An investigation of indanone derivatives as inhibitors of monoamine oxidase

E Aucamp

orcid.org/0000-0003-0949-3377

Dissertation submitted in fulfilment of the requirements for the degree *Master of Science* in *Pharmaceutical Chemistry* at the Potchefstroom Campus of the North West University

Supervisor: Prof. A. Petzer
Co-supervisor: Prof. J.P. Petzer
Co-supervisor: Prof. L.J. Legoabe

Graduation May 2018
Student number: 23401338

The financial assistance of the National Research Foundation (NRF) towards this research is hereby acknowledged. Opinions expressed and conclusions arrived at, are those of the author and are not necessarily to be attributed to the NRF.

TABLE OF CONTENTS

Acknowledgements

First and foremost, I would like to thank Jesus Christ, my Lord and personal saviour, for granting me the opportunity to pursue this degree. Thank You for always listening to my prayers and graciously leading me in life.

I would like to sincerely thank the following people for the support they offered to me during this study. Without them, it would surely not have been completed.

- My first point of call, Douw Steyn. Thank you for your unconditional support and love. Without your calmness, faith in the Lord and good sense of humour, the pursuit of this degree would have been far more stressful.
- Hercu and Linda Aucamp, my loving parents. Thank you for always believing in me and encouraging me to pursue my dreams. Above all, thank you for enabling me to do so.
- My wonderful sister and grandparents, thank you for the support, patience and encouragement you always offered me even though you don't understand chemistry.
- Close friends and colleagues, especially Stefan, Cornel, Franciska, Hernus and Estaleen. Thank you for all the laughs and emotional support during the pursuit of this degree.
- Professors Jacques and Anél Petzer. Thank you for always understanding and offering the guidance and expertise needed to obtain this degree.

"Little science takes you away from God but more of it takes you to Him."

~Louis Pasteur, founder of microbiology and immunology

ABSTRACT

MAO-A and MAO-B are two isoforms of mitochondrial monoamine oxidase (MAO) that are responsible for the deamination of various monoamine substrates. For example tyramine and dopamine are metabolised by both MAO isoforms. MAO-A specifically metabolises noradrenaline and serotonin, while MAO-B metabolises exogenous amines such as benzylamine and 2-phenylethylamine. MAO-B is the dominant isoform in the striatum and hypothalamus of the human brain and inhibitors of this isoform are mainly indicated in Parkinson's disease, while MAO-A dominates the periphery with depression as the main indication for MAO-A inhibitors. Irreversible inhibition of MAO-A may lead to the "cheese reaction" (when taken with tyramine rich foods) or serotonin syndrome (when administered with serotonin-elevating drugs). It is therefore essential to develop highly selective MAO-B inhibitors to eliminate these potentially fatal side effects of irreversible MAO-A inhibition.

Investigation of 1-indanone derivatives is suggested for this purpose as it is structurally similar to previously tested α-tetralones and 1-indanones that exhibited potent and selective MAO-B inhibition. Potent MAO-B inhibition was particularly displayed by α-tetralone inhibitors that were substituted on C6 and C7. In this study 1-indanone was substituted on C5 and C6 (the analogous positions to C6 and C7 of α-tetralone) with the anticipation that this will yield highly potent and specific inhibitors of MAO-B. The structure of 1-indanone is also similar to that of rasagiline, a highly potent MAO-B inhibitor which is used in the treatment of Parkinson's disease. It is postulated that even higher selectivity for the MAO-B isoform may be obtained when rasagiline is substituted on C4 of the indan phenyl ring. It is hypothesised that the entrance and substrate cavities will fuse as the substituent occupies the entrance cavity and rasagiline the substrate cavity of MAO-B. Inhibitors that display this cavity-spanning mode of inhibition generally do not inhibit MAO-A, which would make C4 substituted rasagiline analogues highly specific for MAO-B. Such compounds would possess a low risk of the cheese reaction and serotonin syndrome. Since 1-indanone is similar in structure to rasagiline, this theory was investigated by substitution of 1-indanone on the C4 position with relatively large substituents. The synthesised 1-indanone derivatives were reduced to the corresponding 1-indanol derivatives in order to compare MAO inhibition potencies of the carbonyl and alcohol derivatives.

The structures of the synthesised 1-indanone and 1-indanol derivatives were elucidated by nuclear magnetic resonance (NMR) and mass spectrometry (MS). Purity of the compounds were estimated by high pressure liquid chromatography (HPLC). All compounds were evaluated as inhibitors of human MAO-A and MAO-B by recording their IC_{50} values. 6-(4-

Chlorobenzyloxy)-1-indanone exhibited the highest MAO-B inhibition potency with an IC_{50} value of 0.000076 μM. This study concluded that 1-indanone derivatives are generally more potent inhibitors of human MAO-B than the corresponding 1-indanol derivatives. The most potent 1-indanol derivative, 5-(4-chlorobenzyloxy)-1-indanol, exhibited an IC_{50} value of 0.007 μM for the inhibition of human MAO-B.

Reversibility studies were conducted with the selected 1-indanol derivative that exhibited the highest MAO-B inhibition potency. Previous studies have already shown that 1-indanone derivatives are reversible MAO inhibitors. In addition, the reversibility of MAO-A inhibition of 4-hydroxy-1-indanone (IC_{50} = 2.15 μM) was also examined since this compound displayed the most potent MAO-A inhibition of the series. The results obtained showed that both compounds are reversible inhibitors of MAO.

KEYWORDS

Monoamine oxidase (MAO); MAO-A; MAO B; cheese reaction; serotonin syndrome; α-tetralone; 1-indanone; indanol; rasagiline; reversibility.

UITTREKSEL

Monoamienoksidase (MAO)-A en -B is twee isovorme van mitochondriale MAO wat vir die deaminering van verskeie monoamiensubstrate verantwoordelik is. Beide isovorme van MAO metaboliseer tiramien en dopamien. MAO-A metaboliseer spesifiek noradrenalien en serotonien, terwyl MAO-B eksogene amiene soos bensielamien en 2-fenieletielamien metaboliseer. MAO-B is die mees algemene isovorm in die striatum en hipotalamus van die menslike brein en inhibeerders van hierdie isovorm word hoofsaaklik aangewend vir die behandeling van Parkinson se siekte. MAO-A is die belangrikste isovorm in die periferie en MAO-A-inhibeerders word aangewend vir die behandeling van depressie. Onomkeerbare inhibisie van MAO-A kan tot die “kaasreaksie” (wanneer dit saam met tiramienryke voedsel ingeneem word) of die serotoniensindroom (wanneer dit saam met middels wat serotonienvlakke verhoog toegedien word), lei. Dit is dus noodsaaklik om hoogs selektiewe MAO-B-inhibeerders te ontwikkel om sodoende hierdie gevaarlike newe-effekte van onomkeerbare MAO-A-inhibisie te vermy.

Vir die doel van hierdie studie is die MAO-inhiberende eienskappe van 1-indanoonderivate ondersoek aangesien dit struktureel verwant is aan α-tetraloon- en 1-indanoonderivate wat in vorige studies potente en selektiewe MAO-B-inhibisie getoon het. Die α-tetraloonderivate wat op die C6- en C7-posisies gesubstitueer is, het veral potente MAO-B-inhibisie getoon. In hierdie studie is 1-indanoon op C5 en C6 gesubstitueer (wat ooreenstem met C6 en C7 op α-tetraloon) met die verwagting dat dit potente en spesifieke MAO-B-inhibeerders sal lewer. Die struktuur van 1-indanoon is ook verwant aan dié van rasagilien, ’n potente MAO-B-inhibeerder wat vir die behandeling van Parkinson se siekte gebruik word. Daar is voorgestel dat die selektiwiteit van rasagilien vir die MAO-B-isoform verbeter kan word deur rasagilien op C4 van die indaanfenielring te substitueer. Die hipotese is dat die ingangs- en substraatholtes van die aktiewe setel sal saamsmelt omdat die substituent die ingangsholte beset terwyl rasagilien in die substraatholte van MAO-B bind. Verbindings wat beide bindingsetels beset, tree oor die algemeen nie as MAO-A-inhibeerders op nie en dus sal rasagilien-analoë, wat op C4 gesubstitueer is, baie spesifiek vir MAO-B wees. Hierdie verbindings behoort ’n lae risiko vir die kaasreaksie en serotoniensindroom in te hou. Dié teorie is ondersoek deur 1-indanoon ook met relatiewe groot substituente op C4 te substitueer aangesien 1-indanoon se struktuur soortgelyk is aan dié van rasagilien. Die gesintetiseerde 1-indanoonderivate is tot die ooreenstemmende 1-indanolderivate gereduseer ten einde die potensie van MAO inhibisie van die karboniel- en alkoholbevattende derivate te vergelyk.

Die strukture van die gesintetiseerde 1-indanoon- en 1-indanolderivate is deur kernmagnetieseresonans (KMR) en massa spektrometrie (MS) opgeklaar. Die suiwerheid van die verbindings is met hoë-prestasie vloeistofchromatografie (HPVC) bepaal. Alle verbindings is as inhibeerders van menslike MAO-A en MAO-B geëvalueer deur die IC_{50}-waardes daarvan te bepaal. 6-(4-Chlorobensieloksie)-1-indanoon het die mees potente MAO-B-inhibisie getoon met 'n IC_{50}-waarde van 0.000076 µM. Hierdie studie kom tot die gevolgtrekking dat 1-indanoonderivate oor die algemeen meer potente inhibeerders van menslike MAO-B is as die ooreenstemmende 1-indanolderivate. Die mees potente 1-indanolderivaat, 5-(4-chlorobensieloksie)-1-indanol, het 'n IC_{50}-waarde van 0.007 µM vir die inhibisie van menslike MAO-B getoon.

Omkeerbaarheidstudies is met die 1-indanolderivaat uitgevoer wat die mees potente MAO-B-inhibisie getoon het. Vorige studies het getoon dat 1-indanoonderivate omkeerbare MAO-inhibeerders is. Die omkeerbaarheid van MAO-A-inhibisie van 4-hidroksie-1-indanoon (IC_{50} = 2.153 µM) is ook ondersoek aangesien hierdie verbinding die mees potente MAO-A-inhibisie van die reeks verbindings getoon het. Die resultate het aangedui dat beide hierdie verbindings omkeerbare inhibeerders van MAO is.

SLEUTELWOORDE

Monoamienoksidase; MAO-A; MAO-B; kaasreaksie, serotoniensindroom, α-tetraloon; 1-indanoon; indanol; rasagilien; omkeerbaar.

LIST OF ABBREVIATIONS

4-HQ	4-Hydroxyquinoline
5-HT	5-Hydroxytriptamine / serotonin
A	
A	Adrenaline
ADAGIO	Attenuation of disease progression with azilect given once-daily
ADHD	Attention-deficit hyperactivity disorder
Ala	Alanine
APCI	Atmospheric-pressure chemical ionisation
APP	Amyloid precursor protein
Arg	Arginine
ATP	Adenosine triphosphate
B	
BSAO	Bovine serum amine oxidase
C	
CNS	Central nervous system
C-terminal	Carboxy terminal
CuAO	Copper-containing amine oxidase
Cys	Cysteine
D	
DA	Dopamine
F	
FAD	Flavin adenine dinucleotide

G

GABA	Gamma-aminobutyric acid
GIT	Gastrointestinal tract
Gln	Glutamine
Glu	Glutamic acid

H

His	Histidine
HMRS	High resolution mass spectra
HPLC	High pressure liquid chromatography

I

Ile	Isoleucine

L

L-DOPA	L-3,4-dihydroxyphenylalanine / levodopa
Leu	Leucine
Lys	Lysine

M

MAO	Monoamine oxidase
MAO-A	Monoamine oxidase type A
MAO-B	Monoamine oxidase type B
MPP^+	1-Methyl-4-phenylpyridinium
MPTP	1-Methyl-4-phenyl-1,2,3,6-tetrahydropyridine
MS	Mass spectrometry

N

NA	Noradrenaline
NMR	Nuclear magnetic resonance

NOS	Nitric oxidase synthase
P	
PD	Parkinson’s disease
PE	2-Phenylethylamine
Phe	Phenylalanine
R	
RIMA	Reversible inhibitor of MAO-A
ROS	Reactive oxygen species
S	
SAR	Structure-activity relationship
SD	Standard deviation
SI	Selectivity index
SNpc	Substantia nigra pars compacta
SSAO	Semicarbazide-sensitive amine oxidase
SSRI	Selective serotonin reuptake inhibitor
STS	Selegiline Transdermal System
T	
TK	Tyrosine kinase
TLC	Thin layer chromatography
TPQ	Topa-quinone
Tyr	Tyrosine
V	
VAP-1	Vascular adhesion protein-1

LIST OF TABLES

LIST OF FIGURES

CHAPTER 1: INTRODUCTION

1.1 Introduction and overview

The monoamine oxidase (MAO) enzymes are flavin adenine dinucleotide (FAD) containing proteins located on the outer mitochondrial membrane that function as catalysts for the deamination of a variety of monoamine substrates. The MAO enzymes are present in two isoforms, MAO-A and MAO-B, which differ in substrate and inhibitor specificity as well as distribution in the human body (Youdim & Bakhle, 2006). These two isoforms exhibit a sequence identity of ~70% and are encoded by different genes on the X chromosome (Grimsby *et al.,* 1991; Bach *et al.,* 1988). MAO-A is responsible for the metabolism of noradrenaline (NA), serotonin (5-hydroxytryptamine; 5-HT), dopamine (DA) and tyramine, and is selectively inhibited by clorgyline. MAO-B catalyses the metabolism of the exogenous amines, benzylamine and 2-phenylethylamine (PE), as well as DA and tyramine, and is specifically inhibited by (R)-deprenyl (Youdim & Bakhle, 2006). Research shows that DA is equally well metabolised by both isoforms and in the event of complete inhibition of one isoform, DA will still be sufficiently metabolised by the other isoform. The steady-state level of DA will therefore not change when either isoform is inhibited although the release of DA in the synaptic cleft may be affected (Riederer & Youdim, 1986).

Regional differences between MAO-A and MAO-B exist in the human body. MAO-B exhibits the highest activity in the striatum (basal ganglia) and hypothalamus (Youdim *et al.,* 2006). The dominant isoform in the periphery is MAO-A, the isoform implicated in the so-called “cheese reaction”, which occurs upon irreversible inhibition of MAO-A. Indirect acting sympathomimetic amines, such as tyramine present in wine and beer, are able to induce the “cheese reaction”. Dietary tyramine is usually inactivated by MAO-A during “first pass” metabolism in the gastrointestinal tract (GIT) and liver. The tyramine uptake from the GI tract increases when MAO-A is irreversibly inhibited, which leads to increased noradrenaline release from the peripheral adrenergic neurons. This leads to an increase in blood pressure which may prove to be fatal (Youdim & Bakhle, 2006).

Research indicates that only MAO-A inhibition leads to the potentiation of tyramine-related pharmacological effects. This is supported by the localisation of MAO-A in the GI tract while MAO-B activity is absent or very low in the GI tract (Lader *et al.,* 1970; Finberg & Tenne, 1982).

MAO-A inhibitors are indicated for the treatment of depression since these drugs elevate the brain levels of NA and 5-HT (Pletscher, 1991). To obtain raised levels of amines in the human brain, the inhibition of MAO enzymes should exceed 90% (Fowler *et al.,* 2015). MAO inhibition leads to an altered amine balance with effects on patients' mood after approximately three weeks of treatment (Fowler *et al.,* 1996). Since 5-HT is metabolised by MAO-A in the brain, MAO-A inhibitors may promote the life-threatening serotonin syndrome when administered together with 5-HT-elevating drugs such as selective serotonin reuptake inhibitors (SSRI's). MAO-B selective inhibitors, however, increase DA levels without affecting MAO-A activity and is therefore a viable option for the treatment of Parkinson's disease (PD). A second reason for using MAO-B inhibitors in PD is linked to the possibly that MAO-B inhibitors may be neuroprotective and have the potential to modify disease progression (Fernandez & Chen, 2007). MAO-B activity increases with age and potentially harmful products of the MAO-B catalytic cycle may contribute to neurodegeneration in PD. MAO-B inhibitors may reduce the central levels of these metabolic by-products and therefore protect the dopaminergic system from degeneration due to an age related increase in MAO-B activity (Fowler *et al*., 1997).

Most of the MAO-B inhibitors under investigation are irreversible inhibitors. An example is (R)-deprenyl, also known as selegiline, the first selective MAO-B inhibitor to be used in the clinic. MAO-B inhibitors can be divided into two classes, reversible and irreversible inhibitors. The structures of reversible, competitive inhibitors are related to MAO substrates and these drugs therefore bind to the active site of the MAO-B enzyme. Irreversible ("suicide") inhibitors initially bind in the same way (reversible and competitive) as reversible inhibitors with subsequent oxidation to the active inhibitor. The active inhibitor then binds covalently to the enzyme via the cofactor (FAD) and therefore the enzyme is permanently unable to metabolise amines (Foley *et al.,* 2000). For the completion of the catalytic cycle, the FAD cofactor reacts with oxygen to produce the oxidised flavin and hydrogen peroxide (H_2O_2). An increase in hydrogen peroxide

levels as a result of MAO-B activity may lead to apoptosis of dopamine-producing cells and, as mentioned above, may be responsible for neurodegeneration in PD (Edmondson *et al.,* 2009). Hydrogen peroxide is also a source of hydroxyl radicals which contribute to oxidative stress. MAO inhibitors are therefore also valuable in the treatment of oxidative stress related tissue damage as in the case of a stroke (Youdim *et al.,* 2006). The inhibition caused by the irreversible inhibitors is more persistent than that of reversible inhibitors. Treatment with reversible inhibitors provides the option of immediately regaining enzyme activity after elimination of the inhibitor from the tissue, while enzyme activity is only regained after several weeks following withdrawal of an irreversible inhibitor. After irreversible inhibition, *de novo* synthesis of the enzyme is required to overcome the effects of inhibition (Foley *et al.,* 2000). It is considered safer to use a reversible inhibitor (in comparison with an irreversible inhibitor) as potential side effects, that may occur due to MAO inhibition, can be terminated immediately when drug treatment is stopped (Van den Berg *et al.,* 2007).

1.2 Rationale

The MAO inhibition properties of a series of 1-indanones were determined by Mostert and colleagues (2015), and it was concluded that, similar to α-tetralones studied by Legoabe and colleagues (2014), various substituted 1-indanones exhibit good potency MAO inhibition. Indanone is the 5-membered ring analogues of α-tetralone. This study will expand on the previous study by Mostert *et al*. (2015) by attempting to discover new indanone and indanol derivatives as MAO-B inhibitors by substitution on C4, C5 and C6 of the indanone ring system. For this study, the benzyloxy moiety will be considered as first substituent, since it was shown that substitution with the benzyloxy moiety at C6 or C7 of α-tetralone leads to potent MAO-B inhibition. It is therefore expected that indanones substituted with the benzyloxy moiety on C4, C5 or C6 will produce highly potent MAO-B inhibitors. The previous study on the MAO inhibition properties of indanones concluded that substitution on C6, and to a lesser extent C5, produces selective, potent inhibitors of MAO-B and it is expected that the results obtained in this study will be similar and thus support the previous study (Mostert *et al*., 2015). Three other substituents, 3-chlorobenzyloxy, 4-chlorobenzyloxy and 2-phenoxyethoxy were also selected as substituents for this study, and will be compared to benzyloxy substitution. In particular, Legoabe and colleagues (2014) have shown that substituents

that contain a halogen atom lead to increased MAO inhibition potency of α-tetralones compared to homologues that do not contain a halogen on the side chain phenyl ring. It is therefore expected that the inhibitors that possess substituents with a halogen (e.g. 3-chlorobenzyloxy, 4-chlorobenzyloxy) will be more potent MAO inhibitors than the inhibitors with a benzyloxy or 2-phenoxyethoxy side chains. However, it has to be noted that side chain length may also determine MAO-B inhibition potency, and it has been shown that the caffeine derivatives substituted with the 2-phenoxyethoxy side chain are particularly potent MAO-B inhibitors, possibly because the longer side chain protrudes deeper in the entrance cavity of MAO-B where it establishes productive interactions with hydrophobic residues (Strydom *et al*., 2010).

A major objective of this study will be to reduce the 1-indanones to the corresponding 1-indanol derivatives. The MAO inhibition properties of 1-indanol derivatives have not yet been investigated and this study will provide the opportunity to compare 1-indanones to the corresponding 1-indanol derivatives.

A crystal structure of rasagiline, a highly potent MAO-B inhibitor, bound to MAO-B was published by Hubálek and colleagues (2004). The structure shows that rasagiline binds in the substrate cavity of MAO-B and therefore leaves the entrance cavity unoccupied. Rasagiline may, however, lose selectivity at high dosages and inhibit MAO-A irreversibly. This is of concern since irreversible inhibition of MAO-A may induce the “cheese reaction”. This is also of significance to the present study since rasagiline possess a similar structure to the 1-indanone and 1-indanol derivatives of this study. Substitution on C4 of rasagiline may increase the selectivity of rasagiline for MAO-B and thus reduce the possibility of interaction with MAO-A and the cheese reaction. An appropriate substituent on C4 of rasagiline will project into the entrance cavity so that the entrance and substrate cavities of MAO-B may fuse. Such larger cavity-spanning inhibitors of MAO-B are in general selective for MAO-B and do not bind to MAO-A. Phe208 of MAO-A prevents the binding of large inhibitors to MAO-A. It is therefore expected that C4 substituted 1-indanone and 1-indanol derivatives may produce inhibitors that are selective for MAO-B with poor affinity for MAO-A. The liability of the “cheese reaction” will therefore be avoided.

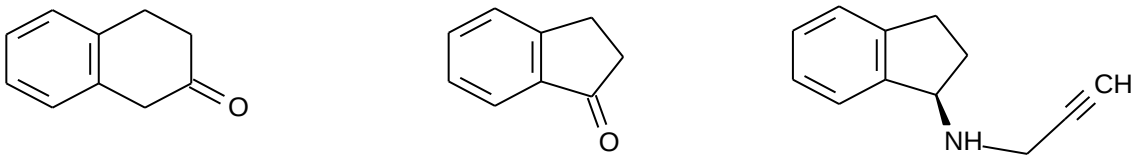

Figure 1.1 The structures of α-tetralone (left), 1-indanone (middle) and rasagiline (right).

Table 1.1 The indanone **(1a-h)**, indanol **(1i-n)** and hydroxy-1-indanone **(2a, c)** derivatives that will be synthesised in this study.

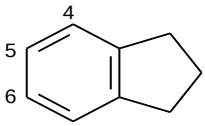

Substitution at C4	Substitution at C5	Substitution at C6
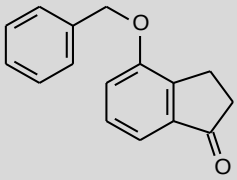 **1a**	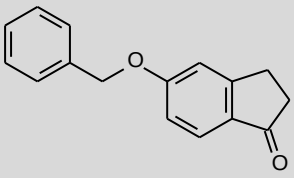 **1b**	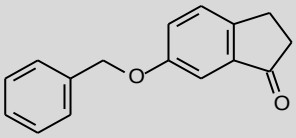 **1c**
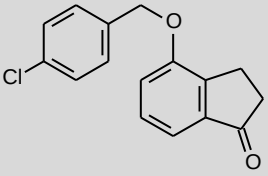 **1d**	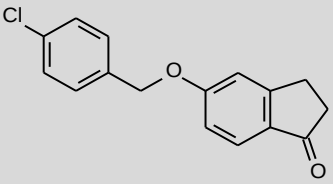 **1e**	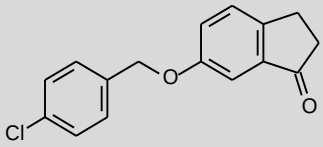 **1f**
		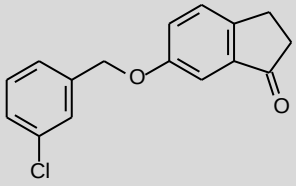 **1g**

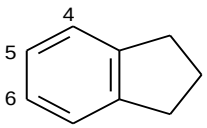

Substitution at C4	Substitution at C5	Substitution at C6
	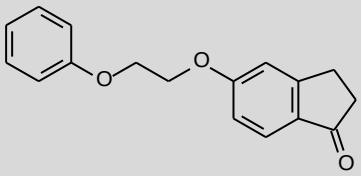 **1h**	
	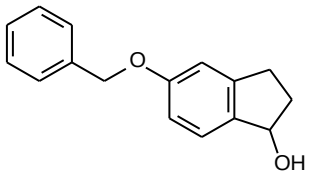 **1i**	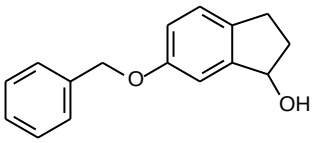 **1j**
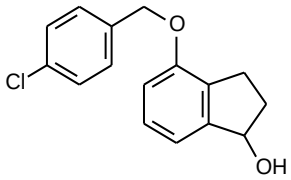 **1k**	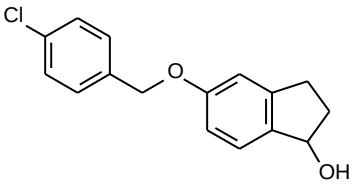 **1l**	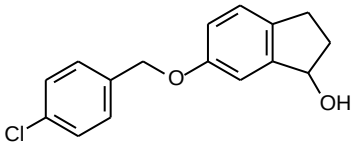 **1m**
		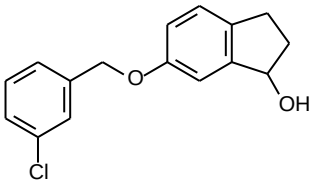 **1n**

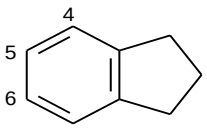

Substitution at C4	Substitution at C5	Substitution at C6
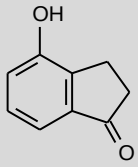 **2a**		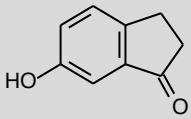 **2c**

1.3 Hypothesis

Based on the finding that α-tetralone and 1-indanone derivatives are highly potent MAO-B inhibitors, it is postulated that the 1-indanone and 1-indanol derivatives synthesised in this study will also exhibit high potency MAO-B inhibition. It may also be postulated that substitution on the C5 and C6 positions will produce particularly potent MAO-B inhibitors since substitution of α-tetralone on C6 and C7 (the analogous positions to C5 and C6 on 1-indanone) yield high potency MAO-B inhibitors. It is postulated that substitution of 1-indanone and 1-indanol on C4 will yield highly selective inhibitors due to possibility that the entrance and substrate cavity will be occupied by the inhibitors. It is also postulated that the compounds substituted with halogen-containing side chains will exhibit higher MAO inhibition potencies compared to compounds that do not contain halogens in their side chains. 1-Indanone and 1-indanol may therefore prove to be promising scaffolds for the design of MAO-B inhibitors with high potencies.

1.4 Objectives

- Eight 1-indanone derivatives will be synthesised that are substituted with the benzyloxy, 3-chlorobenzyloxy, 4-chlorobenzyloxy and 2-phenoxyethoxy moieties on C4, C5 or C6.

- Six 1-indanol derivatives will be synthesised through the reduction of the appropriate 1-indanone derivatives.

- The indanone and indanol derivatives will be evaluated as potential inhibitors of human MAO-A and MAO-B, and the inhibition potencies will be presented as the IC_{50} values.

- The reversibility of MAO-B inhibition of a selected 1-indanol derivative will be determined by dialysis experiments.

CHAPTER 2: LITERATURE STUDY

2.1 MAO

2.1.1 General background

Mary Hare-Bernheim was the first person to give account of the enzyme responsible for the oxidative deamination of tyramine in 1928. She named it tyramine oxidase. Hugh Blaschko later discovered that tyramine oxidase is in fact the same enzyme as those previously described, noradrenaline oxidase and aliphatic amine oxidase, which is responsible for the metabolism of primary, secondary and tertiary amines. Diamines such as histamine are not metabolised by tyramine oxidase. Eventually the enzyme was named mitochondrial monoamine oxidase (MAO) by Zeller (Youdim & Bakhle, 2006).

The MAOs are flavin-containing proteins found on the outer mitochondrial membrane that catalyse the deamination of a range of monoamine substrates and follow the overall oxidative deamination reaction represented in the following figure:

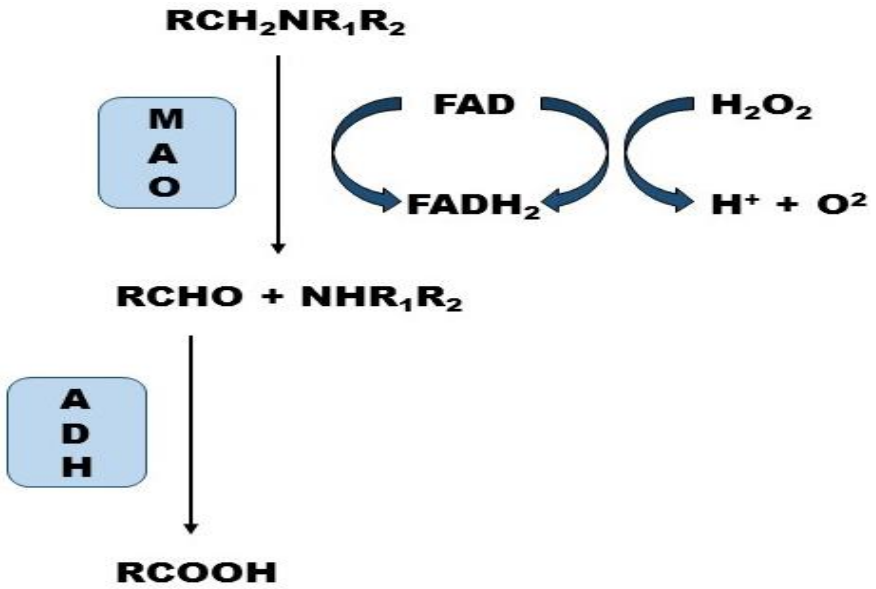

Figure 2.1 A representation of the reaction pathway of the metabolism of monoamines by oxidative deamination (facilitated by the MAO enzymes).

The primary product of this reaction is the corresponding aldehyde which is usually quickly further oxidised by aldehyde dehydrogenase to a carboxylic acid (the final excreted metabolite). The FAD-$FADH_2$ cycle produces hydrogen peroxide that needs to be inactivated by catalase or glutathione peroxidase in the brain. Figure 2.1 was adapted from Youdim & Bakhle (2006) with permission from John Wiley and Sons, British Journal of Pharmacology.

The most important substrates for the MAO enzymes are neurotransmitters in the central nervous system (CNS). These are DA, adrenaline (A), NA, 5-HT and PE (Foley *et al*., 2000). Hydrogen peroxide, the corresponding aldehyde and ammonia (from a primary amine) or a substituted amine (in the case of a secondary amine) are produced through the oxidative deamination reaction. Hydrogen peroxide is a source of hydroxyl radicals and MAO inhibitors may therefore be of use in the management of oxidative stress related tissue damage such as in a stroke (Youdim *et al.,* 2006). The dopaminergic neurons in the substantia nigra pars compacta (SNpc) are densely packed and have a high tonicity, hence they are susceptible to oxidative stress. The extent to which oxidative stress influences these neurons increases in early PD as some of the neurons have been destroyed and the others are increasing in activity to compensate for those lost (Aluf *et al.,* 2011; Finberg & Rabey, 2016). An increase in the hydrogen peroxide levels may lead to apoptosis of dopaminergic cells and, as mentioned above, may be responsible for neurodegeneration in PD (Edmondson *et al.,* 2009).

The metabolism of monoamines by MAO yields a significant amount of hydrogen peroxide in the brain. As mentioned in the text, glutathione peroxidase usually inactivates hydrogen peroxide, but hydrogen peroxide is also chemically converted to highly reactive hydroxyl radicals through the Fenton reaction (facilitated by Fe^{2+}). Hydroxyl radicals have various damaging effects that can lead to neuronal injury or death. The possibility that hydrogen peroxide will act as a substrate for the Fenton reaction increases when glutathione peroxidase levels are low and the levels of MAO and Fe^{2+} are higher than usual. This will lead to neurons being damaged by oxidative stress to a greater extent. MAO inhibitors are therefore used to reduce the generation of hydrogen peroxide and Fe^{2+} ions are removed through iron chelation, which results in a reduction of the formation of hydroxyl radicals and consequently oxidative stress (Youdim & Bakhle, 2006). This figure was adapted from

Youdim & Bakhle (2006) with permission from John Wiley and Sons, British Journal of Pharmacology.

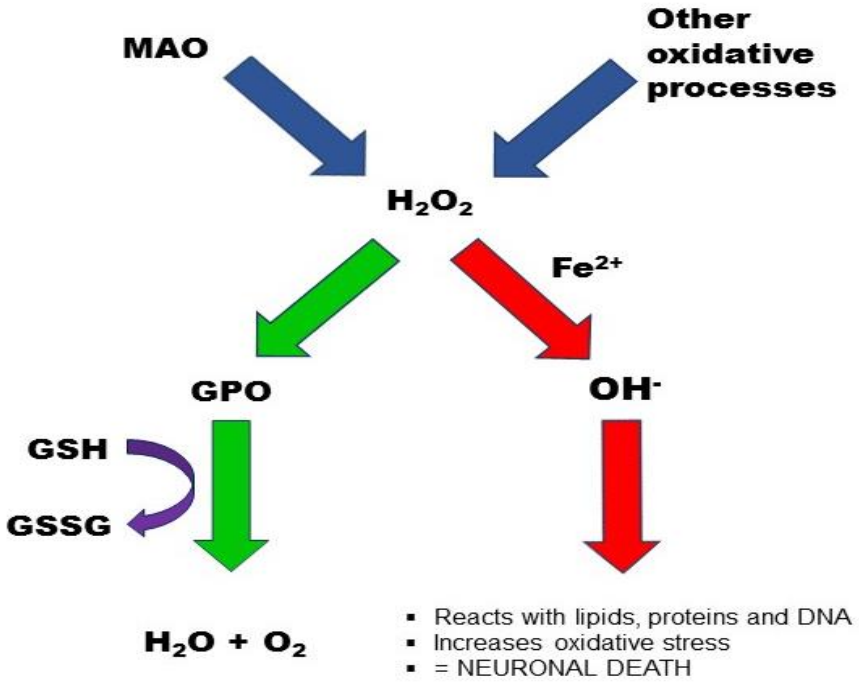

Figure 2.2 A representation of the Fenton reaction, the mechanism through which iron and hydrogen peroxide (H_2O_2) induces neurotoxicity.

Two isoforms of MAO exist, namely MAO-A and MAO-B, which differ in substrate and inhibitor specificity as well as distribution in the human body. They also differ in sensitivity to heat inactivation and in pH optima. MAO-A is inhibited by clorgyline and metabolises NA, 5-HT, tyramine and DA, whereas MAO-B is inhibited by benzylamine and metabolises tyramine and DA. DA is equally well metabolised by both forms of the enzyme (Youdim & Bakhle, 2006). The oxidation of different substrates takes place at very different rates. The kinetic parameters that were measured indicate that MAO-A and MAO-B are equally efficient at metabolising DA with K_{cat}/K_M values greater than those values for other physiological substrates (Youdim *et al.,* 2006; Edmondson *et al*., 2009; Ramsay *et al.,* 2011). Research suggests that in the case of complete inhibition of one of the MAO isoforms, DA would still be adequately metabolised by the other isoform. The steady-state level of DA will therefore not change with selective inhibition of either one of the isoforms, but the release of DA into the synaptic cleft will be affected (Riederer & Youdim, 1986). Furthermore, the metabolism of 5-HT by MAO-A is 40-fold better than by MAO-B, whereas

the metabolism of PE by MAO-B is about 35-fold better than by MAO-A as can be seen in the k_{cat} and k_M differences. These kinetic measurements indicate that DA and NA are metabolised by both MAO-A and MAO-B, but 5-HT is metabolised selectively by MAO-A. Serotonergic neurons contain mainly MAO-B, which functions to protect the mitochondria and the nerve terminals from the other neurotransmitters (Youdim *et al*., 2006; Edmondson *et al*., 2009; Ramsay *et al.,* 2011).

In order to obtain raised levels of brain amines in humans, the inhibition of MAO should exceed 90% (Fowler *et al.,* 2015). The inhibition of MAO leads to an altered amine balance, and the effects on mood can be detected after approximately three weeks. Most of the MAO inhibitors are irreversible and recovery from inhibition is therefore slow (Fowler *et al*., 1996; Zajecka & Zajecka, 2014).

MAO has a unique ability to modulate the neurotransmission of monoamines and may be a target for drugs used to modulate brain functions. These drugs could therefore be used in the treatment of various mental diseases such as mood disorders (Rivera *et al.,* 2009; Shulman *et al.,* 2013), schizophrenia (Samson *et al.,* 1995; Siever and Coursey, 1985; Sun *et al.,* 2012), anxiety (Tyrer & Shawcross, 1988; Tadic *et al.,* 2003), anorexia nervosa (Urwin & Nunn, 2005), attention-deficit hyperactivity disorder (ADHD) (Jiang *et al.,* 2001; Wargelius *et al.,* 2012), migraine (Filic *et al.,* 2005; Merikangas & Merikangas, 1995) and neurodegenerative disorders (Cai, 2014; Youdim *et al.,* 2004). MAO inhibitors may also find application in the treatment of Alzheimer's disease (Saura *et al.,* 1994).

Isoniazid, an anti-tuberculosis drug, was the first drug to exhibit potent MAO inhibitory activity. The first compound to be successfully used as a MAO inhibitor in depression, was iproniazid (a compound related to isoniazid). In the late 1950's it was discovered that iproniazid exhibits significant antidepressant action, but due to serious side effects its clinical value was undermined. It was established that its hydrazine structure was responsible for liver toxicity and hepatitis in patients. Most of the other developed non-selective, irreversible MAO inhibitors with a hydrazide structure, such as iproclozide, mebanazine, nialamide, octamoxin and safrazine have also been taken off the market due to hepatotoxicity and only a few are still in use (Fišar, 2016). This problem was resolved by developing new MAO inhibitors that did not have a hydrazine structure, such as

tranylcypromine. Unfortunately, these new MAO inhibitors were responsible for another serious side effect, the “cheese reaction”.

2.1.2 Tissue distribution

In the early stages of investigation of the distribution of human MAO enzymes, experiments were based on measuring enzyme activities in crude tissue and cell homogenates by using the favoured substrates for the enzymes, NA and 5-HT as substrates for MAO-A and PE as substrate for MAO-B. Low concentrations of enzyme-specific inhibitors were also used, clorgyline inhibited MAO-A and (R)-deprenyl inhibited MAO-B (Glover & Sandler, 1986). These experiments provided evidence that lymphocytes and platelets in the blood contain only MAO-B (Bond & Cundall, 1977).

The MAO enzymes are mainly bound to the outer mitochondrial membrane and are present in most tissues including the brain. MAO-A is mainly present in the catecholaminergic neurons, whereas MAO-B is mainly found in serotonergic and histaminergic neurons and astrocytes (Saura *et al*., 1996a; Saura *et al*., 1996b; Shih *et al*., 1999; Tong *et al*., 2013). In the brain, MAO-A is mainly expressed in the noradrenergic perikarya of the locus coeruleus, whilst MAO-B is expressed in the glial cells, ependyma and perikaya of the 5-HT neurons of the raphae nucleus. MAO-B’s localisation in 5-HT neurons created controversy seeing that 5-HT acts as an *in vitro* and *in vivo* selective substrate of MAO-A. Studies also indicated that MAO-A is selectively localised in the raphae projection fields of the hypothalamus (Fagervall & Ross, 1986). This selective localisation was studied further and results indicated that MAO-A and MAO-B are expressed in the embryonic and early-postnatal raphe neurons, although the MAO-A component seems to disappear during development. An explanation for this altered expression may be due to selective trafficking of the mitochondria expressing MAO-A to axon terminals (Denney & Denney, 1985). Controversy also exists over the expression of the MAO isoform by the dopaminergic neurons of the substantia nigra. Immunohistochemical studies indicated that only a few neurons in the substantia nigra express MAO-A (Westlund *et al.,* 1993) and very low levels of MAO activity were detected by histochemical techniques (Arai *et al*., 1998). Microdialysis studies revealed that MAO-A mainly metabolises DA in the rat striatum *in vivo* (Wachtel & Abercrombie, 1994). The ^{11}C-harmine brain imaging technique has led to the discovery of raised brain MAO-A levels in the cortical, striatal and midbrain sections of guinea pigs that

suffer from major depressive disorder (Meyer *et al*., 2006). The highest levels of MAO-B activity is observed in the striatum (i.e. basal ganglia) and hypothalamus (Youdim *et al.,* 2006). MAO-B levels in the brain are low in mice and human neonates, but increase swiftly after birth (Holschneider *et al*., 2001; Nicotra *et al*., 2004).

The MAO-A and MAO-B enzymes are encoded by separate genes that are located on the X chromosome. Each gene is composed of fifteen exons and has similar intron-exon composition. This suggests that these enzymes are derived from the same ancestral gene (Grimsby *et al.,* 1991). MAO-A and MAO-B have an amino acid identity of 70% and is made up of 527 and 520 amino acids, respectively (Bach *et al.,* 1988). Studies on the transcriptional regulation of the MAO-A and MAO-B genes indicate that different supporting organisations may underlie different cell- and tissue-specific expressions of the MAO subtypes (Shih *et al.,* 2011). The regulation of MAO-A and MAO-B expressions are also influenced by different transcription factors, components of intracellular signalling pathways and hormones. Transcription factor Sp1 activates MAO-A expression, whereas transcription repressor R1 suppresses it (Chen *et al.,* 2005).

2.1.3 The mechanism of action of MAO

The means of transfer of two hydrogens from the amine to the flavin is a controversial question and three possible mechanisms for the chemical mechanism of MAO have been proposed, seeing as there is no base in the active sites of the MAOs to accept a proton. These mechanisms are the hydride mechanism, the radical mechanism and the polar nucleophilic mechanism. It is assumed that the catalytic rate-limiting step involves heterolytic H-abstraction (hydride mechanism), homolytic H-abstraction (radical mechanism) or deprotonation of a H^+ (polar nucleophilic mechanism) from the substrate's α-carbon atom. The N5 atom on the flavin performs the activating stage in all the mechanisms (Borštnar *et al*., 2011).

The polar nucleophilic mechanism proposed by Miller and Edmondson for human MAO-catalysis, is most generally accepted as the mechanism by which MAO catalysis occurs and will be discussed in this chapter. The polar nucleophilic mechanism is proposed to occur via nucleophilic attack at the oxidised flavin 4a position by the amine. Proton abstraction from the α-carbon of the amine is proposed to occur by the N5 atom of the flavin which

becomes nucleophilic. Formation of the iminium product results from the elimination of the reduced flavin. Deprotonated amines do not appear to exhibit the required nucleophilicity, and thus the isoalloxazine ring of the flavin needs to exist in a bent conformation relatively to the planarity in the oxidised state of the enzyme. This allows the carbon at position 4a to be electrophilic and the N5 to be more nucleophilic (Edmondson *et al*., 2009).

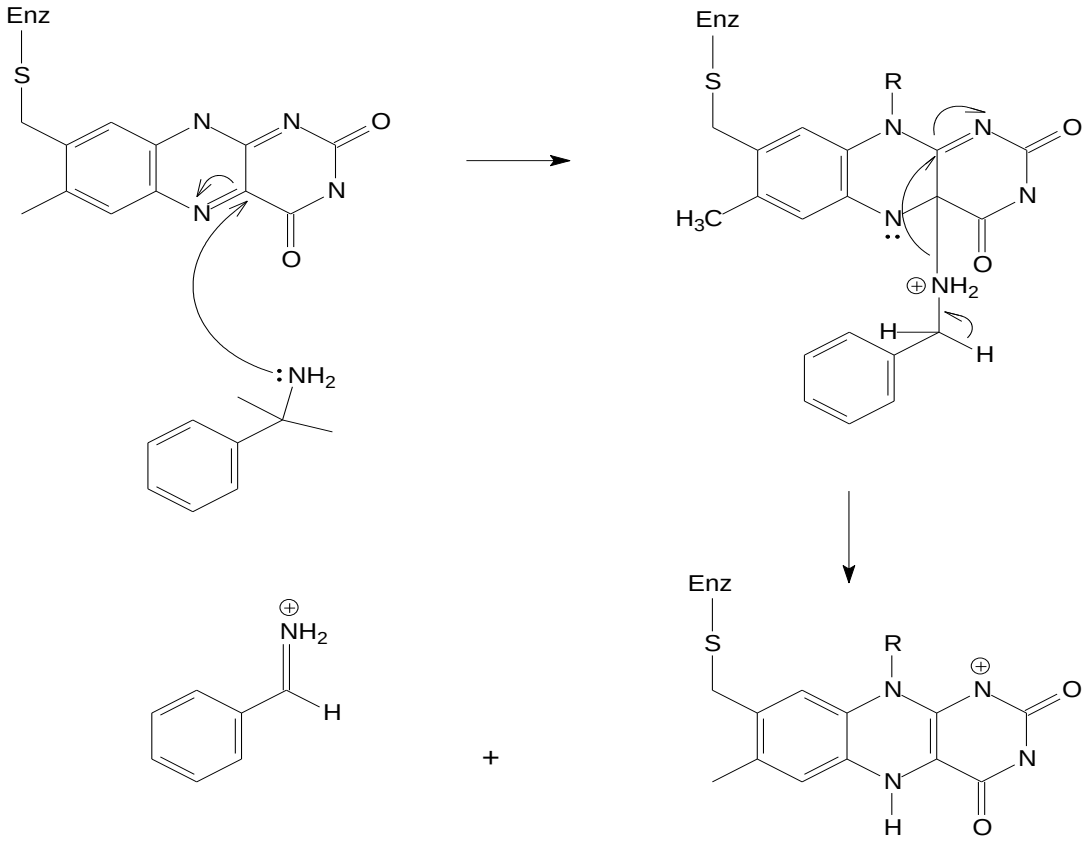

Figure 2.3 The polar nucleophilic mechanism of MAO catalysis.

The transfer of a single electron followed by proton transfer is the mechanism that is well supported by studies on the inactivation of MAO by cyclopropylamines. Importantly, no radical intermediate has been discovered during turnover, even when slow substrates were used (Silverman, 1995). The polar nucleophilic mechanism hypothesises that a short-term adduct to the C4a atom of the FAD cofactor forms where the N5 acts as a base in order to remove the proton. Quantitative structure-activity relationships for a series of substituted benzylamine substrates of MAO-B support this mechanism (Walker & Edmondson, 1994). Although there is no positive evidence to support the simple hydride transfer mechanism, it cannot be ruled out (Kay *et al*., 2007). A synthetic chemical model successfully reproduced

the catalytic properties of MAO-B in a novel approach. Evidence was provided for proton abstraction after a tyrosyl radical cation facilitated an initial charge transfer. Due to the system being an artificial one, it cannot be concluded that it would necessarily follow the mechanism optimised in the protein (Murray *et al*., 2015).

All irreversible MAO inhibitors combine with the N5 atom of the enzyme flavin moiety. The inhibitor molecule can be described as having a substrate-like part that determine the affinity and a "killing group" which binds covalently with the enzyme (Youdim & Finberg, 1983; Youdim *et al*., 1988).

The slowest step in the MAO-A reaction is the breaking of the bond between the α-carbon and the hydrogen in the amine substrate. The re-oxidation of the reduced MAO-B may be slower than the bond-breaking step in the MAO-B reaction. The rate constant for the reduction of MAO-B by PE at 543 s^{-1} clearly indicates this, seeing as it is 500 times faster than the re-oxidation of reduced MAO-B (1 s^{-1}) (Ramsay *et al*., 1987). The hydrogen abstraction is energetically the most difficult step of the reaction as indicated by a deuterium isotope effect of 8.2 on the turnover (5.3 on k_{cat}/K_M) of benzylamine (Walker & Edmondson, 1994).

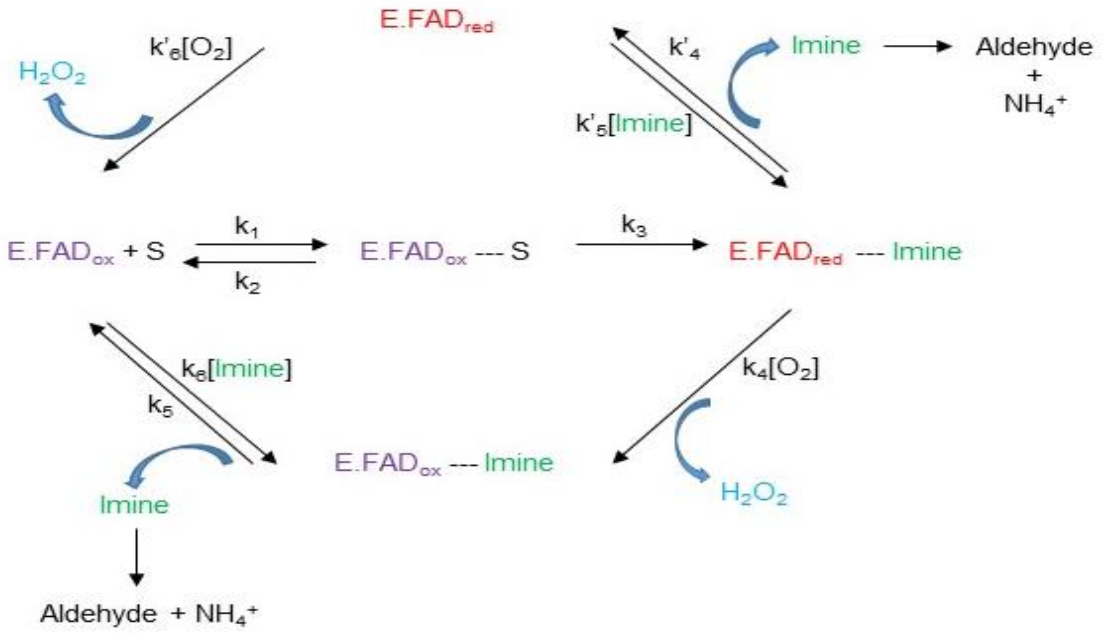

Figure 2.4 The general schematic pathway of MAO catalytic activity.

The top loop of the pathway is followed when PE is used as substrate and the bottom loop when benzylamine is used as substrate. Figure 2.4 was adapted from Edmondson, 1995.

2.2 MAO-A

2.2.1 Biological function of MAO-A

Tyramine and indirect acting sympathomimetic amines that are present in food, such as cheese and fermented drinks (for example wine and beer), are able to induce the “cheese reaction”. Normally, dietary tyramine is inactivated via “first pass” metabolism through MAO in the GIT and then the liver. The remaining tyramine is further metabolised by the MAO present in the lung and vascular endothelial cells (Bakhle, 1990).

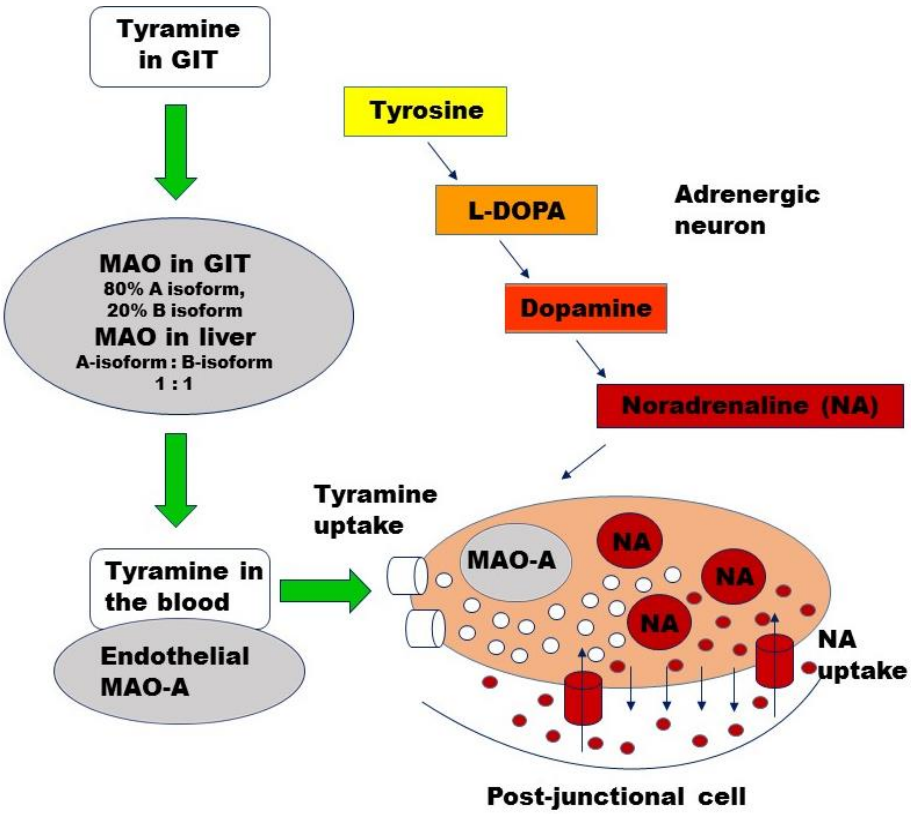

Figure 2.5 A representation of the potentiation of cardiovascular effects due to the simultaneous administration of tyramine and indirectly acting sympathomimetic amines together with irreversible MAO inhibitors.

Figure 2.5 was adapted from Youdim & Bakhle (2006) with permission.

Irreversible inhibition of MAO-A leads to increased tyramine uptake from the GIT and the resulting increased systemic levels of tyramine leads to the release of NA, thus causing the sympatomymetic cardiovascular effects of tyramine. This may lead to a potentially fatal increase in blood pressure. RIMAs, in turn, are displaced from the MAO enzyme by tyramine which leads to normal metabolism of tyramine. The tyramine in the systemic circulation, therefore, never reaches the high levels which result from irreversible MAO-A inhibition (Youdim & Bakhle, 2006). Preclinical and clinical studies indicated that the potentiation of tyramine-related pharmacological effects is a result of MAO-A inhibition only as it is the dominant isoform in the periphery. Due to localisation in the brain, MAO-B inhibition does not lead to the cheese reaction. This can be explained by the localisation of MAO-A in the gut (Lader *et al*., 1970; Finberg & Tenne, 1982; Finberg & Gilman, 2011). The appropriate diet, however, can avoid the cheese reaction and taking this into consideration, it can be argued that MAO inhibitors are exceptional drugs for the treatment of drug-resistant and atypical depression. For this reason, non-selective inhibitors, especially tranylcypromine, are increasingly being used (Finberg & Rabey, 2016).

Due to the metabolism of 5-HT by MAO-A, inhibitors of MAO-A may also promote the life-threatening serotonin syndrome when administered together with serotonin-elevating drugs such as SSRIs. Serotonin syndrome is caused by a toxic build-up of 5-HT and is characterised by fever, hallucinations, tachycardia and gastrointestinal symptoms (Panisset *et al*., 2014). MAO-B selective inhibitors, however, increase levels without affecting MAO-A activity and is therefore considered suitable drugs in treating PD (Fernandez & Chen, 2007). A study carried out by the Parkinson Study Group indicated that only a small fraction of patients (0.24%) treated with (R)-deprenyl together with a SSRI developed symptoms that could possibly relate to that of serotonin syndrome. Only 0.04% of the patients experienced a serious reaction with no fatalities recorded (Panisset *et al*., 2014). It is therefore relatively safe to administer MAO-B inhibitors together with a SSRI. This is an important observation because, due to the high likelihood of co-morbidity of depression and PD, a SSRI will most probably be added to the existing therapy during the course of the disease (Reijnders *et al*., 2008; Richard *et al*., 2012; Weintraub *et al*., 2003).

Interestingly, studies have indicated that insufficient MAO-A levels in humans is responsible for a phenotype of aggressive behaviour (Brunner *et al.,* 1993; Caspi *et al.,* 2002).

2.2.2 Potential role of MAO-A in PD

PD can be defined as a common progressive neurological disorder that currently affects approximately 2% of the American population over the age of 60 years. The pathology of this disease can be described as a loss of dopaminergic cells in the substantia nigra that results in a dopamine deficiency in the striatum. It is characterised by disturbances of the motoric nerve system, primarily bradykinesia, rigidity and tremor at rest. Pre-symptomatic non-motor systems may be involved and include autonomic dysregulation, sleep problems, anxiety, depression and debilitating cognitive changes. These symptoms may also only occur during late stages of the disease (De Lau & Breteler*,* 2006). While MAO-B inhibitors are normally used in the treatment of PD, MAO-A inhibitors may have a twofold role. Firstly, MAO-A inhibitors may be used to treat depression, which is often a co-morbidity of PD. Secondly, MAO-A metabolises DA in the brain, and it may be postulated that nonspecific MAO inhibitors may lead to a more effective enhancement of dopaminergic neurotransmission compared to the inhibition of MAO-B alone (Youdim & Bakhle, 2006).

2.2.3 Inhibitors of MAO-A

MAO-A inhibitors are indicated for the treatment of depression since these drugs elevate the brain levels of NA and 5-HT (Pletscher, 1991). Since 5-HT is metabolised by MAO-A in the brain, inhibitors of MAO-A may promote the life-threatening serotonin syndrome when it is administered together with serotonin-elevating drugs such as SSRIs (Fernandez & Chen, 2007). Reversible MAO-A inhibitors that are still being used clinically include moclobemide, befloxatone and toloxatone (Gareri *et al*., 2000) as well as some non-selective irreversible MAO inhibitors such as tranylcypromine and phenelzine. These compounds will be discussed in the following paragraphs.

2.2.3.1 Non-selective, irreversible MAO inhibitors

Phenelzine:

Besides inhibiting both MAO-A and MAO-B irreversibly, phenelzine blocks gamma-aminobutyric acid (GABA) and alanine transaminases which leads to additional antidepressant activity (Baker *et al.,* 1991; Todd & Baker, 2008). Phenelzine is also the drug

of choice for the treatment of social phobia and refractory social anxiety disorder (Aarre, 2003). Cocaine abuse is also treated with high success with phenelzine as its use is contraindicated upon administration of phenelzine. Phenelzine also reduces patients' craving for cocaine (Golwyn, 1988).

Tranylcypromine:

Tranylcypromine is safe and effective in treating bipolar depression when the appropriate dietary restrictions are applied, particularly when considering that the cheese reaction is a possibility. The limitations it causes, however, have been exaggerated since the quantities of tyramine contained in food are quite low and only a serious deviation from a normal, healthy diet is likely to cause long-term damage or a fatal reaction. The management of such a reaction has been well documented, should it occur (Gillman, 2011). The manufacturers recommend a wash-out period of 7-10 days for tranylcypromine although normal pressor response to an oral tyramine challenge is only regained 30 days after the cessation of tranylcypromine administration (Gahr *et al.,* 2013; Bieck & Antonin, 1988).

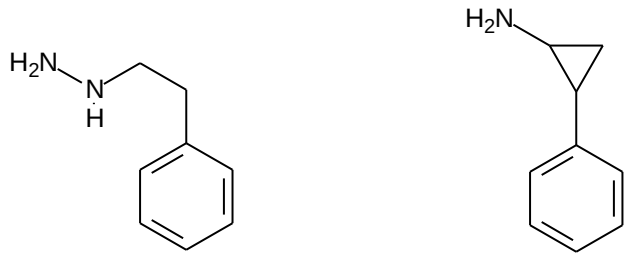

Figure 2.6 The structures of non-selective, irreversible MAO-A inhibitors phenelzine (left) and tranylcypromine (right).

2.2.3.2 Reversible inhibitors of MAO-A (RIMAs)

Da Prada and colleagues (1984) prepared a series of selective RIMAs in the 1980s. They based the design of these compounds on the theory that enzyme inhibition will lead to an increase in substrate levels and that an increase in the displacement of the inhibitor from the active site by the substrate will reverse the degree to which the enzyme is inhibited. A reversible inhibitor will therefore not lead to the cheese reaction when tyramine is ingested as reversibility of inhibition possesses a built-in safety mechanism (Da Prada *et al*.,1984; Finberg, 2014).

Moclobemide and brofaromine:

Moclobemide has shown activity as an antidepressant (Lotufo-Neto *et al.,* 1999) as well as an antiparkinsonian drug (Sieradzan *et al*., 1995; Youdim & Riederer, 2004). It is believed to regulate neuroplasticity in the hippocampus and is therefore responsible for the improvement in attention, memory and vigilance in patients taking the drug (Allain *et al.,* 1992). Moclobemide is currently the only RIMA that is used clinically. Clinical studies carried out directly after its general release, indicated that its effectiveness is equal to that of tricyclic antidepressants in treating depression. However, the studies indicated that its effectivity is lower than those of irreversible MAO inhibitors (Lotufo-Neto *et al.,* 1999; Shulman *et al*., 2013).

Apart from being a RIMA, brofaromine is also a SSRI and is primarily indicated in the treatment of depression and anxiety. It was also found to be equally effective to tricyclic antidepressants (Lotufo-Neto *et al.,* 1999).

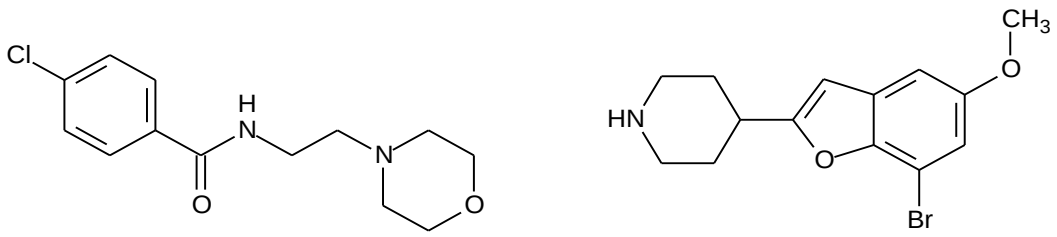

Figure 2.7 The structures of reversible MAO-A inhibitors moclobemide (left) and brofaromine (right).

Methylene Blue:

The use of this drug in depression can be attributed to its various pharmacological activities, such as inhibition of MAO-A, nitric oxidase synthase (NOS) and guanylate cyclase (Naylor *et al.,* 1987; Ramsay *et al*., 2007; Harvey *et al.,* 2010). Methylene blue is an inhibitor of MAO-A with an *in vitro* IC_{50} value of 0.07 µM, while MAO-B is inhibited with an IC_{50} value of IC_{50} = 4.37 µM (Harvey *et al*., 2010).

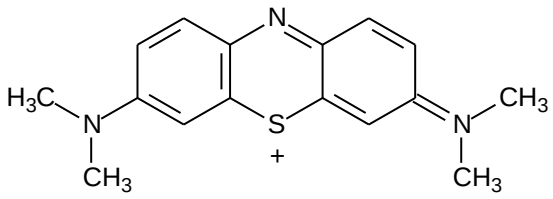

Figure 2.8 The structure of methylene blue.

2.2.4 Three-dimensional structure of MAO-A

Comparison between structures of rat and human MAO-A:

The X-ray structures of rat MAO-A were determined at 3.2 Å (Ma *et al*., 2004) and human MAO-A at 3.0 Å (De Colibus *et al*., 2005). The active site of human MAO-A consists of 5 aromatic and 11 aliphatic residues, which indicates that the cavity is fairly hydrophobic. Despite the fact that human and rat MAO-A display a sequence identity of 92%, MAO-A in rats exhibits a 10-fold higher affinity for the selective irreversible inhibitor, clorgyline, than MAO-A in humans. Important to note is that both rat and human enzymes have single substrate binding cavities with protein loops at the entrances of these cavities. The binding cavity in human MAO-A includes the flavin ring and extends to the cavity-shaping loop which consists of residues 201-216. Two cysteine residues, Cys-321 and Cys-323, are situated close to the entry of the catalytic site. When bound to clorgyline, the side chain of Cys-323 is in contact with the aromatic ring of the inhibitor through van der Waal forces (De Colibus *et al.,* 2005). MAO-A has a monopartite cavity in humans and, although having a monomeric crystal structure, it is dimeric in its membrane-bound form (Binda *et al*., 2011; Son *et al*., 2008, De Colibus *et al*., 2005). This contrasts to rat MAO-A which is dimeric after crystallisation (Edmondson *et al*., 2007b). Differences between the two enzymes can be seen in two important components of the active site, the loop conformations of residues 108-118 and 210-216. This results in a bigger active site cavity volume in human MAO-A (~550 $Å^3$) than in rat MAO-A (~450 $Å^3$). When clorgyline is bound to MAO-A, a conformational change results so that Glu-216 is in direct contact with clorgyline while Gln-215 is projected out of the active site. This altered shape of the active site cavity leads to clorgyline binding in a folded conformation in human MAO-A, whereas it binds in an extended conformation in rat MAO-A (Edmondson *et al*., 2007a; De Colibus *et al.,* 2005).

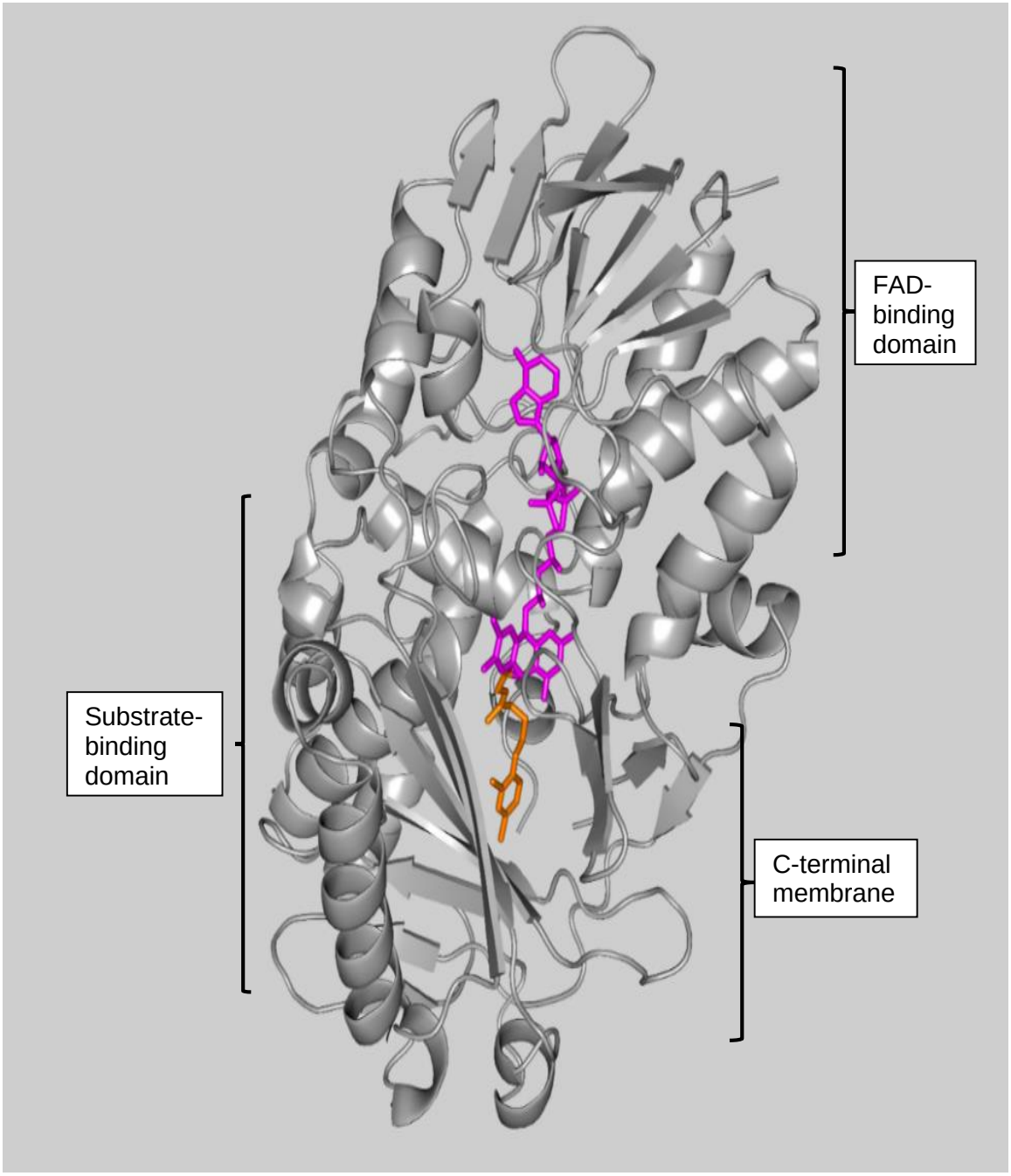

Figure 2.9 A cartoon representation of the structure of human MAO-A.

The FAD-binding domain consists of residues 13–88, 220–294, and 400–462, the substrate-binding domain of residues 89–219 and 295–399 and the C-terminal membrane of residues 463–506. FAD and clorgyline are respectively portrayed as magenta and orange ball-and-stick models. Figure 2.9 was adapted from De Colibus et al. (2005). Copyright (2005) National Academy of Sciences, U.S.A.

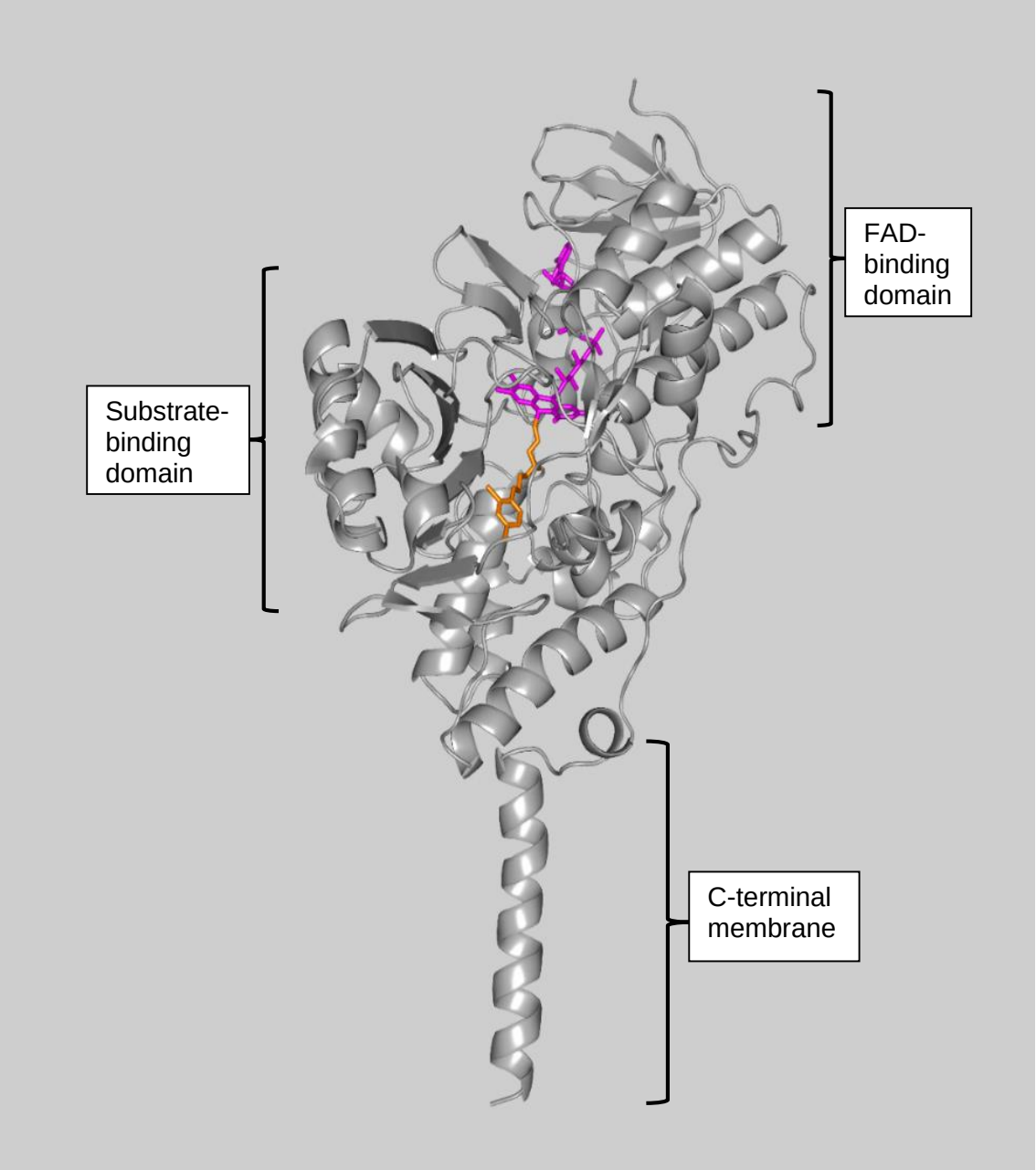

Figure 2.10 A cartoon representation of the structure of rat MAO-A.

FAD and clorgyline are respectively portrayed as magenta and orange ball-and-stick models. Figure 2.10 was adapted from De Colibus et al. (2005). Copyright (2005) National Academy of Sciences, U.S.A.

Comparison between human MAO-A and MAO-B:

The overall chain-folds of MAO-A and MAO-B are more or less the same, but there are differences and similarities in the active site cavities. The structure of the “aromatic cage” in the active site, which consists of two tyrosines as well as the structure of the FAD coenzyme, are identical in both enzymes. Considerable differences between the two enzymes can be found in the proximity of the active sites on the opposite sides of flavin, which controls the recognition of substrates. A further difference is the shapes and sizes of the active site cavities with human MAO-A consisting of a short and wide single cavity of ~550 $Å^3$, whereas human MAO-B consists of a long, narrow cavity of ~700 $Å^3$. Upon entering human MAO-B, an entrance and substrate cavity can be found which are fused together when an inhibitor is bound. The MAO-B active site is therefore bipartite. As already mentioned, MAO-A has a monopartite cavity. The amino acid residues of the enzymes that are displaced by inhibitors, also differ. In MAO-A the conformations of residues Phe-208 and Ile-335 are altered, whereas the conformations Ile-199 and Tyr-326 are altered in MAO-B (De Colibus *et al.,* 2005). Human MAO-A also has a unique, selective Glu-151-Lys mutation. Lys-151 is located on the protein surface, away from the active site cavity and near a group of charged residues that is involved in the contact between two monomers when a dimer is formed, as in the case of human MAO-B and rat MAO-A. It is suggested that this unique mutation is responsible for the destabilisation of the dimeric state of human MAO-A, which then results in the monomeric form of the enzyme (De Colibus *et al*., 2005; Andres *et al.,* 2004).

2.3 MAO-B

2.3.1 Biological function of MAO-B

The therapeutic effects of MAO inhibitors are due to lowered metabolism of monoamine neurotransmitters and decreased production of hydrogen peroxide. The neuroprotective effects of MAO inhibitors can be attributed to their anti-apoptotic nature and modulation of gene expression, which leads to increased neuroplasticity and neuronal survival (Naoi *et al.,* 2016).

Monoaminergic neurotransmitters, of which most are affected by MAO, are involved with processes associated with neuropsychiatric disorders, chronic stress and the aftermath of using many psychotropic drugs. Various drugs can have an effect on the neurotransmission of monoamines through the regulation of neurotransmitter synthesis (Moranta *et al.,* 2004), the regulation of the catabolism of neurotransmitters (Fišar *et al.,* 2012), the inhibition of the uptake or release of the neurotransmitters, changes in the activity of components associated with intracellular signalling pathways (Fišar & Hroudová, 2010) and neuroplasticity.

2.3.2 Potential role of MAO-B in PD

MAO-B activity in the human brain increases with age and is raised in several neurodegenerative diseases. A range of experimental techniques were recently used to show that MAO-B activity in Huntington's, Alzheimer's and PD are increased (Kennedy *et al*., 2003; Zellner *et al*., 2012; Woodard *et al.,* 2014; Ooi *et al*., 2015).

It is proposed that MAO-B plays a primary role in neurodegenerative disorders through generating reactive oxygen species (ROS) and possibly by activating neurotoxins (Naoi *et al.,* 2012; 2016). MPTP (1-methyl-4-phenyl-1,2,3,6-tetrahydropyridine) is a neurotoxic compound and is converted by MAO-B to the active compound 1-methyl-4-phenylpyridinium (MPP^+). This compound is a substrate for the DA transporter, which after being taken up into dopaminergic neurons, can lead to neurotoxicity in humans. MPTP-induced neurotoxicity can be prevented by pre-treatment with MAO-B inhibitors such as (R)-deprenyl and pargyline (Heikkila *et al*., 1984; Langston *et al*., 1984).

2.3.3 Inhibitors of MAO-B

MAO-B selective inhibitors increase DA levels without affecting MAO-A activity and is therefore suitable to treat PD. A second reason for using MAO-B inhibitors in PD is linked to the possibility that MAO-B inhibitors may be neuroprotective and may potentially modify disease progression (Fernandez & Chen, 2007). MAO-B activity stays unchanged until the patient's 60^{th} year and then increases nonlinearly. Most enzymes are believed to have decreased activity with advancing years (Delumeau *et al*., 1994; Dostert *et al*., 1989). Potentially harmful products of the MAO-B catalytic cycle may contribute to neurodegeneration in PD. MAO-B inhibitors may reduce the central levels of these

metabolic by-products and thus protect the dopaminergic system from degeneration, particularly at advanced ages (Fowler *et al*., 1997). Selective MAO-B inhibitors thus not only decrease the oxidation of substrates, but also prevent the production of ROS (Naoi *et al*., 2012; 2016).

The MAO-B inhibitors currently used in the clinic are irreversible inhibitors. An example is (R)-deprenyl, the first selective MAO-B inhibitor to be used. MAO-B inhibitors can be divided into two classes: reversible and irreversible inhibitors. The structures of reversible, competitive inhibitors are related to MAO substrates and these drugs therefore bind to the active site of the MAO-B enzyme. Irreversible ("suicide") inhibitors bind in the same way initially (reversible and competitive) after which they are metabolised by the MAO enzyme to the active inhibitor. The active inhibitor then binds covalently to the N5 atom of FAD and the enzyme is permanently unable to metabolise amines. The inhibition caused by irreversible inhibitors is more persistent than that of reversible inhibitors, with the latter lasting only a few hours, rather than weeks (Foley *et al.,* 2000). Another difference between reversible and irreversible inhibitors, is that reversible inhibitors can be displaced from the binding site when the concentration of the enzyme's substrate increases. It is impossible for irreversible inhibitors to be displaced by another molecule and new enzymes need to be produced to restore the enzyme's activity. This process takes 2-3 weeks (Fišar, 2016). Where irreversible MAO inhibitors are used in practice, it is administered daily at a dose that only provides partial enzyme inhibition. After several days of daily administration, it will lead to a cumulative inhibition of more than 90% of the enzyme in the brain. Continued administration of the drug ensures inhibition of *de novo*-synthesised enzyme and therefore the activity of the enzyme remains at a constant low (Finberg & Rabey, 2016). Examples of reversible and irreversible MAO-B inhibitors will be discussed in the following paragraphs.

2.3.4 Irreversible inhibitors

(R)-Deprenyl:

The synthesis of (R)-deprenyl and similar compounds were first described by Knoll and co-workers in Hungary in 1965 (Knoll *et al.,* 1965). (R)-Deprenyl was established as a selective inhibitor of MAO-B. It was found that (R)-deprenyl does not induce the cheese reaction (Knoll & Magyar, 1972). (R)-Deprenyl was found to possess antiparkinsonian effects

(Birkmayer *et al*.,1975; Birkmayer *et al.,* 1977) which can be explained by the well-defined amphetamine-like catecholamine releasing effect. This effect describes (R)-deprenyl's ability to release catecholamines at extremely low concentrations (Yoneda *et al*., 2001). MAO-B is irreversibly inhibited by (R)-deprenyl as it forms a covalent bond at the N-5 position of the isoalloxazine moiety of the FAD cofactor (Maycock *et al*., 1976; Riederer *et al.,* 1982; Youdim, 1978). The action of (R)-deprenyl in PD thus also entails an increase in the availability of dopamine at central synapses and the consequential lengthening of DA activity (Fišar, 2016). (R)-Deprenyl is a propargyl-derivative of methamphetamine and is metabolised by cytochrome P-450 enzymes. Although (R)-deprenyl does not possess amphetamine-like properties, it is similar in structure to methamphetamine and is metabolised to major potentially toxic metabolites, L-amphetamine or L-methamphetamine. (Reynolds *et al.,* 1978; Fišar, 2016).

(R)-Deprenyl was tested as monotherapy and auxiliary treatment to levodopa (L-DOPA) in PD (DeMaagd & Philip, 2015). No effects with regards to the delay of the progression of the disease could be established but (R)-deprenyl appears to have a positive effect on motor fluctuations (Macleod *et al*., 2005). Other MAO-B inhibitors were developed because the prevention of MPTP-induced nigrostriatal dopaminergic neurodegeneration by (R)-deprenyl suggests that this compound may indeed possess neuroprotective properties. This suggestion, however, is not apparent in clinical trials (Fišar, 2016).

(R)-Deprenyl also possesses a significant antidepressant effect in treatment-resistant depression when administered at a high dosage of 30-60 mg daily. At a lower dosage of 10 mg daily, (R)-deprenyl is ineffective in treating depression (Mann *et al.,* 1989; Sunderland *et al.,* 1994). This indicates that (R)-deprenyl is only MAO-B selective at low dosages and non-selective towards MAO inhibition in higher dosages (Magyar, 2011). These positive results led to the development of the Selegiline Transdermal System (STS) which allowed a greater measure of the administered dose to penetrate the CNS. This gives drug tissue levels that result in non-selective MAO inhibition while inactivation of the gastro-intestinal and hepatic MAO enzymes is avoided (Mawhinney *et al*., 2003). STS was confirmed to be a success in humans seeing that it was indicated to be an effective antidepressant and does not cause the cheese effect in antidepressant dosages (Azzaro *et al*., 2006; Blob *et al*., 2007).

MAO inhibitors have also been proposed in the treatment of depression caused by cocaine addiction. The reasoning behind this is based on the fact that chronic administration of cocaine diminishes the activity of monoamine neurotransmitter systems, which is increased by the use of MAO inhibitors (Ho *et al.,* 2009). Dosages of (R)-deprenyl and pargyline that are adequate to inhibit both MAO enzymes have been evaluated in clinical trials, but only modest responses were recorded (Elkashef *et al.,* 2006).

A placebo-controlled study done on children suffering from ADHD indicated that (R)-deprenyl significantly improves attention but not impulsivity. In three other studies, (R)-deprenyl was compared to methylphenidate, the prescribed treatment for ADHD, and it was established that these two drugs are equally efficient (Akhondzadeh *et al.,* 2003; Niederhofer, 2003; Rubinstein *et al*., 2006; Mohammadi *et al*., 2004).

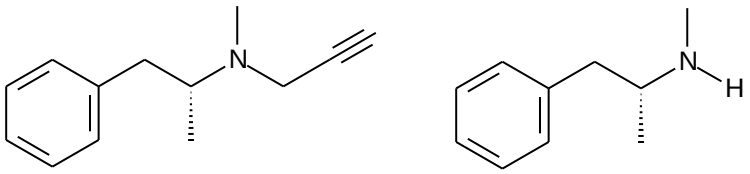

Figure 2.11 The structures of (R)-Deprenyl, on the left, and its main metabolite, L-methamphetamine, on the right.

Rasagiline:

Another highly potent propargylamine MAO-B selective inhibitor, rasagiline (N-propargyl-1-(*R*)-aminoindan), was introduced (Youdim *et al.,* 2001; Finberg & Youdim, 2002; Weinreb *et al.,* 2010). It does not exhibit significant pharmacological activity other than MAO inhibition, and is a more selective MAO inhibitor than (R)-deprenyl (Finberg & Youdim, 2002). These two compounds are relatively selective for MAO-B inhibition but only at high dosages, and therefore high concentrations, MAO-A inhibition may also occur. Rasagiline is used as monotherapy in patients with early and late PD, while it is used as auxiliary therapy to L-dopa in patients in the moderate to advanced stages of the disease (Oldfield *et al*., 2007; Youdim, 2003). Patients with early and advanced PD both described rasagiline to be effective in the treatment of motor as well as non-motor symptoms. It was also

recorded to have a placebo-like tolerability profile. Rasagiline is thus deemed effective in the treatment of all stages of PD (McCormack, 2014; Pistacchi *et al.,* 2013; Stocchi *et al*., 2015). A phase III clinical study, ADAGIO (Attenuation of Disease Progression with Azilect Given Once-daily), recently indicated that rasagiline is the first drug that could potentially slow the progression of PD (Olanow *et al*., 2008; 2009). Rasagiline was also established to be effective in the treatment of depression associated with PD at a dosage of 2 mg/day (the normal dose for PD treatment is 1 mg/day). The reason for the higher dosage is that a greater inhibitory effect on MAO-A is achieved (Korchounov *et al*., 2012). Rasagiline is also used to restore behavioural activity once lost. In a recent study, the drug was tested on aged animals and their learning ability together with their performance in the forced-swim test, were equal to those of young animals (Weinreb *et al.,* 2015).

It is important to note that, unlike (R)-deprenyl, rasagiline is not metabolised to yield a neurotoxic methamphetamine derivative. Rasagiline prevents mitochondrial permeability transition pores from opening and thus improves cell viability. Rasagiline and its metabolite, as well as other propargylamines, may therefore control apoptosis and have neuroprotective effects. It is also believed to regulate Bcl-2 family proteins and through the stabilisation of the permeability transition of the mitochondria, the functionality thereof is supported (Naoi *et al.,* 2003; Weinreb *et al.,* 2004). Another neuroprotective effect of rasagiline and propargylamines is linked to the regulation of the non-amyloidogenic conversion of the amyloid precursor protein (APP), present in Alzheimer's disease (Bar-Am *et al*., 2004a; Yogev-Falach *et al.,* 2002; 2003).

Neurorestorative activity is induced *in vivo* in the SNpc in the human midbrain, when rasagiline is administered in post-MPTP-induced parkinsonism. This is linked to the activation of the tyrosine kinase (TK) receptor as well as the stimulation of diverse transduction pathways related to cell signaling (Sagi *et al.,* 2007).

Rasagiline is predominantly metabolised by cytochrome P-450 isoenzyme 1A2 in the liver where it undergoes N-dealkylation to produce 1-(*R*)-aminoindan, a non-toxic compound (Chen & Swope, 2005; Chen *et al.,* 2007). Laboratory experiments indicate that 1-(*R*)-aminoindan is a weak reversible inhibitor of MAO and therefore not suitable as a substrate for MAO (Sterling *et al*., 1998; Binda *et al.,* 2005). It was recently revealed that 1-(*R*)-

aminoindan has neuroprotective effects. This suggests that it possibly contributes to the overall neuroprotective and anti-apoptotic effects of its mother compound, rasagiline (Bar-Am *et al*., 2004b; Bar-Am *et al*., 2007; 2010). When the administration of rasagiline is discontinued, the activity of MAO-B in platelets returns to baseline levels within two weeks after cessation. Enzyme activity in the brain, however, takes significantly longer to return to baseline levels (Thebault *et al.,* 2004).

Figure 2.12 The structures of rasagiline, on the left, and its main metabolite, 1-(*R*)-aminoindan, on the right.

2.3.5 Reversible MAO-B inhibitors

Safinamide:

Safinamide is a α-aminoamide derivative that possesses dopaminergic as well as non-dopaminergic/glutamatergic properties (Kulisevsky, 2016) and is the only new compound that has been approved to treat PD in the last decade. In the European Union, safinamide is approved to treat fluctuations in mid- to late-stage PD and is combined with a stable dose of L-DOPA or another antiparkinsonian medication. In a 24-week, placebo-controlled clinical trials, the administration of a fixed or flexible dose of safinamide remarkably increased daily 'on' time in patients who suffered from PD (in the mid- to late-stages) and experienced motor fluctuations. Other outcomes that were improved by safinamide administration include motor function and quality of life due to improved health as well as the overall clinical status of patients (Borgohain *et al*., 2014a; Schapira *et al*., 2016). Long-term safinamide administration sustained the treatment benefits of these other outcomes (Borgohain *et al.,* 2014b).

Safinamide's principal mechanism of action involves potent and highly selective, reversible inhibition of MAO-B, which results in increased DA levels in the brain (Rascol *et al*., 2015).

With the glutamatergic mechanism of action, voltage-gated sodium channels are blocked and N-type calcium channels are modulated, which led to the inhibition of glutamate release (Caccia *et al.,* 2006). In animal models, safinamide was established to possess neuroprotective (Caccia *et al.,* 2006; Podurgiel *et al.,* 2013; Sadeghian *et al.,* 2016), neurorescuing (Caccia *et al.,* 2006), tremorolytic (Podurgiel *et al.,* 2013) and anti-inflammatory (Sadeghian *et al.,* 2016) effects. Studies on parkinsonian monkeys also revealed a reduction in the duration and intensity of dyskinesia as a result of L-DOPA treatment, after safinamide administration (Gregoire *et al.,* 2013). Safinamide also does not result in the cheese effect when oral or intravenous tyramine is administered at therapeutic or supratherapeutic dosages (Cattaneo *et al.,* 2003; Di Stefano & Rusca*,* 2011; Marquet *et al*., 2012). It is therefore not necessary to restrict dietary tyramine following safinamide administration.

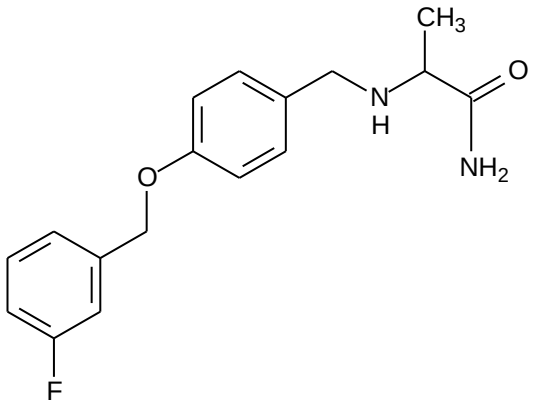

Figure 2.13 The structure of the reversible MAO-B inhibitor safinamide.

2.3.6 Three-dimensional structure of MAO-B

The three-dimensional structure of MAO was elucidated by the groups of Binda, de Colibus and Son by crystallising the enzymes and modelling the proteins and their active sites in a three-dimensional manner (Binda *et al.,* 2002, 2007; De Colibus *et al.,* 2005; Son *et al*., 2008). They proposed that human MAO-B consists of a long and narrow two-site cavity having entrance and active site cavities, respectively (De Colibus *et al.,* 2005). The active site in human MAO-B consists of FAD, situated at the back of the cavity, and tyrosines, Tyr-398 and Tyr-435, forming an aromatic cage with FAD for substrate recognition (Binda *et al.,* 2002). The human MAO-B enzyme is dimeric meaning it consists of two monomers that each has a globular domain and is anchored to the membrane by means of a C-terminal

transmembrane polypeptide segment (Mitoma & Ito, 1992). Each subunit of the homo-dimer contains one FAD that is covalently bound and linked to Cys-397 (Edmondson *et al*., 2009). The MAO enzyme, in an ATP-dependent process, is inserted in the membrane by means of ubiquitin (Zhuang *et al.,* 1988; 1992). The binding of an inhibitor to the enzyme does not lead to a noteworthy change in the conformation of the overall enzyme structure. As mentioned, the active site of MAO-B consists of two cavities, located relatively deep inside the protein. The highly hydrophobic substrate cavity, exhibits a volume of 390 A^3 and is situated in front of the flavin, whereas the similarly hydrophobic entrance cavity exhibits a volume of 290 A^3, is situated under the protein surface and is closed by a loop which consists of residues 99-112 (Binda *et al.,* 2007). A substrate has to cross this protein loop at the entrance cavity first before it can bind to the enzyme (Edmondson *et al.,* 2007b). The entrance cavity functions as the passageway for diffusion of the substrate into the catalytic site (Binda *et al.,* 2002). Furthermore, the Ile-199 side chain functions as a gate that opens and closes the space between the two cavities. The opened and closed conformation of the side chain depends on the substrate or bound inhibitor and is important in determining the enzyme's specificity for the inhibitor (Edmondson *et al*., 2007b; Hubálek, *et al*., 2005). In the case of a closed conformation, Ile-199 physically separates the cavities, whilst the presence of bulky ligands causes the residue to rotate into an open conformation and therefore allows the ligand to expand into the entrance cavity. The substrate cavity space has the shape of an ellipsoidal disk where Leu-171, Cys-172 and Tyr-398 are positioned on the one side and Ile-198, Ile-199 and Tyr-435 on the opposite side. The floor of the cavity is formed by the Tyr-188 side chain and the roof is made up of the aromatic residues Tyr-60, Tyr-326 and Phe-343 (Binda *et al.,* 2003). As mentioned, the FAD coenzyme is situated at the end of the substrate cavity and forms a covalent bond to Cys-397 in an 8α-thioether linkage (Kearney *et al*., 1971). The flavin ring exists in a distorted nonplanar conformation which is observed in all known MAO-B crystal structures (Binda *et al*., 2003).

Three distinct domains, with regards to functionality, can be distinguished in the following figure. The entrance cavity is located in the outer space and leads to the substrate binding cavity in the inner space. The substrate cavity is therefore closer to the flavin cofactor. The FAD molecule is presented as a magenta and safinamide as an orange ball-and-stick molecule. Figure 2.14 was adapted with permission from Binda *et al*., 2007.

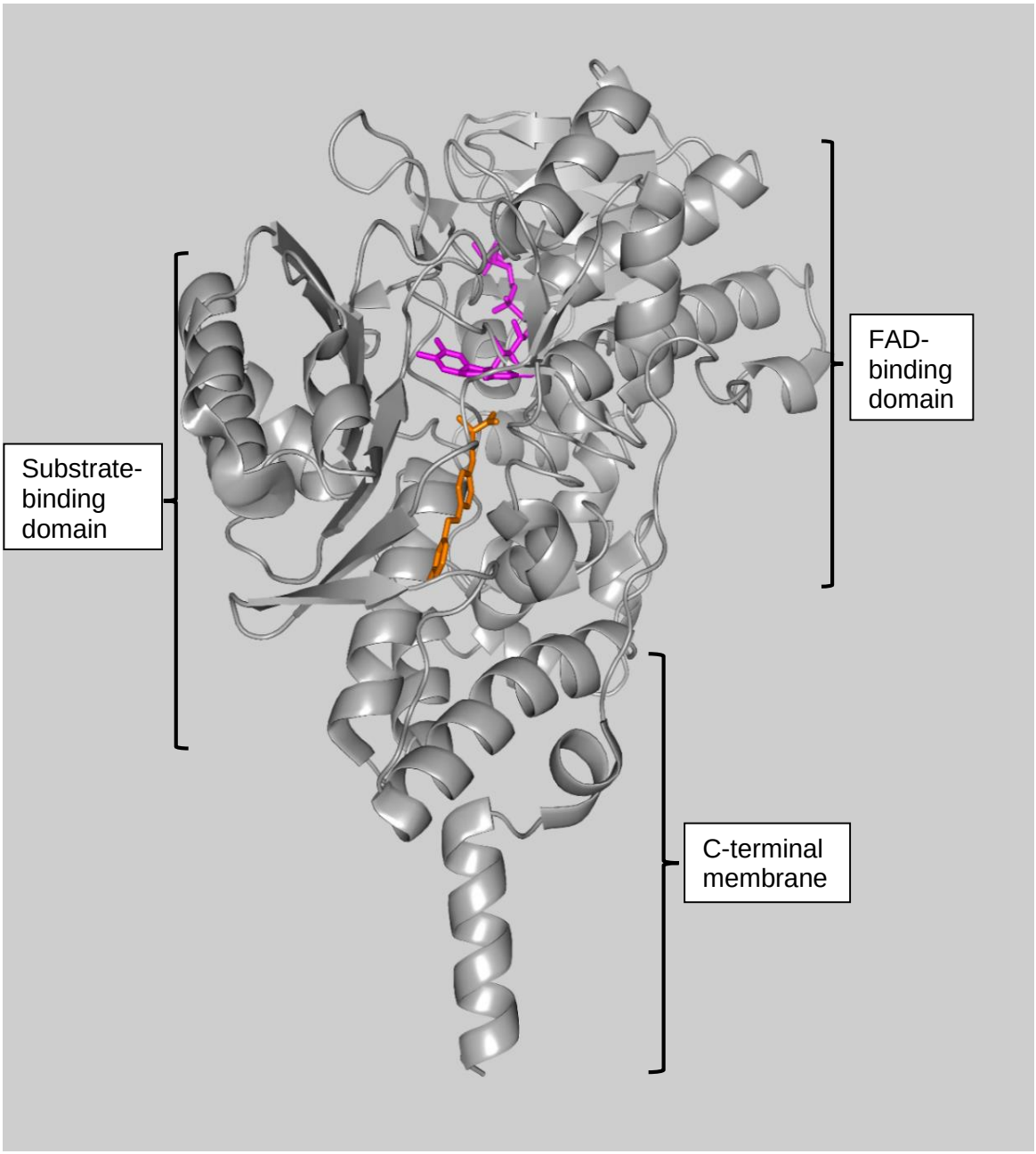

Figure 2.14 A cartoon representation of the crystal structure of human MAO-B.

2.4 *In vitro* measurements of MAO activity

The first heterologous expression of human MAO to be successful, was announced in 1990 when *Saccharomyces cerevisiae* was used as the host system for expression (Urban *et al.,* 1991). Further studies indicated that it is possible for *S. cerevisiae* to function as an adequate source of human MAO-A as its levels of expression is sufficient for the isolation of tens of milligrams of purified enzyme. This unfortunately does not hold true for large quantities of human MAO-B expression (Weyler *et al.,* 1990). A breakthrough came when it was established that it is possible to use the methylotrophic yeast, *Pichia pastoris*, for the heterologous expression of human MAO-B in large quantities (Newton-Vinson *et al.,* 2000). The same was later discovered for human MAO-A (Li *et al*., 2002). This expression system of MAO-A and MAO-B is reliable and convenient and also permits site-directed mutants to be produced which is of importance in structural and mechanistic investigations (Edmondson *et al.,* 2007b). Another discovery regarding the successful expression of the MAO-A and MAO-B enzymes in the baculovirus insect cell, was made. This system leads to the development of active enzymes situated on the outer membrane of the mitochondria (Rebrin *et al.,* 2001). Unfortunately, the reported specific activities of this system was established to be lower than those of the *Pichia pastoris* system (Edmondson *et al.,* 2007b). During the mid-1990s, however, bovine liver was most commonly used as a source of MAO-B, being the most convenient (Salach*,* 1979; Edmondson *et al.,* 2007b), whereas human placental mitochondria was the best available source of MAO-A (Weyler & Salach, 1985).

In recent years, human platelets became the most used biological markers to be used in MAO-B associated psychiatric disorders since it contains almost exclusively MAO-B (Bongioanni *et al*., 1997; Wirz-Justice, 1988). Platelet MAO-B and MAO-B in the human brain are similar seeing that their amino acid sequences are identical (Chen *et al*., 1993). A useful peripheral model to indirectly assess MAO-B activity in the brain, is therefore provided by the platelets. Numerous sources are available to measure platelet MAO-B activity, including whole blood (van Kempen *et al*., 1985), platelet homogenate (Donnelly & Murphy, 1977; Kruk *et al*., 1980), platelet rich plasma (McEntire *et al*., 1979) and the purified platelet mitochondrial fraction (Collins & Sandler, 1971). The screening of MAO-B inhibitors on platelet rich plasma and whole blood may however lead to faulty values, as MAO-B substrates generally are also substrates of plasma amine oxidases (Boomsma *et al.,* 2000). The measure of purity of the enzyme preparation is indirectly correlated to the risk of

incorrect results ascribed to contaminants and the higher the purity, the lower the risk of incorrect results. MAO-B is located on the outer membrane of the mitochondria and therefore provides an opportunity for an altered enzyme with a very low specific activity to be produced, if the micro-environment where the enzyme is inserted is not closely controlled. The preferred MAO-B isolation method is therefore simple separation of platelets from plasma. This avoids further purification and the opportunity for contamination or altering of the mitochondrial environment where MAO-B is attached (Novaroli *et al*., 2005).

In recent years it has become possible to produce large quantities of purified human MAO-B via expression systems. MAO-B is expressed from human MAO-B-cDNA by using different transferring vectors such as *Baculovirus* (Geha *et al*., 2001) and plasmids (Newton-Vinson, *et al*. 2000), and using a variety of expression systems such as *Pichia pastoris* (Newton-Vinson, *et al*. 2000). Until 2005, the depiction of the catalytic behaviour of recombinant MAO-B was generally carried out by comparing its kinetic constant values with those of MAO-B obtained from tissue preparations. The interaction of the recombinant MAO-B with different substrates was also commonly investigated for this purpose (Newton-Vinson, *et al*. 2000).

2.5 Copper-containing amine oxidases

2.5.1 General background and classification

According to Goding and Howard (1998) an increasing amount of enzymes are being acknowledged as proteins on the cell surface where they catalyse enzymatic reactions in the immediate vicinity, and by that monitor the concentration and functions of their often biologically active substrates and end-products. A class of ubiquitous enzymes, namely copper-containing amine oxidases (CuAOs) or semicarbazide-sensitive amine oxidase (SSAO), have been described. These enzymes catalyse the oxidation of primary amines to the corresponding aldehydes, with the reduction of molecular oxygen to hydrogen peroxide. This catalytic cycle releases ammonia in the process (Knowles & Dooley, 1994; Klinman & Mu, 1994; Wertz & Klinman, 2001).

SSAOs are present in various organs and organisms, from mammals to bacteria. In mammals it is present in, amongst other, the vascular smooth cells, adipocytes, placenta, kidney, liver, spleen and plasma, and are expressed tissue specific in different species (Boomsma *et al*., 2000). The SSAOs are present in two forms, one form being soluble and

found in the plasma and the other membrane-bound (Lyles *et al*., 1996). It is presumed that the soluble form emerges from the proteolytic cleavage of the membrane-bound enzyme (Stolen *et al.,* 2004) of which vascular adhesion protein-1 (VAP-1) is an example (Salminen *et al*., 1998; Smith *et al.*, 1998). The SSAOs contain a cofactor that appears to be topa-quinone (TPQ) in most cases (Klinman & Mu, 1994; Klinman, 1996; Lyles, 1996). TPQ is produced via a self-processing event that entails bound copper ion and molecular oxygen and involves an intrinsic tyrosine molecule as starting material (Mu *et al.,* 1992).

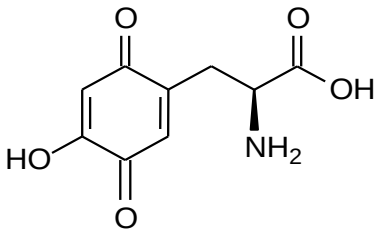

Figure 2.15 The structure of topa-quinone (TPQ).

2.6 Substrates and known inhibitors of CuAOs

α-Methyl substituted monoamines:

Primary aromatic monoamines which contain a methyl substituent on the α-carbon atom, which is attached to the amine group, are recognised inhibitors of SSAO activity and also present with MAO inhibition. Examples are mexiletine (an anti-arrhythmic drug) and amphetamine (a psychostimulant). Both drugs are competitive inhibitors of SSAO activity and possess a reversible mode of inhibition (Callingham, 1977; Garret *et al.*, 1976). MD 780236 is a selective MAO-B inhibitor, which is also able to inhibit SSAO activity in rat tissue (Kinemuchi *et al.,* 1986). Examples of MAO-A inhibitors which also inhibit SSAO activity are the dextro and levo forms of α-methylbenzylamine. The (+)-compound exhibits greater potency than the corresponding (-)-form, which indicates that optical isomerisation plays a role in inhibition of SSAO activity (Kinemuchi, *et al.,* 2004).

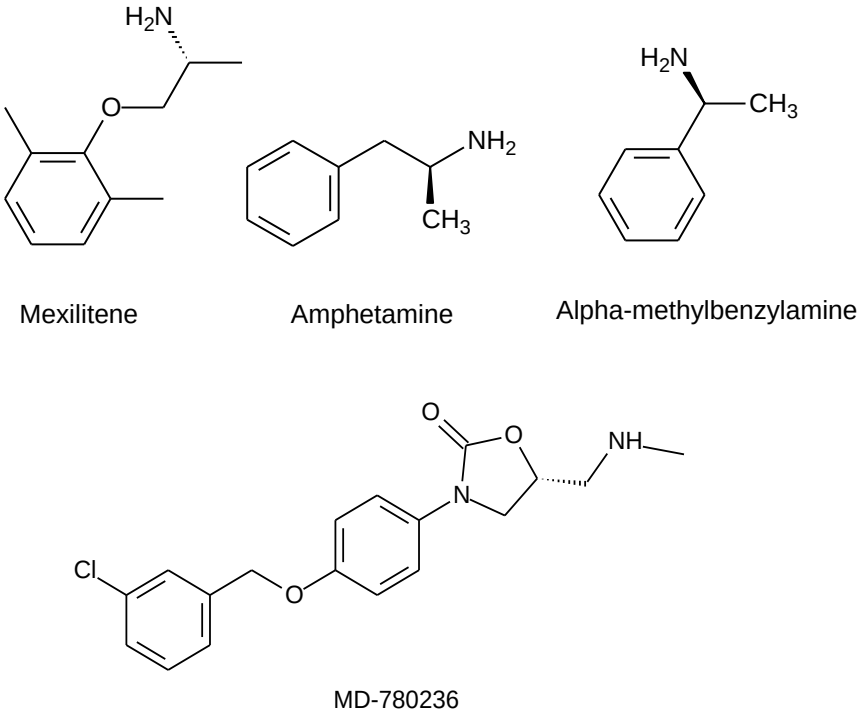

Figure 2.16 The structures of α-methyl substituted monoamines

Hydrazine derivatives:

Various carbonyl reagent compounds, specifically those that are hydrazine derivatives, are known to inhibit SSAO activity (Lyles, 1995; 1996; Andree & Clark, 1982). Semicarbazide is another example of a hydrazine derivative which is able to inhibit SSAO, hence the name SSAO. Semicarbazide is also useful in distinguishing between the SSAO and MAO enzymes in human tissue (Kinemuchi *et al.,* 1982). Other hydrazine derivatives have recently come into focus, some compounds being irreversible, non-selective MAO inhibitors, such as phenelzine, iproniazide (antidepressants), hydralazine (peripheral vasodilator), isoniazide (anti-tuberculant), benzerazide and carbidopa (PD drugs). It is speculated that these drugs inhibit SSAO activity through the formation of covalent bonds with the prosthetic group, TPQ, the enzyme's cofactor (Kinemuchi *et al.,* 2004).

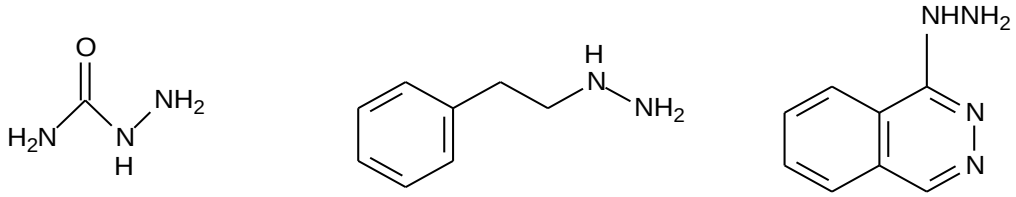

Semicarbazide Phenelzine Hydralazine

Figure 2.17 The structures of hydrazine derivatives

Allylamine derivatives:

Allylamine is an unsaturated aliphatic amine and a SSAO substrate. Its enzymatic product by SSAO, acrolein, is however toxic for the human cardiovascular system and the cytotoxic effects of this metabolite can be observed on cultured vascular smooth muscle cells (Boor *et al*., 1990; Hysmith *&* Boor, 1988). Studies have identified dual MAO-B and SSAO inhibitors (Lyles *et al*., 1987). Among these, MDL 72145 [(*E*)-2-(3',4'-dimethoxyphenyl)-3-fluoro allylamine] was established to be a selective, irreversible MAO-B inhibitor (Zreika *et al*., 1984) as well as an irreversible SSAO inhibitor (*in vivo* and *in vitro*) with equal potency against both enzymes (Lyles *et al*., 1987). The irreversibility of MDL 72145 is useful in determining the half-life and turnover rates of SSAO molecules (Fitzgerald *et al.,* 1998).

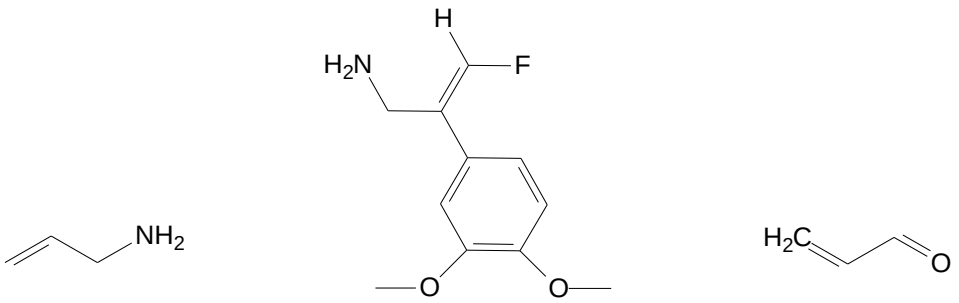

Allylamine MDL 72145 Acrolein

Figure 2.18 The structures of allylamine derivatives

Selective inhibitors of SSAO activity:

No notable membrane-bound SSAO inhibition can be observed by propargylamine inhibitors of MAO-A and MAO-B such as clorgyline, (R)-deprenyl and pargyline. It has, however, been established that propargylamine selectively inhibits SSAO activity at low

concentrations. Hydroxylamine is another example of a potent, selective SSAO inhibitor with little effect on MAO activity (Kinemuchi *et al.,* 2004).

Figure 2.19 The structures of selective inhibitors of SSAO activity, propargylamine (left) and hydroxylamine (right).

2.6.1 Biological function and mechanism of action of the SSAOs

SSAOs have a well-defined role in the metabolism of prokaryotes such as bacteria. The organism uses the proper amine as sources of carbon and nitrogen to support growth. The enzyme reduces toxic amines produced during exposure to stress conditions and is involved in the process of alkaloid biosynthesis. An interesting hypothesis was made that amine oxidase may also serve as a cytokinin oxidase (Hare & Van Staden, 1994). These enzymes are possibly involved in the catabolism of putrescine, spermine and spermidine and play important roles in a wide variety of processes such as tissue differentiation, cell proliferation, tumor growth and the transformation of cultured cells, programmed cell death, apoptosis, cell signaling and wound healing (McIntire & Hartmann, 1992). It is also suggested that SSAOs are key components in complicated processes such as the trafficking of leukocytes that involves VAP-1 (Salmi & Jalkanen, 2002).

Recent biochemical studies in different laboratories have led to proposals regarding the mechanism of action for the reactions catalysed by the SSAOs. The SSAOs catalyse three different reactions via a ping-pong mechanism: (i) the biogenesis of 2,4,5-trihydroxyphenylalanine quinone (TPQ), (ii) the reductive half-reaction and (iii) the oxidative half-reaction (Mure *et al.,* 2002; Dooley, 1999). The second step involves TPQ being reduced to an aminoquinol form and the amine substrate being oxidised to an aldehyde. The third step involves the re-oxidation of the organic cofactor at the expense of molecular

oxygen. It is ultimately reduced and produces hydrogen peroxide (Mure *et al.,* 2002).

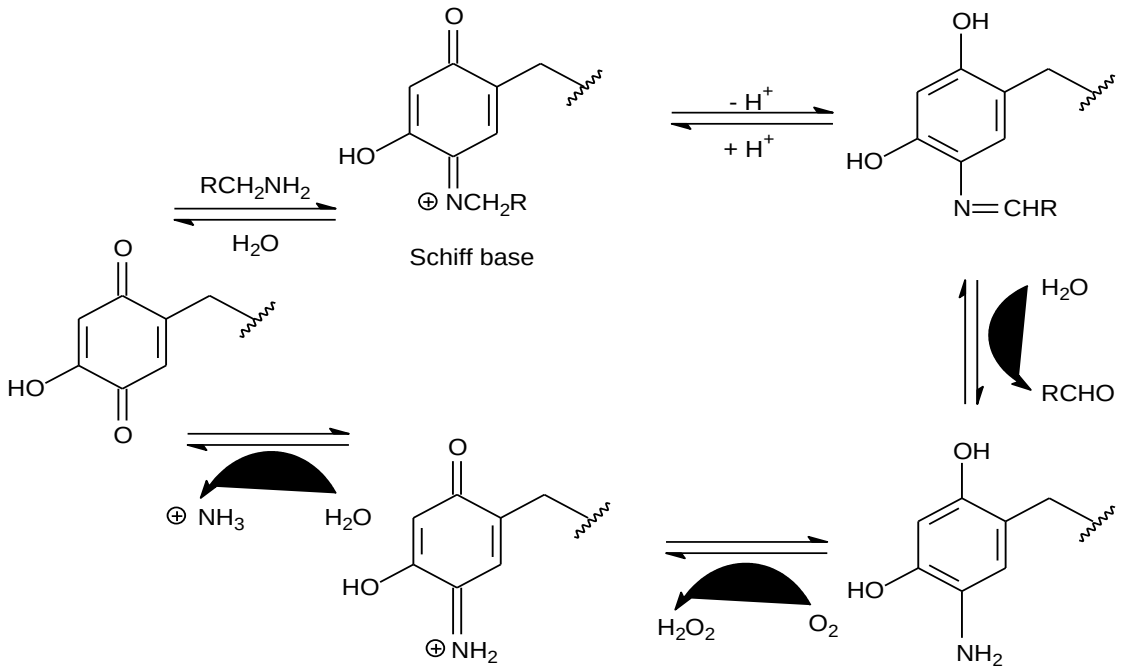

Figure 2.20 A proposed mechanism of action for the SSAOs, which exhibits the Schiff base formation.

2.6.2 The three-dimensional structure of SSAO

The molecular characterisation of the SSAOs started with the isolation of the enzymes based on its amine oxidase activity and physiochemical properties. These enzymes are mostly dimeric glycoproteins that contain two copper atoms per dimer (Klinman & Mu, 1994; Lyles, 1996; Klinman 1996).

Structure of amine oxidase retrieved from Bovine Serum:

Bovine serum amine oxidase (BSAO) was the first mammalian structure of a CuAO to be solved and was found to be rather conserved in comparison to other CuAO structures (Lunelli *et al.,* 2005).

The overall typology and secondary structure of the BSAO monomer consists of three domains, namely D2, D3 and D4. D2 (residues 57-161) is the smallest and consists of a four-stranded antiparallel β-helix connected to a α-helix and forming a N-terminal. Ten residues connect domain D2 to D3 (residues 171-282). The overall folding of D3 is similar to that of D2. D3 consists of a five-stranded antiparallel β-helix connected to a long bipartite

α-helix. Domains D3 and D4 are connected by residues 283-321. Domain D4 is located at the C-terminal and is the largest of the domains, consisting of about 400 residues. It contains the active site and is seen as the molecule's core. The structure of D4 is the most conserved and consists of two extended β-sheets, packed together as a β-sandwich, and a smaller sub-domain consisting of three β-strands and a helix-turn. The structure is completed by a few small loops and peripheral α-helices (Lunelli *et al*., 2005).

In the following figure, D2 to D4 represents the domains of the BSAO monomer. The beginning and end of the secondary structure's residues are numbered. The location of TPQ is indicated by an asterisk (*) and the His residues coordinating Cu(II), are indicated by X. Red arrows represent the two long arms that extend from domain D4 of one monomer and wrap around the other. The two β-sheets appear anti-parallel in the typology but are, in reality, heavily bent with the two arms extending in the same direction. The two large sheets respectively consist of nine and ten β-strands. Figure 2.21 was adapted from Lunelli *et al.* (2005).

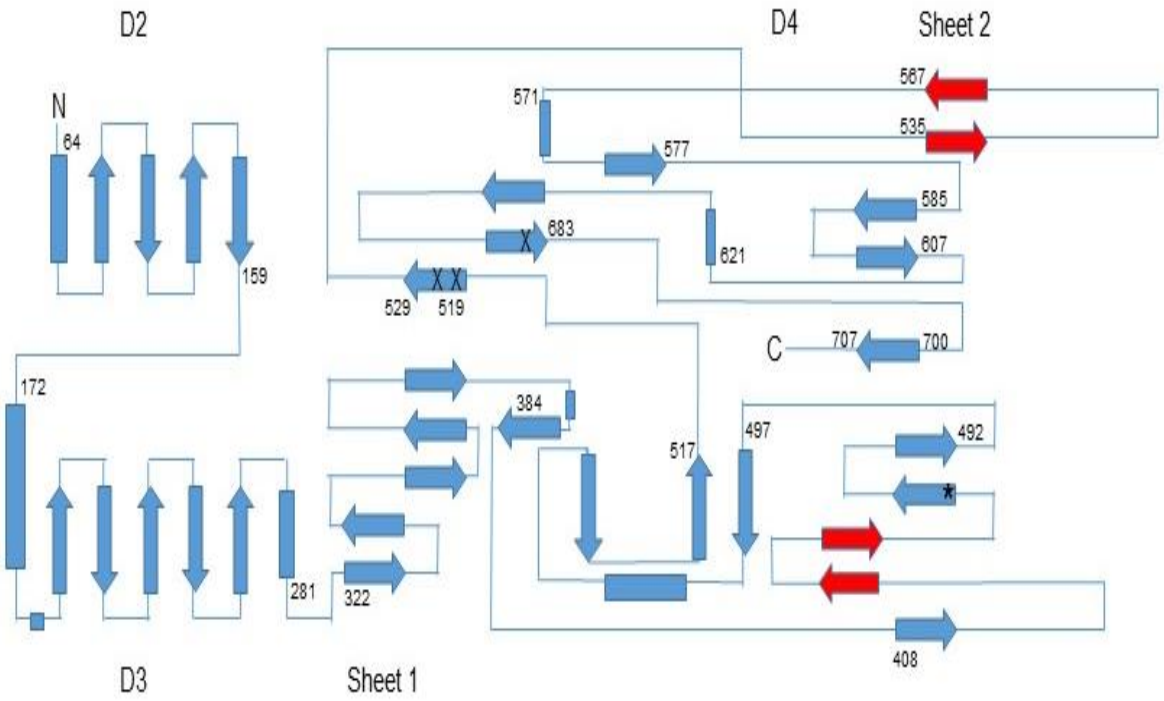

Figure 2.21 A representation of the overall topology of the BSAO monomer.

The quaternary organisation of BSAO resembles that of the already determined structures of other amine oxidases. It is a parallel-piped homodimer and consists of two monomers

linked by a large contact area, which is a product of the β-sandwich of domain D4. A 2-fold axis connects the two sandwiches and leads to the formation of a disk that represents the core of the structure. The two active sites as well as a large portion of the residues involved in the catalytic mechanism are situated in the disk. Domains D2 and D3 are situated opposite the 2-fold axis and have no interaction with the dimer. Between the monomers, a spacious internal cavity, which contains about twelve H_2O molecules to strengthen the interaction between the monomers, is situated symmetrically along the axis of the dimer. Three small channels linked to a wide external mouth along the 2-fold axis of the dimer, connect the internal cavity to the external solvent. The mouth is situated between residues Gly-579 and Arg-584 of the subunits. The central of the three channels is small and has hydrophobic walls lined by the side-chains of Val-607 and Phe-609. Residues Arg-584, Tyr-585, Arg-603 and Gln-605 of the one subunit forms a lateral side channel and residues Phe-609, Ala-620, Phe-681 and Leu-682 of the other subunit, forms the other lateral side channel. This enzyme has a reduced buried surface area in comparison with the other CuAOs and can be explained by the large external mouth as well as the monomer's unique shape (Lunelli *et al.,* 2005). The internal cavity connects with the copper site which is defined by residue His-683. It is therefore possible that this could serve as a pathway for the substrate, molecular oxygen and the reaction product, hydrogen peroxide, as has been suggested for other CuAOs (Li *et al.,* 1998).

The active site of the molecule is situated between the two sheets of the β-sandwich and consists of two well-defined components with unique functions, a Cu(II) ion as well as cofactor TPQ. Three histidine residues, His-519, His-521 and His-683, coordinate the Cu(II) ion, with two of them located on the same strand and the third near the terminal C-atom. Only one H_2O molecule, located between the Cu(II) ion and TPQ, forms a hydrogen bond with the ion. The inactive enzyme is switched to the active formation when the TPQ side-chain rotates around its X_1 torsion angle. This results in the cofactor facing away from the Cu(II) ion, a state which is termed "off copper". TPQ was found to be "off copper" in both subunits in its crystal form. It was also discovered that the most reactive carbonyl atom located at the quinone ring, is carbonyl 5. When the TPQ ring is in its productive orientation, carbonyl 5 is able to give access to the substrate by pointing to the base of the active site. A nucleophilic attack by the amine is then possible due to the abstraction of the hydrogen (Lunelli *et al.,* 2005).

In the following figure, the cyan sphere represents the copper ion. The ball-and-stick models represent TPQ (orange), aspartic acid as proton acceptor (green) and the three histidine residues which coordinate the Cu(II) ion (yellow). Figure 2.22 was adapted from Ernberg *et al*. (2010) with permission from IUCr. https://doi.org/10.1107/S1744309110041515

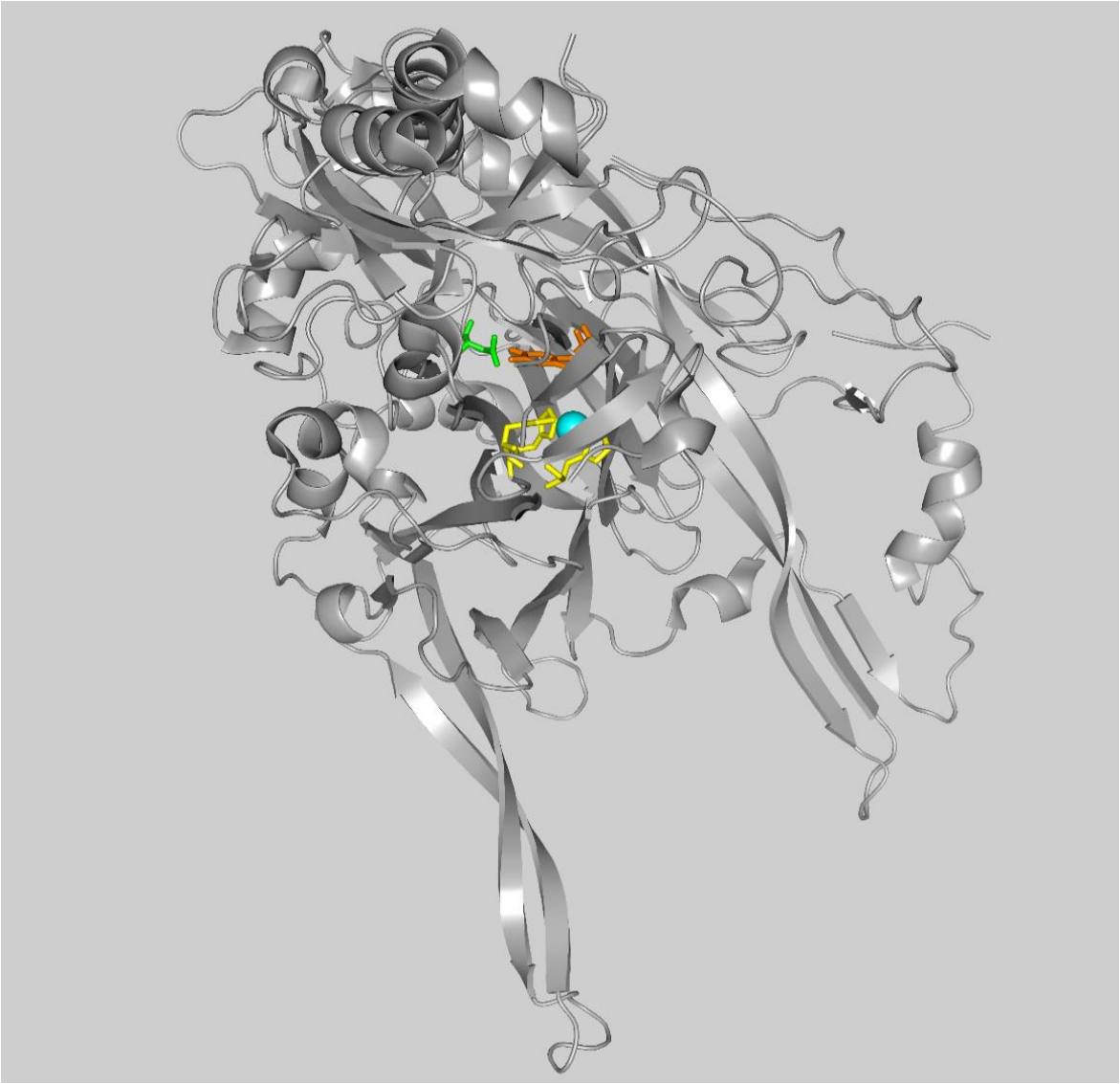

Figure 2.22 A cartoon representation of a monomer for the BSAO structure.

2.7 Conclusion

This chapter includes a brief background on the MAOs followed by a detailed discussion on both isoforms of the enzyme. The biological function of the MAOs, their potential role in PD and known MAO inhibitors were discussed. More detail on MAO-B was provided as the main aim of this study is to synthesise reversible 1-indanone derivatives as selective MAO-B inhibitors. A detailed discussion of the three-dimensional structures of MAO-A and MAO-B is also provided as this offers insight on the interactions between inhibitors and the MAO enzymes, which is important for future drug design. A discussion on the *in vitro* measurements of MAO activity was given as background to the enzymology section of this study (Chapter 4). This chapter also provides an overview of copper containing amine oxidases, especially those derived from bovine serum, as these enzymes are closely linked in function to the MAOs, and certain SSAO inhibitors also exhibit MAO inhibition.

CHAPTER 3: SYNTHESIS

3.1 Introduction

Recent discovery of the high potency MAO inhibition exhibited by α-tetralones (Legoabe *et al*., 2014), led to the search for structurally similar compounds which may also exhibit high potency MAO inhibition. 1-Indanones are the 5-membered ring analogues of α-tetralones. Based on structural similarity to α-tetralones, 1-indanones were postulated to act as a potential scaffold for the design of MAO inhibitors. A subsequent study therefore explored the MAO inhibition properties of a series of 1-indanone derivatives and found that, similar to α-tetralones, various substituted 1-indanones are good potency MAO inhibitors (Mostert *et al*., 2015).

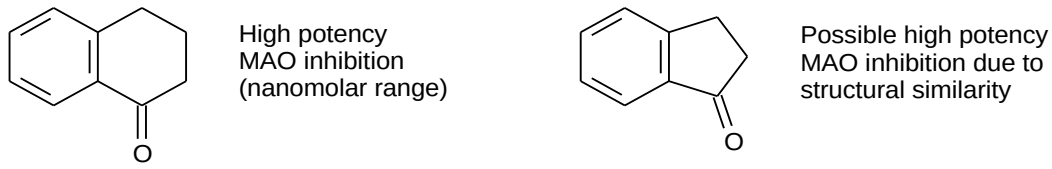

Figure 3.1 The structure of α-tetralone (left) compared to that of 1-indanone (right).

This study is a continuation of the published study and aims to compare the MAO inhibition properties of a small series of 1-indanones with their corresponding reduced alcohol derivatives. For the present study, the benzyloxy moiety was substituted on positions C4, C5 and C6 of 1-indanone. The selection of the benzyloxy moiety was based on the observation that this substituent leads to high potency MAO inhibition when substituted on either C6 or C7 of α-tetralone. Furthermore, the benzyloxy is present in various MAO-B inhibitors such as safinamide (Binda *et al.,* 2007). It is therefore expected that 1-indanones substituted on C6 with the benzyloxy moiety will yield highly potent inhibitors. In support of this, the previous study which investigated the MAO inhibition properties of 1-indanones found that that substitution on C6 and to a lesser extent C5, leads to selective, potent inhibition of MAO-B (Mostert *et al*., 2015). Legoabe and colleagues (2014) also reported that substituents containing a halogen atom lead to increased MAO-A and MAO-B inhibition

potencies compared to the unsubstituted homologues. For this reason the 3-chlorobenzyloxy and 4-chlorobenzyloxy moieties were also considered as substituents for the 1-indanones in the present study. As mentioned, all 1-indanone derivatives prepared in this study were reduced to the corresponding 1-indanol derivatives for comparison.

Hubálek and colleagues (2004) recently published a X-ray crystal structure of rasagiline bound to MAO-B which indicated that rasagiline binds in the enzyme's substrate cavity and leaves the entrance cavity vacant. This is noteworthy as rasagiline and the 1-indanone possess similar structures. Upon inspection of the complex between rasagiline and MAO-B, the observation can be made that substitution on C4 would yield compounds that occupy both cavities, where rasagiline will occupy the substrate cavity and the substituent will extend into the entrance cavity. It is expected that such a compound will display a high degree of selectivity towards MAO-B. The two cavities of MAO-B may fuse together after rotation of the Ile-199 side chain, which enables large inhibitors to bind to MAO-B. Contrary to this, Phe-208 (residue equivalent to Ile-199 in MAO-A) in MAO-A impedes the binding of large inhibitors to MAO-A. For this reason, a C4 substituted rasagiline analogue as well as substituted 1-indanones may likely exhibit poor binding to MAO-A and should thus act as highly selective MAO-B inhibitors without the possibility of causing the cheese reaction.

Table 3.1 The structures of the 1-indanone (**1a-h**) and 1-indanol (**1i-n**) derivatives that were synthesised in this study. The indanone derivatives are depicted in the shaded entries and the alcohol derivatives in the unshaded entries.

	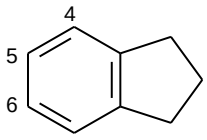	
Substituted at C4	Substituted at C5	Substituted at C6
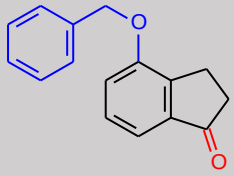 **1a**	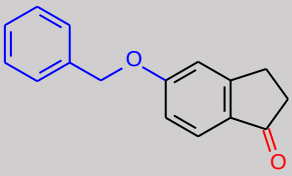 **1b**	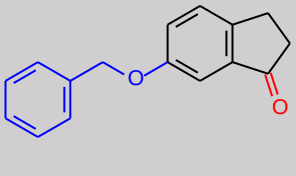 **1c**

	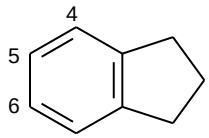	
Substituted at C4	Substituted at C5	Substituted at C6
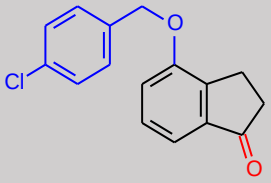 **1d**	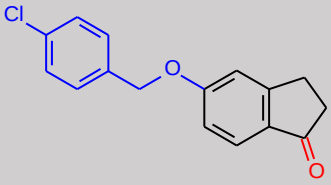 **1e**	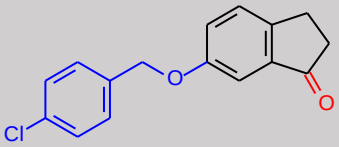 **1f**
		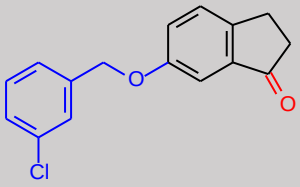 **1g**
	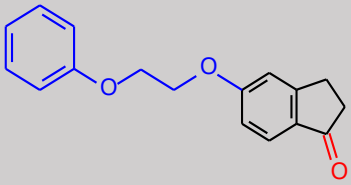 **1h**	
	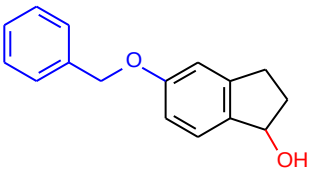 **1i**	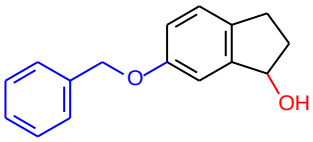 **1j**
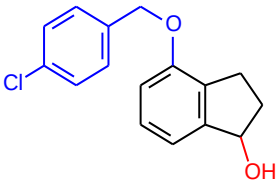 **1k**	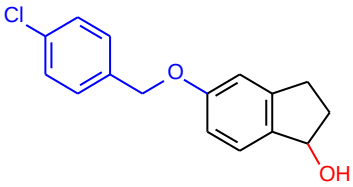 **1l**	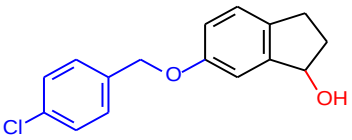 **1m**

	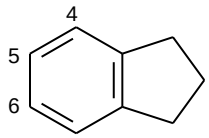	
Substituted at C4	Substituted at C5	Substituted at C6
		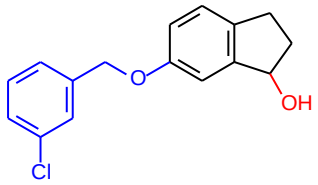 **1n**
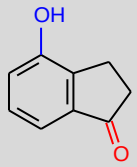 **2a**		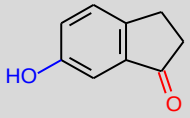 **2c**

3.2 Materials and instrumentation

Materials: All the solvents and reagents used in the synthesis were purchased from Sigma-Aldrich, and were used without further purification.

Thin-layer chromatography (TLC): TLC was used to establish if reactions proceeded to completion. Silica gel 60 (Merck) TLC sheets containing UV_{254} fluorescent indicator were used for TLC. The mobile phase consisted of ethyl acetate and petroleum ether in a ratio of 3:7. The developed TLC sheets were observed under a UV-lamp at a wavelength of 254 nm. The R_f values of the indanone derivatives were calculated and can be found in the results section of this chapter.

Melting Points: The melting points of the synthesised compounds were determined with a Buchi B-545 melting point apparatus. None of the melting points were corrected.

Mass Spectra: A Bruker micrOTOF-Q II mass spectrometer was used to record nominal mass spectra (MS) and high resolution mass spectra (HMRS). This was done in the atmospheric-pressure chemical ionisation (APCI) mode.

Nuclear magnetic resonance (NMR): A Bruker Avance III 600 spectrometer was used to record proton (^{1}H) and carbon (^{13}C) spectra. Proton spectra were recorded at a wavelength of 600 MHz and carbon spectra at 151 MHz. $CDCL_3$ was used as solvent for the NMR spectra of derivatives 1**a-h**, 1**i-n** and DMSO-$_{d6}$ for derivatives 2**a-c**. The signals of tetramethylsilane, which was added to the deuterated solvent, was used as reference and the chemical shifts of the synthesised compounds are reported in parts per million downfield from tetramethylsilane. Spin multiplicities are given as s (singlet), d (doublet), dd (doublet of doublets), t (triplet), qn (quintet) and m (multiplet). The coupling constants (J) of multiplets are given in Hertz (Hz).

High pressure liquid chromatography (HPLC):

HPLC was used to determine the purity of the synthesised indanone derivatives. An Agilent 1100 HPLC system equipped with a quaternary pump and diode array detector was used for the analyses. HPLC grade acetonitrile (purchased from Merck) and Milli-Q water (Millipore), were used to prepare the mobile phase for the chromatography. Separation was carried out with a Venusil XBP C18 column (4.60 x 150 mm, 5 µm) with acetonitrile and Milli-Q water serving as mobile phase in a ratio of 3:7. The flow rate was set to 1 ml/min. A solvent gradient program was initiated at the beginning of each run in which the percentage acetonitrile in the mobile phase was increased linearly to 80% over a 5 min period. Each run was completed within 15 min and an equilibration time of 5 min between runs was allowed. The synthesised compounds were prepared in concentrations of 1 mM and 100 µM in acetonitrile and injected at a volume of 20 µl into the HPLC system. The eluent was monitored at a wavelength of 254 nm.

3.3 General method for the synthesis of indanone derivatives

In the first step of the synthetic route, 4-, 5- and 6-hydroxy-1-indanone (**2a**-**c**) were synthesised by reacting the corresponding methoxy-1-indanone derivatives (**3a**-**c**) with anhydrous $AlCl_3$ (aluminium chloride). In the subsequent steps the hydroxy-1-indanones were alkylated with benzyl bromide, 3-chlorobenzyl bromide, 4-chlorobenzyl bromide or 2-phenoxyethoxy β-bromophenethole to yield the substituted 1-indanone derivatives (**1a**-**h**). The alcohol derivatives (**1i**-**n**) were synthesised by reduction of the 1-indanone derivatives with $NaBH_4$ (sodium borohydride).

3.3.1 Detailed synthesis of 4-, 5- and 6-hydroxy-1-indanone (2a-c)

Legoabe and colleagues described the synthesis of hydroxy-1-tetralones from the corresponding methoxy derivatives (Legoabe *et al.,* 2014). In this study, 4-, 5- and 6-hydroxy-1-indanone (**2a**-**c**) were synthesised according to this published protocol. The methoxy-1-indanone derivatives (**3a**-**c**) (10 mmol) were placed in a round bottom flask and $AlCl_3$ (25 mmol) and toluene (50 ml) were added. The reaction was heated to 140 ºC under reflux for 2 h. With time, the reaction underwent a colour change from bright yellow to dark yellow-brown. TLC was carried out to establish if the reaction has proceeded to completion. Upon completion the reaction mixture of each derivative was cooled on ice and added to distilled water (50 ml), also precooled on ice. The crude products were extracted with ethyl acetate (3 x 75 ml) and each organic phase was dried over anhydrous $MgSO_4$ (magnesium sulphate) at room temperature for 15 min. A clear and transparent light yellow solution was obtained after removal of the $MgSO_4$ by filtration. The organic phase of each derivative was removed under reduced pressure and the analytical pure samples were obtained after recrystallization from ethyl acetate.

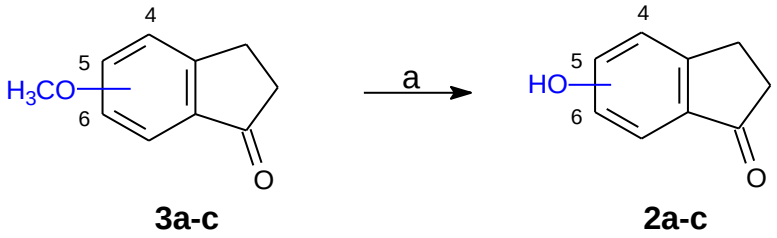

3a-c **2a-c**

Figure 3.2 The reaction pathway for the synthesis of 4-, 5- and 6-hydroxy-1-indanone.

Key: (a) $AlCl_3$, toluene, reflux, 2 h. Substitution: C4 = a; C5 = b; C6 = c.

3.3.2 Detailed synthesis of substituted indanone derivatives (1a-h)

4-, 5- or 6-Hydroxy-1-indanone (**2a**-**c**) (10 mmol), anhydrous K_2CO_3 (potassium carbonate; 20 mmol) and acetone (80 ml) were added to a round bottom flask. Using a glass syringe, the appropriate alkyl bromide (11 mmol) was added. The reaction mixture of each derivative was heated to 80 ºC under reflux for 20 h. The reaction colour changed from orange-brown to creamy white. TLC was carried out to establish if the reaction has proceeded to completion. Upon completion the reaction mixture of each derivative was allowed to cool to room temperature and the K_2CO_3 was removed by filtration. Acetone, the solvent in the

reaction mixture of each derivative, was removed under reduced pressure and the crude product of each derivative was recrystallized from cyclohexane to obtain analytical pure samples. The resulting products were the substituted 1-indanone derivatives (**1a**-**h**).

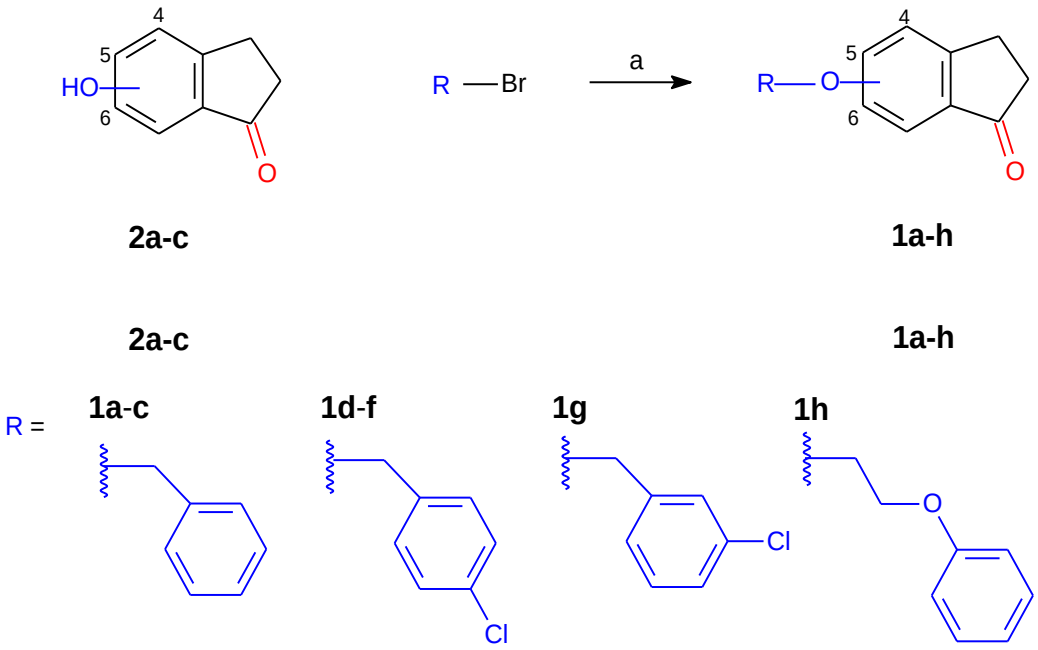

Figure 3.3 The reaction pathway for the synthesis of 4-, 5- and 6- substituted 1-indanone derivatives (**1a**-**h)**.

Key: (a) K_2CO_3, acetone, reflux, 20 h. Substitution: C4 = **1a**, **1d**; C5 = **1b**, **1e**, **1h**; C6 = **1c**, **1f**, **1g**.

3.3.3 Detailed synthesis of the alcohol derivatives (1i-n)

The 4-, 5- and 6-substituted indanone derivatives (**1a**-**h**) (10 mmol) were dissolved in 80 ml ethanol in a round bottom flask. The reaction mixture of each derivative was heated to 90 ºC and $NaBH_4$ (20 mmol) was added. The reaction mixture of each derivative was then heated under reflux for 18 h during which the colour changed from creamy white to colourless. TLC was carried out to establish if the reaction has proceeded to completion and the reaction was allowed time to cool to room temperature. The ethanol solvent was removed under reduced pressure and water (70 ml) was added to the crude residue of each derivative. The reaction mixture of each derivative was extracted with dichloromethane (3 x 50 ml) and the organic phase was subsequently dried over anhydrous $MgSO_4$ for 15 min.

The $MgSO_4$ was removed by filtration and the organic phase of each derivative evaporated under reduced pressure. The obtained crude product of each derivative was recrystallized from cyclohexane to yield the alcohol derivatives **1i**-**n**.

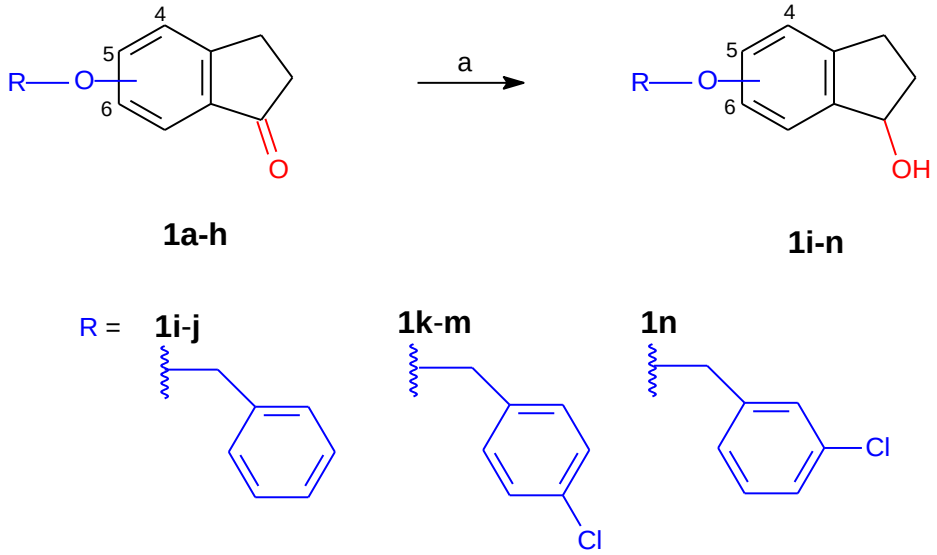

Figure 3.4 The reaction pathway for the synthesis of alcohol derivatives of 1-indanone, compounds (**1i**-**n**).

Key: (a) $NaBH_4$, ethanol, reflux, 18 h. Substitution: C4 = **1k**; C5 = **1i**, **1l**; C6 = **1j**, **1m**, **1n**.

3.4 Physical characterisation

The 1-indanone and 1-indanol derivatives that were synthesised in this study was characterized by ^{1}H NMR, ^{13}C NMR and HRMS, and the purities were estimated by HPLC analyses. Also provided in this section are the yields obtained for the final reactions, melting points and R_f values for the TLC. The obtained ^{1}H NMR and MS data of each compound correspond with the proposed structure although some of the ^{13}C NMR signals overlap. As an example, the NMR spectra of a selected 1-indanone and 1-indanol derivative will be discussed, thereafter the physical data will be presented in table format.

3.4.1 NMR analysis and data

*1-Indanone derivative **1b***: On the ^{13}C NMR spectra, 10 signals are observed in the aromatic region (165>δ>110 ppm) which corresponds to the 10 aromatic C atoms of this compound. The carbonyl carbon yields a signal at 205.30 ppm. In the aliphatic region (δ<70 ppm), 3

signals are observed, which corresponds to the three aliphatic carbons of this compound, including the benzylic CH_2. On the ^1H NMR spectrum, the aromatic protons (δ>6 ppm) integrate for 8 protons as expected for this compound. Unfortunately the multiplets for aromatic protons of the 1-indanone moiety are not clearly seen. The benzyloxy CH_2 was observed as a singlet at 5.06 ppm.The remaining aliphatic protons (4H) are represented by signals at 1.53-3.03 (4H in total).

1-Indanol derivative ***1i***: On the ^{13}C NMR spectra, 10 signals are observed in the aromatic region (δ>110 ppm) which corresponds to the 10 aromatic C atoms of this compound. In the aliphatic region (δ<76 ppm), 4 signals are observed, which corresponds to the four aliphatic carbons of this compound, including the secondary alcohol carbon. The absence of a signal for a carbonyl carbon indicates the successful reduction to the alcohol. On the ^1H NMR spectrum, the aromatic protons (δ>6 ppm) integrate for 8 protons as expected for this compound. Unfortunately the multiplets for aromatic protons of the 1-indanol moiety are not clearly seen. The benzyloxy CH_2 was observed as a singlet at 4.98 ppm, while the aliphatic proton at C1 of the ring corresponds to the triplet at 5.10 ppm (1H). The multiplicity of signal is the result of coupling with two protons on C2, which are not equivalent due to the chiral center at C1. The remaining aliphatic protons (4H) are represented by signals at 1.82-3.01 (4H in total). Since this compound is chiral and represents two enantiomers, the multiplicities of the aliphatic signals are rather complex, indicating non-equivalence of protons attached to the same carbons and complex splitting patterns.

4-Benzyloxy-1-indanone (**1a**)

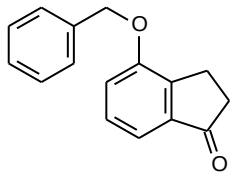	**Melting point:** 75.0 – 78.0 ºC **Purity:** 98.6% (1 mM); 99.1% (100 µM) **R_f:** 0.47 **Yield (final step):** 87.5%
^{1}H NMR:	**^{13}C NMR:**
^{1}H NMR (600 MHz, $CDCl_3$) δ 7.38 – 7.31 (m, 4H), 7.30 – 7.22 (m, 3H), 7.00 (d, *J* = 7.8 Hz, 1H), 5.09 (s, 2H), 3.06 – 2.98 (m, 2H), 2.67 – 2.53 (m, 2H).	^{13}C NMR (151 MHz, $CDCl_3$) δ 207.25, 156.23, 144.52, 138.80, 136.60, 128.83, 128.70, 128.15, 127.24, 116.28, 115.68, 70.08, 36.19, 22.71.
APCI-HRMS m/z calcd for $C_{16}H_{15}O_2$ (MH^+), found 239.1076, calcd. 239.1067	

5-Benzyloxy-1-indanone (**1b**)

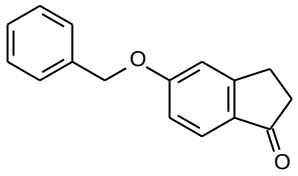	**Melting point:** 105.2 – 106.7 ºC **Purity:** 99.8% (1 mM); 99.6% (100 µM) **R_f:** 0.27 **Yield (final step):** 92.6%
^{1}H NMR:	**^{13}C NMR:**
^{1}H NMR (600 MHz, $CDCl_3$) δ 7.63 – 7.60 (m, 1H), 7.37 – 7.31 (m, 4H), 7.30 – 7.26 (m, 1H), 6.91 – 6.89 (m, 2H), 5.06 (s, 2H), 3.03 – 2.96 (m, 2H), 2.64 – 2.53 (m, 2H).	^{13}C NMR (151 MHz, $CDCl_3$) δ 205.30, 164.38, 158.14, 136.10, 130.66, 128.76, 128.32, 127.48, 125.43, 115.92, 110.82, 70.32, 36.47, 25.92.
APCI-HRMS m/z calcd for $C_{16}H_{15}O_2$ (MH^+), found 239.1081, calcd 239.1067	

6-Benzyloxy-1-indanone (**1c**)

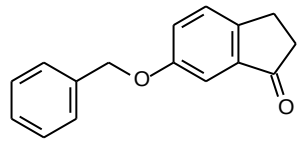	**Melting point:** 48.9 – 55.0 ºC **Purity:** 98.3% (1 mM); 98.1% (100 µM) **R_f:** 0.41 **Yield (final step):** 92.7%
^{1}H NMR:	**^{13}C NMR:**
^{1}H NMR (600 MHz, $CDCl_3$) δ 7.36 (d, *J* = 7.3 Hz, 2H), 7.34 – 7.29 (m, 1.3 Hz, 3H), 7.28 – 7.24 (m, 1H), 7.21 – 7.18 (m, 2H), 5.01 (s, 2H), 3.04 – 2.96 (m, 2H), 2.69 – 2.60 (m, 2H).	^{13}C NMR (151 MHz, $CDCl_3$) δ 207.00, 158.49, 148.25, 138.26, 136.45, 128.67, 128.16, 127.57, 127.50, 124.63, 106.15, 70.32, 37.03, 25.17.
APCI-HRMS m/z calcd for $C_{16}H_{15}O_2$ (MH^+), found 239.1089, calcd 239.1067	

4-(4-Chlorobenzyloxy)-1-indanone (**1d**)

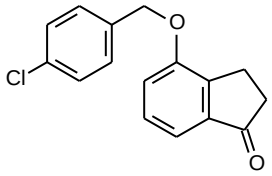	**Melting point:** 101.9 - 122.8 ºC **Purity:** 83.0% (1 mM); 83.0% (100 µM) **R_f:** 0.48 **Yield (final step):** 93.5%
^{1}H NMR:	**^{13}C NMR:**
^{1}H NMR (600 MHz, $CDCl_3$) δ 7.34 – 7.27 (m, 5H), 7.24 (t, *J* = 7.7 Hz, 1H), 6.99 (dd, *J* = 7.9, 0.9 Hz, 1H), 5.05 (s, 2H), 3.05 – 2.97 (m, 2H), 2.72 – 2.51 (m, 2H).	^{13}C NMR (151 MHz, $CDCl_3$) δ 207.13, 155.98, 144.41, 138.87, 135.06, 133.99, 128.90, 128.86, 128.58, 116.19, 115.90, 69.32, 36.16, 22.68.
APCI-HRMS m/z calcd for $C_{16}H_{14}ClO_2$ (MH^+), found 273.0682, calcd 273.0677	

5-(4-Chlorobenzyloxy)-1-indanone (**1e**)

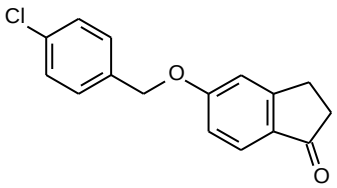	**Melting point:** 115.5-117.6 ºC **Purity:** 99.1% (1 mM); 99.5% (100 µM) **R_f:** 0.56 **Yield (final step):** 85.0%
^{1}H NMR:	**^{13}C NMR:**
^{1}H NMR (600 MHz, $CDCl_3$) δ 7.34 – 7.26 (m, 5H), 7.21 – 7.15 (m, 2H), 4.98 (s, 2H), 3.03 – 2.99 (m, 2H), 2.67 – 2.62 (m, 2H).	^{13}C NMR (151 MHz, $CDCl_3$) δ 206.91, 158.21, 148.41, 138.28, 134.95, 133.96, 128.85, 127.58, 124.56, 106.13, 69.50, 37.02, 25.17.
APCI-HRMS m/z calcd for $C_{16}H_{14}ClO_2$ (MH^+), found 273.0671, calcd 273.0677	

6-(4-Chlorobenzyloxy)-1-indanone (**1f**)

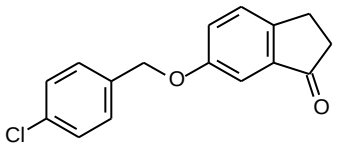	**Melting point:** 98.5 – 138.8 ºC **Purity:** 85.4% (1 mM); 84.4% (100 µM) **R_f:** 0.57 **Yield (final step):** 84.6%
^{1}H NMR:	**^{13}C NMR:**
^{1}H NMR (600 MHz, $CDCl_3$) δ 7.33 – 7.24 (m, 4H), 7.19-7.14 (m, 2H), 7.16 (s, 1H), 4.98 (s, 2H), 3.00 – 2.91 (m, 2H), 2.66 – 2.62 (m, 2H).	^{13}C NMR (151 MHz, $CDCl_3$) δ 206.91, 158.21, 148.41, 138.28, 134.96, 133.96, 128.84, 127.58, 124.55, 106.14, 69.57, 37.02, 25.17.
APCI-HRMS m/z calcd for $C_{16}H_{14}ClO_2$ (MH^+), found 273.0678, calcd 273.0677	

6-(3-Chlorobenzyloxy)-1-indanone (**1g**)

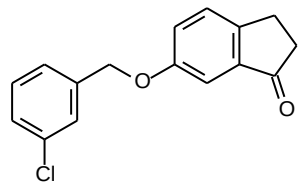	**Melting point:** 81.5 – 93.2 ºC **Purity:** 97.2% (1 mM); 81.3% (100 µM) **R_f:** 0.41 **Yield (final step):** 58.0%
^{1}H NMR:	**^{13}C NMR:**
^{1}H NMR (600 MHz, $CDCl_3$) δ 7.36 (s, 1H), 7.33 (dd, *J* = 8.3, 0.9 Hz, 1H), 7.27 – 7.21 (m, 3H), 7.19 (dd, *J* = 7.4, 2.5, 1H), 7.17 (d, *J* = 2.6 Hz, 1H), 4.99 (s, 2H), 3.06 – 2.97 (m, 2H), 2.68 – 2.61 (m, 2H).	^{13}C NMR (151 MHz, $CDCl_3$) δ 206.91, 158.17, 148.48, 138.52, 138.29, 134.61, 129.94, 128.27, 127.62, 127.45, 125.41, 124.55, 106.09, 69.41, 37.02, 25.18.
APCI-HRMS m/z calcd for $C_{16}H_{14}ClO_2$ (MH^+), found 273.0689, calcd 273.0677	

5-(2-Phenoxyethoxy)-1-indanone (**1h**)

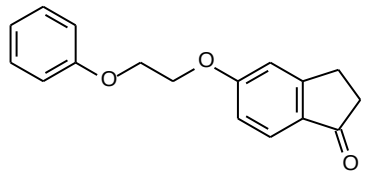	**Melting point:** 135.0 – 137.4 ºC **Purity:** 99.6% (1mM); 99.5% (100 µM) **R_f:** 0.66 **Yield (final step):** 65.0%
^{1}H NMR:	**^{13}C NMR:**
^{1}H NMR (600 MHz, $CDCl_3$) δ 7.63 (d, 9.2 Hz, 1H), 7.24 (t, *J* = 8.0 Hz, 2H), 6.95 – 6.85 (m, 5H), 4.35 – 4.31 (m, 2H), 4.31 – 4.27 (m, 2H), 3.11 – 2.92 (m, 2H), 2.71 – 2.48 (m, 2H).	^{13}C NMR (151 MHz, $CDCl_3$) δ 205.29, 164.28, 158.47, 158.10, 130.77, 129.59, 125.44, 121.32, 115.70, 114.69, 110.61, 66.91, 66.20, 36.47, 25.91.
APCI-HRMS m/z calcd for $C_{17}H_{17}O_3$ (MH^+), found 269.1177, calcd269.1172	

5-Benzyloxy-1-indanol (**1i**)

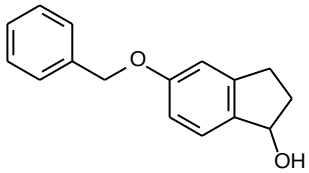	**Melting point:** 82.2 – 90.1 ºC **Purity:** 98.6% (1 mM); 97.5% (100 µM) **R_f:** 0.34 **Yield (final step):** 92.2%
^{1}H NMR:	**^{13}C NMR:**
^{1}H NMR (600 MHz, $CDCl_3$) δ 7.36 – 7.33 (d, *J* = 7.1 Hz, 2H), 7.31 (t, *J* = 7.1 Hz, 2H), 7.27 – 7.21 (m, 2H), 6.83 – 6.71 (m, 2H), 5.10 (t, *J* = 6.9 Hz, 1H), 4.98 (s, 2H), 3.01 – 2.90 (m, 5.4 Hz, 1H), 2.76 – 2.64 (m, 1H), 2.45 – 2.31 (m, 1H), 1.92 – 1.82 (m, 1H).	^{13}C NMR (151 MHz, $CDCl_3$) δ 159.46, 145.31, 137.66, 137.09, 128.61, 127.96, 127.44, 125.11, 113.87, 110.89, 75.89, 70.17, 36.29, 30.02.
APCI-HRMS m/z calcd for $C_{16}H_{16}O_2$ (M^+), found 240.1156, calcd 240.1150	

6-Benzyloxy-1-indanol (**1j**)

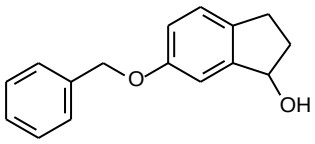	**Melting point:** 74.3 – 83.7 ºC **Purity:** 98.9% (1 mM); 98.2% (100 µM) **R_f:** 0.21 **Yield (final step):** 83.3%
^{1}H NMR:	**^{13}C NMR:**
^{1}H NMR (600 MHz, $CDCl_3$) δ 7.35 (d, *J* = 7.3 Hz, 2H), 7.30 (t, *J* = 7.3 Hz, 2H), 7.27 – 7.15 (m, 1H), 7.06 (d, *J* = 8.2 Hz, 1H), 6.95 (d, *J* = 2.2 Hz, 1H), 6.82 (dd, *J* = 8.2, 2.4 Hz, 1H), 5.10 (s, 1H), 4.98 (s, 2H), 2.93 – 2.84 (m, 1H), 2.73 – 2.59 (m, 1H), 2.46 – 2.36 (m, 1H), 1.90 – 1.80 (m, 1H).	^{13}C NMR (151 MHz, $CDCl_3$) δ 158.28, 146.42, 137.19, 135.45, 128.59, 127.93, 127.48, 125.57, 115.91, 110.00, 76.64, 70.32, 36.59, 29.00.
APCI-HRMS m/z calcd for $C_{16}H_{16}O_2$ (M^+), found 240.1153, calcd 240.1150	

4-(4-Chlorobenzyloxy)-1-indanol (**1k**)

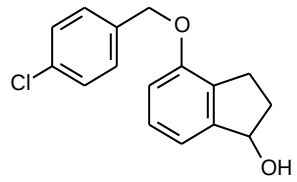	**Melting point:** 120.7 – 122.6 ºC **Purity:** 98.3% (1 mM); 96.9% (100 µM) **R_f:** 0.34 **Yield (final step):** 84.2%
^{1}H NMR:	**^{13}C NMR:**
^{1}H NMR (600 MHz, $CDCl_3$) δ 7.31 – 7.25 (m, 4H), 7.13 (t, *J* = 7.8 Hz, 1H), 6.99 (d, *J* = 7.5 Hz, 1H), 6.72 (d, *J* = 8.1 Hz, 1H), 5.27 – 7.17 (m, 1H), 4.99 (s, 2H), 3.03 – 2.95 (m, 1H), 2.76 – 2.67 (m, 1H), 2.47 – 2.38 (m, 1H), 1.93 – 1.84 (m, 1H).	^{13}C NMR (151 MHz, $CDCl_3$) δ 155.00, 147.14, 135.75, 133.65, 131.65, 128.76, 128.50, 128.39, 116.89, 111.14, 69.11, 35.65, 26.63.
APCI-HRMS m/z calcd for $C_{16}H_{15}ClO_2$ (M^+), found 274.0766, calcd 274.0755	

5-(4-Chlorobenzyloxy)-1-indanol (**1l**)

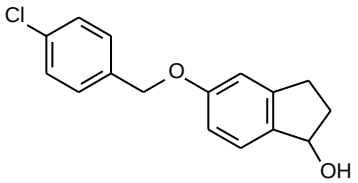	**Melting point:** 130.3 – 132.8 ºC **Purity:** 99.8% (1 mM); 98.4% (100 µM) **R_f:** 0.25 **Yield (final step):** 73.6%
^{1}H NMR:	**^{13}C NMR:**
^{1}H NMR (600 MHz, $CDCl_3$) δ 7.32 – 7.16 (m, 5H), 6.78 – 6.72 (m, 2H), 5.11 (s, 1H), 4.95 (s, 2H), 3.00 – 2.91 (m, 1H), 2.74 – 2.65 (m, 1H), 2.45 – 2.34 (m, 1H), 1.94 – 1.83 (m, 1H).	^{13}C NMR (151 MHz, $CDCl_3$) δ 159.19, 145.38, 137.87, 135.60, 133.73, 128.78, 128.73, 125.17, 113.85, 110.92, 75.89, 69.40, 36.32, 30.04.
APCI-HRMS m/z calcd for $C_{16}H_{15}ClO_2$ (M^+), found 274.0759, calcd 274.0755	

6-(4-Chlorobenzyloxy)-1-indanol (**1m**)

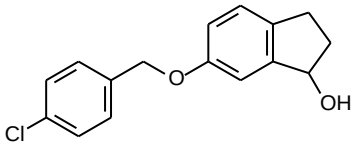	**Melting point:** 109.9 – 114.2 ºC **Purity:** 99.2% (1 mM); 97.7% (100 µM) **R_f:** 0.33 **Yield (final step):** 40.0%
^{1}H NMR:	**^{13}C NMR:**
^{1}H NMR (600 MHz, $CDCl_3$) δ 7.30 – 7.24 (m, 4H), 7.07 (d, *J* = 8.2 Hz, 1H), 6.93 (d, *J* = 2.0 Hz, 1H), 6.79 (dd, *J* = 8.2, 2.3 Hz, 1H), 5.08 (s, 1H), 4.94 (s, 2H), 2.95 – 2.84 (m, 1H), 2.73 – 2.58 (m, 1H), 2.48 – 2.38 (m, 1H), 1.91 – 1.79 (m, 1H).	^{13}C NMR (151 MHz, $CDCl_3$) δ 157.97, 146.46, 135.67, 135.66, 133.70, 128.77, 125.63, 115.85, 109.97, 76.62, 69.50, 36.61, 29.00.
APCI-HRMS m/z calcd for $C_{16}H_{15}ClO_2$ (M^+), found 274.0760, calcd 274.0755	

6-(3-Chlorobenzyloxy)-1-indanol (**1n**)

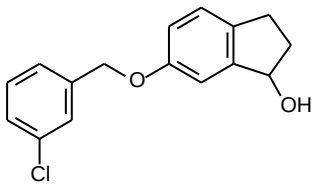	**Melting point:** None - oil **Purity:** 97.3% (1 mM); 97.1% (100 µM) **R_f:** 0.44 **Yield (final step):** 68.9%
^{1}H NMR:	**^{13}C NMR:**
^{1}H NMR (600 MHz, $CDCl_3$) δ 7.30 – 7.17 (m, 5H), 6.76 (d, *J* = 6.3 Hz, 2H), 5.11 (s, 1H), 4.95 (s, 2H), 3.00 – 2.91 (m, 1H), 2.74 – 2.65 (m, 1H), 2.45 – 2.34 (m, 1H), 1.94 – 1.83 (m, 1H).	^{13}C NMR (151 MHz, $CDCl_3$) δ 157.93, 146.48, 139.26, 135.73, 134.52, 129.87, 128.05, 127.41, 125.66, 125.35, 115.84, 109.96, 69.45, 36.58, 29.01.
APCI-HRMS m/z calcd for $C_{16}H_{15}ClO_2$ (M^+), found 274.0766, calcd 274.0761	

4-Hydroxy-1-indanone (**2a**)

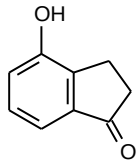	**Melting point:** 244.8 – 247.3 ºC **Purity:** 98.0% (1 mM); 97.0% (100 µM) **R_f:** 0.16 **Yield (final step):** 47.3%
^{1}H NMR:	**^{13}C NMR:**
^{1}H NMR (600 MHz, DMSO-d6) δ 9.75 (s, 1H), 7.05 (t, J = 7.7 Hz, 1H), 6.89 (d, J = 7.5 Hz, 1H), 6.85 (dd, J = 7.8, 1.0 Hz, 1H), 2.78 – 2.69 (m, 2H), 2.45 – 2.36 (m, 2H).	^{13}C NMR (151 MHz, DMSO-$_{d6}$) δ 155.60, 142.31, 138.88, 129.08, 120.23, 113.79, 36.25, 22.76.
APCI-HRMS m/z calcd for $C_9H_9O_2$ (MH^+), found 149.0593, calcd 149.0597	

6-Hydroxy-1-indanone (**2c**)

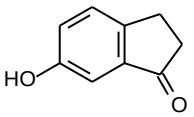	**Melting point:** 101.1 – 102.7 **º**C **Purity:** 99.6% (1 mM); 98.6% (100 µM) **R_f:** 0.25 **Yield (final step):** 51.2%
^{1}H NMR:	**^{13}C NMR:**
^{1}H NMR (600 MHz, DMSO-d_6) δ 10.48 (s, 1H), 7.48 (d, *J* = 8.3 Hz, 1H), 6.85 (d, *J* = 2.1 Hz, 1H), 6.80 (dd, *J* = 8.4, 2.1 Hz, 1H), 3.03 – 2.95 (m, 2H), 2.57 – 2.51 (m, 2H).	^{13}C NMR (151 MHz, DMSO-$_{d6}$) δ 204.48, 164.10, 158.73, 129.08, 125.36, 116.20, 112.52, 36.39, 25.65.
APCI-HRMS m/z calcd for $C_9H_9O_2$ (MH^+), found 149.0605, calcd 149.0597	

3.4.2 TLC

During this study, thin-layer chromatography was used to establish if reactions have proceeded to completion. The mobile phase that was used for this purpose was petroleum ether and ethyl acetate in a ratio of 7:3. The R_f (retention factor) value can be used to indicate the position of a spot of a compound on a TLC sheet. Equation 3.1 was used to calculate the R_f value of each synthesised indanone derivative.

$$Rf = \frac{Distance\ travelled\ by\ analyte\ on\ TLC\ plate}{Distance\ travelled\ by\ solvent\ on\ TLC\ plate}$$

3.1. The equation for the calculation of R_f values.

Table 3.2 The calculated R_f values of the 1-indanone (**1a-h**), 1-indanol (**1i-n**) and hydroxyl-1-indanone (**2a, c**) derivatives.

Compound	**R_f values**	**Compound**	**R_f values**
1a	0.47	**1i**	0.34
1b	0.27	**1j**	0.21
1c	0.41	**1k**	0.34
1d	0.48	**1l**	0.25
1e	0.56	**1m**	0.33
1f	0.57	**1n**	0.44
1g	0.41	**2a**	0.16
1h	0.66	**2c**	0.25

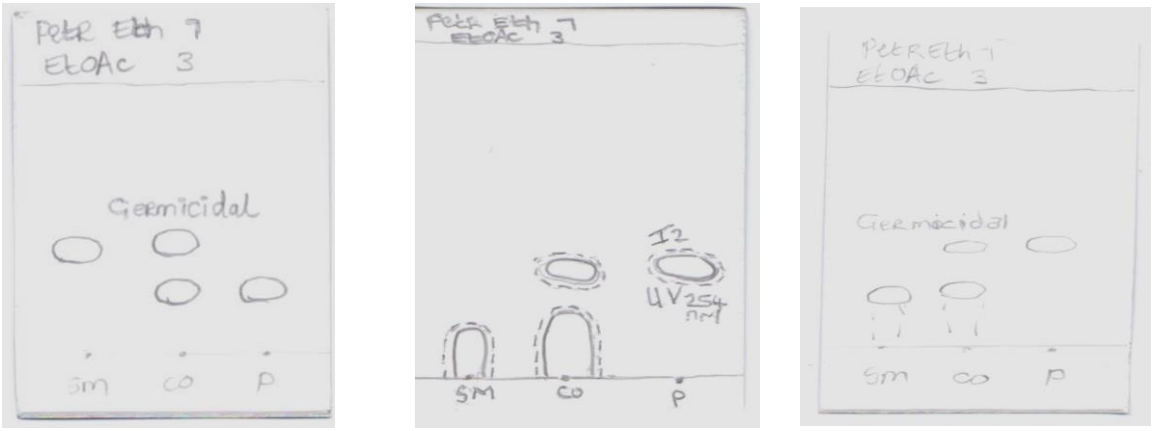

Figure 3.5 Examples of TLC sheets obtained in this study.

On the left is shown an image of a TLC sheet obtained in the first step of synthesis, the preparation of 4-hydroxy-1-tetralone (**2a**). In the centre, a TLC sheet of the second step of synthesis, the preparation of 5-benzyloxy-1-indanone (**1b**) is shown, and on the right, a TLC sheet of the third, and last, step of synthesis is shown, the preparation of 5-benzyloxy-1-indanol (**1i**). The observation can be made that the reactions were complete in each instance as no starting material was present where only the product was spotted. Petroleum ether and ethyl acetate was used as mobile phase in a 7:3 ratio. Key: (sm) = starting material; (co) = starting material + product; (p) = product.

3.4.3 Mass spectrometry

High resolution mass spectrometry was used to characterise the indanone derivatives. Protonated molecular ion (MH^+) was used to ionize the indanone compounds **1a**-**h** and **2a**,**c** as the ketone functional group of these compounds is able to receive a H+ through the breaking of the double bond. Molecular ion (M^+) was used for the ionization of the indanol derivatives (**1i-n**) as these compounds possess an alcohol functional group (-OH). It is impossible for the indanol derivatives (**1i-n**) to also be ionized by MH^+ as it is not possible for H^+ to bind to the alcohol functional group. The estimated and experimentally determined molecular weights of the derivatives are given in table 3.3. The difference between the calculated and experimentally determined molecular weights are expressed in parts per million (ppm) and were calculated according to equation 3.2. A ppm difference of <5 is regarded as acceptable and indicates that the calculated and experimental masses are in agreement. As shown in table 3.3, the results of the mass spectral analysis of this study indicated that the calculated and experimentally determined molecular weights

corresponded well and thus provides evidence that the structures of the synthesised compounds are those depicted in table 3.1.

$$ppm = \frac{[Experimentally\ determined\ mw\ -\ Calculated\ mw]}{[Calculated\ mw]} \times 10^6$$

Equation 3.2. The equation for the calculation of the difference between the calculated and experimentally determined molecular weights. This difference is expressed in parts per million (ppm)

Table 3.3 The calculated and experimentally determined molecular weights of the 1-indanone (**1a-h**), 1-indanol (**1i-n**) and hydroxy-1-indanone (**2a, c**) derivatives.

	Experimental (found)	**Calculated**	**Chemical formula**	**ppm**
1a	239.1076	239.1067	$C_{16}H_{15}O_2$ (MH^+)	3.76
1b	239.1081	239.1067	$C_{16}H_{15}O_2$(MH^+)	5.86
1c	239.1089	239.1067	$C_{16}H_{15}O_2$(MH^+)	9.20
1d	273.0682	273.0677	$C_{16}H_{14}ClO_2$(MH^+)	1.83
1e	273.0671	273.0677	$C_{16}H_{14}ClO_2$(MH^+)	-2.19
1f	273.0678	273.0677	$C_{16}H_{14}ClO_2$(MH^+)	0.37
1g	273.0689	273.0677	$C_{16}H_{14}ClO_2$(MH^+)	4.39
1h	269.1177	269.1172	$C_{17}H_{17}O_3$(MH^+)	1.86
1i	240.1156	240.1150	$C_{16}H_{16}O_2$ (M^+)	4.58
1j	240.1153	240.1150	$C_{16}H_{16}O_2$(M^+)	3.33

	Experimental (found)	**Calculated**	**Chemical formula**	**ppm**
1k	274.0766	274.0755	$C_{16}H_{15}ClO_2(M^+)$	4.01
1l	274.0759	274.0755	$C_{16}H_{15}ClO_2(M^+)$	2.19
1m	274.0760	274.0755	$C_{16}H_{15}ClO_2(M^+)$	1.82
1n	274.0766	274.0761	$C_{16}H_{15}ClO_2(M^+)$	4.01
2a	149.0593	149.0597	$C_9H_9O_2(M^+)$	-2.68
2c	149.0605	149.0597	$C_9H_9O_2(M^+)$	5.37

3.4.4 Purity estimation by HPLC

HPLC analyses were used to determine the purity of the indanone derivatives. The indanone derivatives were dissolved in acetonitrile at concentrations of 1 mM and 100 µM, and were subsequently injected into the HPLC system. The eluent was monitored at a wavelength of 254 nm. The results obtained from these analyses are tabulated in table 3.4. A purity of >95% for the synthesised compounds is considered adequate for further biological evaluation. The results indicated a high degree of purity and a low percentage of impurities for most of the synthesised compounds, which indicate that these compounds may be evaluated as potential inhibitors of the MAO enzymes. Compounds **1d**, **1f** and **1g** exhibited purity of <95% but was also screened for MAO activity. It is important to note that the determination of the purity of the compounds by HPLC is only an estimation of the purity and not an absolute measure. The reason for this is that the indanone derivatives and potential impurities (being organic compounds) possess different molar extinction coefficients at 254 nm. For example, even though two compounds are present in an equal molar concentration, the peak areas would differ if the two compounds possess different molar extinction coefficients.

Table 3.4 The purities of the 1-indanone (**1a-h**), 1-indanol (**1i-n**) and hydroxy-1-indanone (**2a, c**) derivatives as estimated by HPLC analysis.

	Purity		**Purity**
1a	98.6% (1 mM) 99.1% (100 µM)	**1i**	98.6% (1 mM) 97.5% (100 µM)
1b	99.8% (1 mM) 99.6% (100 µM)	**1j**	98.9% (1 mM) 98.2% (100 µM)
1c	98.3% (1 mM) 98.1% (100 µM)	**1k**	98.3% (1 mM) 96.9% (100 µM)
1d	83.0% (1 mM) 83.0% (100 µM)	**1l**	99.8% (1 mM) 98.4% (100 µM)
1e	99.1% (1 mM) 99.5% (100 µM)	**1m**	99.2% (1 mM) 97.7% (100 µM)
1f	85.4% (1 mM) 84.4% (100 µM)	**1n**	97.3% (1 mM) 97.1% (100 µM)
1g	97.2% (1 mM) 81.3% (100 µM)	**2a**	98.0% (1mM) 97.0% (100 µM)
1h	99.6% (1 mM) 99.5% (100 µM)	**2b**	99.6 % (1mM) 98.6% (100 µM)

3.5 Conclusion

In this chapter the syntheses of 4-, 5- and 6-hydroxy-1-indanone from commercially available 4-, 5-, and 6-methoxy-1-indanone and $AlCl_3$ are described. These compounds served as key starting materials and were reacted with appropriately substituted alkyl bromides in the presence of K_2CO_3. In this manner, eight 1-indanone derivatives were synthesised in this study. In the subsequent step, the indanone derivatives were reacted with $NaBH_4$ to yield six alcohol derivatives. The structures of the synthesised compounds were elucidated and confirmed by NMR and MS. The ^{1}H NMR and ^{13}C NMR spectra correlated well with the proposed structures of the compounds. The experimentally determined (through MS) and calculated molecular weights also correlated well and therefore provided further evidence for the structures of the synthesised compounds. The R_f value of each compound was determined as well as the yields of the products that were obtained in the final steps of the synthetic routes. HPLC was used to estimate the purity of the synthesised compounds. It was concluded that the structures of the indanone and alcohol derivatives are those given in this chapter and the majority of compounds are of adequate purity to undergo further biological evaluation.

CHAPTER 4: ENZYMOLOGY

4.1 Introduction

The ability of the synthesised indanone (**1a-h**) and alcohol (**1i-n**) derivatives to inhibit human MAO-A and MAO-B, will be explored in this chapter. IC_{50} values for the synthesised compounds will be determined by fluorescence spectrophotometry with kynuramine as the substrate. MAO-A and MAO-B oxidise kynuramine to generate 4-hydroxyquinoline (4-HQ), a metabolite that fluoresces when dissolved in an alkaline medium. The fluorescence measurements will be carried out at an excitation wavelength (λ_{ex}) of 310 nm and an emission wavelength (λ_{em}) of 400 nm (Strydom *et al.*, 2010). The MAO catalysed generation of 4-hydroxyquinoline may be accurately measured in the presence of the indanone (**1a-h**) and alcohol (**1i-n**) derivatives with the use of fluorescence spectrophotometry since these derivatives do not fluoresce under the specific assay conditions of this study. Sigmoidal dose-response curves will be constructed and IC_{50} values, as an indication of the inhibition potencies of the synthesised compounds, will be estimated from the curves.

In the second section of this chapter, an alcohol derivative will be selected for further enzymatic evaluation. In this respect, the reversibility of MAO inhibition will be determined by dialysis and sets of Lineweaver-Burk plots will be constructed to determine if the mode of MAO inhibition is competitive or non-competitive. These studies will focus on the alcohol derivatives since the reversibility of MAO inhibition by indanones has previously been investigated (Mostert *et al*., 2015).

4.2 MAO activity measurements

4.2.1 General background

Kynuramine, a mixed MAO-A/B substrate, was used as the enzyme substrate to evaluate the inhibition potencies of the synthesised compounds. The fact that certain MAO substrates are oxidised to generate products that fluoresce, served as the basis for the biological evaluations. In this respect, kynuramine undergoes oxidation by MAO-A and

MAO-B to yield 4-hydroxyquinoline (Fig 4.1.), a compound that fluoresces when dissolved in alkaline medium. In this reaction, kynuramine is oxidatively deaminated by the MAO enzyme in the first step to yield an aldehyde intermediate. In the second step of the reaction, the aldehyde can either undergo condensation which generates 4-hydroxyquinoline, or it can undergo further oxidation to generate 2,4-dihydroxyquinoline via an acid intermediate. However, the aldehyde is condensed much faster than it is oxidised *in vitro* since the MAO enzymes are not involved in the process while condensation is spontaneous. Therefore, *in vitro* oxidation of kynuramine by the MAO enzymes generates fluorescent 4-hydroxyquinoline as a product. Weissbach and colleagues (1960) observed that 4-hydroxyquinoline can be accurately measured and quantitated by a fluorescence spectrophotometer, as it fluoresces in alkaline media. This finding resulted in the development of a swift and dependable assay for the evaluation of MAO activity, which will be applied during this study to investigate the MAO-A and MAO-B inhibition properties of the indanone (**1a-h**) and alcohol (**1i-n**) derivatives.

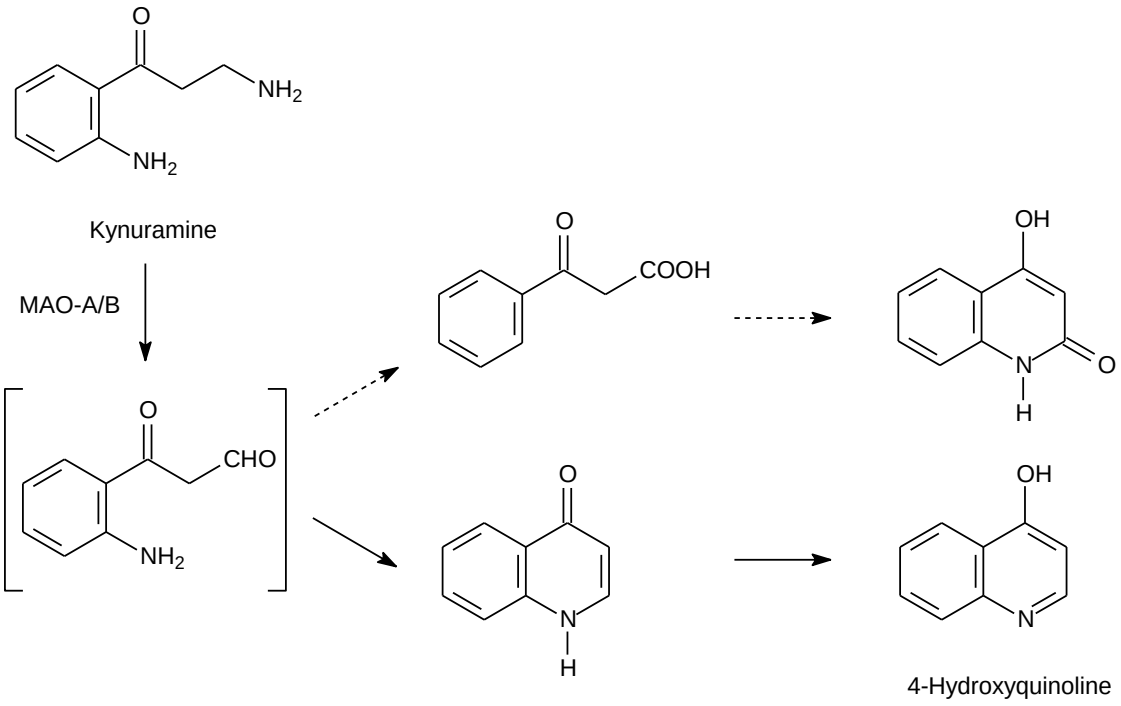

Figure 4.1 The reaction pathway for the oxidation of kynuramine by MAO-A and MAO-B to produce 4-hydroxyquinoline

4.2.2 Materials and instrumentation

The following materials were purchased from Sigma-Aldrich:

- Kynuramine dihydrobromide
- 4-Hydroxyquinoline
- (*R*)-Deprenyl
- Microsomes of insect cells that contain recombinant human MAO-A and MAO-B at a concentration of 5 mg/ml

The following materials were purchased from Merck:

- White polypropylene 96-well microtiter plates
- Potassium phosphate (K_2HPO_4 and KH_2PO_4)
- Potassium chloride (KCl)
- Sucrose
- Sodium hydroxide (NaOH)
- Dimethyl sulfoxide (DMSO)

The following materials were purchased from Thermo Scientific:

- Slide-A-Lyzer dialysis cassettes with a 0.5 to 3 ml sample volume capacity and molecular weight cut-off of 10 000

The fluorometric evaluations were performed with a Varian Cary Eclipse fluorescence spectrophotometer. IC_{50} values of the synthesised products were determined and sigmoidal dose-response curves constructed with the use of the Graphpad Prism 5 software package. All buffers were prepared in Milli-Q deionised water (Millipore).

4.2.3 Experimental determination of IC_{50} values

IC_{50} values give an indication of the MAO-A and MAO-B inhibition potencies of test compounds. The IC_{50} values of the indanone (**1a-h**) and alcohol (**1i-n**) derivatives were determined in this study. MAO activities were recorded in the absence and presence of various concentrations of the test inhibitors and sigmoidal activity-concentration curves were created for the IC_{50} values employing the Prism software package. The compounds that present with low IC_{50} values are the most potent MAO-A and MAO-B inhibitors of the series.

4.2.3.1 Method

Recombinant human MAO-A and MAO-B, at a concentration of 5 mg/ml, were purchased from Sigma-Aldrich. The enzymes were pre-aliquoted and stored at –70 ºC. White polypropylene 96-well microtiter plates were used to carry out all enzymatic reactions, which contained the following:

- 92 µl Potassium phosphate (K_2HPO_4/KH_2PO_4) buffer (100 mM; pH 7.4; made isotonic with the addition of 20.2 mM KCl)
- 50 µl Kynuramine – to produce a final concentration of 50 µM for the MAO-A and MAO-B inhibition studies
- 8 µl of each indanone (**1a-h**) or alcohol (**1i-n**) derivative to produce final concentrations of 0–100 µM. Stock solutions of the compounds were prepared with DMSO as solvent.

The reactions were incubated at 37 ºC for 30 min. A volume of 50 µl of the enzyme was subsequently added to initiate the reactions. The final concentration of the enzymes in the reactions were 0.0075 mg protein/ml for MAO-A and 0.015 mg protein/ml for MAO-B. The reactions were incubated for a further 20 min and were subsequently terminated with the addition of 80 µl NaOH (2 N). The concentration of 4-hydroxyquinoline in the microtiter plate wells were measured with fluorescence spectrophotometry. The fluorescence was measured at an λ_{ex} of 310 nm and an λ_{em} of 400 nm. The PMT voltage of the fluorescence spectrophotometer was set to the medium setting, with an excitation slit width of 5 nm and an emission slit width of 10 nm.

Quantitative estimations of 4-hydroxyquinoline in the enzymatic reactions were made by using a linear calibration curve. In order to make these estimations, known quantities of 4-hydroxyquinoline (0.047 – 1.50 µM) were dissolved in K_2HPO_4/KH_2PO_4 buffer (100 mM, pH 7.4, made isotonic with 20.2 mM KCl) to a final volume of 200 µl. To each calibration standard, 80 µl NaOH (2 N) was added. Control samples were incorporated into the assay procedure to ensure that the synthesised compounds do not fluoresce themselves or otherwise quench the fluorescence of 4-hydroxyquinoline. The control samples, comprising of a volume of 200 µl, contained the test inhibitor (100 µM) and 4-hydroxyquinoline (1.50 µM). To each control sample, 80 µl NaOH (2 N) was added. The fluorescence values of the calibration standards used in this assay should bracket those recorded in the inhibition studies. A linearity of 0.999 should be displayed by the calibration curve to be acceptable.

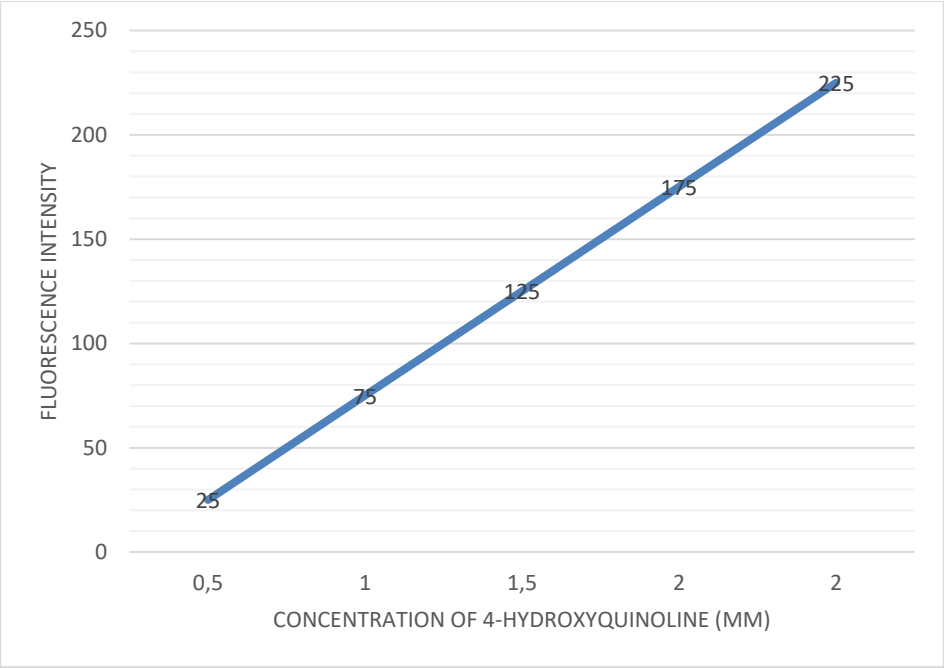

Figure 4.2 Example of a calibration curve constructed in this study.

The graph represents the fluorescence of 4-hydroxyquinoline versus the concentration of authentic 4-hydroxyquinoline.

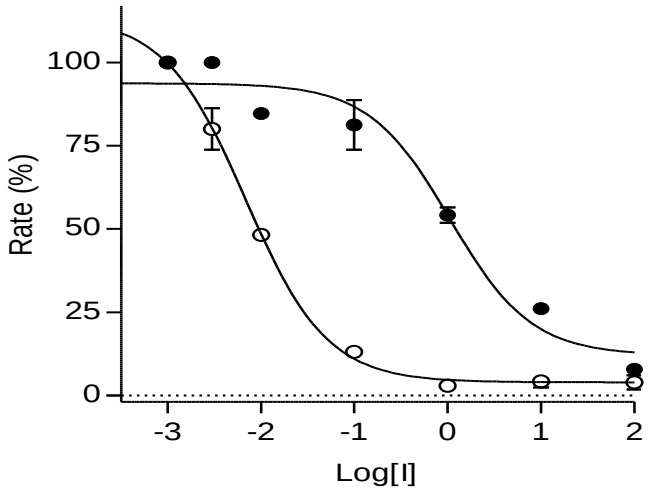

Figure 4.3 Sigmoidal curves for the inhibition of MAO-A by **2a** (filled circles) and the inhibition of MAO-B by **1l** (open circles), respectively.

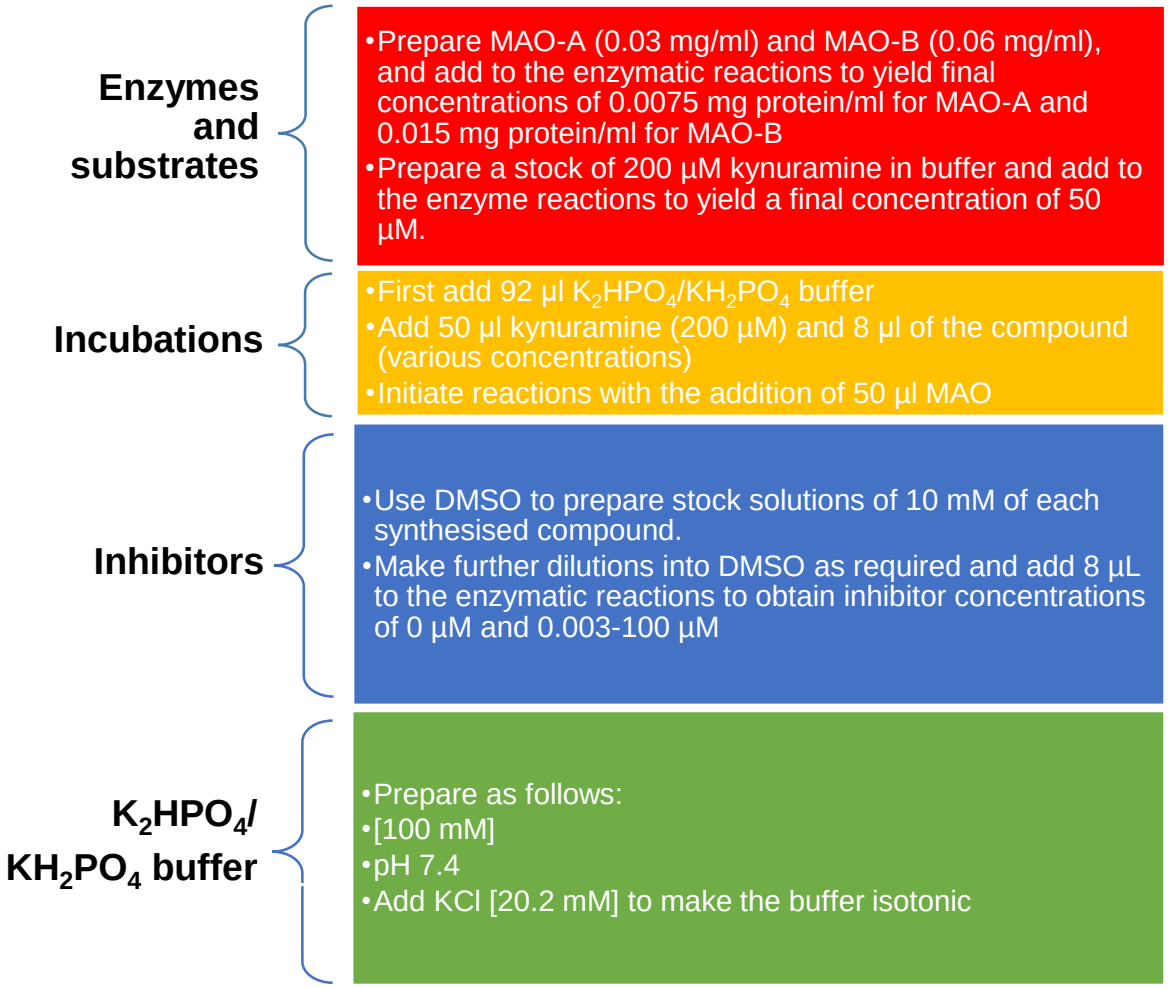

Figure 4.4 A summary of preparation required before performing the MAO inhibition assay.

Concentrations of the solutions are indicated in brackets.

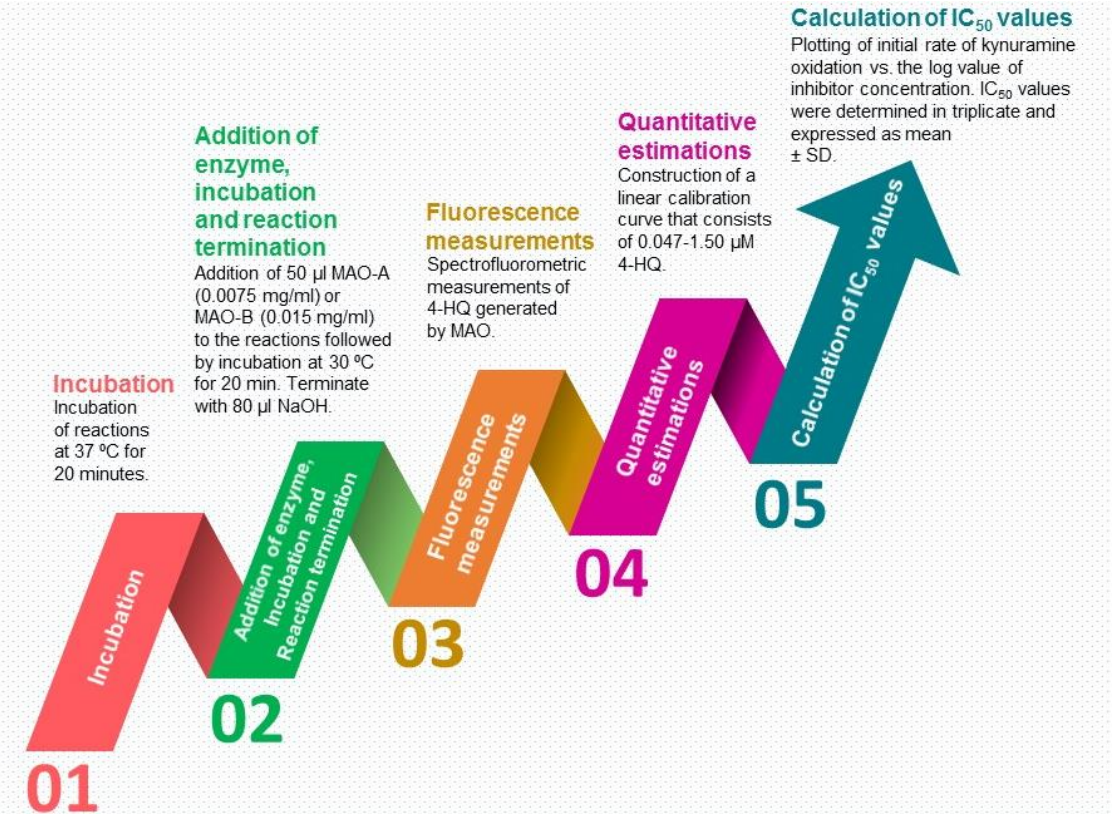

Figure 4.5 Process-flow for the determination of IC_{50} values for MAO inhibition (4-HQ = 4-hydroxyquinoline).

4.2.3.2 Results – IC_{50} values

Table 4.1 The IC_{50} values for the inhibition of human MAO-A and MAO-B by indanone derivatives **1a–h**.

Compound		IC_{50} MAO-A (µM)	IC_{50} MAO-B (µM)	SI[a]
1a	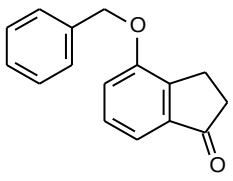	25.5 ± 3.69	6.35 ± 1.39	4

Compound		IC_{50} MAO-A (μM)	IC_{50} MAO-B (μM)	SI[a]
1b	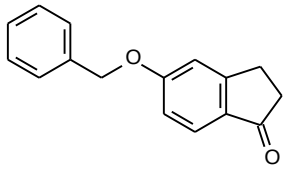	No inhibition[b]	0.048 ± 0.0069	>2083
1c	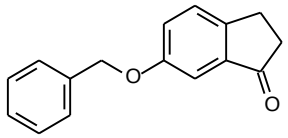	No inhibition[b]	0.00033 ± 0.00010	>303030
1d	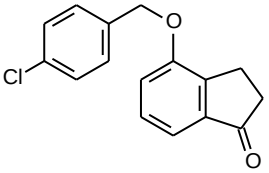	No inhibition[b]	0.351 ± 0.059	>285
1e	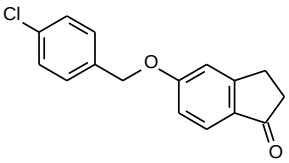	33.5 ± 4.62	0.00013 ± 0.00002	257692
1f	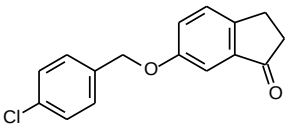	No inhibition[b]	0.000076 ± 0.00003	>1315789

Compound		IC_{50} MAO-A (μM)	IC_{50} MAO-B (μM)	SI[a]
1g	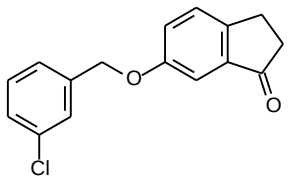	No inhibition[b]	0.00023 ± 0.00002	>434782
1h	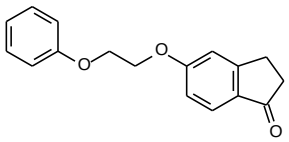	No inhibition[b]	0.070 ± 0.0022	>1429

* All IC_{50} determinations were conducted in triplicate and values are expressed as mean ± SD.

[a] Selectivity index (SI) = IC_{50}(MAO-A)/ IC_{50}(MAO-B). This value indicates the extent to which the test inhibitor is specific for MAO-B compared to MAO-A.

[b] No inhibition was observed at the maximum tested concentration (100 μM).

Table 4.2 The IC_{50} values for the inhibition of human MAO-A and MAO-B by 1-indanol derivatives **1i–n**.

Compound		IC_{50} MAO-A (μM)	IC_{50} MAO-B (μM)	SI[a]
1i	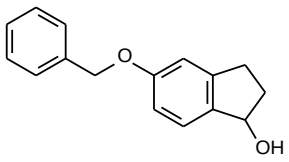	No inhibition[b]	0.075 ± 0.0073	>1333

Compound		IC_{50} MAO-A (μM)	IC_{50} MAO-B (μM)	SI[a]
1j	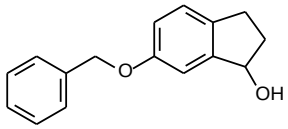	No inhibition[b]	0.030 ± 0.037	>3333
1k	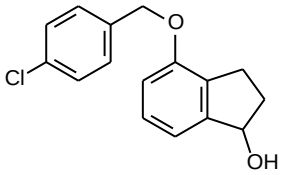	22.3 ± 6.75	0.648 ± 0.093	34
1l	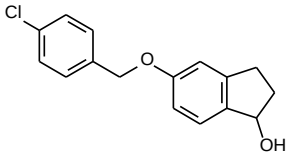	No inhibition[b]	0.007 ± 0.0011	>14286
1m	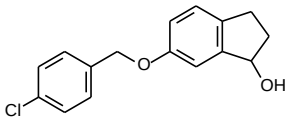	No inhibition[b]	0.074 ± 0.0021	>1351
1n	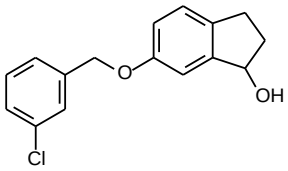	No inhibition[b]	0.063 ± 0.0023	>1587

* All IC_{50} determinations were conducted in triplicate and values are expressed as mean ± SD.

[a] Selectivity index (SI) = IC_{50}(MAO-A)/ IC_{50}(MAO-B). This value indicates the extent to which the test inhibitor is specific for MAO-B compared to MAO-A.

[b] No inhibition was observed at the maximum tested concentration (100 μM).

Table 4.3 The IC_{50} values for the inhibition of human MAO-A and MAO-B by hydroxy-1-indanone derivatives **2a** and **2c**.

Compound		IC_{50} MAO-A (μM)	IC_{50} MAO-B (μM)	SI[a]
2a	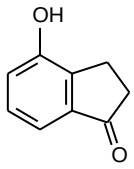	2.15 ± 0.319	63.5 ± 5.95	0.034
2c	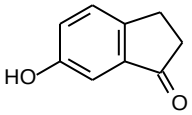	No inhibition[b]	No inhibition[b]	-

* All IC_{50} determinations were conducted in triplicate and values are expressed as mean ± SD.

[a] Selectivity index (SI) = IC_{50}(MAO-A)/ IC_{50}(MAO-B). This value indicates the extent to which the test inhibitor is specific for MAO-B compared to MAO-A.

[b] No inhibition was observed at the maximum tested concentration (100 μM).

Tables 4.1, 4.2 and 4.3 provide the IC_{50} values for the inhibition of human MAO-A and MAO-B by the 1-indanone (**1a-h**), 1-indanol (**1i-n**) and hydroxy-1-indanone derivatives (**2a-c**). All IC_{50} determinations were conducted in triplicate and the values are expressed as the mean ± SD. Low IC_{50} values are indicative of potent MAO inhibition. The SI value is indicative of the selectivity of the inhibitor for MAO-B compared to MAO-A. Only 4 compounds inhibited MAO-A while no MAO-A inhibition was observed with the remaining 12 compounds, even at the maximum tested concentration (100 μM). The lowest possible SI value was given to the 12 compounds that exhibit no MAO-A inhibition with the assumption that IC_{50} = 100 μM. The following observations and comparisons may be made from the tables:

- Several indanone and indanol derivatives are human MAO-A and MAO-B inhibitors, exhibiting IC_{50} values in the micromolar range. All compounds, except **2a**, a hydroxy-1-indanone derivative, are specific inhibitors of the MAO-B isoform with SI values ranging from 4 to 1315789. It can therefore be concluded that all the indanone and indanol derivatives of this study are specific MAO-B inhibitors.

- Examination of the inhibition potencies of the indanone derivatives reveals that compound **1f** exhibits the highest potency MAO-B inhibition (IC_{50} = 0.000076 µM) and compound **1a** exhibits the highest potency MAO-A inhibition (IC_{50} = 25.5 µM). Compound **1f** is 1315789-fold more selective for MAO-B compared to the MAO-A isoform.
- Examination of inhibition potencies of the indanol derivatives reveals that compound **1l** exhibits the highest potency MAO-B inhibition (IC_{50} = 0.007 µM). Compound **1k** is the only indanol derivative that exhibits MAO-A inhibition (IC_{50} = 22.3 µM). Compound **1l** is 14286-fold more specific for MAO-B compared to the MAO-A isoform.
- Compound **1f** is the most potent MAO-B inhibitor of all the tested compounds and exhibits an IC_{50} value of 0.000076 µM. It should be noted that impurities may have possibly contributed to the MAO inhibition activity of compound **1f** with an estimated purity of 85.4% (1mM).
- Compound **2a** is the most potent MAO-A inhibitor of all the tested compounds, exhibiting an IC_{50} value of 2.15 µM. It is also the only compound with a SI value <1 which indicates selectivity for MAO-A over the MAO-B isoform. It is noteworthy that this compound does not contain an alkyloxy substituent.
- Of all compounds, compound **1f** exhibits the highest selectivity for MAO-B with an SI value of >1315789.
- The indanone derivatives are in general more potent MAO-B inhibitors than the indanol derivatives. This is supported by the observation that four indanone derivatives (compounds **1c**, **1e**, **1f** and **1g**) exhibit MAO-B inhibition with IC_{50} values in the sub-nanomolar range (0.000076– 0.00033 µM) while the MAO-B inhibition potencies of the indanol derivatives are in the micromolar range (IC_{50} > 0.007 µM). It may thus be concluded that the 1-indanone scaffold is more suitable for the design of potent MAO-B inhibitors than the 1-indanol scaffold.

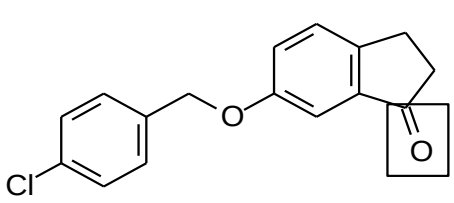

IC_{50} = 0.000076 µM

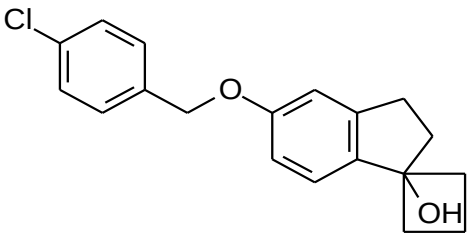

IC_{50} = 0.007 µM

Figure 4.6 **Comparison of the structures of the most potent indanone (**1f**) and indanol (**1l**) derivatives.**

- Evaluation of the effect of halogen (Cl) substitution on the inhibition properties of the indanone and indanol derivatives indicates that chlorine substitution on the benzyloxy ring yields more potent MAO-B inhibitors. For example, the chlorine substituted indanone derivative **1f** (IC_{50} = 0.000076 µM) is 4.3-fold more potent than its unsubstituted derivative **1c** (IC_{50} = 0.00033 µM). A similar observation was made with regards to the chlorine substituted indanol derivatives. The chlorine substituted indanol derivative **1l** (IC_{50} = 0.007 µM) is 11-fold more potent than the unsubstituted derivative **1i** (IC_{50} = 0.075 µM).

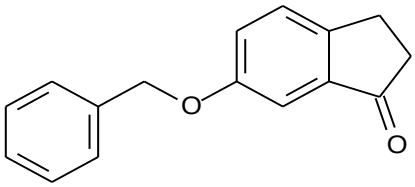

IC_{50} MAO-B = 0.00033 µM

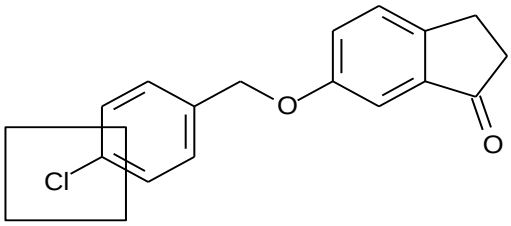

IC_{50} MAO-B = 0.000076 µM

Figure 4.7 Comparison between the MAO-B inhibition potencies of unsubstituted and chlorine substituted indanone derivatives **1c** (left) and **1f** (right).

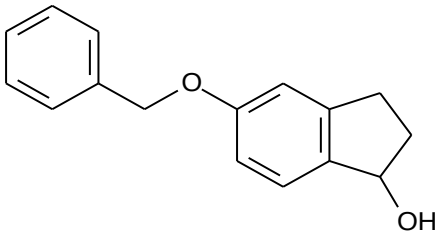

IC_{50} MAO-B = 0.075 µM

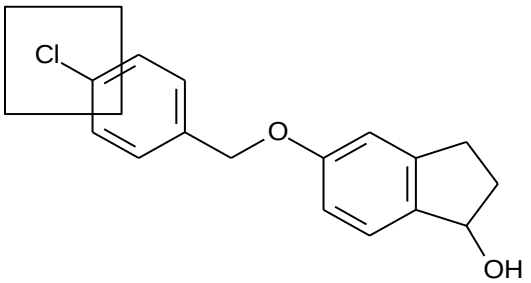

IC_{50} MAO-B = 0.007 µM

Figure 4.8 Comparison between the MAO-B inhibition potencies of unsubstituted and chlorine substituted indanol derivatives **1i** (left) and **1l** (right).

- Evaluation of the effect of chlorine substitution at different positions of the substituent ring reveals that, for the indanone derivatives, chlorine substitution on the *para* position of the benzyloxy side chain produces more potent MAO-B inhibition than substitution on the *meta* position. For example, compound **1f** which is substituted with chlorine on the *para* position of the benzyloxy phenyl ring (IC_{50} = 0.000076 µM), is 3-fold more potent than compound **1g** (IC_{50} = 0.00023), which is substituted with chlorine on the *meta* position of the benzyloxy phenyl ring.

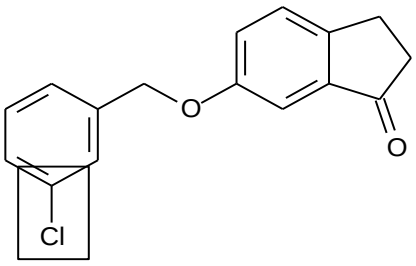

IC_{50} MAO-B = 0.00023 µM

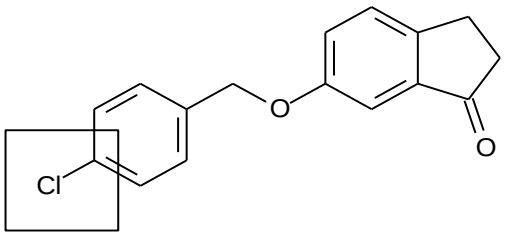

IC_{50} MAO-B = 0.000076 µM

Figure 4.9 Comparison between the MAO-B inhibition potencies of indanone derivatives with *meta* and *para* chlorine substitution on the benzyloxy phenyl ring. Compound **1g** (left) and **1f** (right) are provided as examples.

- Evaluation of the effect of chlorine substitution at different positions reveals that, for the indanol derivatives, chlorine substitution on the *meta* position of the benzyloxy side chain produces more potent MAO-B inhibitors than substitution on the *par*a position. For example, compound **1n** (IC_{50} = 0.063 µM), which is substituted with chlorine on the *meta* position of the benzyloxy ring, is 1.2-fold more potent than compound **1m**

(IC_{50} = 0.074), which is substituted with chlorine on the *para* position of the benzyloxy phenyl ring.

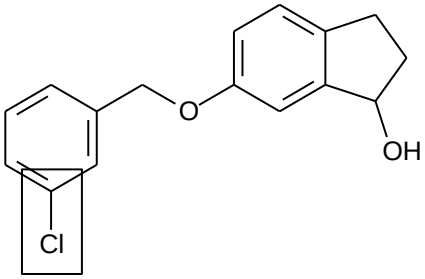

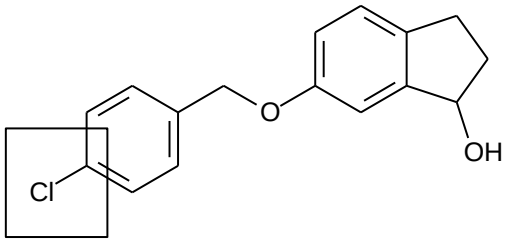

IC_{50} MAO-B = 0.063 µM **IC_{50} MAO-B = 0.074 µM**

Figure 4.10 Comparison between the MAO-B inhibition potencies of indanol derivatives with *meta* and *para* chlorine substitution on the benzyloxy ring. Compound **1n** (left) and **1m** (right) are provided as examples.

- Evaluation of the effect of substitution with 4-chlorobenzyloxy on different positions of 1-indanone reveal that substitution on C6 yields the highest MAO-B inhibition potency (e.g. **1f**, IC_{50} = 0.000076 µM), substitution on C5 yields second best MAO-B inhibition (e.g. **1e**, IC_{50} = 0.00013 µM) and substitution on C4 yields the weakest MAO-B inhibition (**1d**, IC_{50} = 0.351 µM). Compound **1f** is thus 2-fold and 4618-fold more potent than compounds **1e** and **1d**, respectively.

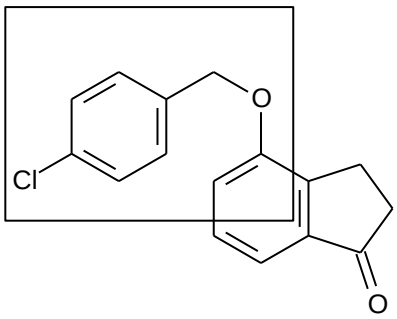

IC_{50} MAO-B = 0.351 µM

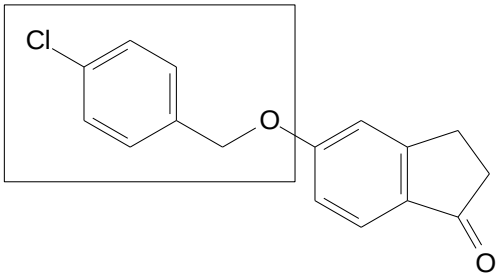

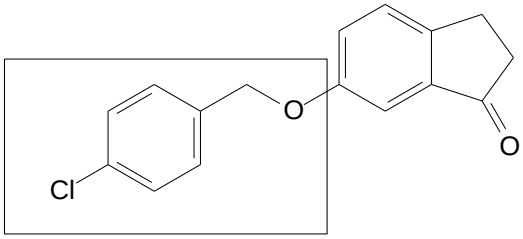

IC_{50} MAO-B = 0.00013 µM **IC_{50} MAO-B = 0.000076 µM**

Inhibition potencies: C4 < C5 < C6

Figure 4.11 Comparison between MAO-B inhibition potencies of indanone derivatives substituted with 4-chlorobenzyloxy on C4, C5 and C6.

- Evaluation of the effect of substitution with 4-chlorobenzyloxy on different positions of 1-indanol reveals that substitution at C5 yields the highest potency MAO-B inhibition (**1l**, IC_{50} MAO-B = 0.007 µM), C6 substitution yields the second highest inhibition (**1m**, IC_{50} = 0.074 µM) and C4 substitution yields the weakest MAO-B inhibition (**1k**, IC_{50} = 0.648 µM). Compound **1l** is thus 11-fold and 92-fold more potent than compounds **1m** and **1k**, respectively. Compound **1k**, the weakest MAO-B inhibitor, is also the only compound of these three that exhibit MAO-A inhibition with an IC_{50} value of 22.3 µM.

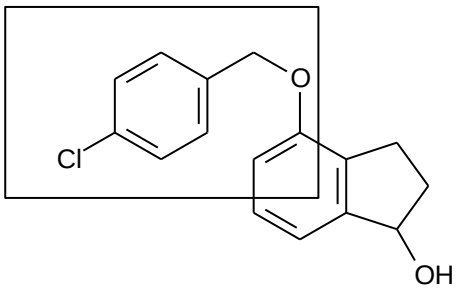

IC_{50} MAO-B = 0.648 µM

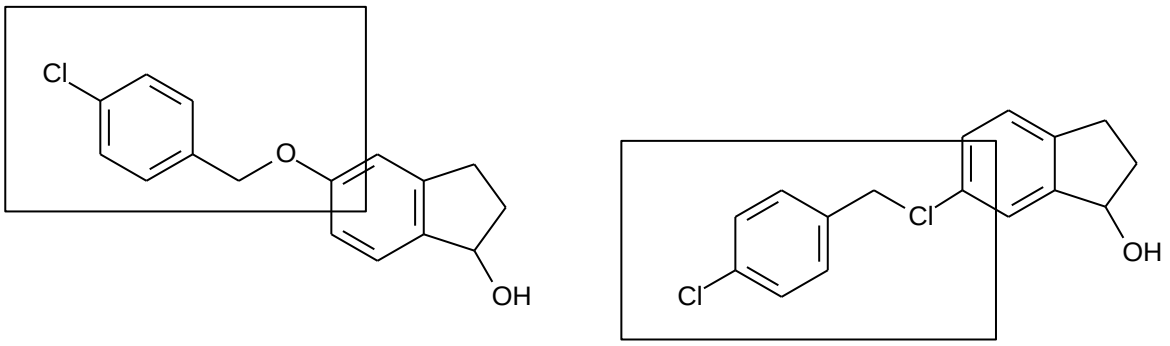

IC_{50} MAO-B = 0.007 µM **IC_{50} MAO-B = 0.074 µM**

Inhibition potencies: C4 < C6 < C5

Figure 4.12 Comparison between MAO-B inhibition potencies of 1-indanol derivatives substituted with the 4-chlorobenzyloxy on C4, C5 and C6.

- Evaluation of the MAO-B inhibition potencies of 1-indanone derivatives with different substituents, i.e. benzyloxy and 2-phenoxyethoxy, reveals that benzyloxy substitution produces compounds with higher potencies. For example, a compound substituted with benzyloxy on C5 (**1b**, IC_{50} = 0.048 µM) is 1.5-fold more potent than a compound substituted with 2-phenoxyethoxy (**1h**, IC_{50} = 0.070 µM). As mentioned, substitution with 4-chlorobenzyloxy (**1e**, IC_{50} = 0.00013 µM) produces inhibitors with higher inhibition potencies than compounds with benzyloxy as substituent (**1b**, IC_{50} = 0.048 µM). It can therefore be concluded that substitution with the 2-phenoxyethoxy side chain (**1h**, IC_{50} = 0.070 µM) produces compounds with lower inhibition potency than substitution with 4-chlorobenzyloxy (**1e**, IC_{50} = 0.00013 µM).

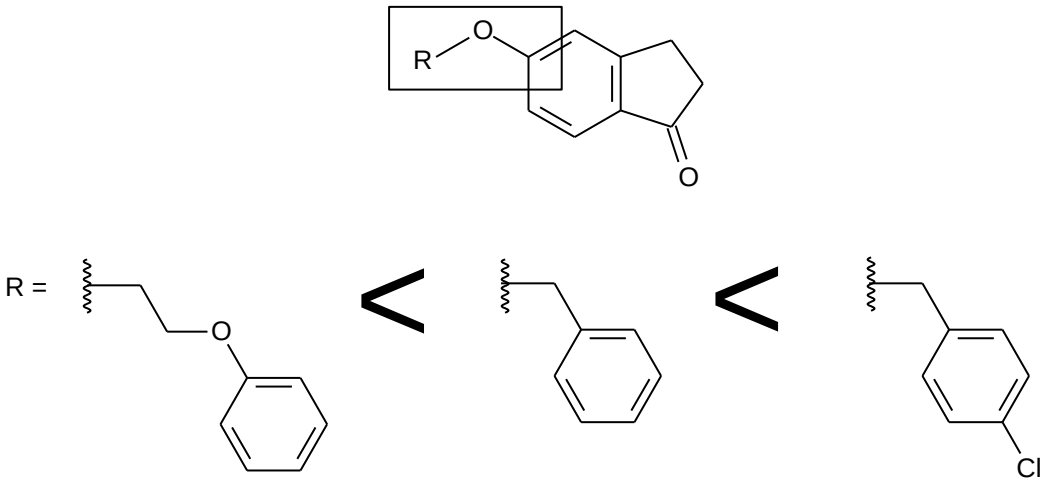

MAO-B inhibition potencies

Figure 4.13 Comparison between the MAO-B inhibition potencies of 1-indanone derivatives with different substituents, i.e. 2-phenoxyethoxy (left), benzyloxy (middle) and 4-chlorobenzyloxy (right).

- Evaluation of the MAO inhibition potencies of 4-hydroxy-1-indanone and 6-hydroxy-1-indanone reveals that 4-hydroxy-1-indanone is a potent MAO-A inhibitor (**2a**, IC_{50} = 2.15 µM) and a weak inhibitor of MAO-B (**2a**, IC_{50} = 63.5 µM). In contrast, 6-hydroxy-1-indanone (**2b**) exhibits no inhibition of either MAO isoform at the maximum tested concentration of 100 µM.

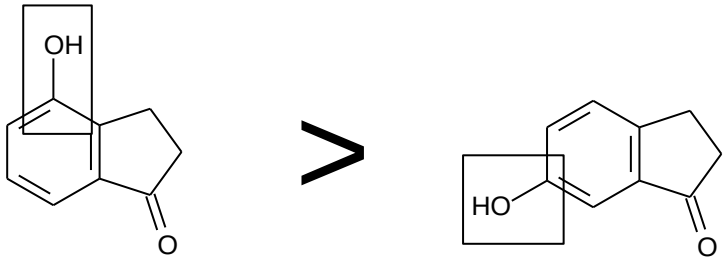

MAO-A and MAO-B inhibition potencies

Figure 4.14 Comparison between MAO inhibition potencies of 4-hydroxy-1-indanone (left) and 6-hydroxy-1-indanone (right).

4.3 Method – Reversibility of inhibition by dialysis

For the reversibility studies, compounds **2a** and **1l** were selected as representative test inhibitors since **2a** is the most potent MAO-A inhibitor of all compounds evaluated, and **1l** is the most potent MAO-B inhibitors among the alcohol derivatives. The reversibility studies were conducted by dialysis with Slide-A-Lyzer dialysis cassettes (Thermo Scientific). The cassettes have a sample volume capacity of 0.5 to 3 ml and a molecular weight cut-off of 10 000. Compounds **2a** and **1l**, at concentrations of 4 x IC_{50}, were pre-incubated with recombinant human MAO-A or MAO-B (0.03 mg protein/ml) at 37 ºC for 15 min. The buffer used for the enzyme-inhibitor incubations was potassium phosphate buffer (100 mM, pH 7.4, made isotonic with KCl) containing 5% sucrose. Control incubations were performed without inclusion of an inhibitor (negative control) and with inclusion of the irreversible inhibitors pargyline ($IC_{50(MAO-A)}$ = 13 µM) or (R)-deprenyl ($IC_{50(MAO-B)}$ = 0.079 µM) (positive controls). The dialysis mixtures consisted of a final of volume of 0.8 ml and DMSO (4%) served as co-solvent in all pre-incubations. The dialysis of the enzyme-inhibitor complexes were carried out for 20 to 25 h at 4 ºC in 80 ml outer buffer (100 mM potassium phosphate, pH 7.4, 5% sucrose). The sucrose buffer was replaced at 3 and 7 h following the start of dialysis. The residual MAO-A and MAO-B activities were determined after two-fold dilution of the reactions with the addition of kynuramine as the substrate. The final MAO concentration after dilution was 0.015 mg protein/ml and final kynuramine concentration, 50 µM. The reactions were incubated for 20 min and subsequently terminated by addition of 1000 µl deionised water and 400 µl NaOH (2 N). The concentrations of 4-hydroxyquinoline generated by MAO catalysis were measured by fluorescence spectrophotometry at λ_{ex} = 310 nm and λ_{em} = 400 nm. The reactions were performed in triplicate and the residual catalytic rates are given as mean ± SD. For comparison, enzyme-inhibitor complexes that did not undergo dialysis were maintained at 4 ºC for the same amount of time and the residual MAO activity subsequently measured as above.

Quantitative estimations of 4-hydroxyquinoline in the enzymatic reactions were made by using a linear calibration curve. In order to make these estimations, known quantities of 4-hydroxyquinoline (0.047 – 1.560 µM) were dissolved in K_2HPO_4/KH_2PO_4 buffer (100 mM, pH 7.4, made isotonic with 20.2 mM KCl) to a final volume of 200 µl. To each calibration standard, 80 µl NaOH (2 N) was added.

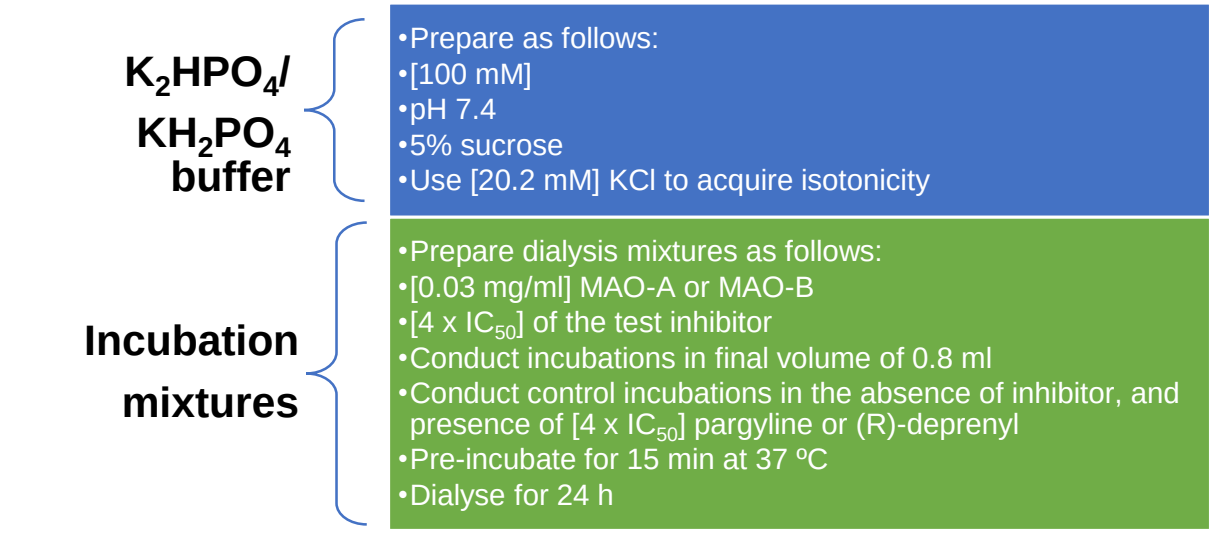

Figure 4.15 Summary of the buffer and dialysis conditions for the reversibility studies.

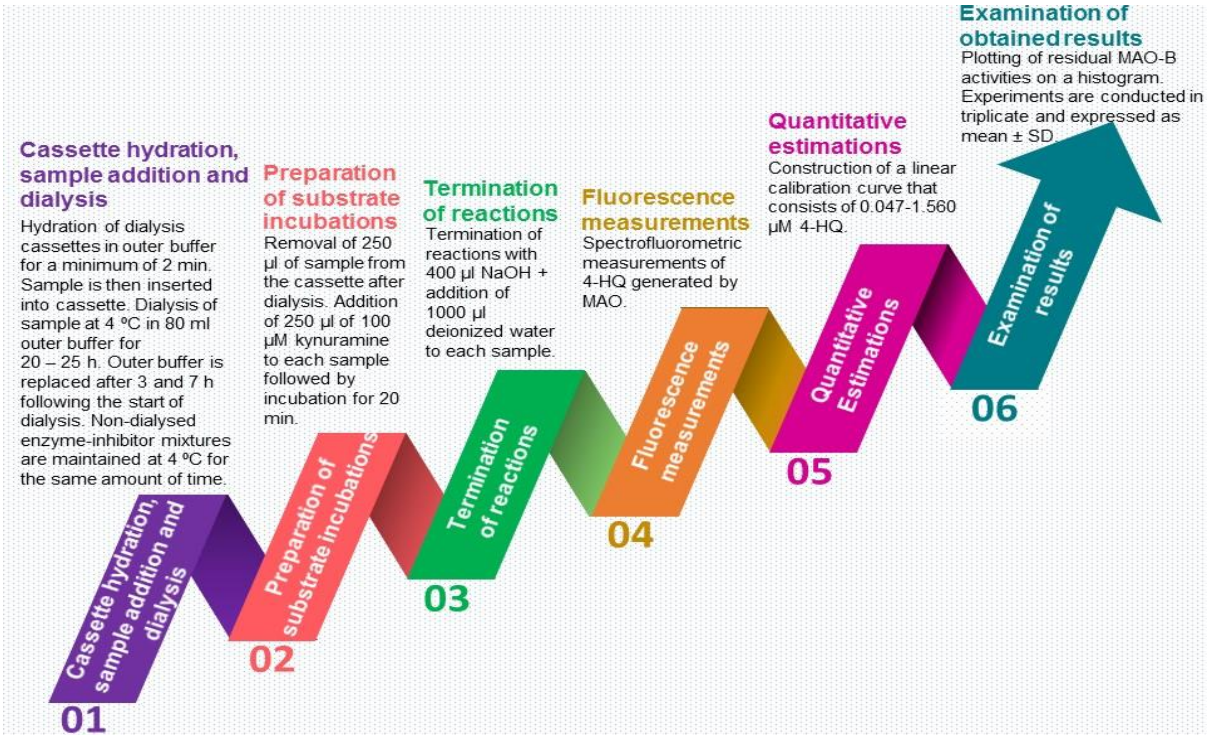

Figure 4.16 Process-flow of the reversibility studies (4-HQ = 4-hydroxyquinoline).

4.3.1 Results of reversibility studies

After dialysis of mixtures of compound **2a** and **1l** and MAO-A and MAO-B, respectively for 24 h, complete recovery of MAO-A and MAO-B activity could be observed (Figure 4.17). Inhibition of MAO-A and MAO-B by compounds **2a** and **1l**, respectively, are therefore completely reversible with the catalytic activity of MAO-A and MAO-B recovering to 85% and 96% of the control value (recorded without the presence of the inhibitor). Contrary to this, non-dialysed mixtures of MAO-A and MAO-B and the test inhibitors yielded residual activities of 72% and 74%, respectively. Dialysis of mixtures of MAO-A and pargyline, and MAO-B and (R)-deprenyl (both irreversible MAO inhibitors) resulted in almost no recovery of MAO-A and MAO-B activity, with residual enzyme activities of only 1.9% and 3%, respectively, of the control value. The conclusion may be made that **2a** and **1l** are reversible inhibitors of human MAO-A and MAO-B, and that all the other indanol derivatives (**1i-n**) synthesised in this study, are most likely also reversible MAO-B inhibitors.

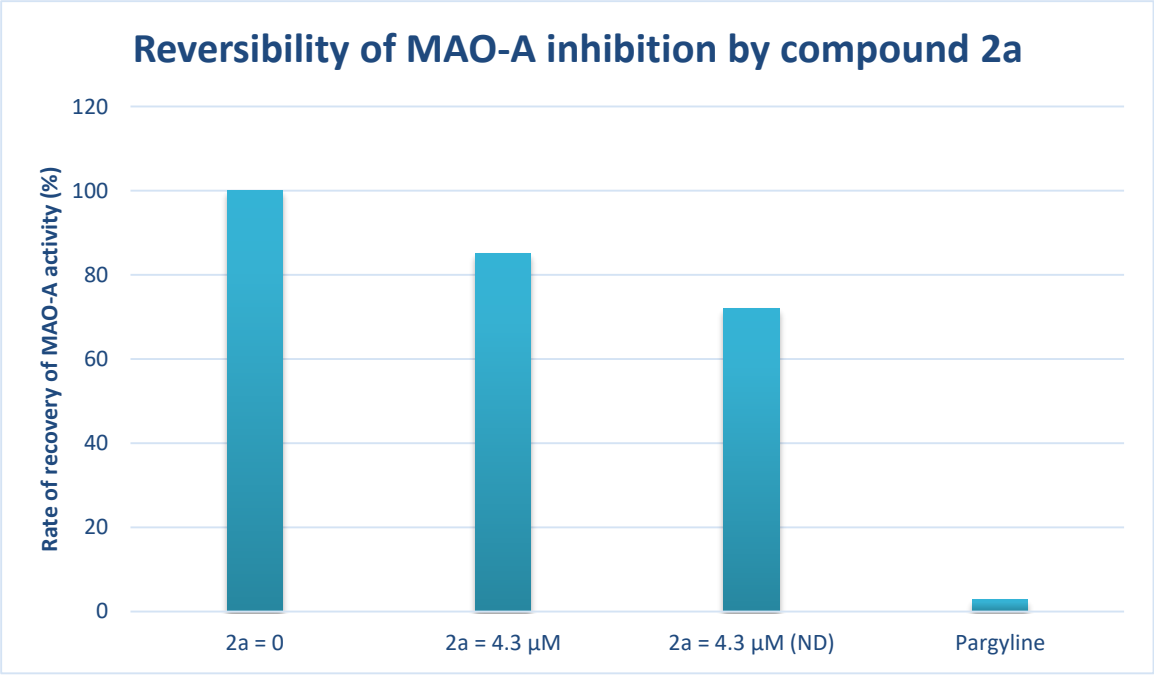

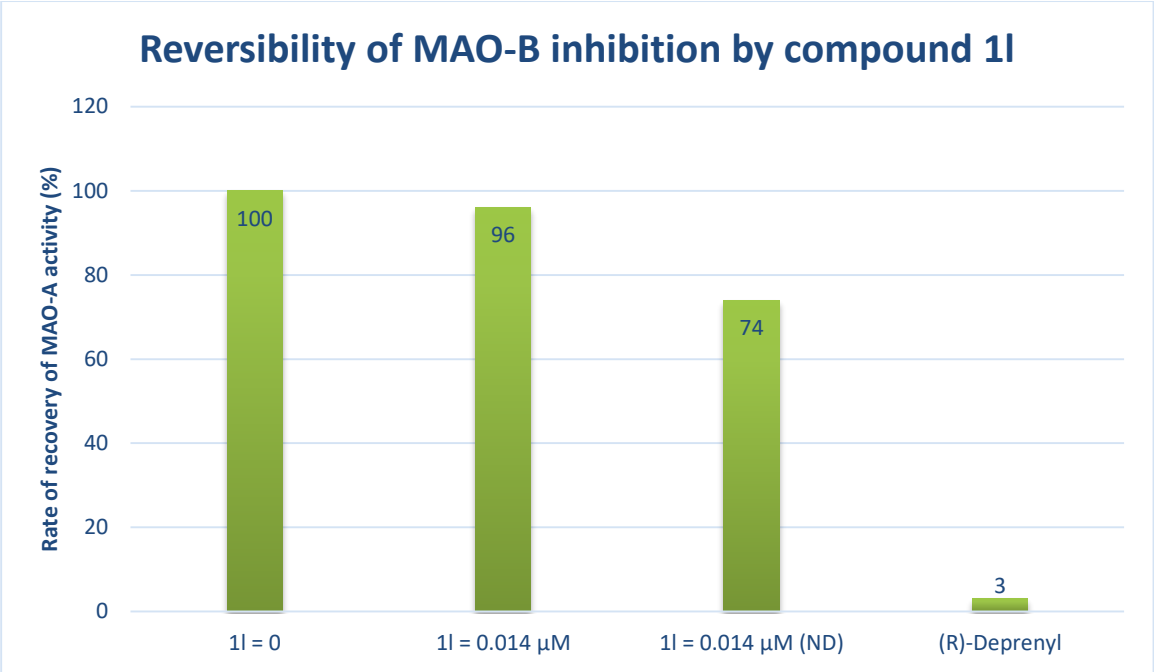

Figure 4.16 Reversibility of inhibition of MAO-A and MAO-B by compounds **2a** and **1l**, respectively.

MAO-A was pre-incubated in the absence of inhibitor (2a = 0) and presence of 2a (**2a** = 4.3 µM) and pargyline (top), and MAO-B was pre-incubated in the absence of inhibitor and presence of 1l (**1l** = 0.014 µM) and (R)-deprenyl (bottom). After dialysis, the residual enzyme activities were measured. For comparison, the MAO-A [**2a** = 4.3 µM (ND)] and MAO-B [(**1l** = 0.014 µM (ND)] activities of non-dialysed mixtures of the MAOs and the test inhibitors were also measured.

4.4 Conclusion

The *in vitro* biological evaluation of the 1-indanone (**1a-h**), 1-indanol (**1i-n**) and hydroxy-1-indanone (**2a**, **c**) derivatives are presented and discussed in this chapter. The IC_{50} values of all compounds were determined as a measure of enzyme inhibition potency. For the determination of IC_{50} values, MAO activity measurements were performed with the use of recombinant MAO-A and MAO-B enzymes and the non-selective MAO-A/B substrate, kynuramine. Kynuramine is oxidised to yield 4-hydroxyquinoline, a fluorescent compound, by MAO. Sigmoidal dose-response curves were constructed from the MAO activity measurements in the presence of different concentrations of the synthesised compounds.

These curves were used for the estimation of IC_{50} values. The conclusion can be made that the indanone derivatives, in general, are potent inhibitors of MAO-B, with compound **1f** (IC_{50} = 0.000076 μM) exhibiting the highest potency inhibition of the series of indanone derivatives. Although not as potent as the indanones, the indanol derivatives are also considered to be potent MAO-B inhibitors, with **1l** (IC_{50} = 0.007 μM) exhibiting the highest potency of the series of indanol derivatives. Compared to the reference MAO-B inhibitor, lazabemide which exhibits an IC_{50} value of 0.091 μM (Petzer *et al.,* 2013), most indanone and indanol derivatives are more potent MAO-B inhibitors. It was also determined that chlorine substitution on the substituent phenyl ring yields more potent MAO-B inhibition. For the indanone derivatives, substitution on the *para* position of the side chain phenyl ring yields more potent inhibitors while substitution on the *meta* position yields more potent inhibition for the indanol derivatives. Compounds **2a** and **1l** were selected for reversibility studies that were performed by dialysis. It was concluded that these compounds are reversible inhibitors of MAO-A and MAO-B, respectively. For a relatively small compound, **2a** exhibits a high inhibition potency for human MAO-A with an IC_{50} value of 2.15 μM. In comparison with a MAO-A inhibitor used in practice, toloxatone which exhibits an inhibition potency of 3.92 μM for MAO-A (Petzer *et al.,* 2013), **2a** is considered highly potent with regards to human MAO-A inhibition.

Figure 4.17 Chemical structures of the MAO-A inhibitor, toloxatone (left) and the MAO-B inhibitor, lazabemide (right).

CHAPTER 5: CONCLUSION

The focus of this study is the design of inhibitors for the MAO enzymes that are located on the outer membrane of the mitochondria. As discussed, two isoforms of the MAOs exist, namely MAO-A and MAO-B. MAO-A catalyses the deamination of NA, 5-HT, DA and tyramine, while MAO-B is responsible for the deamination of exogenous amines such as benzylamine, PE, DA and tyramine. MAO-A is selectively inhibited by clorgyline and MAO-B is selectively inhibited by (R)-deprenyl (Youdim & Bakhle, 2006). The two isoforms also differ with regards to regional distribution in tissues with MAO-A being the dominant isoform in the periphery while MAO-B exhibits the highest activity in the striatum and basal ganglia in the brain (Youdim *et al.,* 2006). An important factor in the biology of the MAOs is the "cheese reaction". The "cheese reaction" is induced when indirect acting sympathomimetic amines, such as tyramine present in food and wine, are consumed and MAO-A is irreversibly inhibited. Tyramine uptake from the GI tract increases which leads to an increase in NA release and ultimately a potentially fatal increase in blood pressure (Youdim & Bakhle, 2006). The MAOs are important drug targets. Inhibitors of MAO-A are indicated for depression and results in raised levels of 5-HT in the human brain (Pletscher, 1991). It is important to notice that MAO-A inhibitors may induce the life-threatening serotonin syndrome when co-administered with SSRI's. MAO-B specific inhibitors, in turn, serve as treatment for PD as it increases DA levels in the human brain with no effect on MAO-A. Inhibitors of MAO-B may also be possibly neuroprotective and possess the potential to modify disease progression (Fernandez & Chen, 2007).

The most noteworthy MAO-B inhibitors are (R)-deprenyl and rasagiline, which are used in the treatment of PD. These inhibitors are irreversible inhibitors and initially bind in the same manner as reversible inhibitors but is subsequently oxidised to the active inhibitor, which binds covalently to the FAD cofactor. The MAO enzyme is therefore permanently unable to metabolise amines (Foley *et al.,* 2000). Reversible inhibitors are thus considered a safer treatment option as potential side effects that may occur with MAO inhibition can be terminated immediately when administration of the drug is discontinued (Van den Berg *et al.,* 2007).

The main objective of this study was to synthesise a series of 1-indanone and related 1-indanol derivatives as potential MAO inhibitors. The compounds were substituted at C4, C5, and C6 of the 1-indanone and 1-indanol rings with the benxyloxy, 3-chlorobenzyloxy, 4-chlorobenzyloxy and 2-phenoxyethoxy moieties. Some of these moieties have previously been substituted on α-tetralone, which led to compounds with high MAO-B inhibition potency (Legoabe *et al.,* 2014). Furthermore, a series of 1-indanones previously synthesised also presented with good MAO-B inhibition potencies (Mostert *et al*., 2015). It was proposed that substitution on C4 of the 1-indanone ring would yield highly selective MAO-B inhibitors without the liability of the "cheese reaction". This hypothesis was made based on the observation that rasagiline binds in the substrate cavity of MAO-B and leaves the entrance cavity empty as shown in a crystal structure of the rasagiline-MAO-B complex published by Hubálek and colleagues (2004). Substitution with an appropriate substituent on C4 of rasagiline is hypothesised to extend into the entrance cavity and result in the fusion of the MAO-B cavities, which would yield highly selective "cavity-spanning" inhibitors of MAO-B. This theory was evaluated with 1-indanones of the present study since 1-indanone resembles the structure of rasagiline.

4-Hydroxy-1-indanone (**2a**) and 6-hydroxy-1-indanone (**2c**) were synthesised from commercially available 4-methoxy-1-indanone and 6-methoxy-1-indanone, respectively, and used as starting materials to synthesise five 1-indanone derivatives (**1a, c, d, f, g**). Commercially available 5-hydroxy-1-indanone, in turn, was used to synthesise a further three 1-indanone derivatives (**1b, e, h**). In total, eight 1-indanone derivatives (**1a-h**) were successfully synthesised. Six of the 1-indanone derivatives were successfully reduced to the corresponding alcohol derivatives (**1i-n**) as the reductions of **1a** and **1h** were unsuccessful even though various attempts were made. The structures of all synthesised compounds were elucidated with NMR and MS analysis and the purity of the compounds were estimated by HPLC analysis. The structures of the synthesised compounds corresponded well to the proposed structures and the compounds was of adequate purity for biological evaluation. The structures of the synthesised compounds and the corresponding IC_{50} values obtained from MAO inhibition studies are tabulated underneath.

Table 5.1 The synthesised 1-indanone derivatives (**1a-h**) and their corresponding IC_{50} values for the inhibition of human MAO-A and MAO-B.

Compound		IC_{50} MAO-A (μM)	IC_{50} MAO-B (μM)
1a	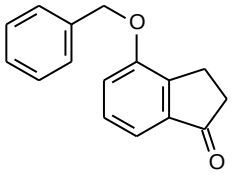	25.5 ± 3.69	6.35 ± 1.39
1b	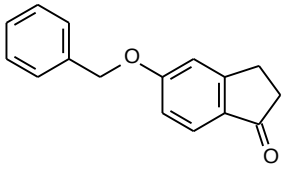	No inhibition[b]	0.048 ± 0.0069
1c	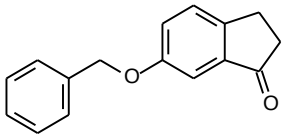	No inhibition[b]	0.00033 ± 0.00010
1d	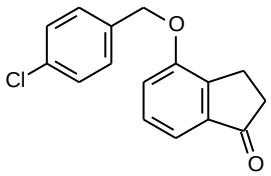	No inhibition[b]	0.351 ± 0.059
1e	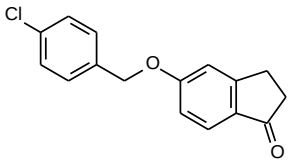	33.5 ± 4.62	0.00013 ± 0.00002
1f	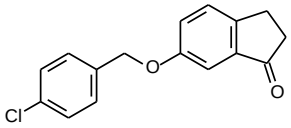	No inhibition[b]	0.000076 ± 0.00003

1g	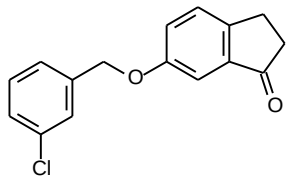	No inhibition[b]	0.00023 ± 0.00002
1h	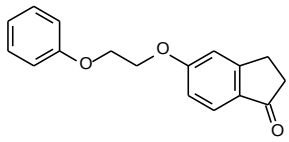	No inhibition[b]	0.070 ± 0.0022

* All IC_{50} determinations were conducted in triplicate and values are expressed as mean ± SD.

[b] No inhibition was observed at the maximum tested concentration (100 μM).

Table 5.2 The synthesised 1-indanol derivatives (**1i-n**) and their corresponding IC_{50} values for the inhibition of human MAO-A and MAO-B.

Compound		IC_{50} MAO-A (μM)	IC_{50} MAO-B (μM)
1i	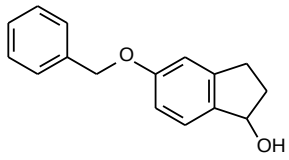	No inhibition[b]	0.075 ± 0.0073
1j	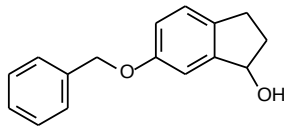	No inhibition[b]	0.030 ± 0.037
1k	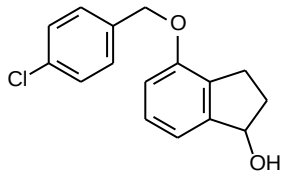	22.3 ± 6.75	0.648 ± 0.093

1l	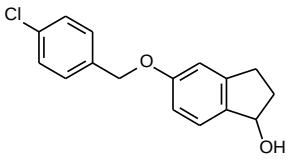	No inhibition[b]	0.007 ± 0.0011
1m	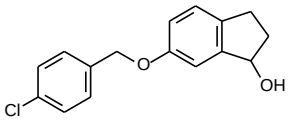	No inhibition[b]	0.074 ± 0.0021
1n	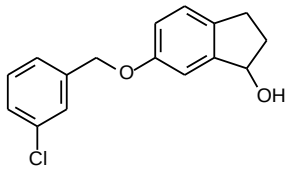	No inhibition[b]	0.063 ± 0.0023

* All IC_{50} determinations were conducted in triplicate and values are expressed as mean ± SD.

[b] No inhibition was observed at the maximum tested concentration (100 μM).

Table 5.3 The synthesised hydroxy-1-indanone derivatives (**2a, c**) and their corresponding IC_{50} values for the inhibition of human MAO-A and MAO-B.

Compound		IC_{50} MAO-A (μM)	IC_{50} MAO-B (μM)
2a	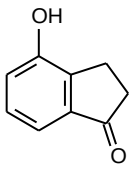	2.15 ± 0.319	63.5 ± 5.95
2c	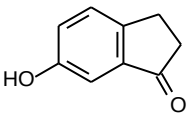	No inhibition[b]	No inhibition[b]

* All IC_{50} determinations were conducted in triplicate and values are expressed as mean ± SD.

[b] No inhibition was observed at the maximum tested concentration (100 μM).

In order to determine the IC_{50} values for the inhibition of MAO by the test compounds, recombinant human MAO-A and MAO-B were used as enzyme sources and kynuramine served as non-selective MAO-A/B substrate. The oxidation of kynuramine by MAO produces 4-hydroxyquinoline, a metabolite which fluoresces. By measuring the MAO catalytic rates at different inhibitor concentrations, sigmoidal dose-response curves were constructed and used to estimate the IC_{50} values. From the results, it was concluded that the 1-indanone (**1a-h**) and 1-indanol (**1i-n**) derivatives are potent inhibitors of MAO-B, with **1a**, **1e** and **1k** also exhibiting MAO-A inhibition, although with low potency. The 1-indanone derivatives in general exhibit higher inhibition potency than the 1-indanol derivatives with compound **1f** (IC_{50} = 0.000076 µM) possessing the highest inhibition potency of the indanones. Compound **1l** (IC_{50}= 0.007 µM) exhibits the highest inhibition potency of the indanol derivatives, although it is 92-fold weaker than compound **1f**. It was interesting to note that 4-hydroxy-1-indanone (**2a**; IC_{50} = 2.15 µM) is a good potency inhibitor of MAO-A and approximately equipotent to the known MAO-A inhibitor, toloxatone (IC_{50}= 3.92 µM). 6-Hydroxy-1-indanone (**2c**), in turn, is not a MAO-A inhibitor.

Compounds **2a** and **1l** were selected for the reversibility studies. Compound **1l** exhibits the highest MAO-B inhibition activity of the 1-indanol derivatives. The results showed that dialysis of mixtures of MAO-A and **2a**, and MAO-B and **1l** restored enzyme activity and it was concluded that these inhibitors are reversible MAO inhibitors. It may thus be concluded that 1-indanol derivatives act as reversible inhibitors of MAO-B. Reversibility studies have previously been carried out with 1-indanone derivatives and the conclusion was made that 1-indanones are also reversible inhibitors of MAO-B (Mostert *et al.,* 2015).

This study proved the hypothesis that 1-indanone and 1-indanol derivatives are promising leads for the design of potent MAO-B inhibitors. Substitution on C6 and C5 proved to yield highly potent MAO-B inhibitors. However, the proposal that substitution on C4 of 1-indanone and 1-indanol derivatives would yield highly selective and potent MAO-B inhibitors, was not substantiated. The C4-substituted 1-indanone and 1-indanol derivatives, compounds **1a** (IC_{50} = 6.35 µM), **1d** (IC_{50} = 0.351 µM) and **1k** (IC_{50} = 0.648 µM), exhibit relatively weaker MAO-B inhibition compared to the C5- and C6-substituted derivatives. The conclusion can therefore be made that 1-indanone and 1-indanol are promising scaffolds for the future design of MAO-B inhibitors with high inhibition potency, especially when substitution takes place on C5 or C6.

Based on the above, the following recommendations can be made for the future design of MAO-B inhibitors:

- 1-Indanone and 1-indanol proved to be suitable scaffolds for the design of potent MAO-B inhibitors in this study. It is recommended to expand the series with a wider variety of substituents on C5 and C6. This would yield more useful SAR.
- Compound **1f** was the most potent MAO-B inhibitor of the 1-indanone derivatives and compound **1l** the most potent MAO-B inhibitor of the 1-indanol derivatives in this study. These could be used as lead compounds in the future design of MAO-B inhibitors. Different halogens and alkyl groups may be substituted on the phenyl ring of the substituent to determine which yields the most potent MAO-B inhibition.
- Compound **1f** also exhibited the highest selectivity for MAO-B inhibition in this study and may be used as lead compound to improve the selectivity of MAO-B inhibitors.
- Compound **2a** exhibited the best MAO-A inhibition potency and can be used as a lead compound in the future design of potent MAO-A inhibitors. It is recommended to use small substituents as this study indicated that large substituents does not lead to potent MAO-A inhibition.
- Since compounds **1a**, **1d** and **1k** did not display the selectivity and high MAO-B inhibition potency that were anticipated, this study shows that substitution on C4 is not a viable option for the design of potent and selective MAO-B inhibitors. It is, however, recommended that the structural basis for the low MAO-B inhibition potency of the C4-substituted 1-Indanone and 1-indanol derivatives be investigated to identify key residues in the MAO-B active site that may restrict the binding of inhibitors. This would assist in the design of inhibitors that avoid interactions with these residues.

Bibliography

Aarre, T.F. 2003. Phenelzine efficacy in refractory social anxiety disorder: a case series. *Nordic journal of psychiatry.* 57:313-315.

Andree, T.H. & Clark, D.E. 1982. Characteristics and specificity of phenelzine and benzerazide as inhibitors of benzylamine oxidase and monoamine oxidase. *Biochemical pharmacology*. 31:825-830.

Akhondzadeh, S., Tavakolian, R., Davari-Ashtiani, R., Arabgol, F. & Amini, H. 2003. (R)-deprenyl in the treatment of attention deficit hyperactivity disorder in children: a double blind and randomized trial. *Progress in neuro-psychopharmacology & biological psychiatry.* 27:841-845.

Arai, R., Horiike, K. & Hasegawa, Y. 1998. Dopamine-degrading activity of monoamine oxidase is not detected by histochemistry in neurons of the substantia nigra pars compacta of the rat. *Brain research.* 812:275-278.

Allain, H., Lieury, A., Brunet-Bourgin, F., Mirabaud, C., Trebon, P., Le Coz, F. & Gandon, J.M. 1992. Antidepressants and cognition: comparative effects of moclobemide, viloxazine and maprotiline. *Psychopharmacology.* 106(Suppl):S56-61.

Aluf, Y., Vaya, J., Khatib, S. & Finberg, J.P. 2011. Alterations in striatal oxidative stress level produced by pharmacological manipulation of dopamine as shown by a novel synthetic marker molecule. *Neuropharmacology*. 61:87-94.

Andres, A.M., Soldevila, M., Navarro, A., Kidd, K.K., Oliva, B. & Bertranpetit, J. 2004. Positive selection in MAOA gene is human exclusive: determination of the putative amino acid change selected in the human lineage. *Human genetics*. 115:377-386.

Azzaro, A.J., VanDenBerg, C.M., Blob, L.F., Kemper, E.M., Sharoky, M., Oren, D.A. & Campbell, B.J. 2006. Tyramine pressor sensitivity during treatment with the selegiline transdermal system 6 mg/24 h in healthy subjects. *Journal of clinical pharmacology*. 46:933-944.

Bach, A.W., Lan, N.C., Johnson, D.L., Abell, C.W., Bembenek, M.E., Kwan, S.W., Seeburg, P.H. & Shih, J.C. 1988. CDNA cloning of human liver monoamine oxidase A and B: molecular basis of differences in enzymatic properties. *Proceedings of the national academy of sciences of the United States of America.* 85:4934-4938.

Bakhle, Y.S. 1990. Pharmacokinetic and metabolic properties of lung. *British journal of anaesthesia*. 65:79-93.

Baker, G.B., Wong, J.T., Yeung, J.M. & Coutts, R.T. 1991. Effects of the antidepressant phenelzine on brain levels of gamma-aminobutyric acid (GABA). *Journal of affective disorders*. 21:207-211.

Bar-Am, O., Amit, T., Youdim, M.B. 2004a. Contrasting neuroprotective and neurotoxic actions of respective metabolites of antiparkinson drugs rasagiline and selegiline. *Neuroscience letters.* 355:169-172.

Bar-Am, O., Yogev-Falach, M., Amit, T., Sagi, Y. & Youdim, M.B.H. 2004b. Regulation of protein kinase C by the antiparkinson drug, MAO-B inhibitor, rasagiline and its derivatives, *in vivo*. *Journal of neurochemistry*. 89:1119-1125.

Bar-Am, O., Amit, T., Youdim, M.B. *2017*. Aminoindan and hydroxyaminoindan, metabolites of rasagiline and ladostigil, respectively, exert neuroprotective properties *in vitro*. *Journal of neurochemistry.* 103:500-508.

Bar-Am, O., Weinreb, O., Amit, T., Youdim, M.B. 2010. The neuroprotective mechanism of 1-(R)-aminoindan, the major metabolite of the antiparkinsonian drug rasagiline. *Journal of neurochemistry.* 112:1131-1137.

Bieck, P.R. & Antonin, K.H. 1988. Oral tyramine pressor test and the safety of monoamine oxidase drugs: comparison of brofaromine and tranylcypromine in healthy subjects. *Journal of clinical pschycopharmacology.* 8:237-245.

Binda, C., Newton-Vinson, P., Hubalek, F., Edmondson, D.E & Mattevi, A. 2002. Structure of human monoamine oxidase B, a drug target for the treatment of neurological disorders. *Nature structural & molecular biology*. 9:22-26.

Binda, C., Li, M., Hubalek, F., Restelli, N., Edmondson, D.E & Mattevi, A. 2003. Insights into the mode of inhibition of human mitochondrial monoamine oxidase B from high-resolution crystal structures. *Proceedings of the national academy of sciences.* 100:9750-9755.

Binda, C., Hubálek, F., Li, M., Herzig, Y., Sterling, J., Edmondson, D.E. & Mattevi, A. 2005. Binding of rasagiline-related inhibitors to human monoamine oxidases: a kinetic and crystallographic analysis. *Journal of medicinal chemistry*. 48:8148-8154.

Binda, C., Wang, J., Pisani, L., Caccia, C., Carotti, A., Salvati, P., Edmondson, D.E. & Mattevi, A. 2007. Structures of human monoamine oxidase B complexes with selective noncovalent inhibitors: safinamide and coumarin analogs. *Journal of medicinal chemistry.* 50:5848–5852.

Binda, C., Mattevi, A. & Edmondson, D.E. 2011. Structural properties of human monoamine oxidases A and B. *International review of neurobiology*. 100:1-11.

Birkmayer, W., Riederer, P., Youdim, M.B.H. & Linauer, W. 1975. The potentiation of the anti-akinetic effect after L-dopa treatment by an inhibitor of MAO-B, L-deprenyl. *Journal of neural transmission*. 36:303–326.

Birkmayer, W., Riederer, P., Abrozi, L. & Youdim, M.B.H. 1977. Implications of combined treatment with "madopar" and L-deprenyl in Parkinson's disease. A long-term study. *Lancet*. 1:439–443.

Blob, L.F., Sharoky, M., Campbell, B.J., Kemper, E.M., Gilmor, M.G., VanDenBerg, C.M. & Azzaro, A.J. 2007. Effects of a tyramine-enriched meal on blood pressure response in healthy male volunteers treated with selegiline transdermal system 6 mg/24 hour. *CNS Spectrums.* 12:25-34.

Bond, P.A. & Cundall, R.L. 1977. Properties of monoamine oxidase (MAO) in human blood platelets, plasma, lymphocyts and granulocytes. *Clinica chimica acta*. 80:317-326.

Bongioanni, P., Gemignani, F., Boccardi, B., Borgna, M. & Rossi, B. 1997. Platelet monoamine oxidase molecular activity in demented patients. *Italian journal of neurological sciences.* 18:151-156.

Boomsma, F., Van Dijk, J., Bhaggoe, U.M., Bouhuizen, A. & Van der Meiracker, A.H. 2000. Variation in semicarbazide-sensitive amine oxidase activity in plasma and tissues of mammals. *Comparative biochemistry and physiology part c: pharmacology, toxicology and endocrinology.*126:69-78.

Boor, P.J., Hysmith, R.M. & Sanduja, R. 1990. A role for a new vascular enzyme in the metabolism of xenobiotic amines. *Circulation research.* 66:249-252.

Borgohain, R., Szasz, J., Stanzione, P., Meshram, C., Bhatt, M., Chirilineau, D., Stocchi, F., Lucini, V., Giuliani, R., Forrest, E., Rice, P., Anand, R. & Study 016 Investigators. 2014a. Randomized trial of safinamide add-on to levodopa in Parkinson's disease with motor fluctuations. *Movement disorders*. 29:229-237.

Borgohain, R., Szasz, J., Stanzione, P., Meshram, C., Bhatt, M.H., Chirilineau, D., Stocci, F., Lucini, V., Giuliani, R., Forrest, E., Rice, P., Anand, R. & Study 018 Investigators. 2014b. Two-year, randomized, controlled study of safinamide as add-on to levodopa in mid to late Parkinson's disease. *Movement disorders*. 29:1273-1280.

Borštnar, R., Repič, M., Kržan, M., Mavri, J. & Vianello, R. 2011. Irreversible inhibition of monoamine oxidase B by the antiparkinsonian medicines rasagiline and selegiline: A computational study. *European journal of organic chemistry.* 32:6419-6433.

Brunner, H.G., Nelen, M.R., Zandvoort, P., Abeling, N., Gennip, A.H., Wolter, E.C., Kuiper, M.A., Roper, H.H. & Oust, B.A. 1993. X-linked borderline mental retardation with prominent behavioral disturbance: phenotype, genetic localization, and evidence for disturbed monoamine metabolism. *American journal of human genetics*. 52:1032-1039.

Caccia, C., Maj, R., Calabresi, M. Maestroni, S., Faravelli, L., Curatolo, L., Salvati, P. & Fariello, R.G. 2006. Safinamide: from molecular targets to a new antiparkinson drug. *Neurology*. 67(Suppl):S18-23.

Cattaneo, C., Caccia, C., Marzo, A., Maj, R & Fariello, R.G. 2003. Pressor response to intravenous tyramine in healthy subjects after safinamide, a novel neuroprotectant with selective, reversible monoamine oxidase B inhibition. *Clinical neuropharmacology*. 26:213-217.

Cai, Z. 2014. Monoamine oxidase inhibitors: promising therapeutic agents for Alzheimer's disease (Review). *Molecular medicine reports.* 9:1533-1541.

Callingham, B.A. 1977. Substrate selective inhibition of monoamine oxidase by mexiletine. *British journal of pharmacology.* 61:118-119.

Caspi, A., McClay, J., Moffitt, T.E., Mill, J., Martin, J., Craig, I.W., Taylor, A. & Poulton, R. 2002. Role of genotype in the cycle of violence in maltreated children. *Science.* 297:851-853.

Chen, K., Wu, H.F. & Shih, J.C. 1993. The deduced amino acid sequences of human platelet and frontal cortex monoamine oxidase B are identical. *Journal of neurochemistry*. 61:187-190.

Chen, K., Ou, X.M., Chen, G., Choi, S.H. & Shih, J.C. 2005. R1, a novel repressor of the human monoamine oxidase A. *Journal of biological chemistry.* 280:11552-11559.

Chen, J.J. & Swope, D.M. 2005. Clinical pharmacology of rasagiline: a novel, second-generation propargylamine for the treatment of Parkinson disease. *Journal of clinical pharmacology.* 45:878-894.

Chen, J.J., Swope, D.M. & Dashtipour, K. 2007. Comprehensive review of rasagiline, a second-generation monoamine oxidase inhibitor, for the treatment of Parkinson's disease. *Clinical therapeutics.* 29:1825-1849.

Collins G.G.S. & Sandler, M. 1971. Human blood platelet monoamine oxidase. *Biochemical pharmacology.* 20:289–296.

Da Prada, M., Kettler, R., Burkard, W.P. & Haefely, W.E. 1984. Moclobemide, an antidepressant with short-lasting MAO-A inhibition: brain catecholamines and tyramine pressor effects in rats. (*In* Tipton, K.F., Dostert, P. & Strolin Benedetti, M., *eds.* Monoamine oxidase and disease. London: Academic press. p. 137-154).

De Colibus, L., Li, M., Binda, C., Lustig, A., Edmondson, D.E. & Mattevi, A. 2005. Three-dimensional structure of human monoamine oxidase A (MAO A): relation to the structures of rat MAO A and human MAO B. *Proceedings of the national academy of sciences of the United States of America.* 102:12684-12689.

De Lau, L.M. & Breteler, M.M. Epidemiology of Parkinson's disease. 2006. *Lancet neurology.* 5:525-535.

DeMaagd, G. & Philip, A. 2015. Parkinson's disease and its management. Part 3: nondopaminergic and nonpharmacological treatment options. *Physical therapy*. 40: 668-679.

Delumeau, J.C., Bentué-Ferrer, D., Gandon, J.M., Amrein, R., Belliard, S. & Allain H. 1994. Monoamine oxidase inhibitors, cognitive functions and neurodegenerative diseases. *Journal of neural transmission.* 41(Suppl):259-266.

Denney, R.M. & Denney, C.B. 1985. An update on the identity crisis of monoamine oxidase: new and old evidence for the independence of MAO-A and B. *Pharmacology & therapeutics.* 30:227-258.

Di Stefano, A.F. & Rusca, A. 2001. Pressor response to oral tyramine during co-administration with safinamide in healthy volunteers. *Naunyn-Schmiedeberg's archives of pharmacology*. 384:505-515.

Donnelly, C.H. & Murphy, D.L. 1977. Substrate- and inhibitor-related characteristics of human platelet monoamine oxidase. *Biochemical pharmacology.* 26:852-858.

Dooley, DM. 1999. Structure and biogenesis of topaquinone and realted cofactors. *Journal of biological inorganic chemistry*. 4:1-11.

Dostert, P.L., Strolin-Benedetti, M., Tipton, K.F. 1989. Interactions of monoamine oxidase with substrates and inhibitors. *Medical research reviews*. 9:45-89.

Edmondson, D.E. 1995. Structure activity studies of the substrate binding site in monoamine oxidase B. *Biochimie*. 77:643-650.

Edmondson, D.E., De Colibus, L., Binda, C., Li, M. & Mattevi, A. 2007a. New insights into the structures and functions of human monoamine oxidases A and B. *Journal of neural transmission.* 114:703-705.

Edmondson, D.E., Binda, C. & Mattevi, A. 2007b. Structural insights into the mechanism of amine oxidation by monoamine oxidases A and B. *Archives of biochemistry and biophysics.* 464:269-276.

Edmondson, D.E., Binda, C., Wang, J. Upadhyay, A.K. & Mattevi, A. 2009. Molecular and mechanistic properties of the membrane-bound mitochondrial monoamine oxidases. *Biochemistry*. 48:4220-4230.

Elkashef, A., Fudala, P.J., Gorgon, L., Li, S.H., Kahn, R., Chiang, N., Vocci, F., Collins, J., Jones, K., Boardman, K. & Sather M. 2006. Double-blind, placebo-controlled trial of selegiline transdermal system (STS) for the treatment of cocaine dependence. *Drug and alcohol dependence*. 85:191-197.

Ernberg, K., McGrath, A.P., Peat, T.S., Adams, T.E., Xiao, X., Pham, T., Newman, J., McDonald, I.A., Collyer, C.A. & Guss, J.M. 2010. A new crystal form of human vascular adhesion protein-1. *Acta crystallographica, section F.* 66:1572-1578.

Fagervall, I. & Ross, S.B. 1986. A and B forms of monoamine oxidase within the mono-aminergic neurons of the rat brain. *Journal of neurochemistry.* 47:569-576.

Fernandez, H. H. & Chen, J. J. 2007. Monoamine oxidase-B inhibition in the treatment of Parkinson's disease. *Pharmacotherapy.* 27(Suppl):174-185S.

Filic, V., Vladic, A., Stefulj, J., Cicin-Sain, L., Balija, M., Sucic, Z. & Jernej, B. 2005. Monoamine oxidases A and B gene polymorphisms in migraine patients. *Journal of* the *neurological sciences.* 228:149-153.

Finberg, J.P. & Tenne, M. 1982. Relationship between tyramine potentiation and selective inhibition of monoamine oxidase types A and B in the rat vas deferens. *British journal of pharmacology*. 77:13-21.

Finberg, J.P. & Youdim, M.B. 2002. Pharmacological properties of the antiparkinson drug rasagiline; modification of endogenous brain amines, reserpine reversal, serotonergic and dopaminergic behaviours. *Neuropharmacology.* 43:1110-1118.

Finberg, J.P. & Gillman, P.K. 2011. Selective inhibitors of monoamine oxidase type B and the cheese effect. (*In* Youdim, M.B. & Riederer, P., *eds.* International Review of Neurobiology. Burlington, VT: Academic Press. p. 169-190).

Finberg, J.P. 2014. Update on the pharmacology of selective inhibitors of MAO-A and MAO-B: focus on modulation of CNS monoamine neurotransmitter release. *Pharmacology & therapeutics.* 143:133-152.

Finberg, J.P.M. & Rabey, J.M. 2016. Inhibitors of MAO-A and MAO-B in Psychiatry and Neurology. *Frontiers in pharmacology.* 7:340-355.

Fišar, Z. & Hroudová, J. 2010. Intracellular signalling pathways and mood disorders. *Folia biologica.* 56:135-148.

Fišar, Z., Hroudová, J. & Raboch, J. 2012. Neurotransmission in mood disorders. (In: Juruena, M.F., *ed*. Clinical, Research and Treatment Approaches to Affective Disorders. Rijeka, Croatia: InTech. P. 191-234).

Fišar, Z. 2016. Drugs related to monoamine oxidase activity. *Progress in neuro-psychopharmacology and biological psychiatry.* 69:112-124.

Fitzgerald, D.H., Tipton, K.F & Lyles, G.A. 1998. Studies on the behaviour of semicarbazide-sensitive amine oxidase in Sprague-Dawley rats treated with the monoamine oxidase inhibitor tranylcypromine. *Journal of neural transmission.* 52(Suppl):259-264.

Foley, P., Gerlach, M., Youdim, M. & Riederer, P. 2000. MAO-B inhibitors: multiple roles in the therapy of neurodegenerative disorders? *Parkinsonism and related disorders.* 6:25-47.

Fowler, J.S., Volkow, N.D., Wang, G.J., Pappas, N., Logan, J., Macgregor, R., Alexoff, D., Shea, C., Schlyer, D., Wolf, A.P., Warner, D., Zezulkova, I. & Cilento, R. 1996. Inhibition of monoamine oxidase B in the brains of smokers. *Nature.* 379:733-736.

Fowler, J. S., Volkow, N.D., Wang, G.J., Logan, J., Pappas, N., Shea, C. & Macgregor, R. 1997. Age-related Increases in brain monoamine oxidase B in living healthy human subjects. *Neurobiology of aging.* 18:431-435.

Fowler, J.S., Logan, J., Shumay, E., Alia-Klein, N., Wang, G.J. & Volkow, ND. 2015. Monoamine oxidase: radiotracer chemistry and human studies. *Journal of labelled compounds and radiopharmaceuticals.* 58:51-64.

Gahr, M., Schonfeldt-Lecuona, C., Kolle, M.A. & Freudenmann, R.W. 2013. Withdrawal and discontinuation phenomena associated with tranylcypromine: a systemic review. *Pharmacopsychiatry.* 46:123-129.

Gareri, P., Falconi, U., De Fazio, P. & De Sarro, G. 2000. Conventional and new antidepressant drugs in the elderly. *Progress in neurobiology.* 61:353-396.

Garret, N.J., Mantle, T.J. & Tipton, K. 1976. Inhibition of monoamine oxidase by amphetamine and related compounds. *Biochemical pharmacology.* 25:2073-2077.

Geha, R.M., Rebrin, I., Chen, K. & Shih, J.C. 2001. Substrate and inhibitor specificities for human monoamine oxidase A and B are influenced by a single amino acid. *Journal of biological chemistry*. 276:9877-9882.

Gillman, P.K. 2011. Advances pertaining to the pharmacology and interactions of irreversible non-selective monoamine oxidase inhibitors. *Journal of clinical psychopharmacology.* 31:66-74.

Glover, V. & Sandler, M. 1986. Clinical chemistry of monoamine oxidase. *Cell biochemistry and function.* 4:89-97.

Goding, J.W. & Howard, M.C. 1998. Ecto-enzymes of lymphoid cells. *Immunological reviews.* 161:5-10.

Golwyn, D.H. 1988. Cocaine abuse treated with phenelzine. *International journal of the addictions.* 23:897-905.

Gregoire, L., Jourdain, V.A., Townsend, M. Roach, A. & Di Paolo, T. 2013. Safinamide reduces diskinesias and prolongs L-dopa antiparkinsonian effect in parkinsonian monkeys. *Parkinsonism & related disorders*. 19:508-514.

Grimsby, J., Chen, K., Wang, L.J., Lan, N.C. & Shih, J.C. 1991. Human monoamine oxidase A and B genes exhibit identical exon-intron organisation. *Proceedings of the national academy of sciences of the United States of America.* 88:3637-3641.

Hare, P.D. & Van Staden, J. 1994. Cytokinin oxidase: biochemical features and physiological significance. *Physiologia plantarum*. 91:128-136.

Harvey, B.H., Duvenhage, I., Viljoen, F., Scheepers, N., Malan, S.F., Wegener, G., Brink C.B. & Petzer, J.P. 2010. Role of monoamine oxidase, nitric oxide synthase and regional brain monoamines in the antidepressant-like effects of methylene blue and selected structural analogues. *Biochemical pharmacology.* 80:1580-1591.

Heikkila, R.E., Manzino, L., Cabbat, F.S. & Duvoisin, R.C. 1984. Protection against the dopaminergic neurotoxicity of 1-methyl-4-phenyl-1,2,5,6-tetrahydropyridine by monoamine oxidase inhibitors. *Nature.* 311:467-469.

Ho, M., Cherng, C.G., Tsai, Y.N., Chiang, C.Y., Chuang, J., Kao, S. & Yu, L. 2009. Chronic treatment with monoamine oxidase-B inhibitors decreases cocaine reward in mice. *Psychopharmacology*. 205:141-149.

Holschneider, D.P., Chen, K., Seif, I. & Shih, J.C. 2001. Biochemical, behavioral, physiologic, and neurodevelopmental changes in mice deficient in monoamine oxidase A or B. *Brain research bulletin.* 56:453-462.

Hubálek, F., Binda, C., Li, M., Herzig, Y., Sterling, J., Youdim, M.B., Mattevi, A. & Edmondson, D.E. 2004. Inactivation of purified human recombinant monoamine oxidases A and B by rasagiline and its analogues. *Journal of medicinal chemistry*. 47:1760-1766.

Hubálek, F., Binda, C., Khalil, A., Li, M., Mattevi, A., Castagnoli, N. & Edmondson, D.E. 2005. Demonstration of isoleucine 199 as a structural determinant for the selective inhibition of human monoamine oxidase B by specific reversible inhibitors. *Journal of biological chemistry.* 280:15761-15766.

Hysmith, R.M. & Boor, P.J. 1988. Role of benzylamine oxidase in the cytotoxicity of allylamine toward aortic smooth muscle cells. *Toxicology.* 51:133-145.

Jiang, S., Xin, R., Lin, S., Qian, Y., Tang, G., Wang, D. & Wu, X. 2001. Linkage studies between attention-deficit hyperactivity disorder and the monoamine oxidase genes. *American journal of medical genetics.* 105:783-788.

Kay, C.W.M., El Mkami, H., Molla, G., Pollegioni, L. & Ramsay, R.R. 2007. Characterisation of the covalently-bound anionic flavin radical in monoamine oxidase A by electron paramagnetic resonance. *Journal of the american chemical society.* 129:16091-16097.

Kearney, E.B., Salach, J.J., Walker, W.H., Seng, R.L., Kenney, W., Zeszotek, E. & Singer, T.P. 1971. The covalently-bound flavin of hepatic monoamine oxidase. 1. Isolation and sequence of a flavin peptide and evidence for binding at the 8alpha position. *European journal of biochemistry*. 24:321-327.

Kennedy, B.P., Ziegler, M.G., Alford, M., Hansen, L.A., Thal, L.J. & Masliah, E. 2003. Early and persistent alterations in prefrontal cortex MAO A and B in Alzheimer's disease. *Journal of neural transmission*. 110:789-801.

Kinemuchi, H., Morikawa, F., Tajima, H. & Kamijo, K. 1982. Enzymatic characteristics of a clorgyline and L-deprenyl-resistant amine oxidase in human placenta. (*In* Kamijo, K., Usdin, E. & Nagatsu, T., *eds.* Monoamine oxidase: basic and clinical frontiers. Amsterdam: Excerpta Medica. p. 112-124).

Kinemuchi, H., Morikawa, F., Ueda, T. & Arai, Y. 1986. Studies of monoamine oxidase and semicarbazide-sensitive amine oxidase. Part I. Inhibition by a selective monoamine oxidase-B inhibitor MD 780236. *Japanese journal of pharmacology.* 41:183-189.

Kinemuchi, H., Sugimoto, H., Obata, T., Satoh, N. & Ueda, S. 2004. Selective inhibitors of membrane-bound semicarbazide-sensitive amine oxidase (SSAO) activity in mammalian tissues. *Neurotoxicology.* 25:325-335.

Klinman, J.P. & Mu, D. 1994. Quinoenzyme in biology. *Annual review of biochemistry.* 63:299-344.

Klinman, J.P. 1996. New quinofactors in eukaryotes. *Journal of biological chemistry.* 271:27189-27192.

Knoll, J., Ecseri, Z., Kelemen, K., Nievel, J., & Knoll, B. 1965. Phenylisopropylmethylpropinylamine (E-250), a new spectrum psychic energizer. *Archives internationales de pharmacodynamie et de thérapie.* 155:154-164.

Knoll, J. & Magyar, K. 1972. Some puzzling pharmacological effects of monoamine oxidase inhibitors. *Advances in biochemical psychopharmacology.* 5:393-408.

Knowles, P.F. & Dooley, D.M. 1994. Amine oxidases. (*In* Sigel, H. & Sigel, A., *eds*. Metal ions in biological systems. New York: Marcel Dekker. p. 361-403).

Korchounov, A., Winter, Y. & Rossy, W. 2012. Combined beneficial effect of rasagiline on motor function and depression in *de novo* Parkinson's disease. *Clinical neuropharmacology.* 35:121-124.

Kruk, Z.L., Moffet, A. & Scott, D.F.J. 1980. Platelet monoamine oxidase activity in epilepsy. *Journal of neurology, neurosurgery & psychiatry.* 43:68-70.

Kulisevsky, J. 2016. Safinamide- a unique treatment targeting both dopaminergic and non-dopaminergic systems. *European neurological review*. 11:101-105.

Kurkijärvi, R., Adams, D.H., Leino, R., Möttönen, T., Jalkanen, S. & Salmi, M. 1998. Circulating form of human vascular adhesion protein-1 (VAP-1): increased serum levels in inflammatory liver disease. *Journal of immunology.* 161:1549-1557.

Lader, M.H., Sakalis, G. & Tansella, M. 1970. Interactions between sympathomimetic amines and a new monoamine oxidase inhibitor. *Psychopharmacologia.* 18:118-123.

Langston, J.W., Irwin, I., Langston, E.B. & Forno, L.S. 1984. Pargyline prevents MPTP-induced parkinsonism in primates. *Science.* 225:1480-1482.

Legoabe, L.J., Petzer, A. & Petzer, J.P. 2014. α-Tetralone derivatives as inhibitors of monoamine oxidase. *Bioorganic & medicinal chemistry letters.* 24:2758-2763.

Li, M., Hubálek, F., Newton-Vinson, P. & Edmondson, D.E. 2002. High-level expression of human liver monoamine oxidase A in *Pichia pastoris*: comparison with the enzyme expressed in *Saccharomyces cerevisiae*. *Protein expression and purification*. 24:152-162.

Lotufo-Neto, F., Trivedi, M. & Thase, M.E. 1999. Meta-analysis of the reversible inhibitors of monoamine oxidase type A moclobemide and brofaromine for the treatment of depression. *Neuropsychopharmacology*. 20:226-247.

Lunelli, M., Di Paolo, M.L., Biadene, M., Calderone, V., Battistutta, R., Scarpa, M., Rigo, A. & Zanotti, G. 2005. Crystal structure of amine oxidase from bovine serum. *Journal of molecular biology.* 346:991-1004.

Lyles, G.A., Marshall, C.M.S., McDonald, I.A., Bey, P. & Ralfreyman, M.G. 1987. Inhibition of rat aorta semicarbazide-sensitive amine oxidase by 2-phenyl-3-haloallylamines and related compounds. *Biochemical pharmacology.* 36:2847-2853.

Lyles, G.A. 1995. Substrate-specificity of mammalian tissue-bound semicarbazide-sensitive amine oxidase. *(In* Yu, P.M., Tipton, K.F. & Boulton, A.A., *eds.* Current neurochemical and pharmacological aspects of biogenic amines. Utrecht: Elsevier. p. 293-303).

Lyles, G.A. 1996. Mammalian plasma and tissue-bound semicarbazide-sensitive amine oxidase: biochemical, pharmalogical and toxicological aspects. *International journal of biochemistry & cell biology.* 28:259-274.

Ma, J., Yoshimura, M., Yamashita, E., Nakagawa, A., Ito, A. & Tsukihara, T. 2004. Structure of rat monoamine oxidase A and its specific recognitions for substrates and inhibitors. *Journal of molecular biology.* 338:103-114.

Macleod, A.D., Counsell, C.E., Ives, N. & Stowe, R. 2005. Monoamine oxidase B inhibitors for early Parkinson's disease. The *Cochrane database of systematic reviews*. 20:CD004898.

Magyar, K. 2011. The pharmacology of selegiline. *International review of neurobiology.* 100:65-84.

Mann, J.J., Aarons, S.F., Wilner, P.J., Keilp, J.G., Sweeney, J.A., Pearlstein, T., Frances A.J., Kocsis, J.H. & Brown, R.P. 1989. A controlled study of the antidepressant efficacy and side effects of (-)-deprenyl. A selective monoamine oxidase inhibitor. *Archives of general psychiatry.* 46:45-50.

Marquet, A., Kupas, K., Johne, A., Astruc, B., Patat, A., Krösser, S. & Kovar, A. 2012. The effect of safinamide, a novel drug for Parkinson's disease, on pressor response to oral tyramine: a randomized, double-blind, clinical trial. *Clinical pharmacology and therapeutics*. 92:450-457.

Mawhinney, M., Cole, D. & Azzaro, A.J. 2003. Daily transdermal administration of selegiline to guinea-pigs preferentially inhibits monoamine oxidase activity in brain when compared with intestinal and hepatic tissues. *Journal of pharmacy and pharmacology*. 55:27-34.

Maycock, A.L., Abeles, R.H., Salach, J.I. & Singer, T.P. 1976. The structure of the covalent adduct formed by the interaction of 3-dimethylamino-1-propyne and the flavine of mitochondrial amine oxidase. *Biochemistry.* 15:114-125.

McCormack, P.L. 2014. Rasagiline: a review of its use in the treatment of idiopathic Parkinson's disease. *Cns drugs.* 28:1083-1097.

McIntire, W.S. & Hartmann, C. 1992. Copper-containing amine oxidases. (*In* Davidson, V.L., *ed.* Principles and applications of quinoproteins. New York: Marcel Dekker. p. 97-171).

McEntire, J.E., Buchok, S.J. & Papermaster, B.W. 1979. Determination of platelet monoamine oxidase activity in human platelet-rich plasma – a new microfluorescent assay utilizing kynuramine as substrate. *Biochemical pharmacology.* 28:2345-2347.

Meyer, J.H., Ginovart, N., Boovariwala, A., Sagrati, S., Hussey, D., Garcia, A., Young, T., Praschak-Rieder, N., Wilson, A.A. & Houle, S. 2006. Elevated monoamine oxidase a levels in the brain: an explanation for the monoamine imbalance of major depression. *Archives of general psychiatry.* 63:1209-1216.

Merikangas, K.R. & Merikangas, J.R. 1995. Combination monoamine oxidase inhibitor and beta-blocker treatment of migraine, with anxiety and depression. *Biological psychiatry.* 38:603-610.

Mitoma, J. & Ito, A.J. 1992. Mitochondrial targeting signal of rat liver monoamine oxidase B is located at its carboxy terminus. *Journal of biochemistry.* 111:4-20.

Mohammadi, M.R., Ghanizadeh, A., Alaghband-Rad, J., Tehranidoost, M., Mesgarpour, B. & Soori H. 2004. Selegiline in comparison with methylphenidate in attention deficit hyperactivity disorder children and adolescents in a double-blind, randomized clinical trial. *Journal of child and adolescent psychopharmacology.* 14:418-425.

Moranta, D., Esteban, S. & García-Sevilla, J.A. 2004. Differential effects of acute cannabinoid drug treatment, mediated by CB1 receptors, on the *in vivo* activity of tyrosine and tryptophan hydroxylase in the rat brain. *Naunyn-Schmiedeberg's archives of pharmacology.* 369:516-524.

Mostert, S., Petzer, A. & Petzer, J.P. 2015. Indanones as high potency reversible inhibitors of monoamine oxidase. *Chemmedchem.* 10:862-873.

Mu, D., Janes, S.M., Smith, A.J., Brown, D.E., Dooley, D.M. & Klinman, J.P. 1992. Tyrosine codon corresponds to topa-quinone at the active site of copper amine oxidases. *Journal of biological chemistry*. 267:7979-7982.

Mure, M., Mills, S.A. & Klinman, J.P. 2002. Catalytic mechanism of the topa quinone containing copper amine oxidases. *Biochemistry.* 41:9269-9278.

Murray, A. T., Dowley, M. J. H., Pradaux-Caggiano, F., Baldansuren, A., Fielding, A. J., Tuna, F., Hendon, C. H., Walsh, A., Lloyd-Jones, G. C., John, M. P. & Carbery, D. R., 2015. Catalytic amine oxidation under ambient aerobic conditions: mimicry of monoamine oxidase B. *Angewandte chemie- international edition*. 54:8997-9000.

Naoi, M., Maruyama, W., Youdim, M.B. Yu, P. & Boulton, A.A. 2003. Anti-apoptotic function of propargylamine inhibitors of type-B monoamine oxidase. *Inflammopharmacology.* 11:175-181.

Naoi, M., Maruyama, W. & Inaba-Hasegawa, K. 2012. Type A and B monoamine oxidase in age-related neurodegenerative disorders: their distinct roles in neuronal death and survival. *Current topics in medicinal chemistry.* 12:2177-2188.

Naoi, M., Riederer, P. & Maruyama, W. 2016. Modulation of monoamine oxidase (MAO) expression in neuropsychiatric disorders: genetic and environmental factors involved in type A MAO expression. *Journal of neural transmission*. 123:91-106.

Naylor, G.J., Smith, A.H. & Connelly, P. 1987. A controlled trial of methylene blue in severe depressive illness. *Biological psychiatry.* 22:657-659.

Newton-Vinson, P., Hubälek, F. & Edmondson, D.E. 2000. High-level expression of human liver monoamine oxidase B in *Pichia pastoris*. *Protein expression and purification.* 20:334-345.

Nicotra, A., Pierucc, F., Parvez, H. & Senatori, O. 2004. Monoamine oxidase expression during development and aging. *Neurotoxicology.* 25:155-165.

Niederhofer, H. 2003. Selegiline and methylphenidate in treatment of ADHD. *Psychiatria danubina*. 15:3-6.

Novaroli, L., Reist, M., Favre, E., Carotti, A., Catto, M. & Carrupt, P.A. 2005. Human recombinant monoamine oxidase B as reliable and efficient enzyme source for inhibitor screening. *Bioorganic & medicinal chemistry*. 13:6212-6217.

Obata, T. & Yamanaka, Y. 2000. Inhibition of monkey brain semicarbazide-sensitive amine oxidase by various antidepressants. *Neuroscience letters.* 286:131-133.

Olanow, C.W., Hauser, R.A., Jankovic, J., Langston, W., Lang, A., Poewe, W., Tolosa, E., Stocchi, F., Melamed, E., Eyal, E. & Rascol, O. 2008. A randomized, double-blind, placebo-controlled, delayed start study to assess rasagiline as a disease modifying therapy in Parkinson's disease (the ADAGIO study): rationale, design, and baseline characteristics. *Movement disorders.* 23:2194-2201.

Olanow, C.W., Rascol, O., Hauser, R., Feigin, P.D., Jankovic, J., Lang, A., Langston, W., Melamed, E., Poewe, W., Stocchi, F., Tolosa, E & ADAGIO Study Investigators. 2009. A double-blind, delayed-start trial of rasagiline in Parkinson's disease. *The new England journal of medicine.* 361:1268-1278.

Oldfield, V., Keating, G.M. & Perry, C.M. 2007. Rasagiline: a review of its use in the management of Parkinson's disease. *Drugs*. 67:1725-1747.

Ooi, J., Hayden, M.R. & Pouladi, M.A. 2015. Inhibition of excessive monoamine oxidase A/B activity protects against stress-induced neuronal death in Huntington disease. *Molecular neurobiology*. 52:1850-1861.

O'Sullivan, J., Unzeta, M., Healy, J., O'Sullivan, M., Davey, G. & Tipton, K. 2004. Semicarbazide-sensitive amine oxidases: enzymes with quite a lot to do. *Neurotoxicology.* 25:303-315.

Panisset, M., Chen, J.J., Rhyee, S.H., Conner, J. & Mathena, J. 2014. Serotonin toxicity association with concomitant antidepressants and rasagiline treatment: retrospective study (STACCATO). *Pharmacotherapy*. 34:1250-1258.

Petzer, A., Pienaar, A. & Petzer, J.P. 2013. The inhibition of monoamine oxidase by esomeprazole. *Drug research (Stuttgart).* 63:462-467.

Pistacchi, M., Martinello, F., Gioulis, M. & Zambito Marsala, S. 2013. Rasagiline and rapid symptomatic motor effect in Parkinson's disease: review of literature. *Neurology and therapy.* 3:41-66.

Pletscher, A. 1991. The discovery of anti-depressants: A winding path. *Experientia.* 47:4-8.

Podurgiel, S., Collins-Praino, L.E., Yohn, S., Randall, P.A., Roach, A., Lobianco, C. & Salamone, J.D. 2013. Tremorolytic effects of safinamide in animal models of drug-induced parkinsonian tremor. *Pharmacology, biochemistry and behaviour*. 105:105-111.

Rascol, O., Perez-Lloret, S. & Ferreira, J.J. 2015. New treatments for levodopa-induced motor complications. *Movement disorders.* 30:1451-1460.

Ramsay, R.R., Koerber, S.C. & Singer, T.P. 1987. Stopped-flow studies on the mechanism of oxidation of N-methyl-4-phenyltetrahydropyridine by bovine liver monoamine oxidase B. *Biochemistry.* 26:3045-3050.

Ramsay, R.R., Dunford, C. & Gillman, P.K. 2007. Methylene blue and serotonin toxicity: inhibition of monoamine oxidase A (MAO A) confirms a theoretical prediction. *British journal of pharmacology.* 152:946-951.

Ramsay, R.R., Olivieri, A. & Holt, A. 2011. An improved approach to steady-state analysis of monoamine oxidases. *Journal of neural transmission*. 118:1003-1019.

Rebrin, I., Geha, R.M., Chen, K. & Shih, J.C. 2001. Effects of carboxyl-terminal truncations on the activity and solubility of human monoamine oxidase B. *Journal of biological chemistry.* 276:29499-29506.

Reijnders, J.S., Ehrt, U., Weber, W.E., Aarsland, D. & Leentjens, A.F. 2008. A systematic review of prevalence studies of depression in Parkinson's disease. *Movement disorders.* 23:183-189.

Reynolds, G.P., Elsworth, J.D., Blau, K., Sandler, M., Lees, A.J. & Stern, G.M. 1978. Deprenyl is metabolized to methamphetamine and amphetamine in man. *British journal of clinical pharmacology.* 6:542-544.

Richard, I.H., McDermott, M.P., Kurlan, R., Lyness, J.M., Como, P.G., Pearson, N., Factor, S.A., Juncos, J., Serrano Ramos, C., Brodsky, M., Manning, C., Marsh, L., Shulman, L., Fernandez, H.H., Black, K.J., Panisset, M., Christine, C.W., Jiang, W., Singer, C., Horn, S., Pfeiffer, R., Rottenberg, D., Slevin, J., Elmer, L., Press, D., Hyson, H.C., McDonald, W. & SAD-PD Study Group. 2012. A randomized, double-blind, placebo-controlled trial of antidepressants in Parkinson's disease. *Neurology.* 78:1229-1236.

Riederer, P., Reynolds, G.P., Youdim, M.B.H. & Jellinger, K. 1982. *In vitro* tests of MAO inhibitors in human brain tissue: chemical structure and pharmacological action. (In: Kamijo, K., Usdin, E., Nagatsu, T., *eds*. Monoamine oxidase, basic and clinical frontiers.

Excerpta Medica, Amsterdam Oxford Princeton, International Congress Series 564, p 345).

Riederer, P. & Youdim, M.B.H. 1986. Monoamine oxidase activity and monoamine metabolism in brains of parkinsonian patients treated with L-deprenyl. *Journal of neurochemistry.* 46:1359-1365.

Rivera, M., Gutiérrez, B., Molina, E., Torres-González, F., Bellón, J.A., Moreno-Küstner, B., King, M., Nazareth, I., Martínez-González, L.J., Martínez-Espín, E., Muñoz-García, M.M., Motrico, E., Martínez-Cañavate, T., Lorente, J.A., Luna, J.D. & Cervilla, J.A. 2009. High-activity variants of the uMAOA polymorphism increase the risk for depression in a large primary care sample. *American journal of medical genetics.* 150B:395-402.

Rubinstein, S., Malone, M.A., Roberts, W. & Logan, W.J. 2006. Placebo-controlled study examining effects of (R)-deprenyl in children with attention-deficit/hyperactivity disorder. *Journal of child and adolescent psychopharmacology.* 16:404-415.

Sadeghian, M., Mullali, G., Pocock, J.M., Piers, T., Roach, A. & Smith, K.J. 2016. Neuroprotection by safinamide in the 6-hydroxydopamine model of Parkinson's disease. *Neuropathology and applied neurobiology*. 42:423-435.

Sagi, Y., Mandel, S., Amit, T. & Youdim, M.B. 2007. Activation of tyrosine kinase receptor signaling pathway by rasagiline facilitates neurorescue and restoration of nigrostriatal dopamine neurons in post-MPTP-induced parkinsonism. *Neurobiology of disease*. 25:35-44.

Salach, J.I. 1979. Monoamine oxidase from beef liver mitochondria: simplified isolation procedure, properties, and determination of its cysteinyl flavin content. *Archives of biochemistry and biophysics.* 192:128-137.

Salmi, M. & Jalkanen, S. 2002. Enzymatic control of leukocyte traffcking: Role of VAP-1. *Advances in experimental medicine and biology journal.* 512:57-63.

Salminen, T., Smith, D., Jalkanen, S. & Johnson, M. 1998. Structural model of the catalytic domain of an enzyme with cell adhesion activity: human vascular adhesion protein-1 (HVAP-1) D4 domain is an amine oxidase. *Protein engineering, design & selection.* 11:1195-1204.

Samson, J.A., Gurrera, R.J., Nisenson, L. & Schildkraut, J.J. 1995. Platelet monoamine oxidase activity and deficit syndrome schizophrenia. *Psychiatry research*. 56:25-31.

Saura, J., Luque, J.M., Cesura, A.M., Da Prada, M., Chan-Palay, V., Huber, G., Löffler, J. & Richards, J.G. 1994. Increased monoamine oxidase B activity in plaque-associated

astrocytes of Alzheimer brains revealed by quantitative enzyme radioautography. *Neuroscience*. 62:15-30.

Saura, J., Bleuel, Z., Ulrich, J., Mendelowitsch, A., Chen, K., Shih, J.C., Malherbe, P., Da Prada, M. & Richards, J.G. 1996a. Molecular neuroanatomy of human monoamine oxidases A and B revealed by quantitative enzyme radioautography and in situ hybridization histochemistry. *Neuroscience.* 70:755-774.

Saura, J., Nadal, E., van den Berg, B., Vila, M., Bombi, J.A. & Mahy, A. 1996b. Localization of monoamine oxidases in human peripheral tissues. *Life sciences.* 59:1341-1349.

Schapira, A.H.V., Fox, S.H., Hauser, R.A., Jankovic, J., Jost, W.H., Kenney, C., Kulisevsky, J., Pahwa, R., Poewe, W. & Anand, R. 2016. Assessment of safety and efficacy of safinamide as a levodopa adjunct in patients with Parkinson's disease and motor fluctuations: a randomized clinical trial. *Jama neurology*. 74:216-224

Shih, J.C., Chen, K. & Ridd, M.J. 1999. Monoamine oxidase: from genes to behavior. *Annual review of neuroscience.* 22:197-217.

Shih, J.C., Wu, J.B. & Chen, K. 2011. Transcriptional regulation and multiple functions of MAO genes. *Journal of neural transmission.* 118:979-986.

Shulman, K.I., Hermann, N. & Walker, S.E. 2013. Current place of monoamine oxidase inhibitors in the treatment of depression. *Cns drugs.* 27:789-797.

Sieradzan, K., Channon, S., Ramponi, C., Stern, G.M., Lees, A.J. & Youdim, M.B. 1995. The therapeutic potential of moclobemide, a reversible selective monoamine oxidase A inhibitor in Parkinson's disease. *Journal of clinical psychopharmacology.* 15(Suppl):S51-S59.

Siever, L.J. & Coursey, R.D. 1985. Biological markers for schizophrenia and the biological high-risk approach. *The journal of nervous and mental disease.* 173:4-16.

Silverman, R.B. 1995. Radical ideas about monoamine-oxidase. *Accounts of chemical research.* 28:335-342.

Smith, D.J. Salmi, M., Bono, P., Hellman, J., Leu, T. & Jalkanen, S. 1998. Cloning of vascular adhesion protein-1 reveals a novel multifunctional adhesion molecule. *Journal of experimental medicine.* 188:17-27.

Son, S.Y., Ma, J., Kondou, Y., Yoshimura, M., Yamashita, E. & Tsukihara, T. 2008. Structure of human monoamine oxidase A at 2.2-A resolution: the control of opening

the entry for substrates/inhibitors. *Proceedings of the national academy of sciences.* 105:5739-5744.

Sterling, J., Veinberg, A., Lerner, D., Goldenberg, W., Levy, R., Youdim, M. & Finberg, J. 1998. (R)(+)-N-propargyl-1-aminoindan (rasagiline) and derivatives: highly selective and potent inhibitors of monoamine oxidase B. *Journal of neural transmission.* 52(Suppl):301-305.

Stocchi, F., Fossati, C. & Torti, M. 2015. Rasagiline for the treatment of Parkinson's disease: an update. *Expert opinion on pharmacotherapy.* 16:2231-2241.

Stolen, C.M., Yegutkin, G.G., Kurkijärvi, R., Bono, P., Alittalo, K. & Jalkanen, S. 2004. Origins of serum semicarbazide-sensitive amine oxidase. *Circulation research*. 95:50-57.

Strydom, B., Bergh, J.J. & Petzer, J.P. 2010. 8-Aryl- and alkyloxycaffeine analogues as inhibitors of monoamine oxidase. *European journal of medicinal chemistry.* 46:3474-3485.

Sun, Y., Zhang, J., Yuan, Y., Yu, X., Shen, Y. & Xu, Q. 2012. Study of a possible role of the monoamine oxidase A (MAOA) gene in paranoid schizophrenia among a Chinese population. *American journal of medical genetics part B: neuropsychiatric genetics.* 159B:104-111.

Sunderland, T., Cohen, R.M., Molchan, S., Lawlor, B.A., Mellow, A.M., Newhouse, P.A., Tariot, P.N., Mueller, E.A. & Murphy, D.L. 1994. High-dose selegiline in treatment-resistant older depressive patients. *Archives of general psychiatry*. 51:607-615.

Tadic, A., Rujescu, D., Szegedi, A., Giegling, I., Singer, P., Möller, H.J. & Dahmen, N. 2003. Association of a MAOA gene variant with generalized anxiety disorder, but not with panic disorder or major depression. *American journal of medical genetics part B neuropsychiatric genetics.* 117B(1):1-6.

Thebault, J.J., Guillaume, M. & Levy, R. 2004. Tolerability, safety, pharmacodynamics and pharmacokinetics of rasagiline: a potent, selective and irreversible monoamine oxidase type B inhibitor. *Pharmacotherapy*. 24:1295-1305.

Todd, K.G. & Baker, G.B. 2008. Neurochemical effects of the monoamine oxidase inhibitor phenelzine on brain GABA and alanine: A comparison with vigabatrin. *Journal of pharmacy & pharmaceutical sciences.* 11:14s-21s.

Tong, J., Meyer, J.H., Furukawa, Y., Boileau, I., Chang, L.J., Wilson, A.A., Houle, S. & Kish, S.J. 2013. Distribution of monoamine oxidase proteins in human brain:

implications for brain imaging studies. *Journal of cerebral blood flow & metabolism.* 33:863-871.

Tyrer, P. & Shawcross, C. 1988. Monoamine oxidase inhibitors in anxiety disorders. *Journal of psychiatric research.* 22(Suppl):87-98.

Urban, P., Andersen, J.K., Hsu, H.P.P. & Pompom, D. 1991. Comparative membrane locations and activities of human monoamine oxidases expressed in yeast. *Federation of European biochemical societies Letters*. 286:142-146.

Urwin, R.E. & Nunn, K.P. 2005. Epistatic interaction between the monoamine oxidase A and serotonin transporter genes in anorexia nervosa. *European journal of human genetics.* 13:370-375.

Van Den Berg, D., Zoellner, K.R., Ogunrombi, M.O., Malan, S.F., Terre'Blanche, G., Castagnoli, N., Jr., Bergh, J.J. & Petzer, J.P. 2007. Inhibition of monoamine oxidase B by selected benzimidazole and caffeine analogues. *Bioorganic and medicinal chemistry*. 15:3692-3702.

Van Kempen, G.M.J., van Brussel, J.L. & Pennings, E.J.M. 1985. Assay of platelet monoamine oxidase in whole blood. *Clinica chimica acta.* 153:197-202.

Walker, M.C. & Edmondson, D.E. 1994. Structure-activity relationships in the oxidation of benzylamine analogues by bovine liver mitochondrial monoamine oxidase B. *Biochemistry.* 33:7088-7098.

Wachtel, S.R. & Abercrombie, E.D. 1994. L-3,4-dihydroxyphenylalanine-induced dopamine release in the striatum of intact and 6-hydroxydopamine-treated rats: differential effects of monoamine oxidase A and B inhibitors. *Journal of neurochemistry.* 63:108-117.

Wargelius, H.L., Malmberg, K., Larsson, J.O. & Oreland, L. 2012. Associations of MAOA-VNTR or 5HTT-LPR alleles with attention-deficit hyperactivity disorder symptoms are moderated by platelet monoamine oxidase B activity. *Psychiatric genetics.* 22:42-45.

Weinreb, O., Bar-Am, O., Amit, T., Chillag-Talmor, O. & Youdim, M.B. 2004. Neuroprotection via pro-survival protein kinase C isoforms associated with Bcl-2 family members. *Faseb journal.* 18:1471-1473.

Weinreb, O., Amit, T., Bar-Am., O. & Youdim, M.B.H. 2010. Rasagiline: A novel antiparkinsonian monoamine oxidase-B inhibitor with neuroprotective activity. *Progress in neurobiology*. 92:330-344.

Weinreb, O., Badinter, F.T., Bar-AM, O. & Youdim, M.B. 2015. Effect of long-term treatment with rasagiline on cognitive deficits and related molecular cascades in aged mice. *Neurobiology of aging.* 36:2628-2636.

Weintraub, D., Moberg, P.J., Duda, J.E., Katz, I.R. & Stern, M.B. 2003. Recognition and treatment of depression in Parkinson's disease. *Journal of geriatric psychiatry and neurology.* 16:178-183.

Weissbach, H., Smith, T.E., Daly, J.W., Witkop, B. & Udenfriend, S. 1960. A rapid spectrophotometric assay of monoamine oxidase based on the rate of disappearance of kynuramine. *Journal of biological chemistry*. 235:1160-1163.

Wertz, D.L. & Klinman, J.P. 2001. Eucariotic copper amine oxidase. (*In* Huber, A., Poulos, T. & Wiegahardt, K., *eds.* Handbook of Metalloproteins. New York: John Wiley. p. 1258-1271).

Westlund, K.N., Krakower, T.J., Kwan, S.W. & Abell, C.W. 1993. Intracellular distribution of monoamine oxidase A in selected regions of rat and monkey brain and spinal chord. *Brain research.* 612:221-230.

Weyler, W. & Salach, J.I. 1985. Purification and properties of mitochondrial monoamine oxidase type A from human placenta. *Journal of biological chemistry*. 260:13199-13207.

Weyler, W., Titlow, C.C. & Salach, J.I. 1990. Catalytically active monoamine oxidase type A from human liver expressed in *Saccharomyces cerevisiae* contains covalent FAD. *Biochemical and biophysical research communications.* 173:1205-1211.

Wirz-Justice, A. 1988. Platelet research in psychiatry. *Experientia.* 44(Suppl):145-152.

Woodard, C.M., Campos, B.A., Kuo, S.H., Nirenberg, M.J., Nestor, M.W., Zimmer, M., Mosharov, E.V., Sulzer, D., Zhou, H., Paull, D., Clark, L., Schadt, E.E., Sardi, S.P., Rubin, L., Eggan, K., Brock, M., Lipnick, S., Rao, M., Chang, S., Li, A. & Noggle, S.A. 2014. iPSC-derived dopamine neurons reveal differences between monozygotic twins discordant for Parkinson's Disease. *Cell reports.* 9:1173-1182.

Yogev-Falach, M., Amit, T., Bar-Am, O., Sagi, Y., Weinstock, M. & Youdim, M.B.H. 2002. Involvement of MAP kinase in the regulation of amyloid precursor protein processing by novel cholinesterase inhibitors derived from rasagiline. *Faseb journal.* 16:1674-1676.

Yogev-Falach, M., Amit, T., Bar-Am, O. & Youdim, M.B.H. 2003. The importance of propargylamine moiety in the antiparkinson drug rasagiline and its derivatives for MAPK-dependent amyloid precursor protein processing. *Faseb journal.* 17:2325-2327.

Youdim, M.B.H. 1978. The active centers of monoamine oxidase types “A” and “B”: binding with (^{14}C)-clorgyline and (^{14}C)-deprenyl. *Journal of neural transmission.* 43:199-208.

Youdim, M.B. & Finberg, J.P. 1983. Monoamine oxidase inhibitor antidepressants. *(*In Grahame-Smith, D.G. & Cowen, P.J., *eds*. Psychopharmacology. Amsterdam: Excerpta Medica. p. 38-70).

Youdim, M.B.H., Finberg, J.P.M. & Tipton, K.F. 1988. Monoamine Oxidase. (*In* Trendelenburg, U. & Wiener, N. Handbook of Experimental Pharmacology. Berlin: Springer-Verlag. p. 119-192).

Youdim, M.B., Gross, A. & Finberg, J.P. 2001. Rasagiline [N-propargyl-1R(+)-aminoindan], a selective and potent inhibitor of mitochondrial monoamine oxidase B. *British journal of pharmacology.* 132:500-506.

Youdim, M.B. 2003. Rasagiline: an antiparkinson drug with neuroprotective activity. *Expert review of neurotherapeutics*. 3:737-749.

Youdim, M.B., Fridkin, M. & Zheng, H. 2004. Novel bifunctional drugs targeting monoamine oxidase inhibition and iron chelation as an approach to neuroprotection in Parkinson’s disease and other neurodegenerative diseases. *Journal of neural transmission.* 111:1455-1471.

Youdim, M.B. & Riederer, P.F. 2004. A review of the mechanisms and role of monoamine oxidase inhibitors in Parkinson’s disease and depressive illness. *British journal of pharmacology.* 147(Suppl):S287-S296.

Youdim, M. & Bakhle, Y. 2006. Monoamine oxidase: isoforms and inhibitors in Parkinson’s disease and depressive illness. *British journal of pharmacology.* 147:S287-296.

Youdim, M., Edmondson, D. & Tipton, K. 2006. The therapeutic potential of monoamine oxidase inhibitors. *Nature reviews* | *Neuroscience.* 7:295-309.

Yoneda, F., Moto, T., Sakae, M., Ohde, H., Knoll, B., Miklya, L. & Knoll, J. 2001. Structure-activity studies leading to (-)1-(benzofuran-2-yl)-2-propylaminopentane, ((-)BPAP), a highly potent, selective enhancer of the impulse propagation mediated release of catecholamines and serotonin in the brain. *Bioorganic & medicinal chemistry.* 9:1197-1212.

Zajecka, J.M. & Zajecka, A.M. 2014. A clinical overview of monoamine oxidase inhibitors: pharmacological profile, efficacy, safety/tolerability, and strategies for

successful outcomes in the management of major depressive disorders. *Annals of general psychiatry.* 44:513-523.

Zellner, M., Baureder, M., Rappold, E., Bugert, P., Kotzailias, N., Babeluk, R., Baumgartner, R., Attems, J., Gerner, C., Jellinger, K., Roth, E., Oehler, R. & Umlauf, E. 2012. Comparative platelet proteome analysis reveals an increase of monoamine oxidase-B protein expression in Alzheimer's disease but not in non-demented Parkinson's disease patients. *Journal of proteomics*. 75:2080-2092.

Zhuang, Z., Hogan, M. & McCauley, R. 1988. The *in vitro* insertion of monoamine oxidase B into mitochondrial outer membrane. *Febs letters.* 238:90-185.

Zhuang, Z., Marks, B. & McCauley, R.B. 1992. The insertion of monoamine oxidase A into the outer membrane of rat liver mitochondria. *Journal of biological chemistry*. 267:591-596.

Zreika, M., McDonald, I.A., Bey, P. & Palfreyman, M.G. 1984. MDL 72145, an enzyme-activated irreversible inhibitor with selectivity for monoamine oxidase type B. *Journal of neurochemistry*. 43:448-454.

ANNEXURE A: ^{1}H-NMR and ^{13}C-NMR spectra

4-Benzyloxy-1-indanone (**1a**)

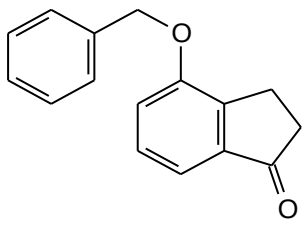

^{1}H NMR (600 MHz, $CDCl_3$) δ 7.38 – 7.31 (m, 4H), 7.30 – 7.22 (m, 3H), 7.00 (d, *J* = 7.8 Hz, 1H), 5.09 (s, 2H), 3.06 – 2.98 (m, 2H), 2.67 – 2.53 (m, 2H).

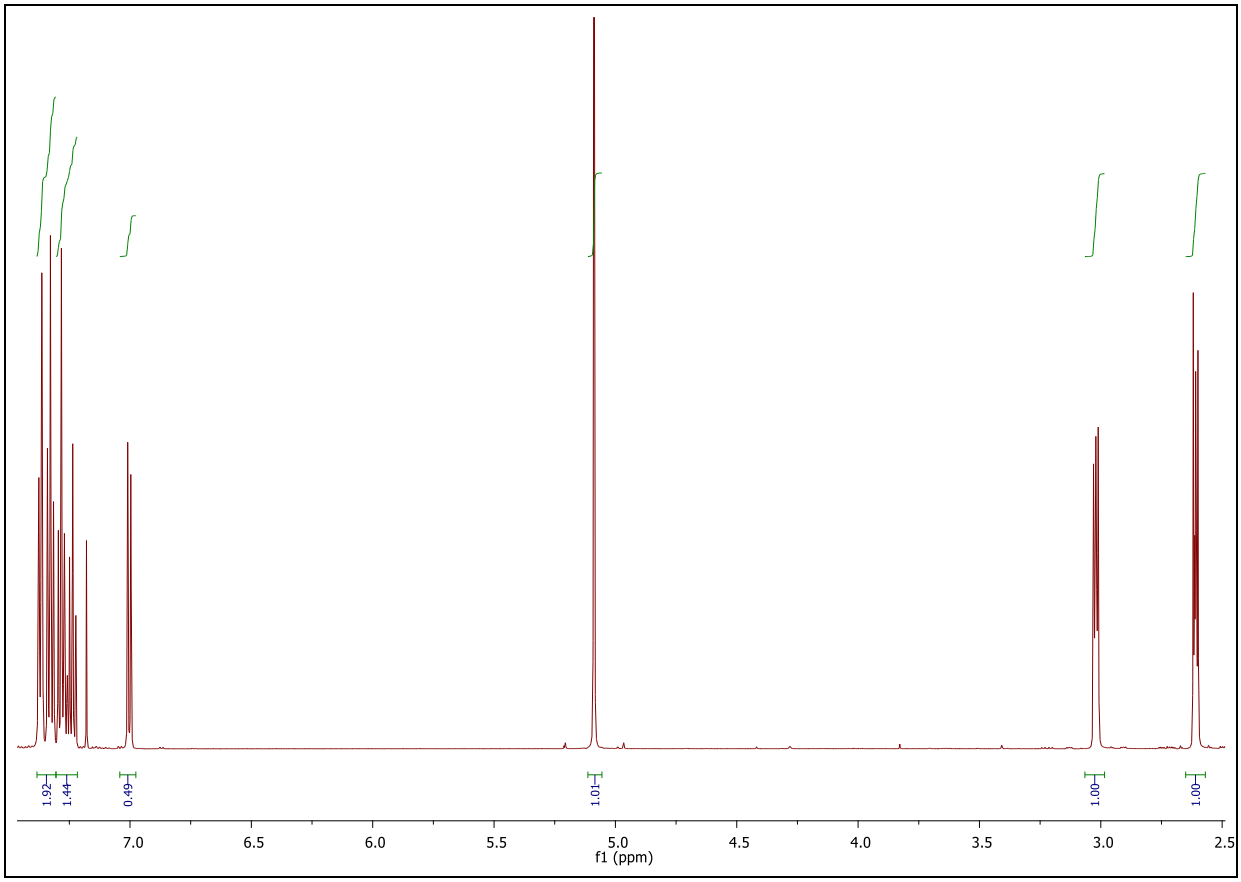

4-Benzyloxy-1-indanone (**1a**)

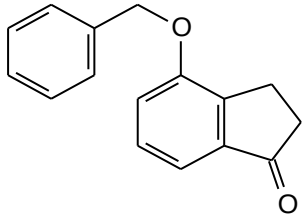

^{13}C NMR (151 MHz, $CDCl_3$) δ 207.25, 156.23, 144.52, 138.80, 136.60, 128.83, 128.70, 128.15, 127.24, 116.28, 115.68, 70.08, 36.19, 22.71.

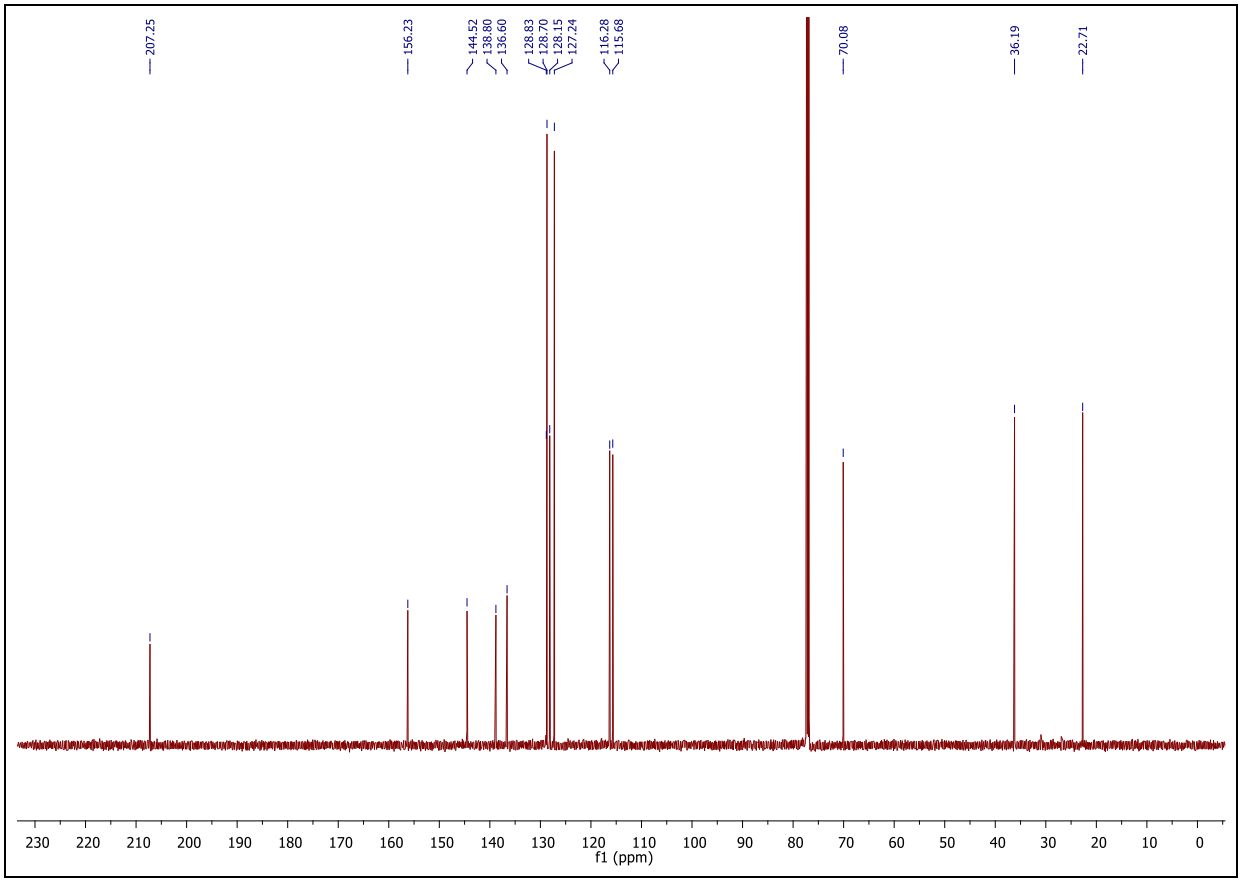

5-Benzyloxy-1-indanone (**1b**)

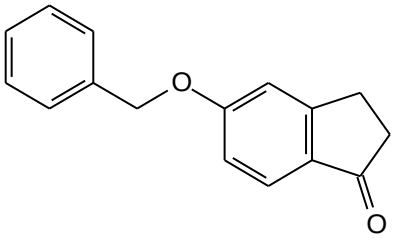

^{1}H NMR (600 MHz, $CDCl_3$) δ 7.63 – 7.60 (m, 1H), 7.37 – 7.31 (m, 4H), 7.30 – 7.26 (m, 1H), 6.91 – 6.89 (m, 2H), 5.06 (s, 2H), 3.03 – 2.96 (m, 2H), 2.64 – 2.53 (m, 2H).

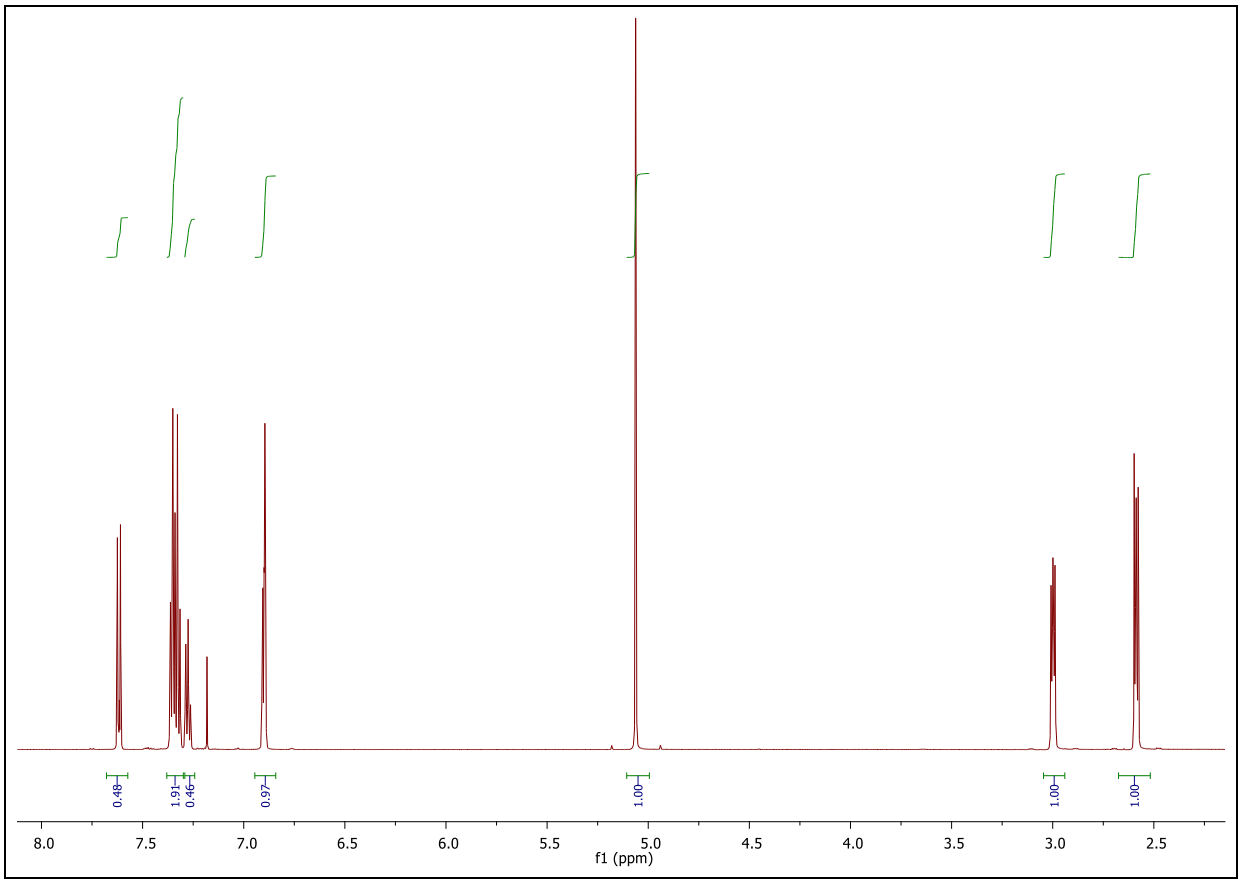

5-Benzyloxy-1-indanone (**1b**)

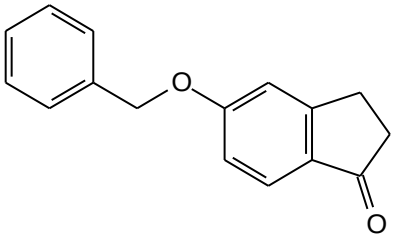

^{13}C NMR (151 MHz, $CDCl_3$) δ 205.30, 164.38, 158.14, 136.10, 130.66, 128.76, 128.32, 127.48, 125.43, 115.92, 110.82, 70.32, 36.47, 25.92.

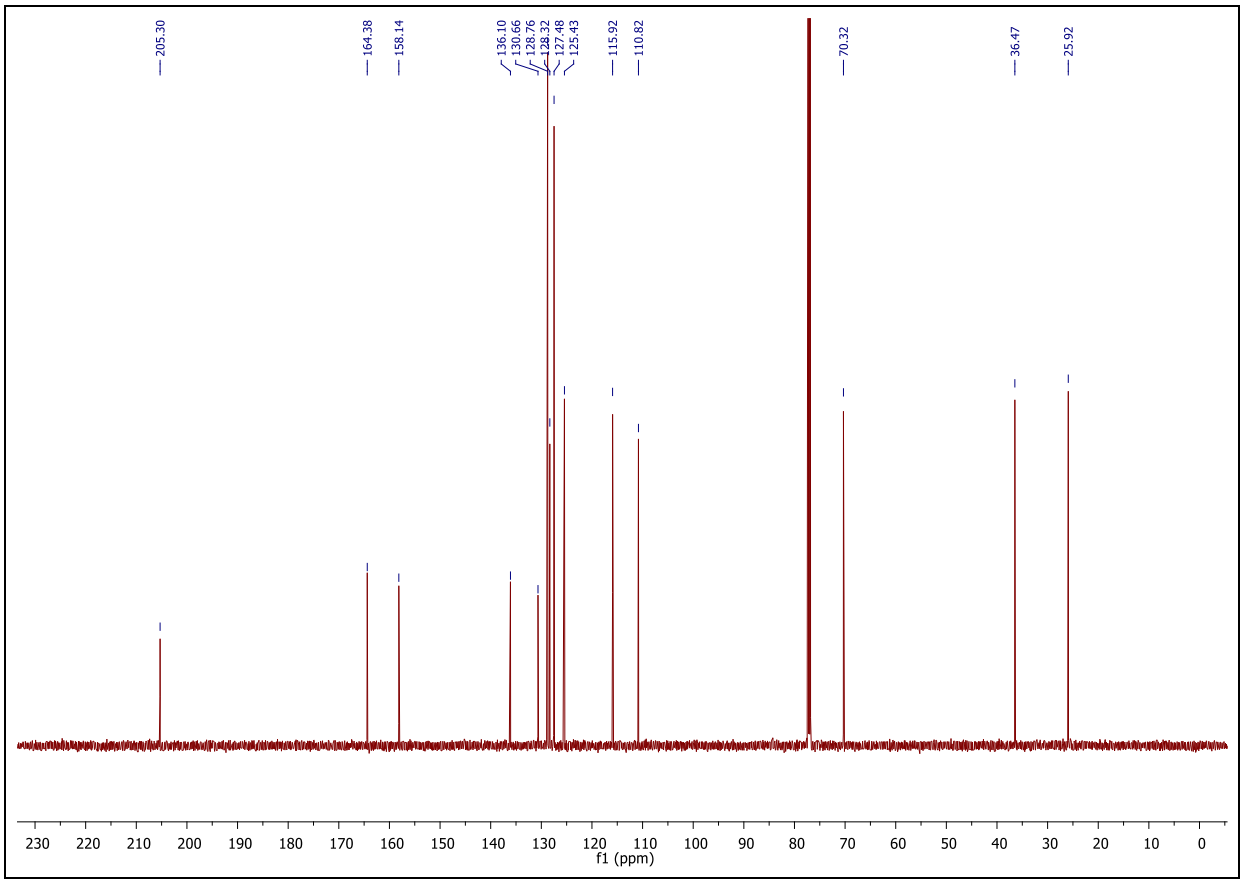

6-Benzyloxy-1-indanone (**1c**)

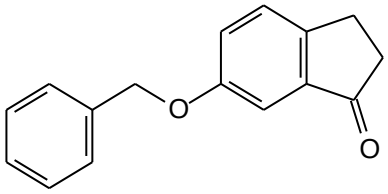

^{1}H NMR (600 MHz, $CDCl_3$) δ 7.36 (d, *J* = 7.3 Hz, 2H), 7.34 – 7.29 (m, 1.3 Hz, 3H), 7.28 – 7.24 (m, 1H), 7.21 – 7.18 (m, 2H), 5.01 (s, 2H), 3.04 – 2.96 (m, 2H), 2.69 – 2.60 (m, 2H).

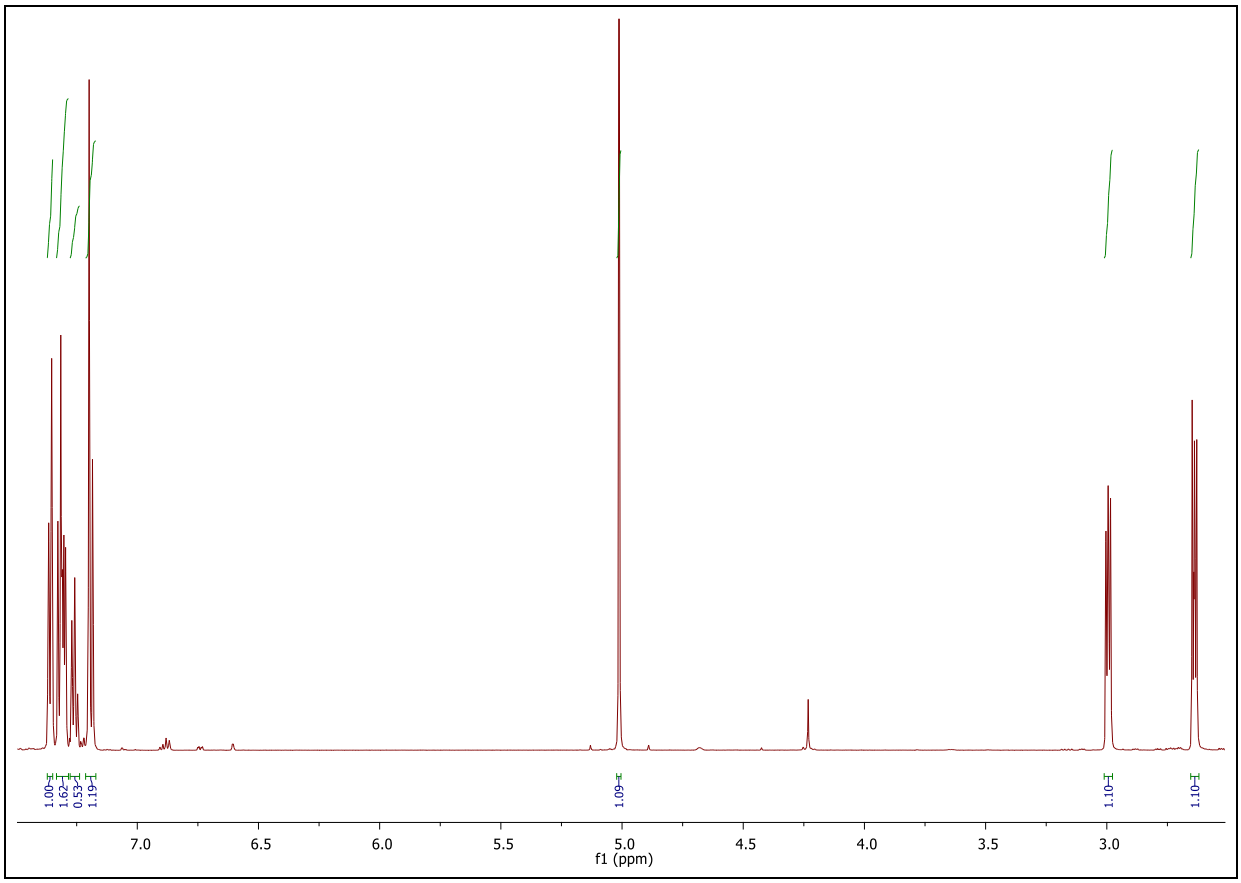

6-Benzyloxy-1-indanone (**1c**)

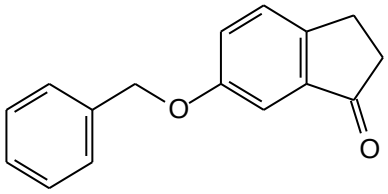

^{13}C NMR (151 MHz, $CDCl_3$) δ 207.00, 158.49, 148.25, 138.26, 136.45, 128.67, 128.16, 127.57, 127.50, 124.63, 106.15, 70.32, 37.03, 25.17.

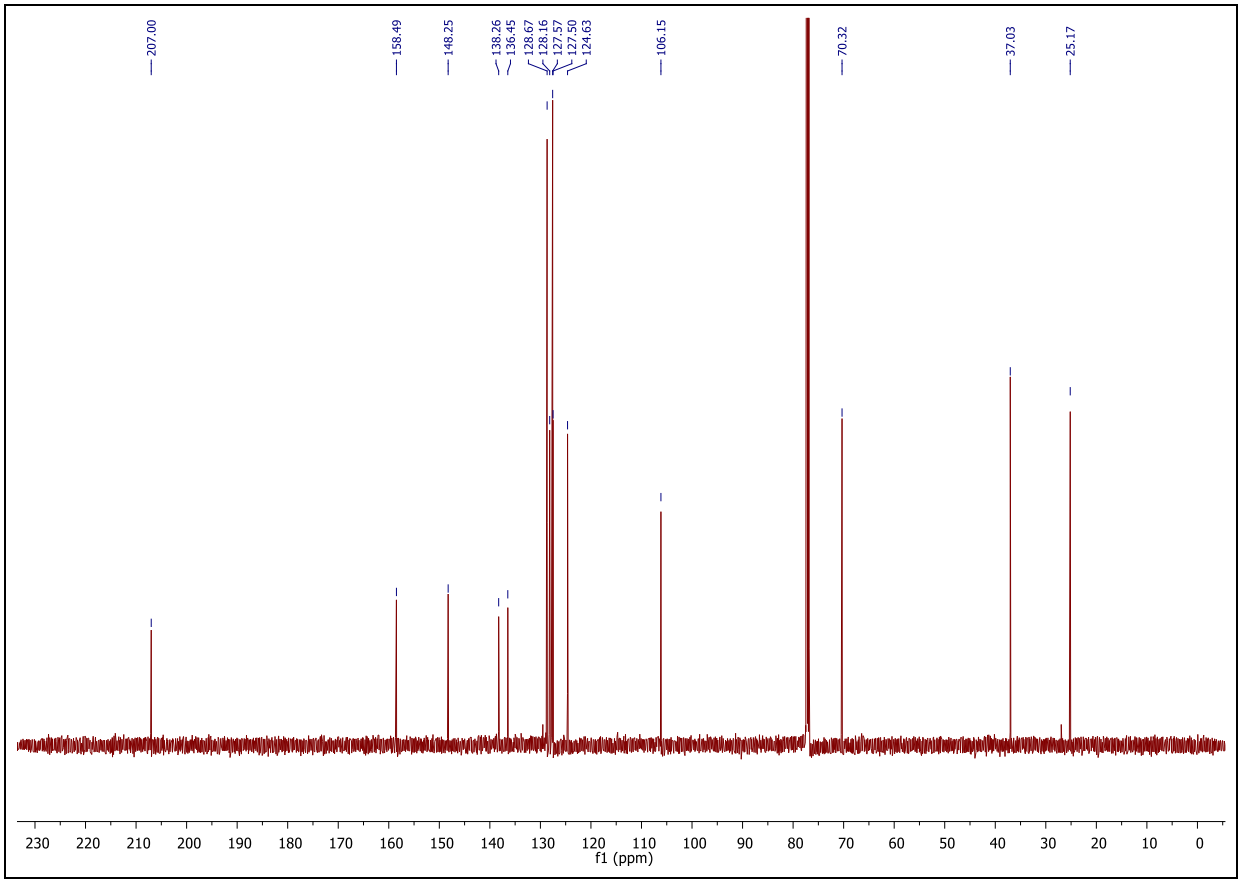

4-(4-Chlorobenzyloxy)-1-indanone (**1d**)

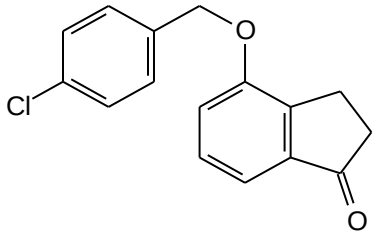

^{1}H NMR (600 MHz, $CDCl_3$) δ 7.34 – 7.27 (m, 5H), 7.24 (t, *J* = 7.7 Hz, 1H), 6.99 (dd, *J* = 7.9, 0.9 Hz, 1H), 5.05 (s, 2H), 3.05 – 2.97 (m, 2H), 2.72 – 2.51 (m, 2H).

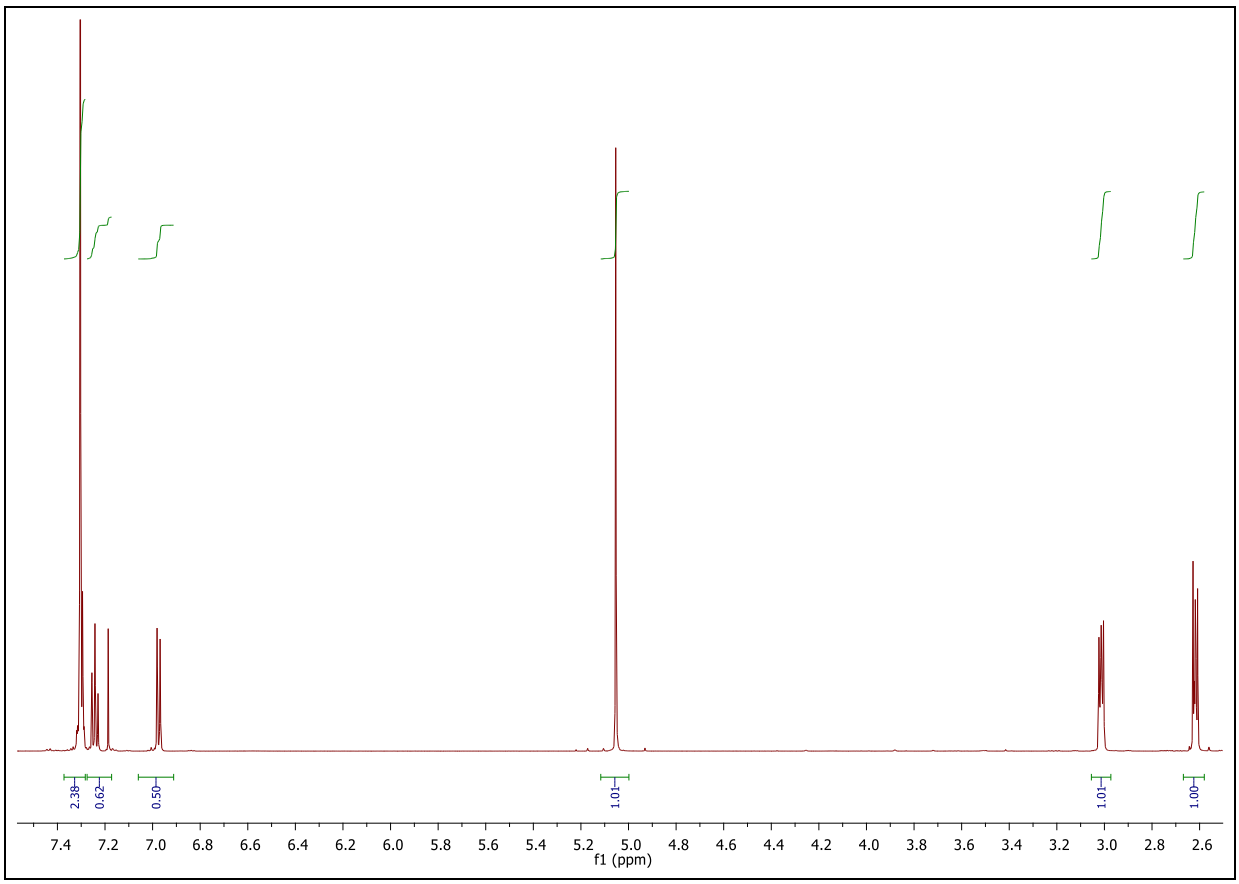

4-(4-Chlorobenzyloxy)-1-indanone (**1d**)

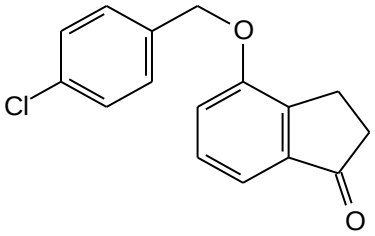

^{13}C NMR (151 MHz, $CDCl_3$) δ 207.13, 155.98, 144.41, 138.87, 135.06, 133.99, 128.90, 128.86, 128.58, 116.19, 115.90, 69.32, 36.16, 22.68.

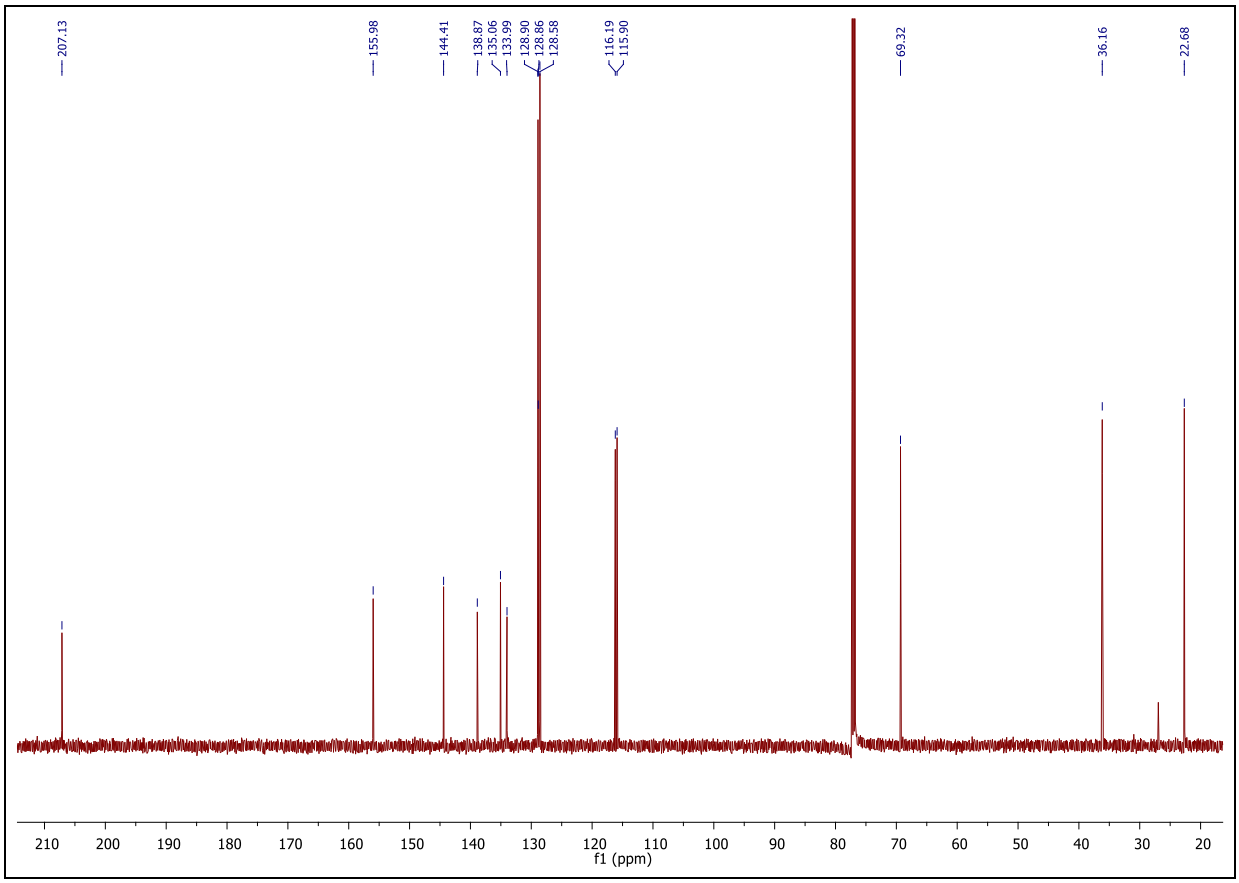

5-(4-Chlorobenzyloxy)-1-indanone (**1e**)

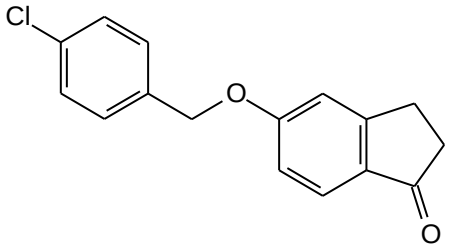

^{1}H NMR (600 MHz, $CDCl_3$) δ 7.34 – 7.26 (m, 5H), 7.21 – 7.15 (m, 2H), 4.98 (s, 2H), 3.03 – 2.99 (m, 2H), 2.67 – 2.62 (m, 2H).

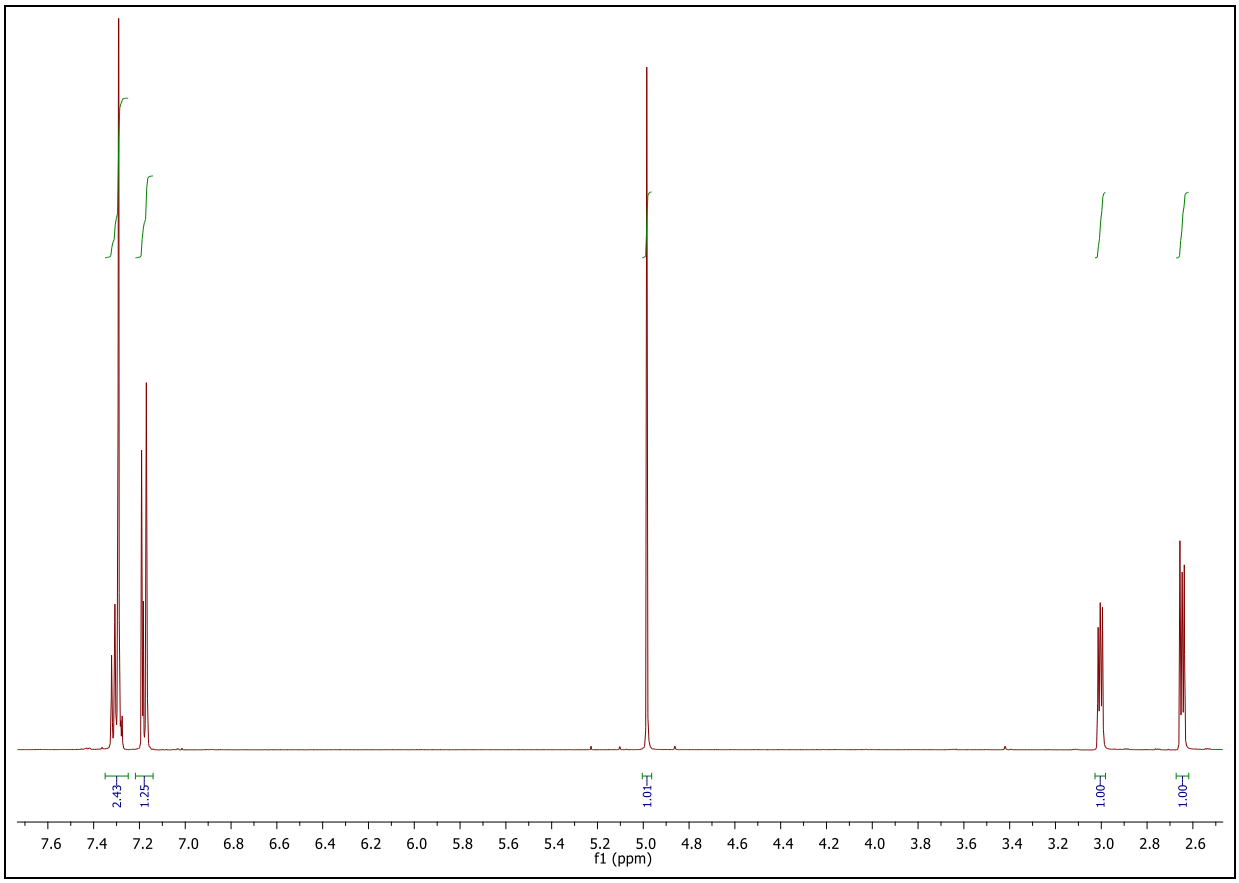

5-(4-Chlorobenzyloxy)-1-indanone (**1e**)

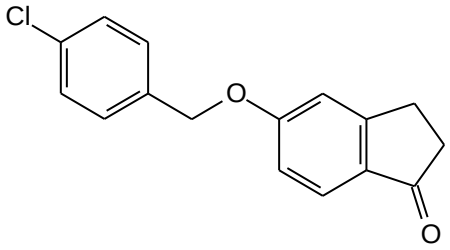

^{13}C NMR (151 MHz, $CDCl_3$) δ 206.91, 158.21, 148.41, 138.28, 134.95, 133.96, 128.85, 127.58, 124.56, 106.13, 69.50, 37.02, 25.17.

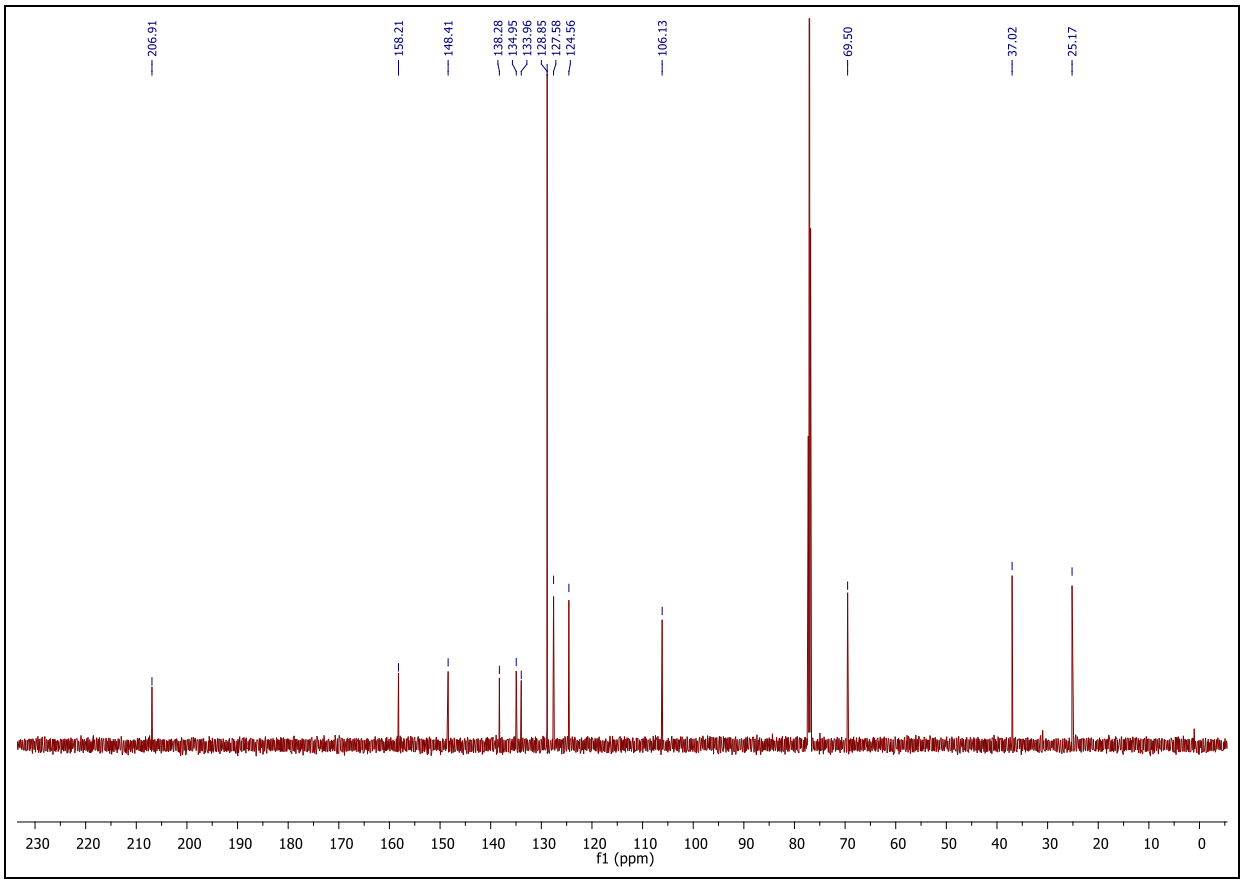

6-(4-Chlorobenzyloxy)-1-indanone (**1f**)

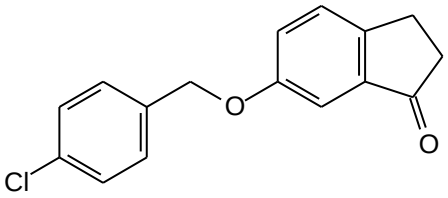

^{1}H NMR (600 MHz, $CDCl_3$) δ 7.33 – 7.24 (m, 4H), 7.19-7.14 (m, 2H), 7.16 (s, 1H), 4.98 (s, 2H), 3.00 – 2.91 (m, 2H), 2.66 – 2.62 (m, 2H).

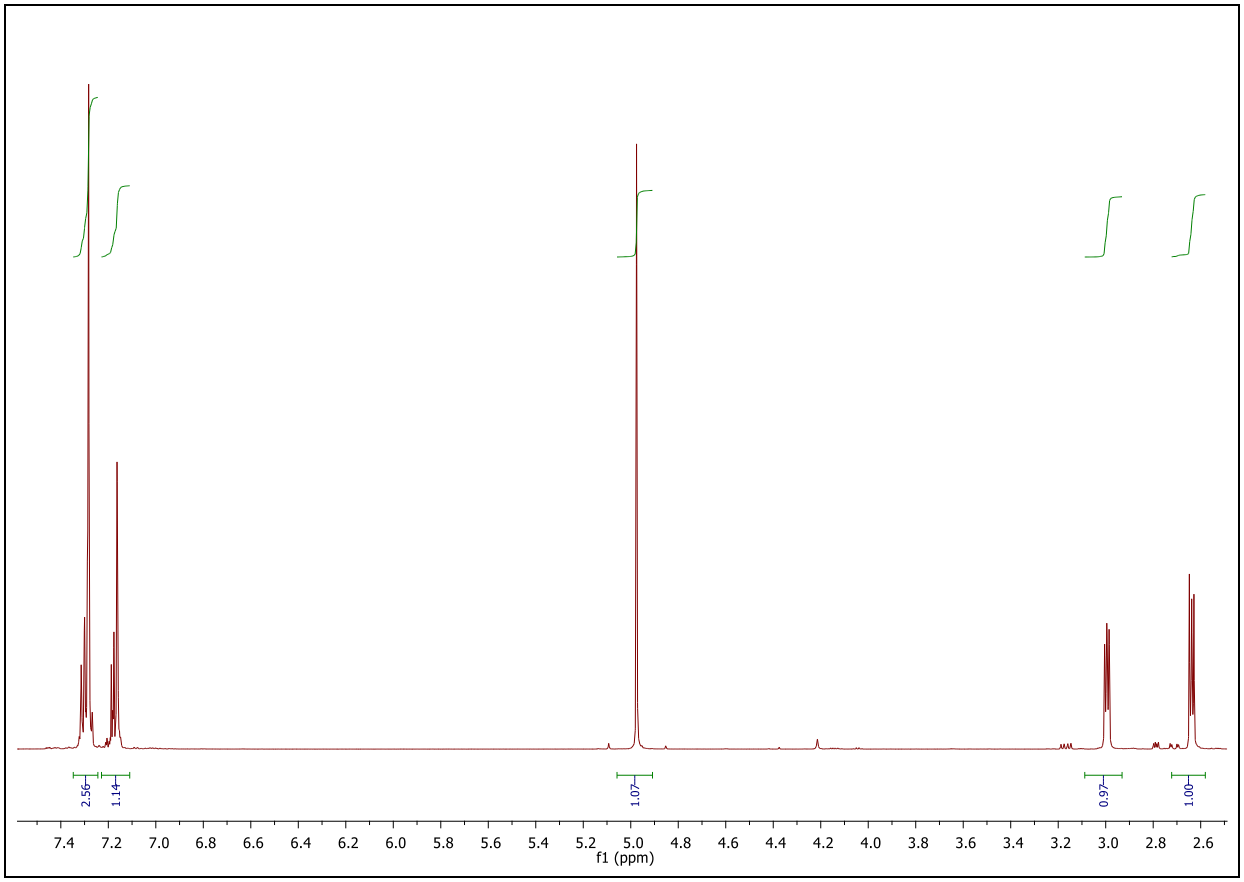

6-(4-Chlorobenzyloxy)-1-indanone (**1f**)

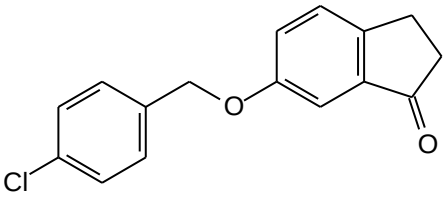

^{13}C NMR (151 MHz, $CDCl_3$) δ 206.91, 158.21, 148.41, 138.28, 134.96, 133.96, 128.84, 127.58, 124.55, 106.14, 69.57, 37.02, 25.17.

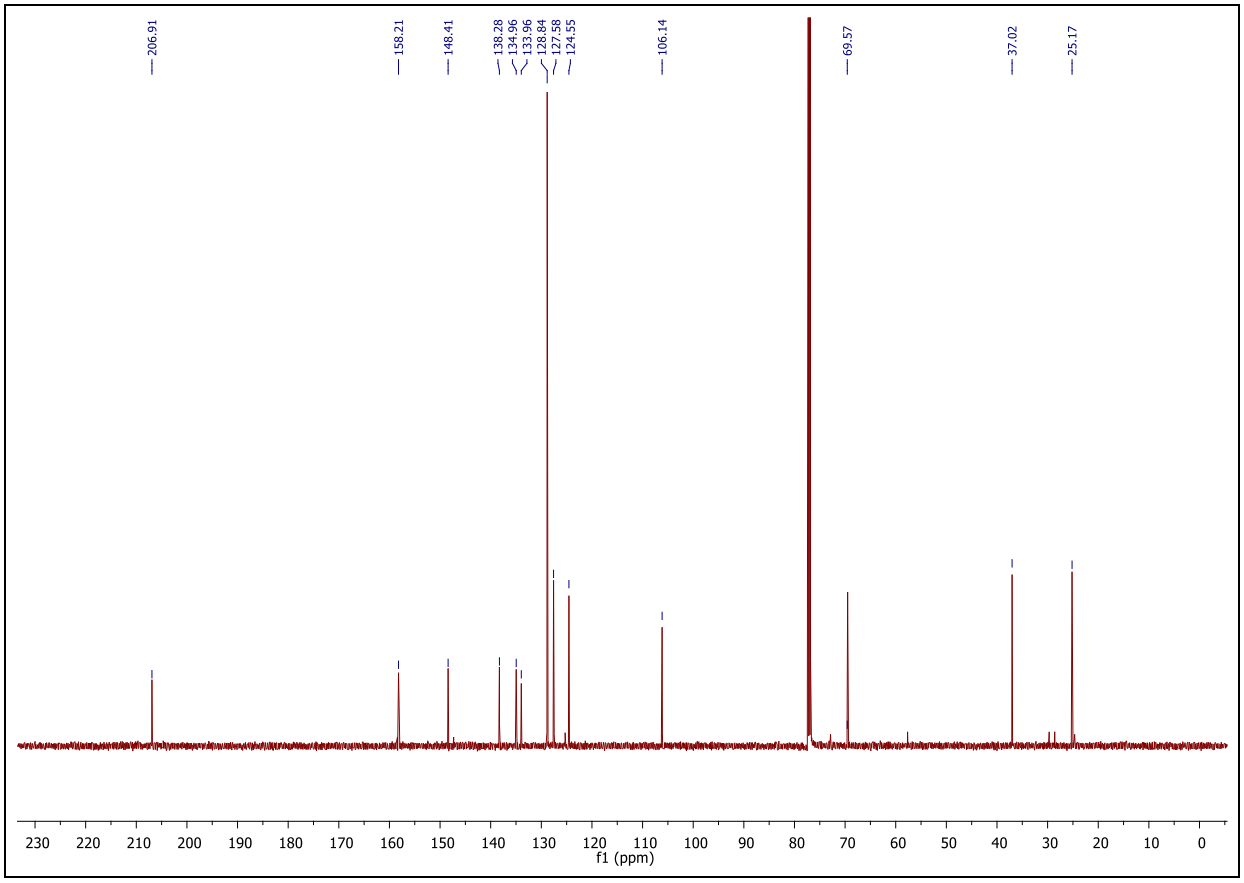

6-(3-Chlorobenzyloxy)-1-indanone (**1g**)

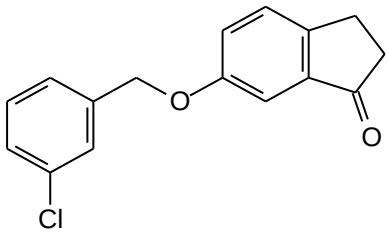

^{1}H NMR (600 MHz, $CDCl_3$) δ 7.36 (s, 1H), 7.33 (dd, *J* = 8.3, 0.9 Hz, 1H), 7.27 – 7.21 (m, 3H), 7.19 (dd, *J* = 7.4, 2.5, 1H), 7.17 (d, *J* = 2.6 Hz, 1H), 4.99 (s, 2H), 3.06 – 2.97 (m, 2H), 2.68 – 2.61 (m, 2H).

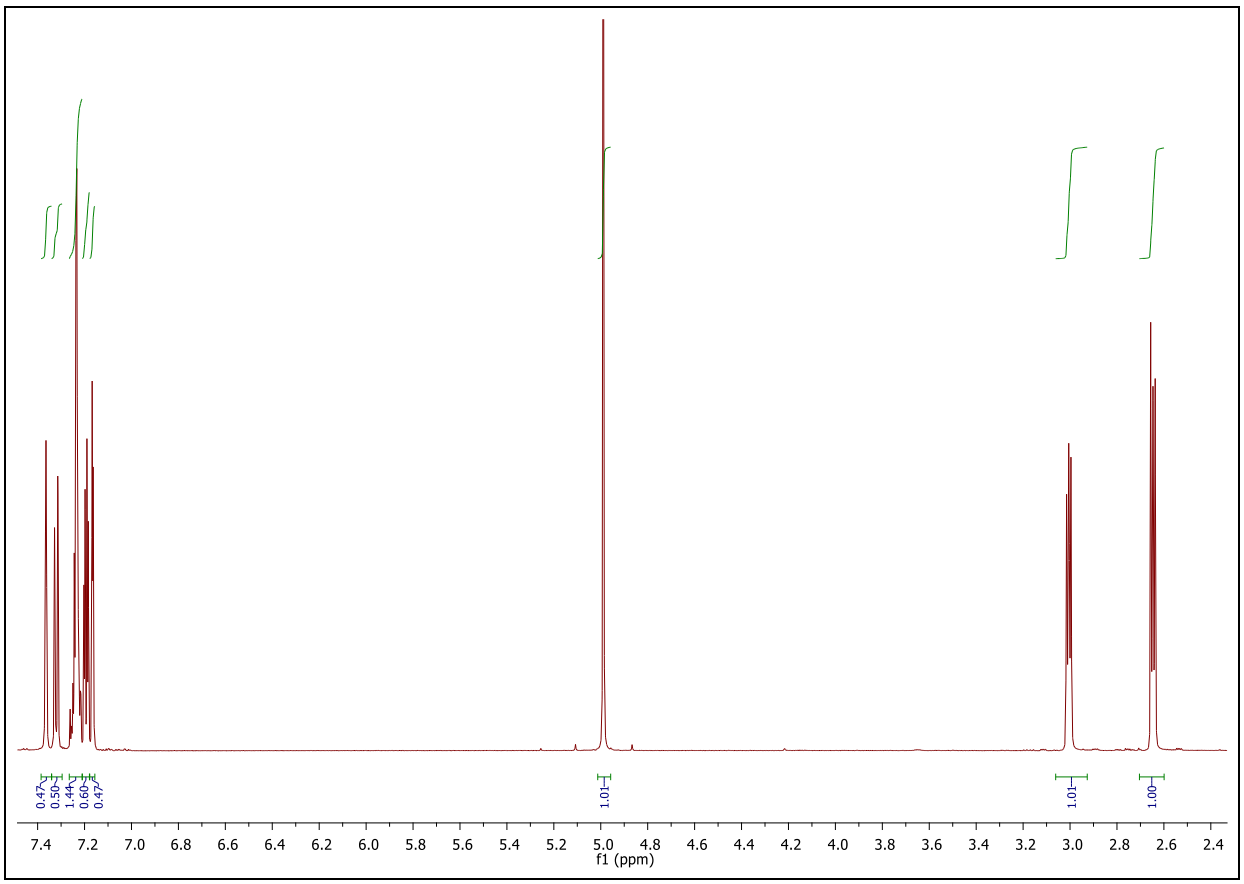

6-(3-Chlorobenzyloxy)-1-indanone (**1g**)

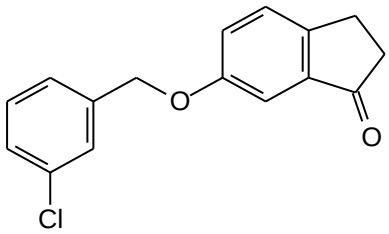

^{13}C NMR (151 MHz, $CDCl_3$) δ 206.91, 158.17, 148.48, 138.52, 138.29, 134.61, 129.94, 128.27, 127.62, 127.45, 125.41, 124.55, 106.09, 69.41, 37.02, 25.18.

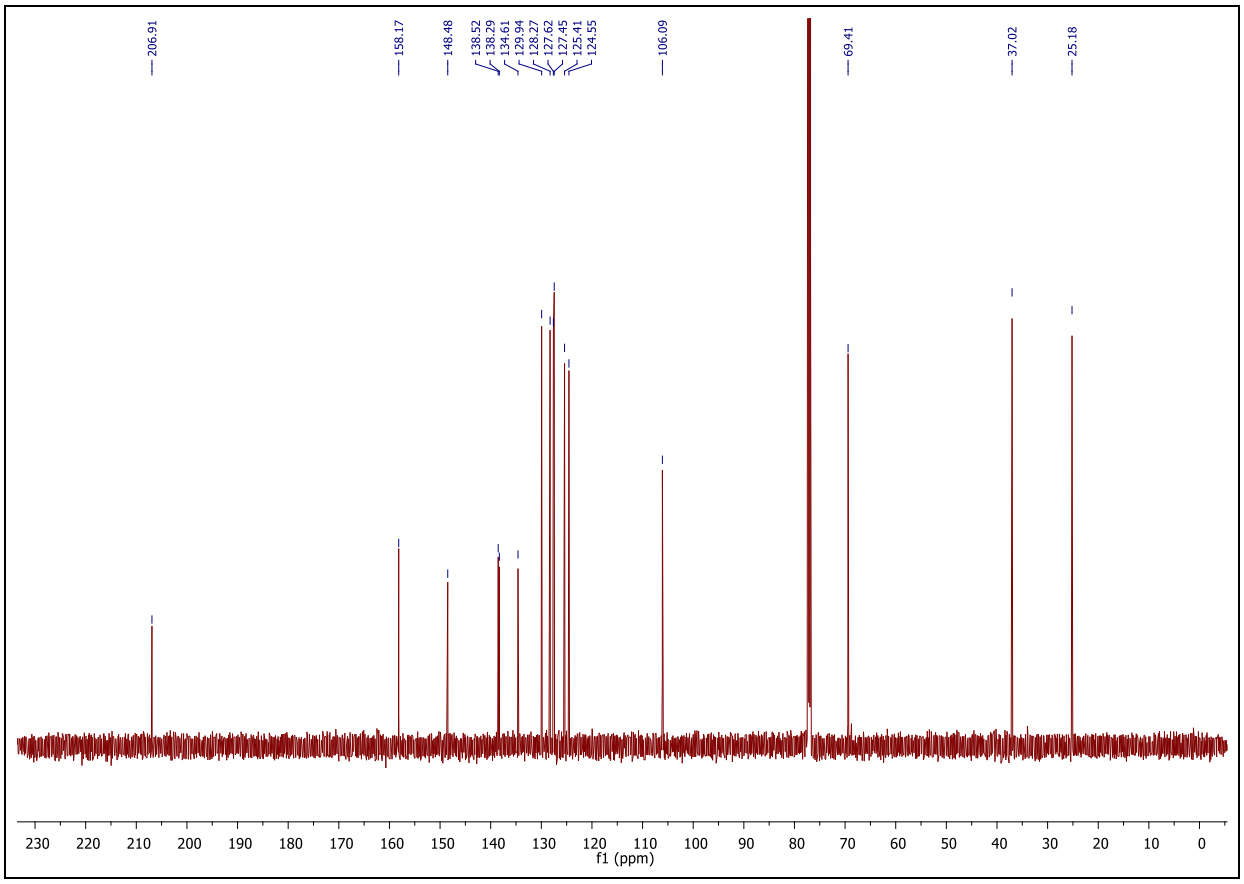

5-(2-Phenoxyethoxy)-1-indanone (**1h**)

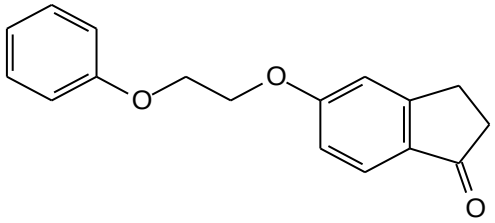

^{1}H NMR (600 MHz, $CDCl_3$) δ 7.63 (d, 9.2 Hz, 1H), 7.24 (t, *J* = 8.0 Hz, 2H), 6.95 – 6.85 (m, 5H), 4.35 – 4.31 (m, 2H), 4.31 – 4.27 (m, 2H), 3.11 – 2.92 (m, 2H), 2.71 – 2.48 (m, 2H).

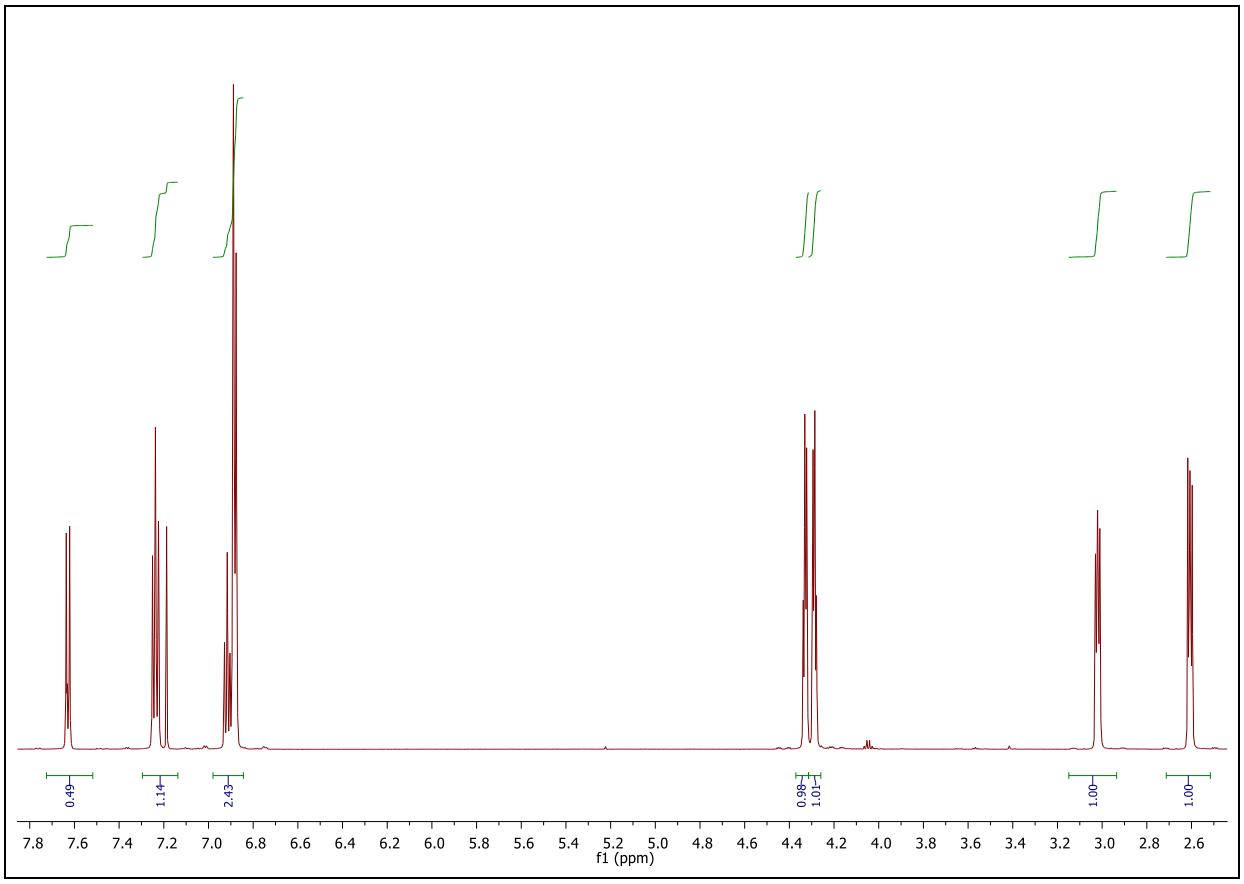

5-(2-Phenoxyethoxy)-1-indanone (**1h**)

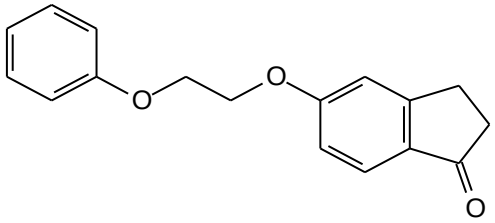

^{13}C NMR (151 MHz, $CDCl_3$) δ 205.29, 164.28, 158.47, 158.10, 130.77, 129.59, 125.44, 121.32, 115.70, 114.69, 110.61, 66.91, 66.20, 36.47, 25.9

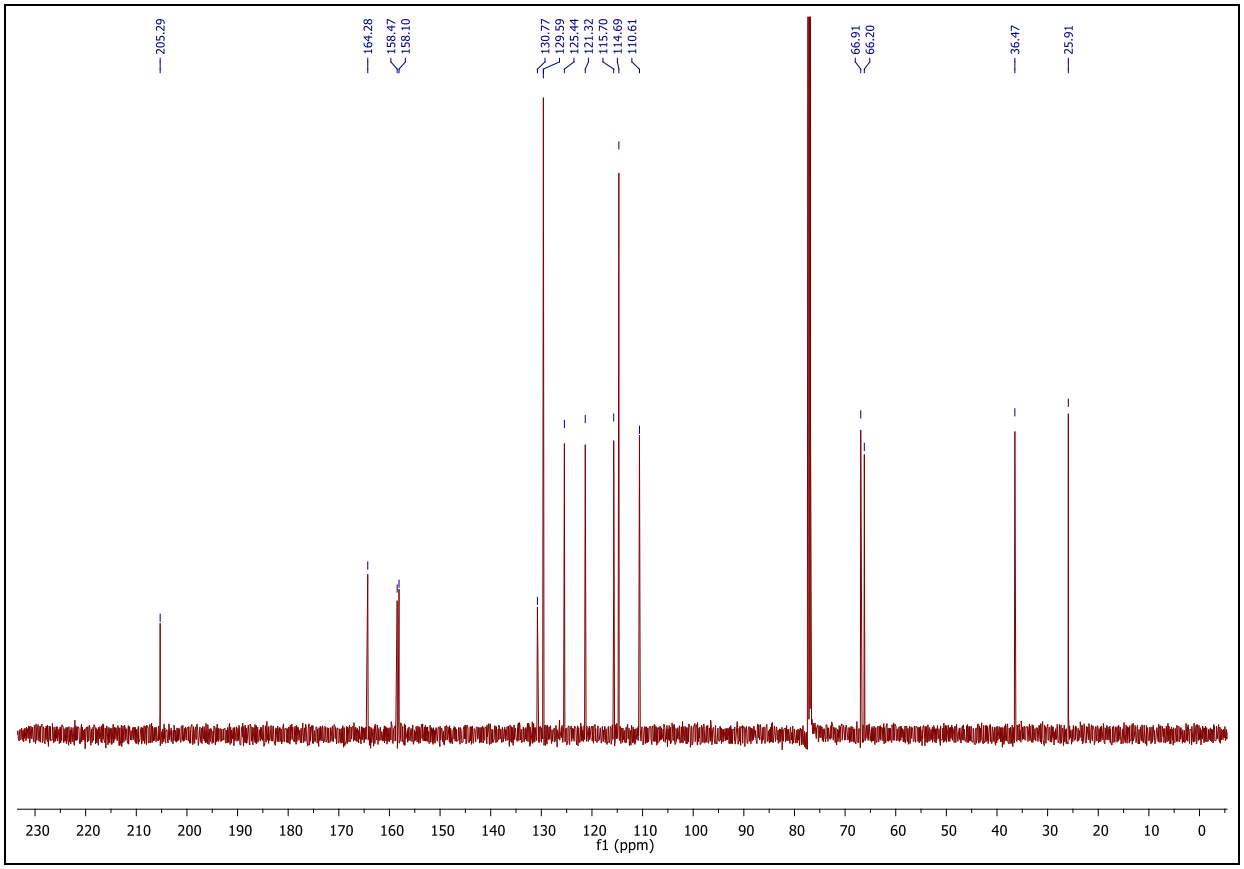

5-Benzyloxy-1-indanol (**1i**)

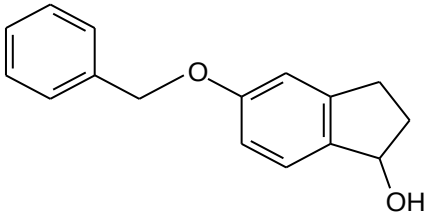

^{1}H NMR (600 MHz, $CDCl_3$) δ 7.36 – 7.33 (d, *J* = 7.1 Hz, 2H), 7.31 (t, *J* = 7.1 Hz, 2H), 7.27 – 7.21 (m, 2H), 6.83 – 6.71 (m, 2H), 5.10 (t, *J* = 6.9 Hz, 1H), 4.98 (s, 2H), 3.01 – 2.90 (m, 5.4 Hz, 1H), 2.76 – 2.64 (m, 1H), 2.45 – 2.31 (m, 1H), 1.92 – 1.82 (m, 1H).

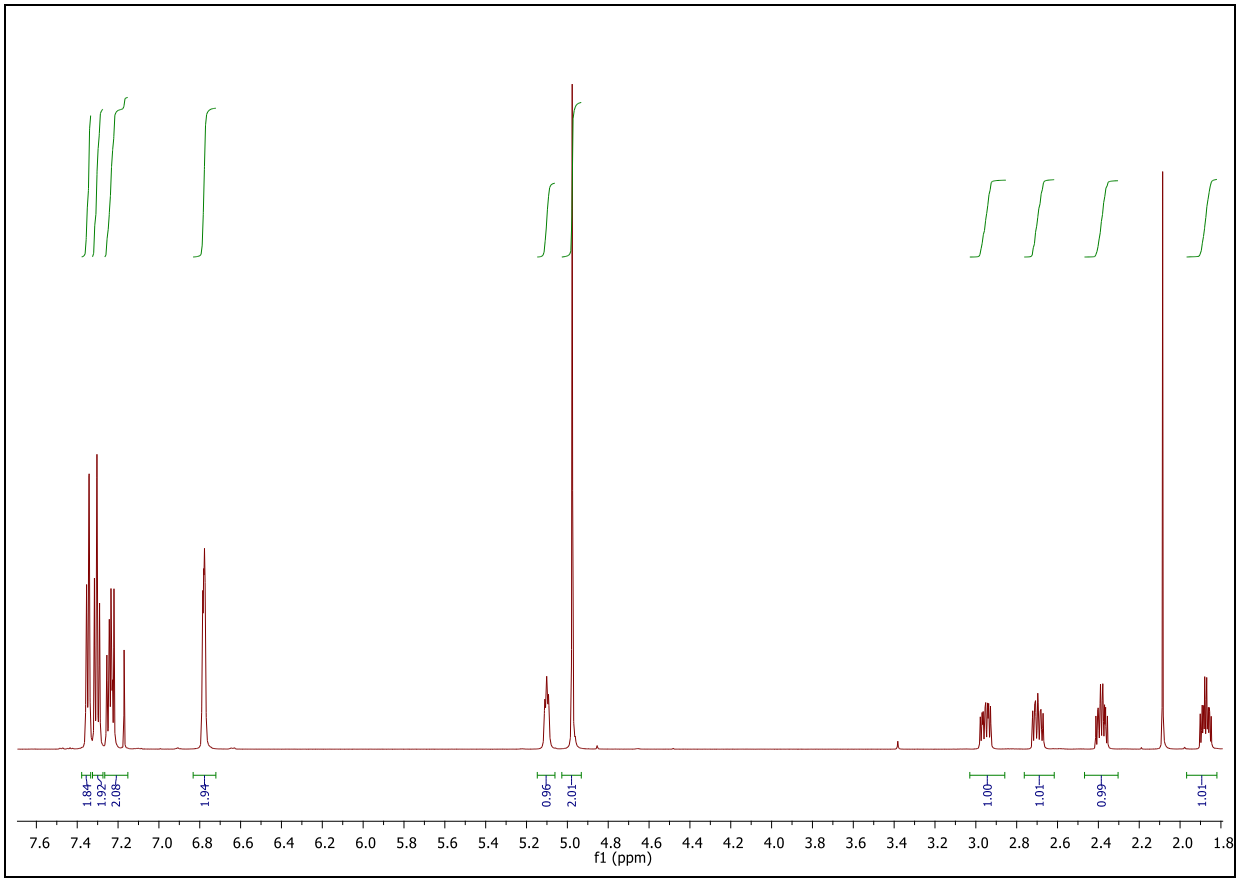

5-Benzyloxy-1-indanol (**1i**)

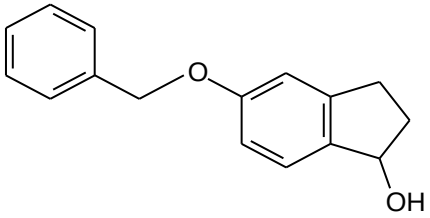

^{13}C NMR (151 MHz, $CDCl_3$) δ 159.46, 145.31, 137.66, 137.09, 128.61, 127.96, 127.44, 125.11, 113.87, 110.89, 75.89, 70.17, 36.29, 30.02.

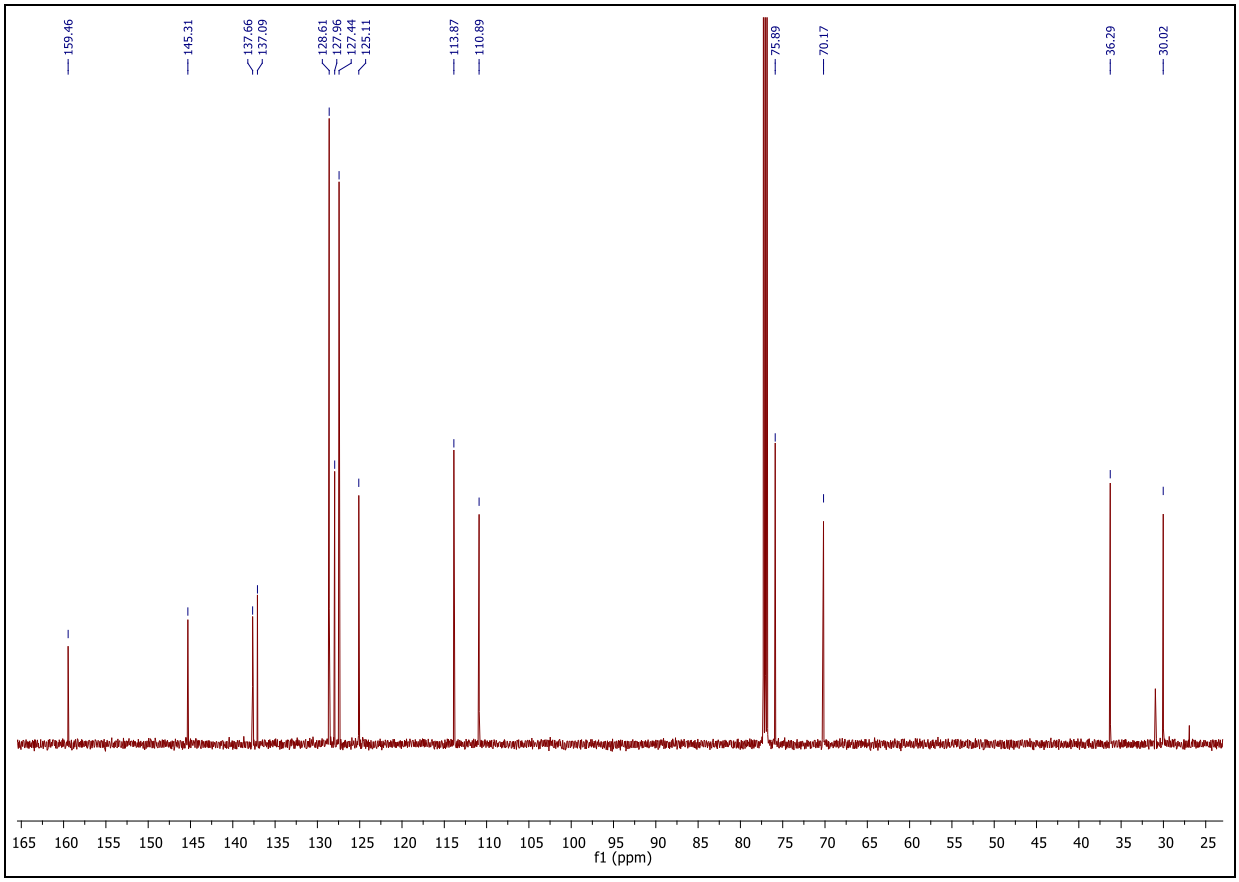

6-Benzyloxy-1-indanol (**1j**)

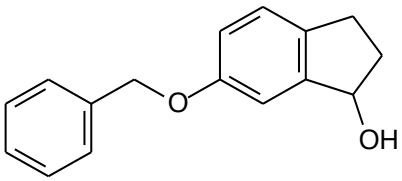

^{1}H NMR (600 MHz, $CDCl_3$) δ 7.35 (d, *J* = 7.3 Hz, 2H), 7.30 (t, *J* = 7.3 Hz, 2H), 7.27 – 7.15 (m, 1H), 7.06 (d, *J* = 8.2 Hz, 1H), 6.95 (d, *J* = 2.2 Hz, 1H), 6.82 (dd, *J* = 8.2, 2.4 Hz, 1H), 5.10 (s, 1H), 4.98 (s, 2H), 2.93 – 2.84 (m, 1H), 2.73 – 2.59 (m, 1H), 2.46 – 2.36 (m, 1H), 1.90 – 1.80 (m, 1H).

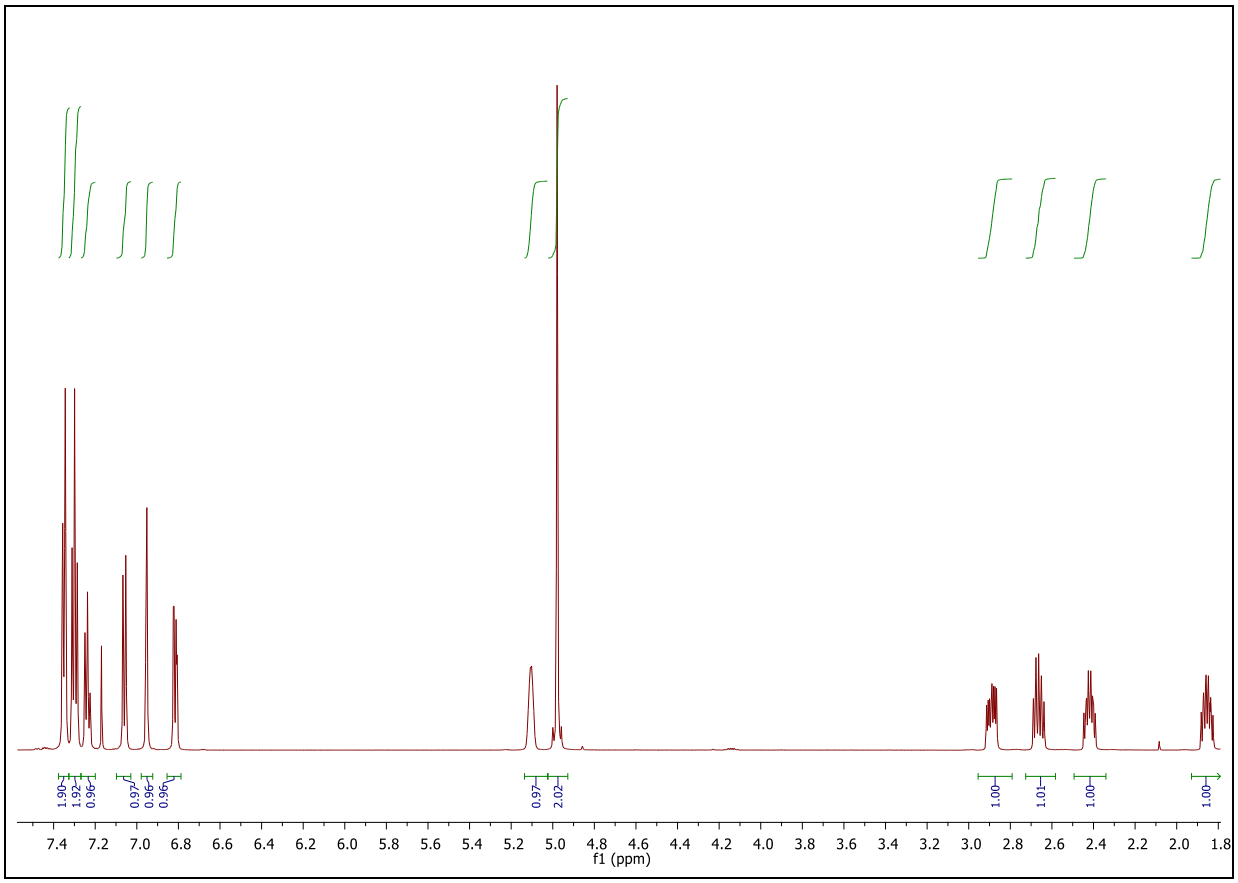

6-Benzyloxy-1-indanol (**1j**)

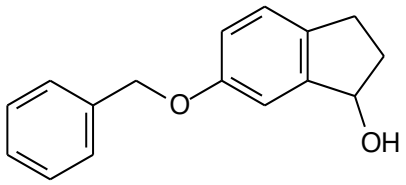

^{13}C NMR (151 MHz, $CDCl_3$) δ 158.28, 146.42, 137.19, 135.45, 128.59, 127.93, 127.48, 125.57, 115.91, 110.00, 76.64, 70.32, 36.59, 29.00.

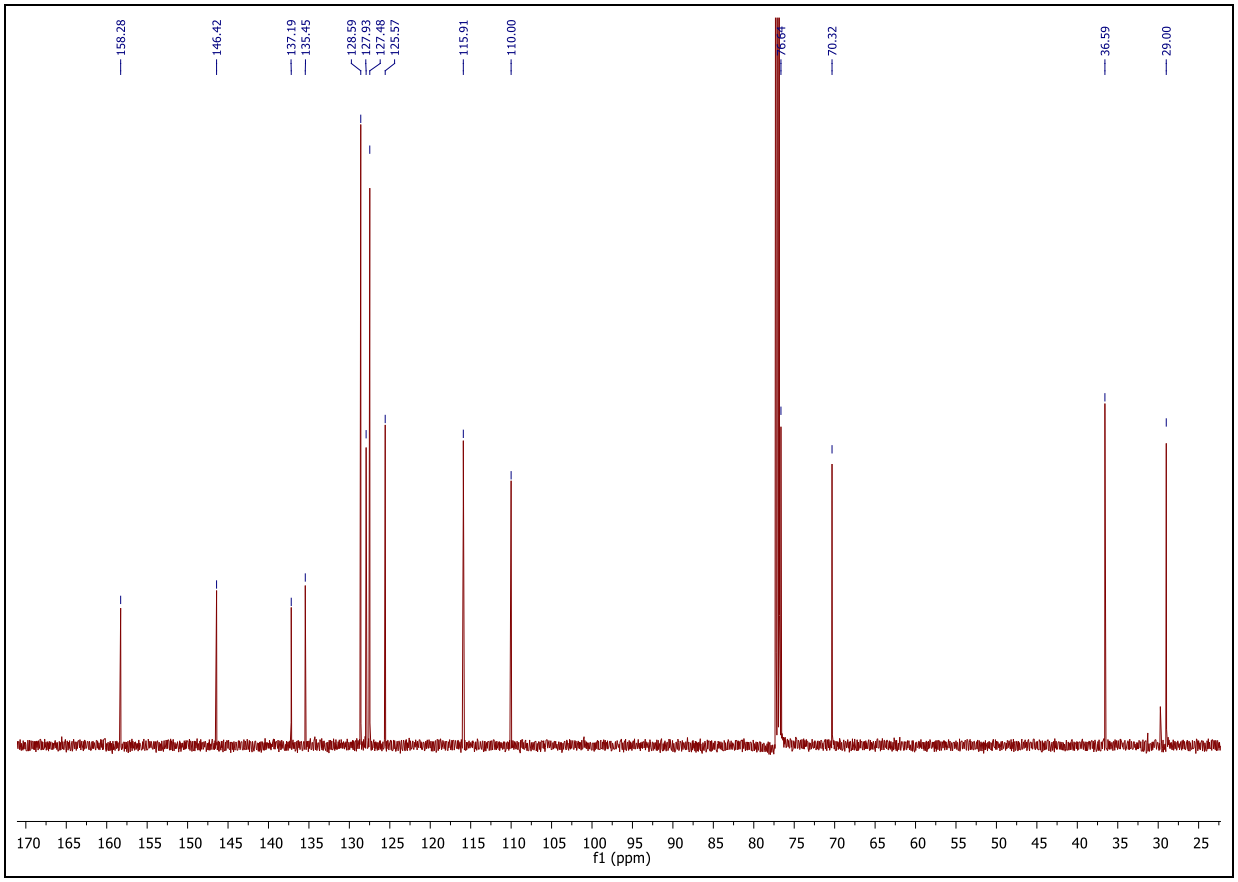

4-(4-Chlorobenzyloxy)-1-indanol (**1k**)

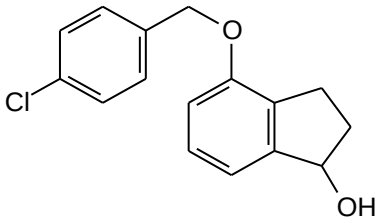

^{1}H NMR (600 MHz, $CDCl_3$) δ 7.31 – 7.25 (m, 4H), 7.13 (t, *J* = 7.8 Hz, 1H), 6.99 (d, *J* = 7.5 Hz, 1H), 6.72 (d, *J* = 8.1 Hz, 1H), 5.27 – 7.17 (m, 1H), 4.99 (s, 2H), 3.03 – 2.95 (m, 1H), 2.76 – 2.67 (m, 1H), 2.47 – 2.38 (m, 1H), 1.93 – 1.84 (m, 1H).

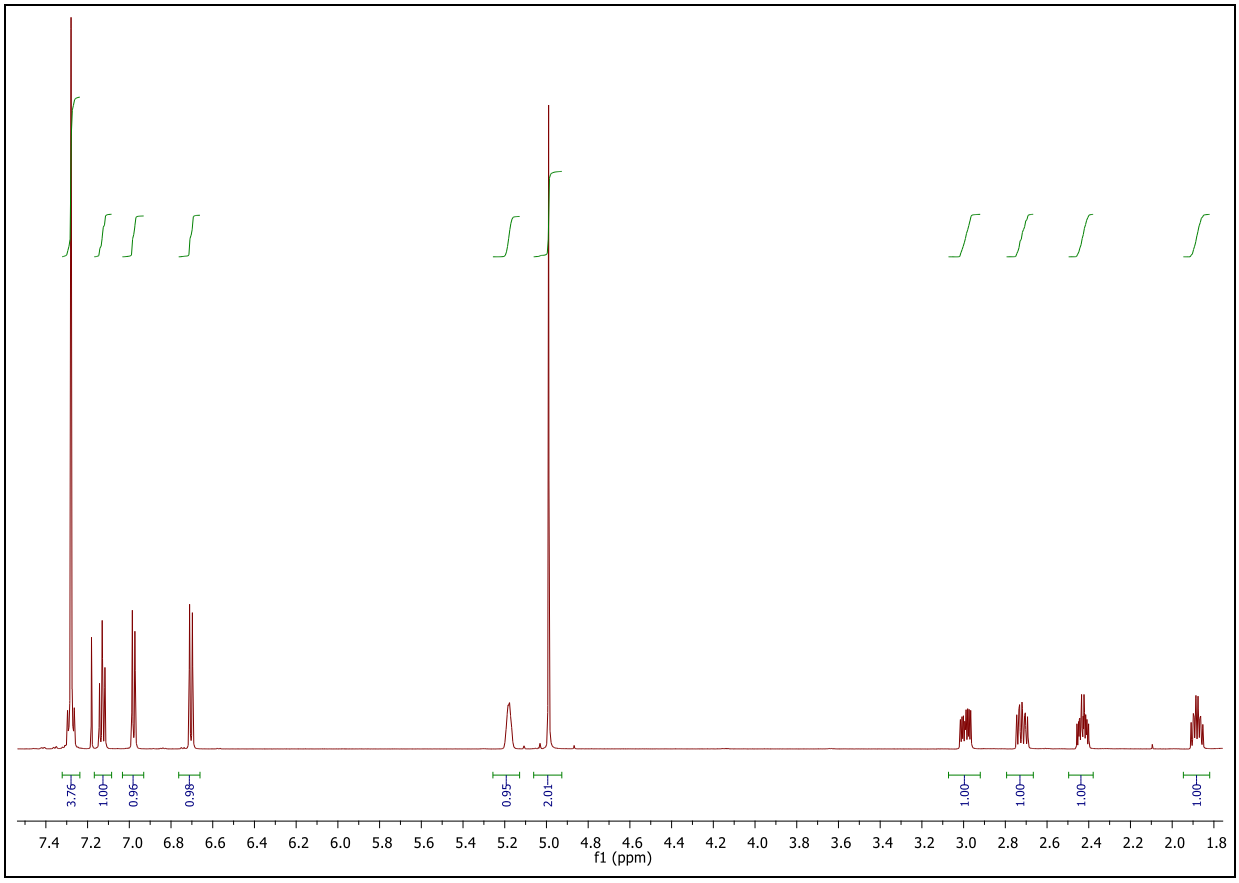

4-(4-Chlorobenzyloxy)-1-indanol (**1k**)

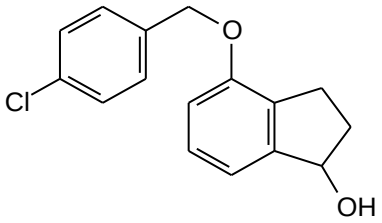

^{13}C NMR (151 MHz, $CDCl_3$) δ 155.00, 147.14, 135.75, 133.65, 131.65, 128.76, 128.50, 128.39, 116.89, 111.14, 69.11, 35.65, 26.63.

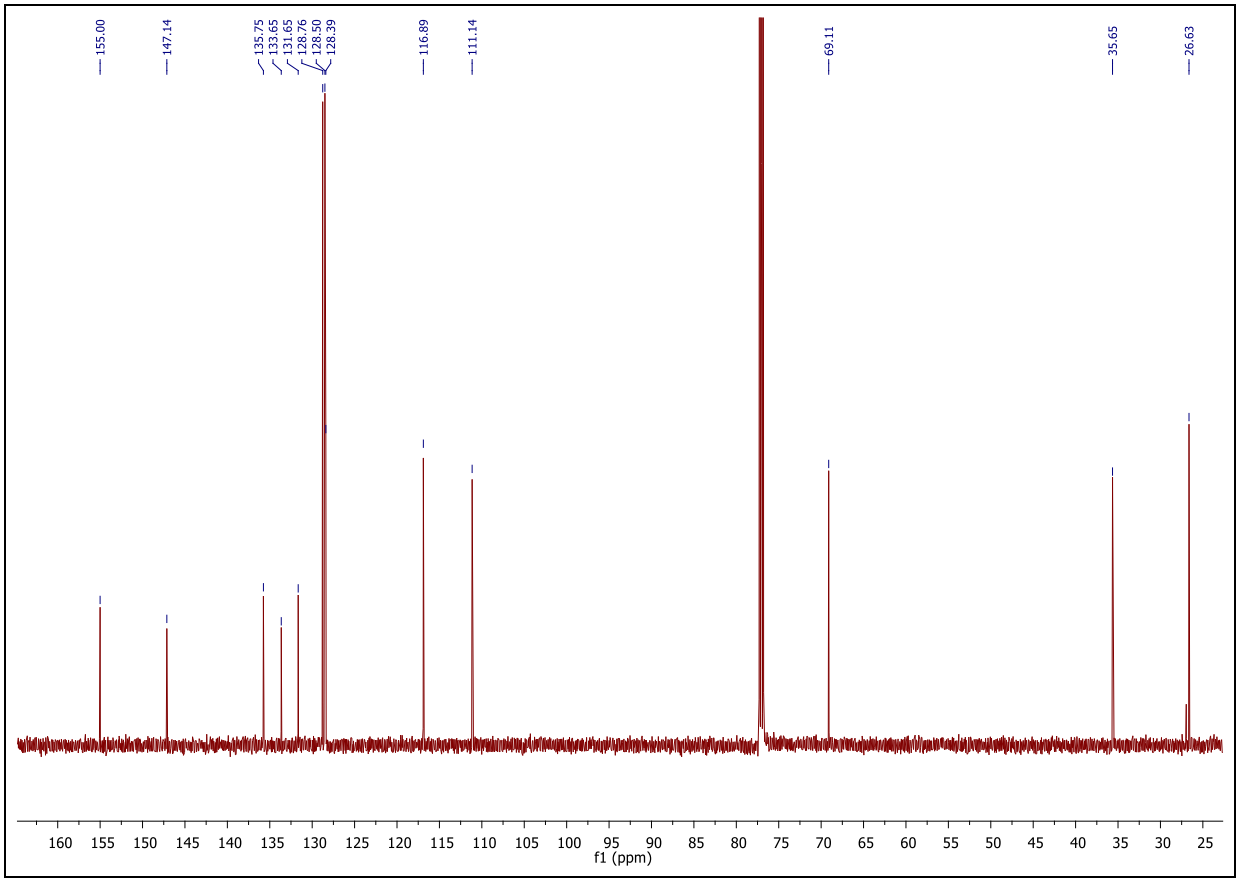

5-(4-Chlorobenzyloxy)-1-indanol (**1l**)

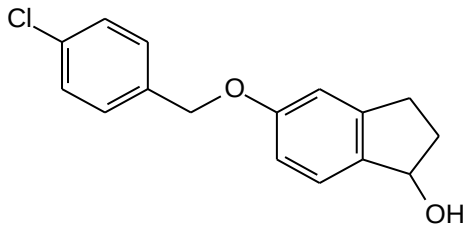

^{1}H NMR (600 MHz, $CDCl_3$) δ 7.32 – 7.16 (m, 5H), 6.78 – 6.72 (m, 2H), 5.11 (s, 1H), 4.95 (s, 2H), 3.00 – 2.91 (m, 1H), 2.74 – 2.65 (m, 1H), 2.45 – 2.34 (m, 1H), 1.94 – 1.83 (m, 1H).

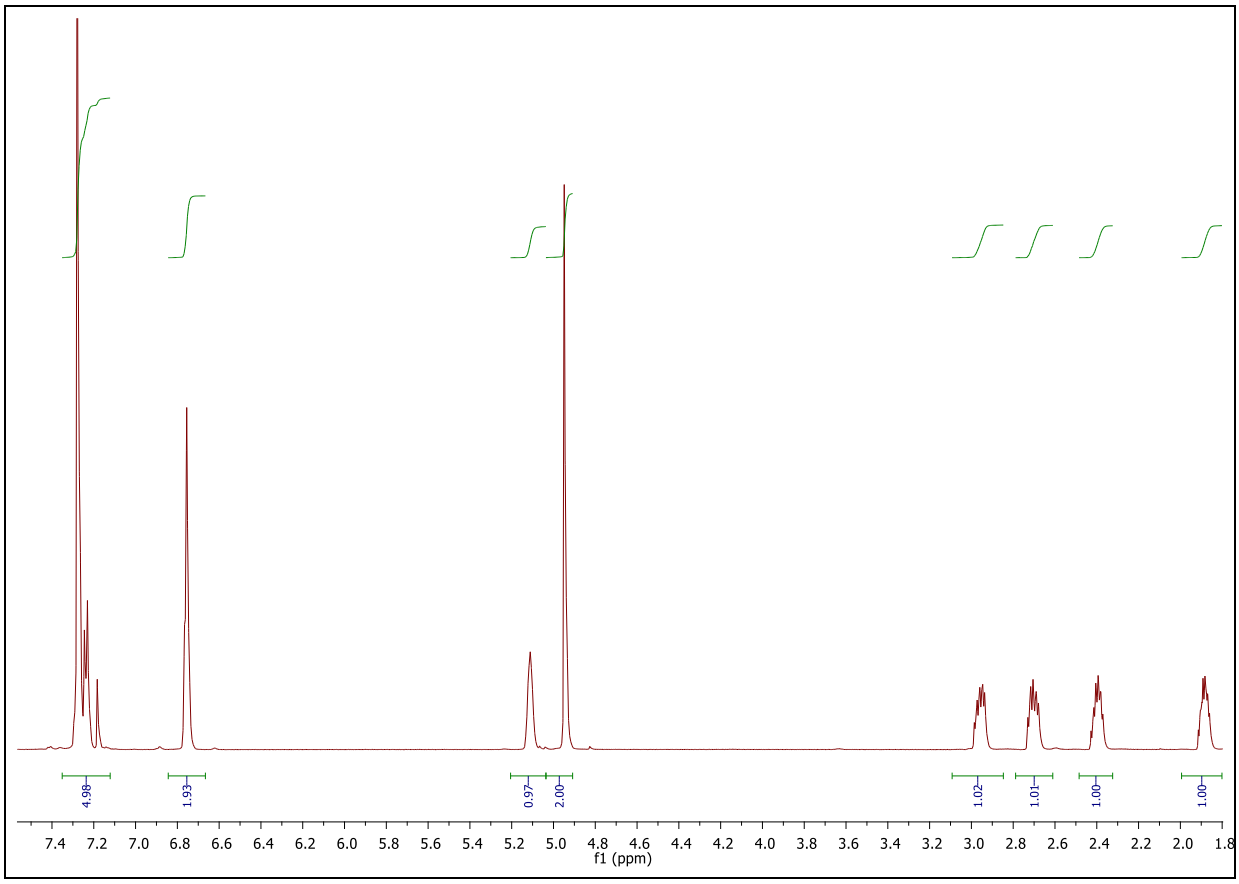

5-(4-Chlorobenzyloxy)-1-indanol (**1l**)

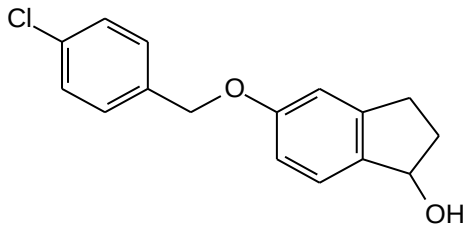

^{13}C NMR (151 MHz, $CDCl_3$) δ 159.19, 145.38, 137.87, 135.60, 133.73, 128.78, 128.73, 125.17, 113.85, 110.92, 75.89, 69.40, 36.32, 30.04.

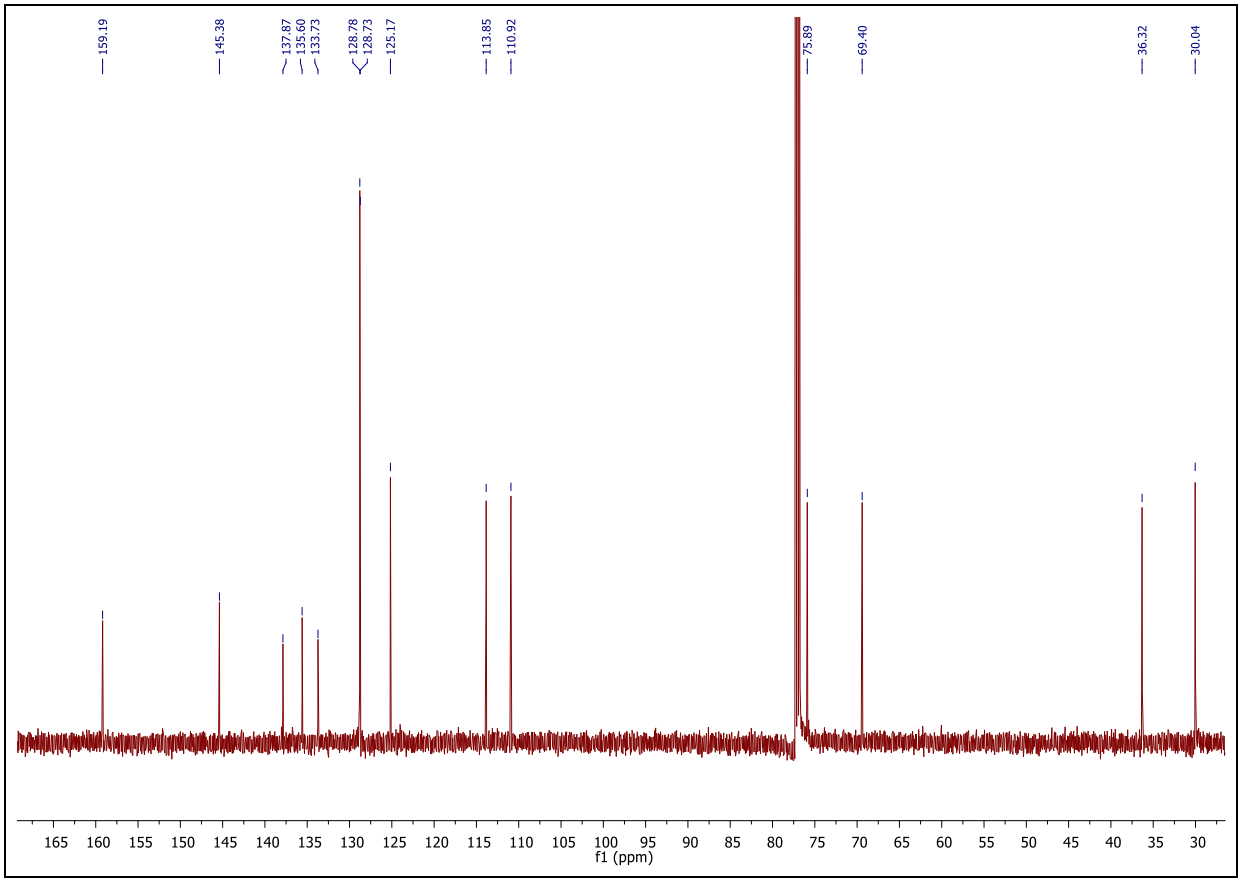

6-(4-Chlorobenzyloxy)-1-indanol (**1m**)

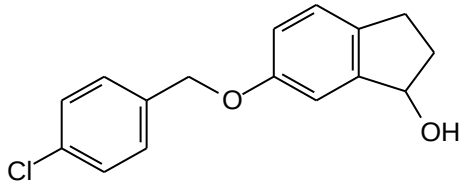

^{1}H NMR (600 MHz, $CDCl_3$) δ 7.30 – 7.24 (m, 4H), 7.07 (d, *J* = 8.2 Hz, 1H), 6.93 (d, *J* = 2.0 Hz, 1H), 6.79 (dd, *J* = 8.2, 2.3 Hz, 1H), 5.08 (s, 1H), 4.94 (s, 2H), 2.95 – 2.84 (m, 1H), 2.73 – 2.58 (m, 1H), 2.48 – 2.38 (m, 1H), 1.91 – 1.79 (m, 1H).

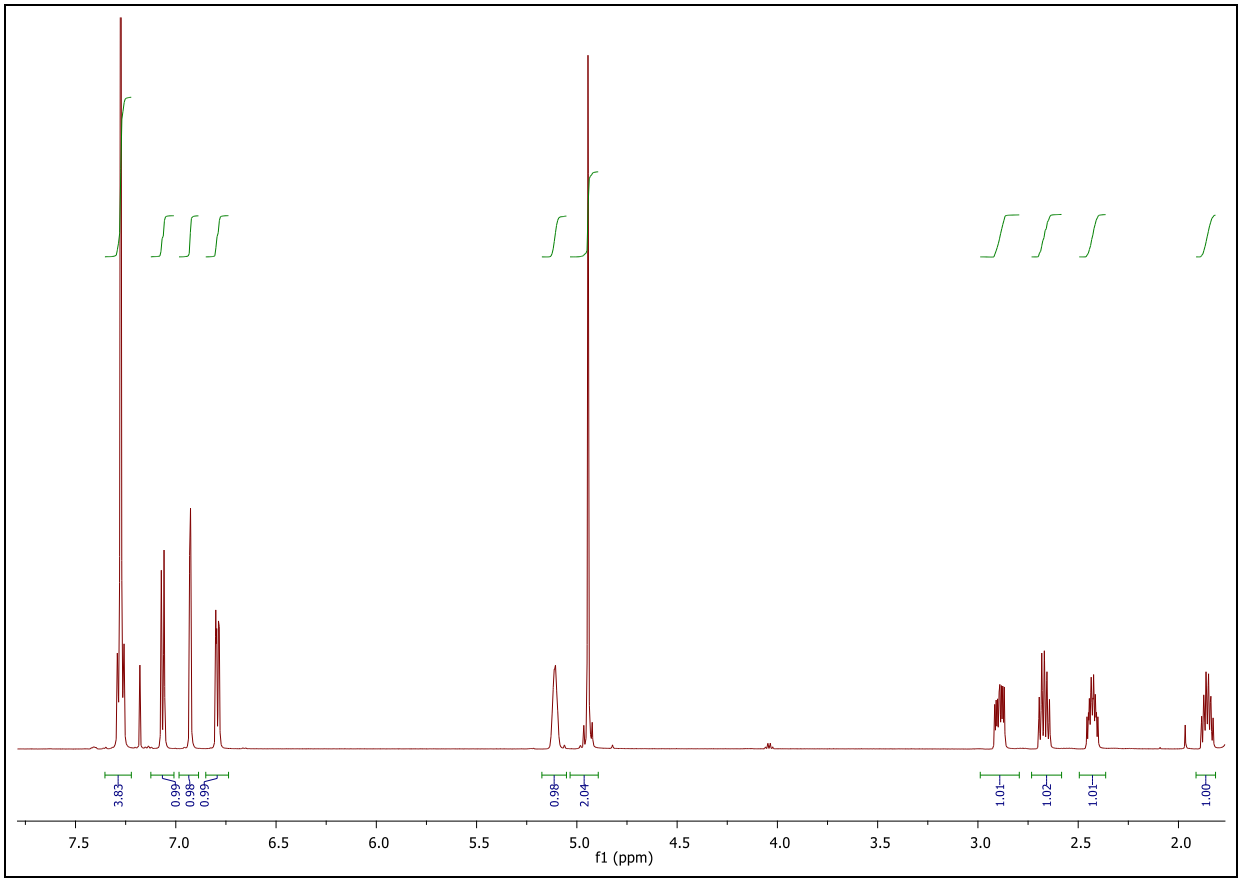

6-(4-Chlorobenzyloxy)-1-indanol (**1m**)

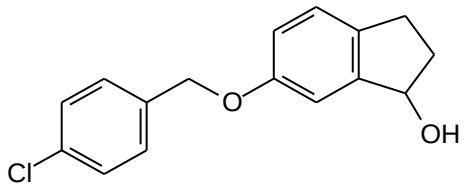

^{13}C NMR (151 MHz, $CDCl_3$) δ 157.97, 146.46, 135.67, 135.66, 133.70, 128.77, 125.63, 115.85, 109.97, 76.62, 69.50, 36.61, 29.00.

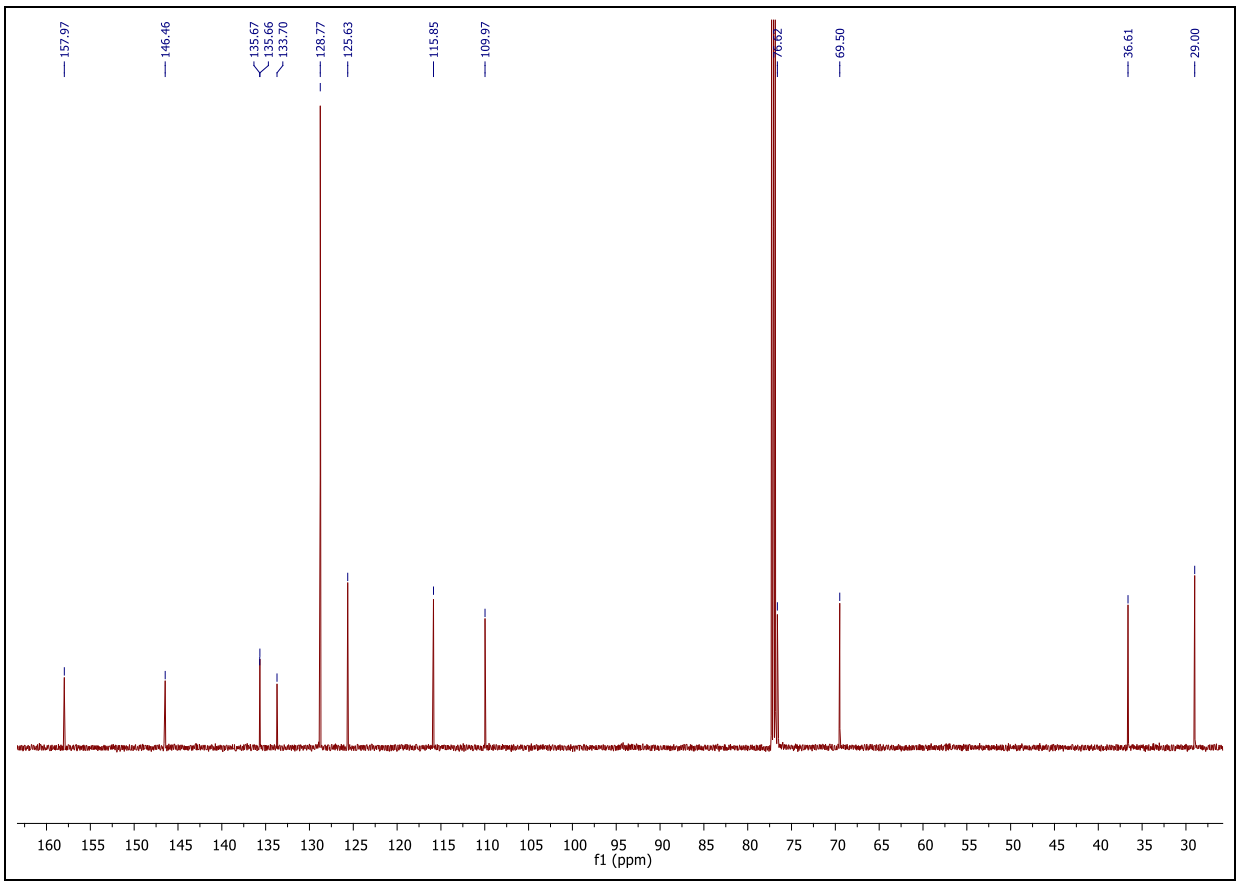

6-(3-Chlorobenzyloxy)-1-indanol (**1n**)

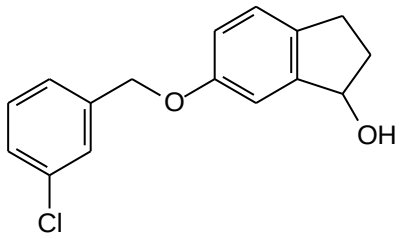

^{1}H NMR (600 MHz, $CDCl_3$) δ 7.30 – 7.17 (m, 5H), 6.76 (d, *J* = 6.3 Hz, 2H), 5.11 (s, 1H), 4.95 (s, 2H), 3.00 – 2.91 (m, 1H), 2.74 – 2.65 (m, 1H), 2.45 – 2.34 (m, 1H), 1.94 – 1.83 (m, 1H).

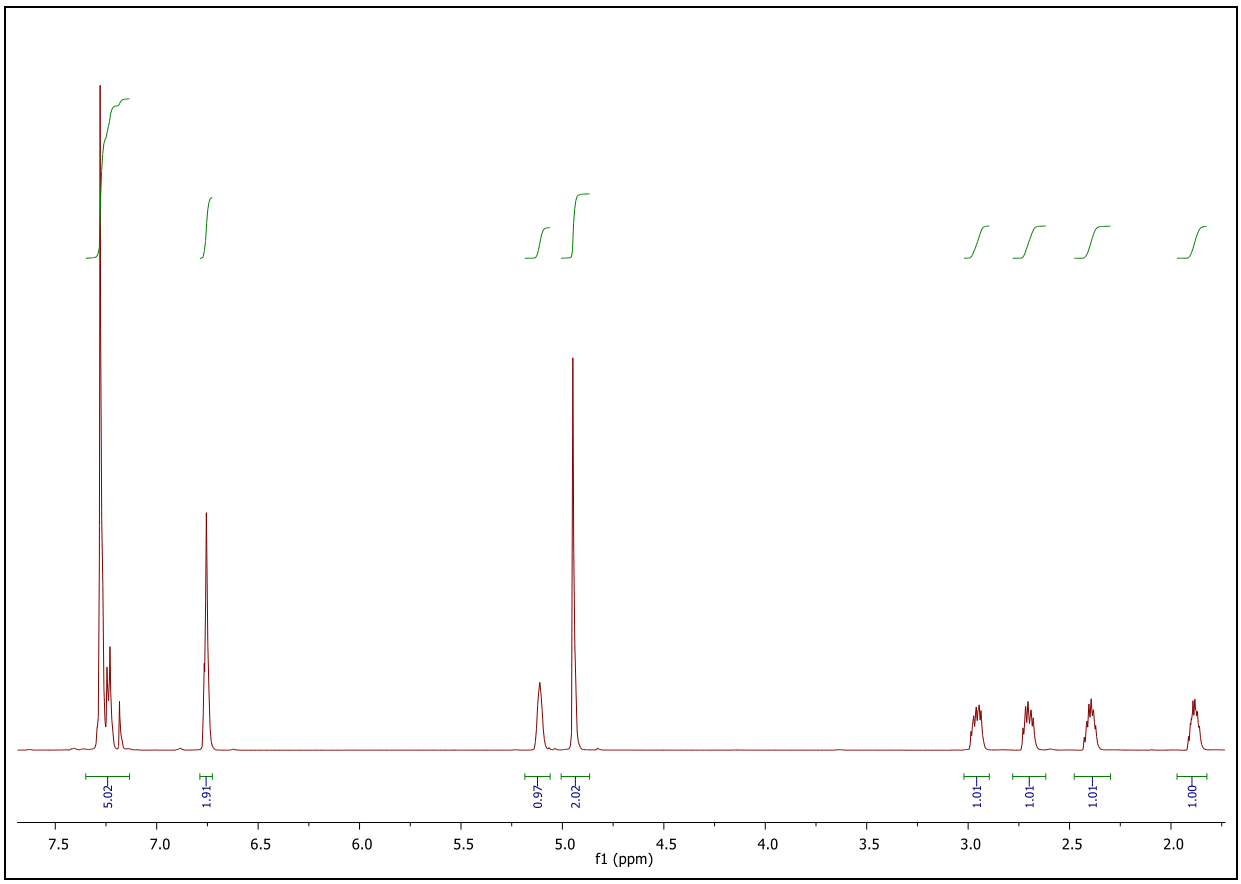

6-(3-Chlorobenzyloxy)-1-indanol (**1n**)

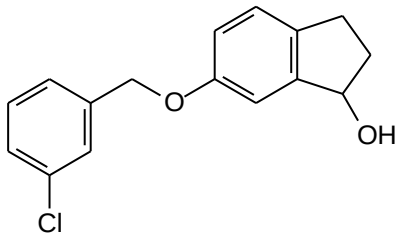

^{13}C NMR (151 MHz, $CDCl_3$) δ 157.93, 146.48, 139.26, 135.73, 134.52, 129.87, 128.05, 127.41, 125.66, 125.35, 115.84, 109.96, 69.45, 36.58, 29.01, 14.10.

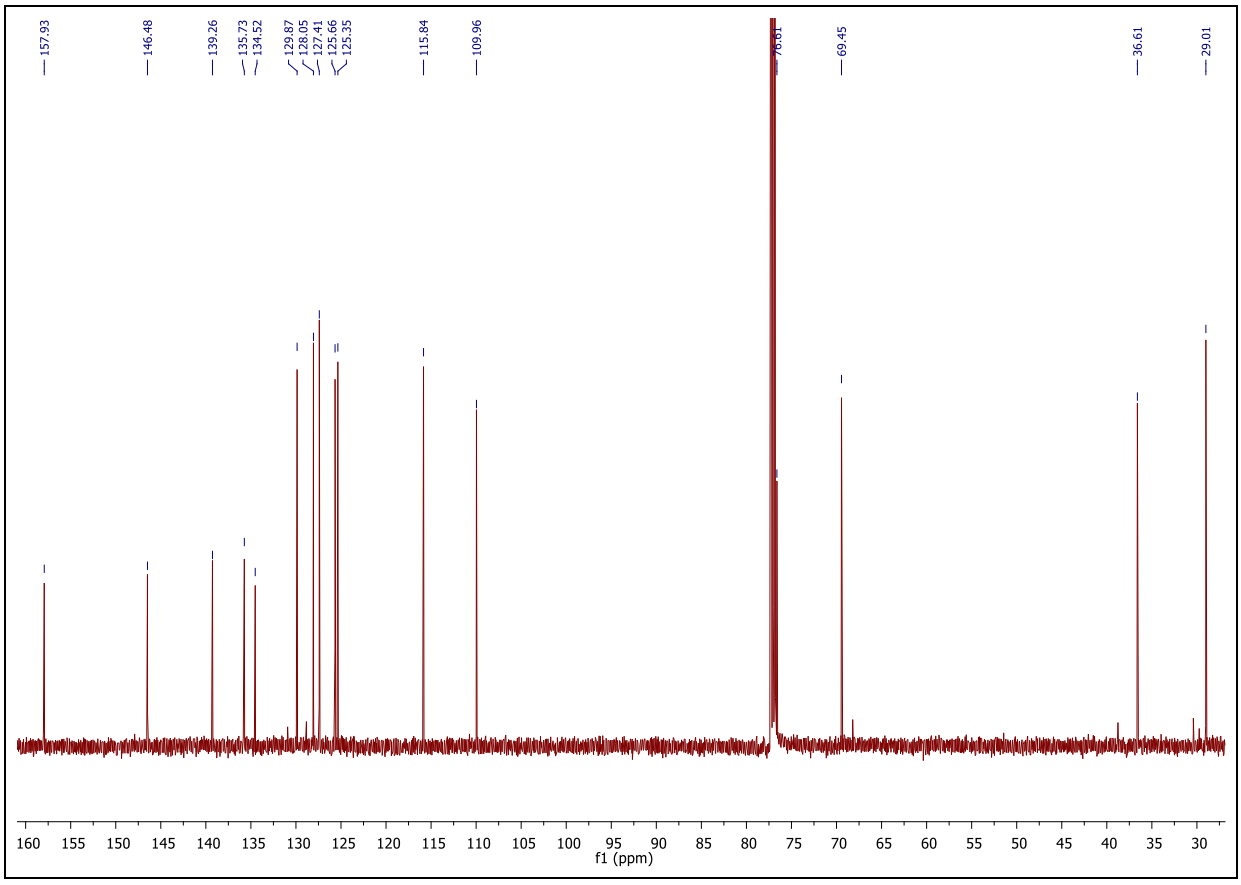

4-Hydroxy-1-indanone (**2a**)

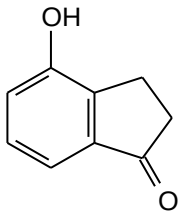

^{1}H NMR (600 MHz, DMSO-d_6) δ 9.75 (s, 1H), 7.05 (t, J = 7.7 Hz, 1H), 6.89 (d, J = 7.5 Hz, 1H), 6.85 (dd, J = 7.8, 1.0 Hz, 1H), 2.78 – 2.69 (m, 2H), 2.45 – 2.36 (m, 2H).

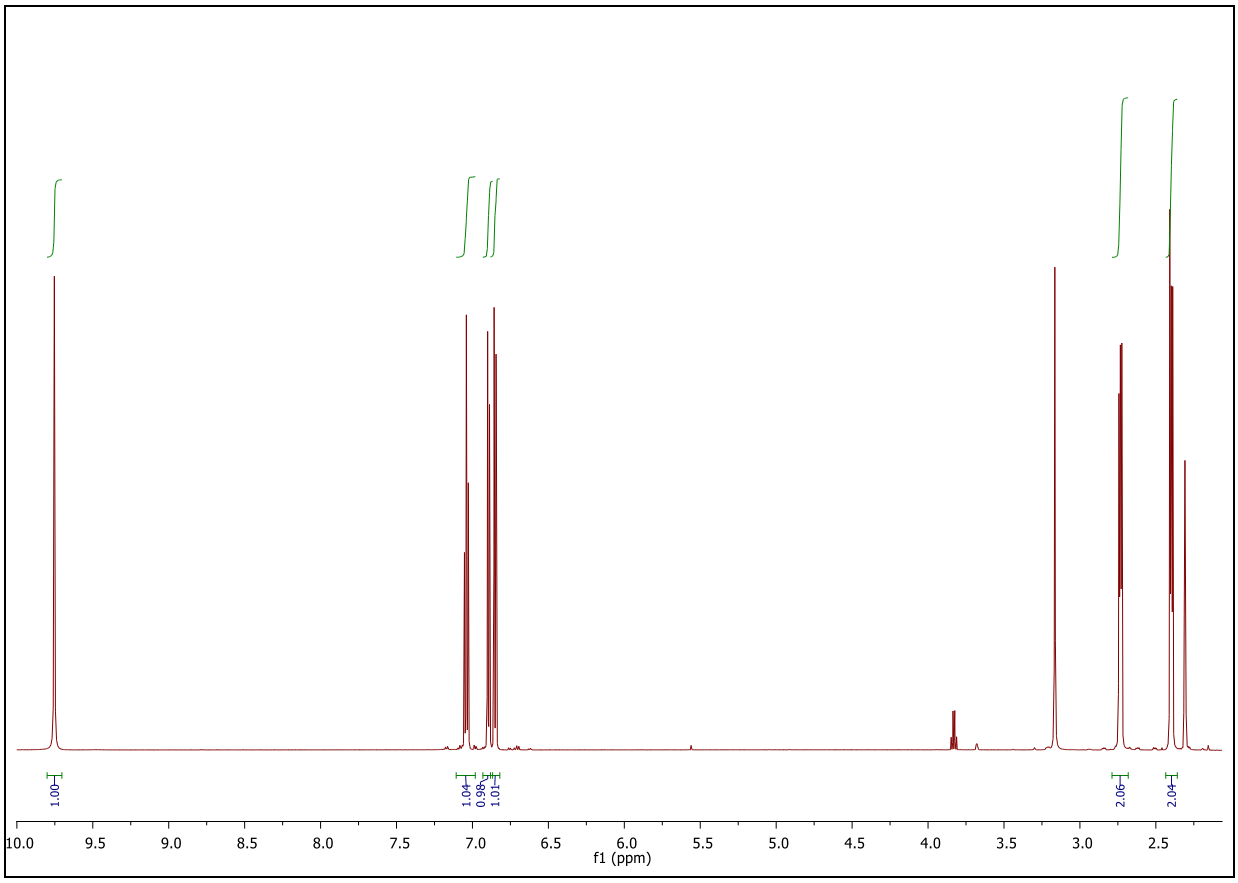

4-Hydroxy-1-indanone (**2a**)

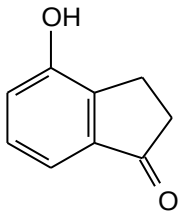

^{13}C NMR (151 MHz, DMSO) δ 155.60, 142.31, 138.88, 129.08, 120.23, 113.79, 36.25, 31.14, 22.76.

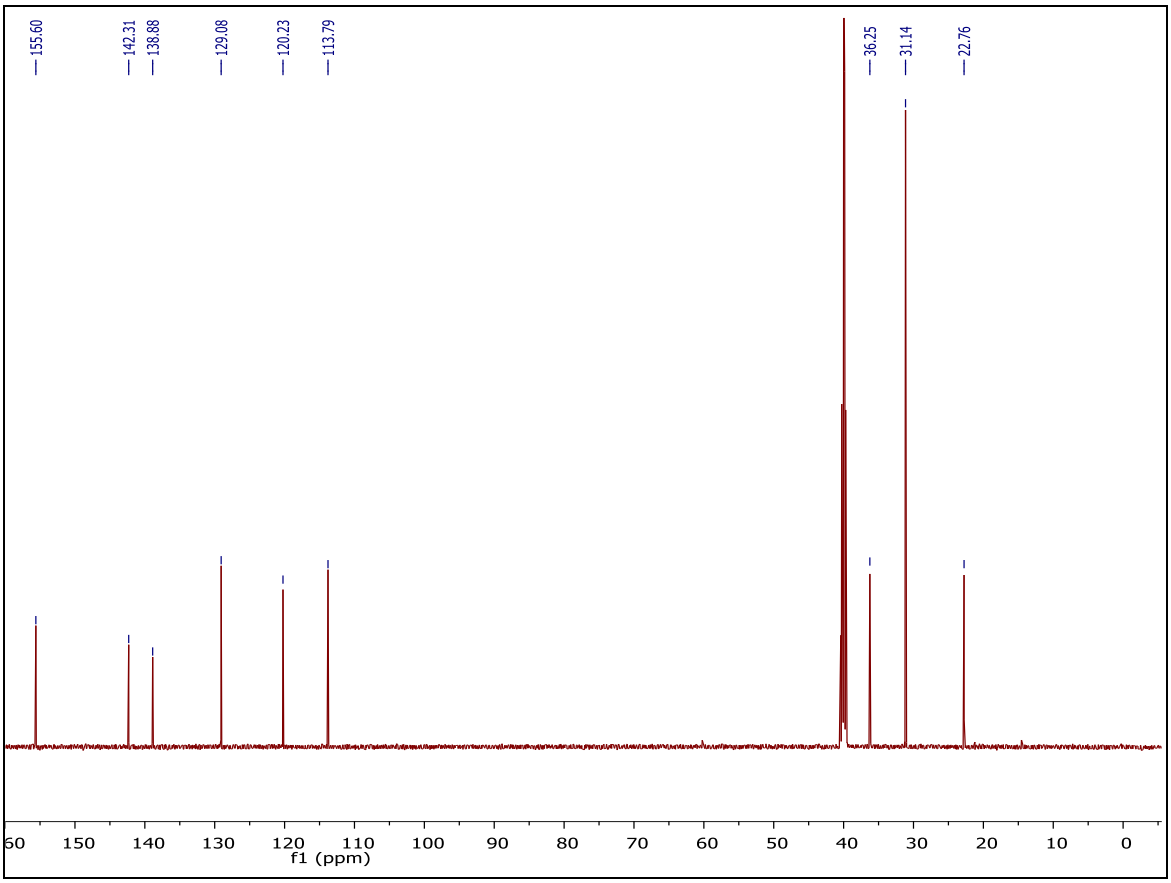

6-Hydroxy-1-indanone (**2c**)

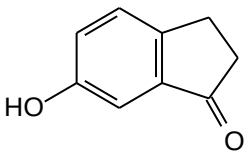

^{1}H NMR (600 MHz, DMSO-d_6) δ 10.48 (s, 1H), 7.48 (d, J = 8.3 Hz, 1H), 6.85 (d, J = 2.1 Hz, 1H), 6.80 (dd, J = 8.4, 2.1 Hz, 1H), 3.03 – 2.95 (m, 2H), 2.57 – 2.51 (m, 2H).

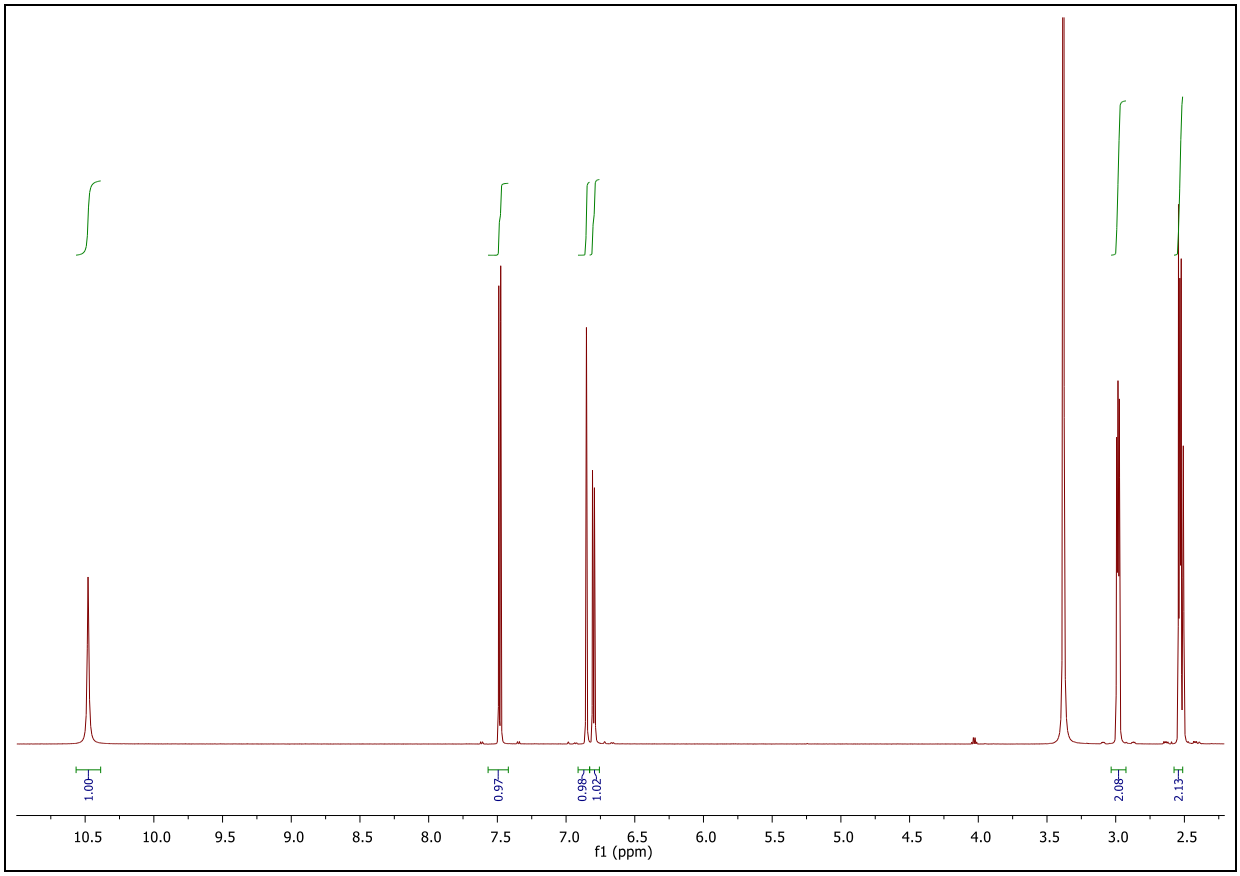

6-Hydroxy-1-indanone (**2c**)

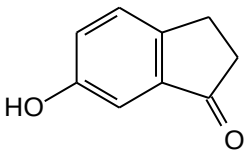

^{13}C NMR (151 MHz, DMSO) δ 204.48, 164.10, 158.73, 129.08, 125.36, 116.20, 112.52, 36.39, 25.65.

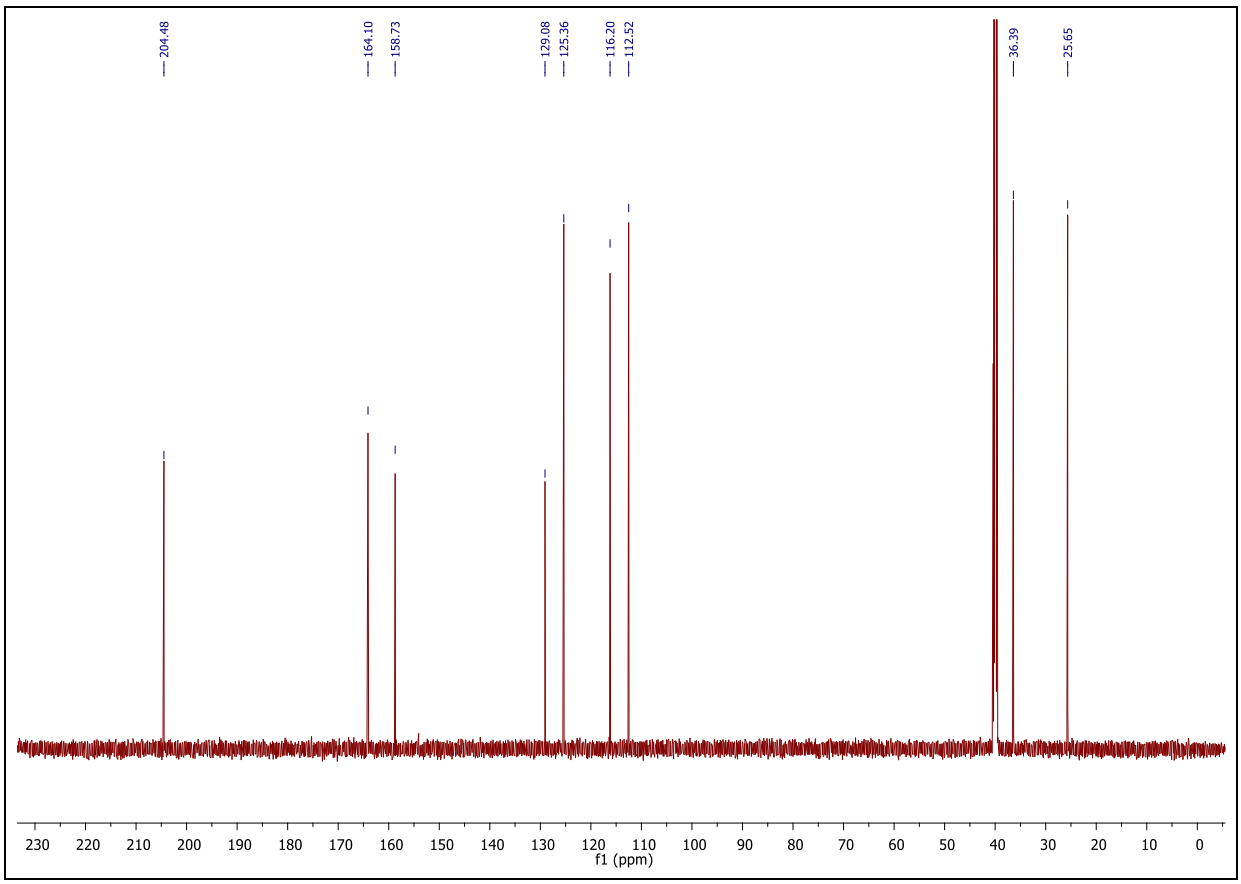

ANNEXURE B: MASS SPECTRA

4-Benzyloxy-1-indanone (**1a**)

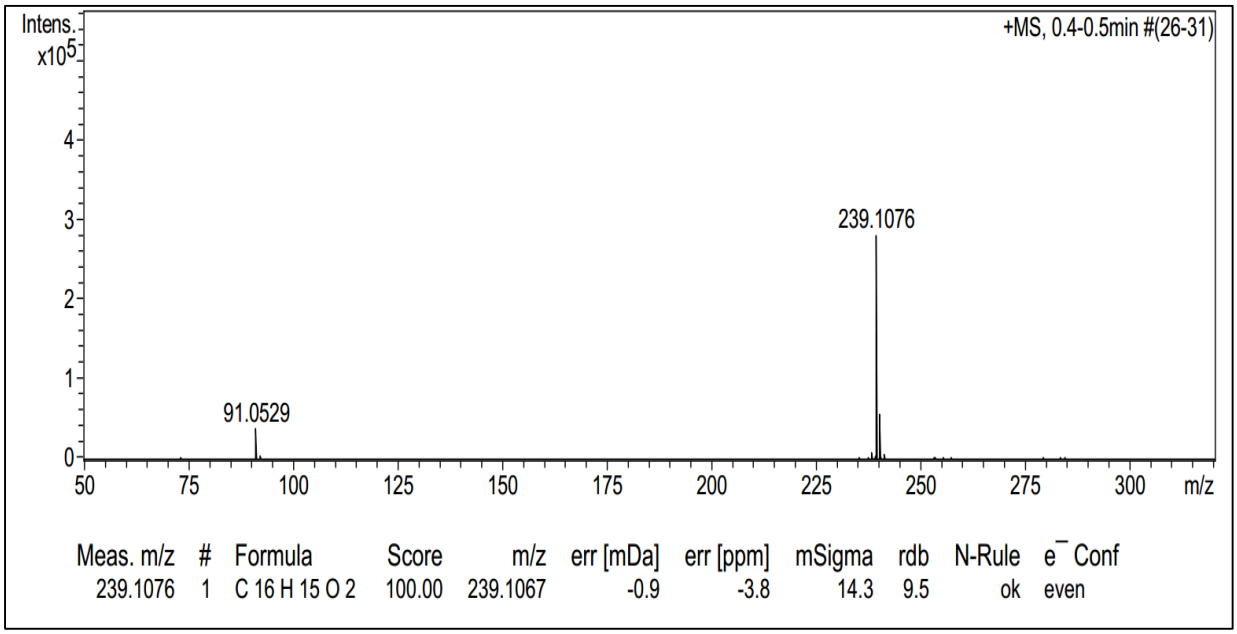

Meas. m/z	#	Formula	Score	m/z	err [mDa]	err [ppm]	mSigma	rdb	N-Rule	e⁻ Conf
239.1076	1	C 16 H 15 O 2	100.00	239.1067	-0.9	-3.8	14.3	9.5	ok	even

5-Benzyloxy-1-indanone (**1b**)

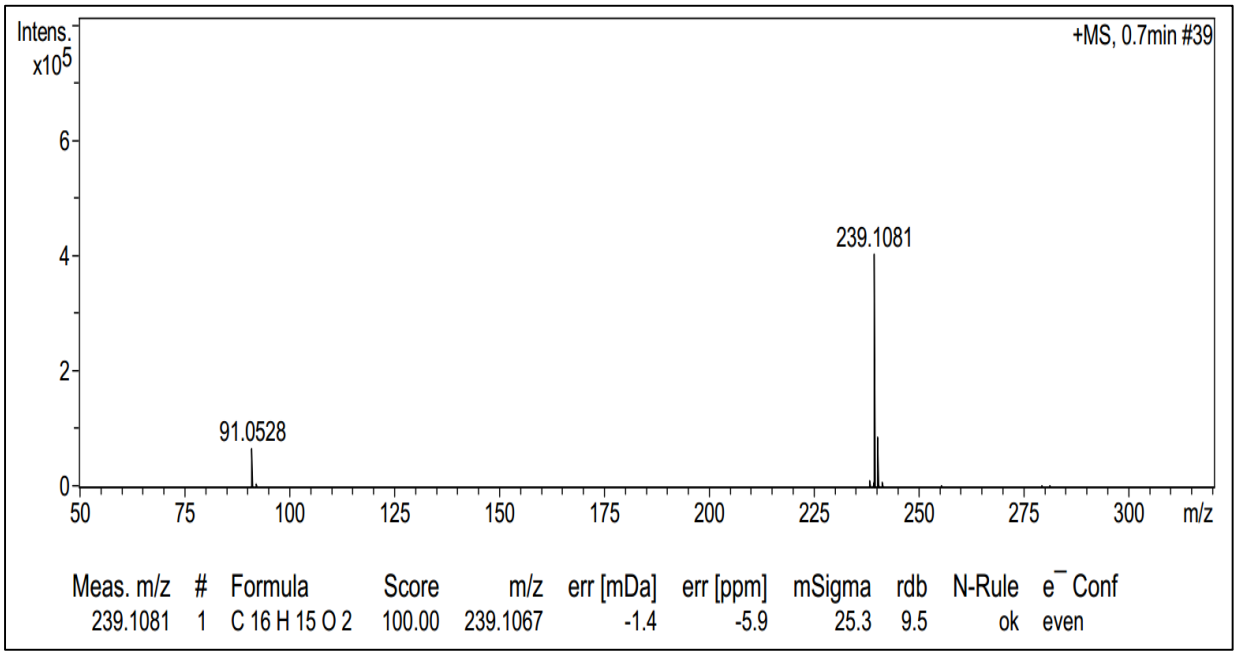

Meas. m/z	#	Formula	Score	m/z	err [mDa]	err [ppm]	mSigma	rdb	N-Rule	e⁻ Conf
239.1081	1	C 16 H 15 O 2	100.00	239.1067	-1.4	-5.9	25.3	9.5	ok	even

6-Benzyloxy-1-indanone (**1c**)

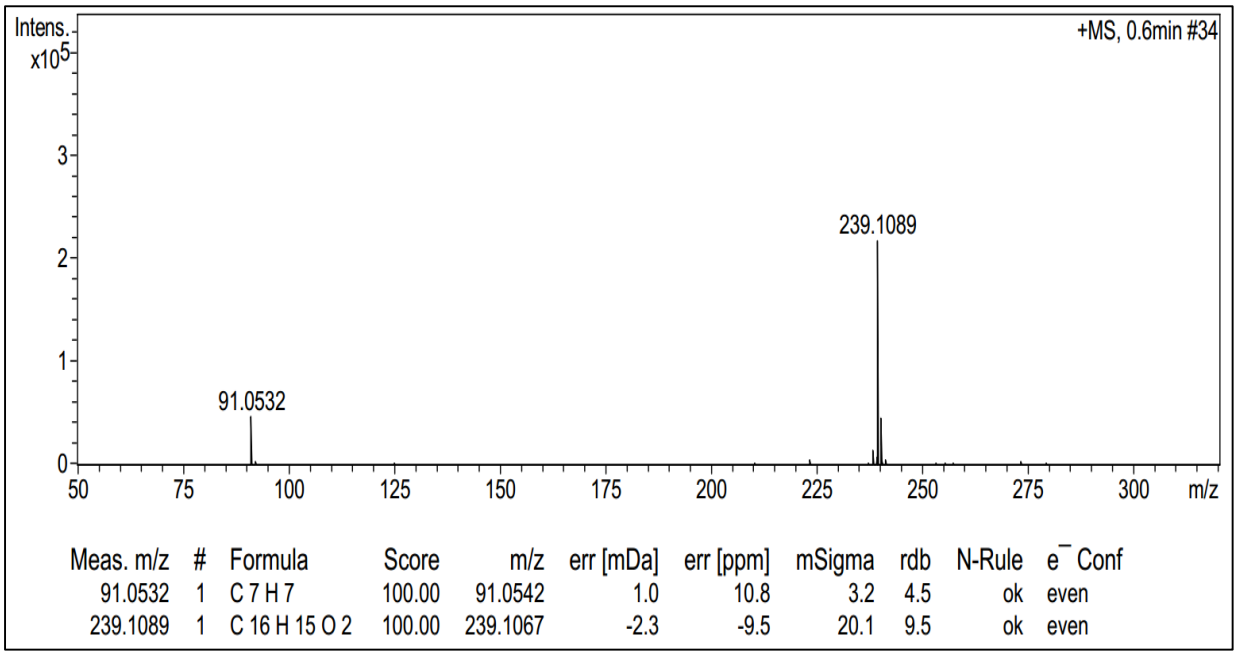

Meas. m/z	#	Formula	Score	m/z	err [mDa]	err [ppm]	mSigma	rdb	N-Rule	e⁻ Conf
91.0532	1	C 7 H 7	100.00	91.0542	1.0	10.8	3.2	4.5	ok	even
239.1089	1	C 16 H 15 O 2	100.00	239.1067	-2.3	-9.5	20.1	9.5	ok	even

4-(4-Chlorobenzyloxy)-1-indanone (**1d**)

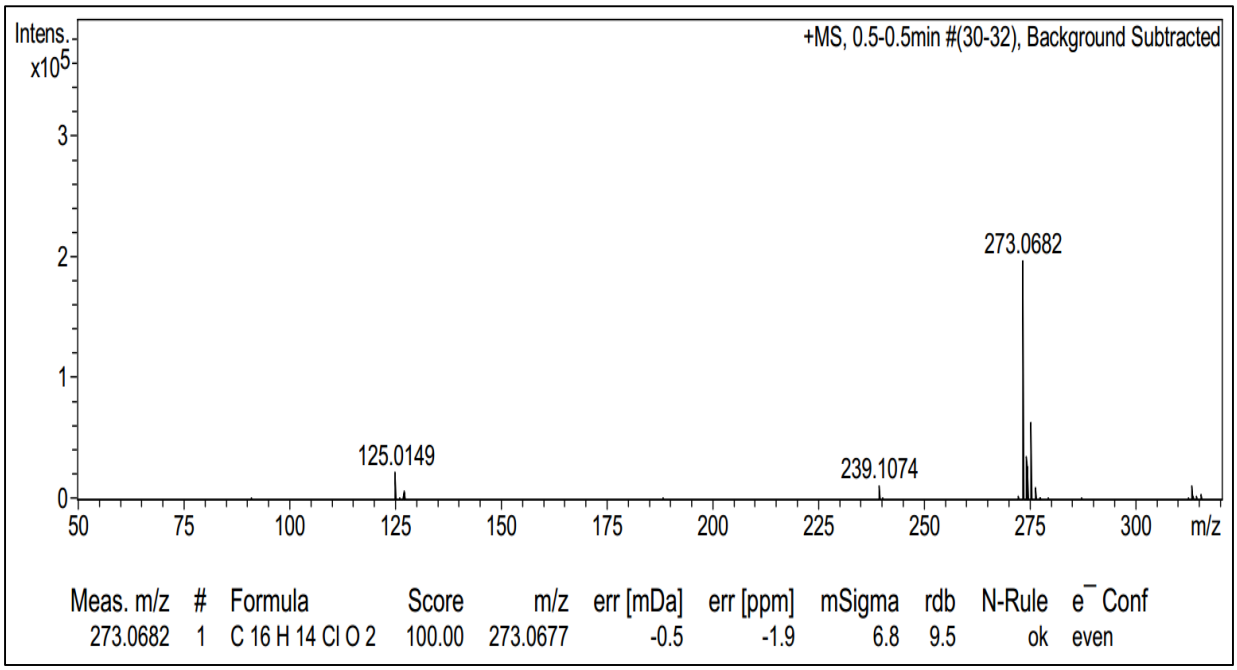

Meas. m/z	#	Formula	Score	m/z	err [mDa]	err [ppm]	mSigma	rdb	N-Rule	e⁻ Conf
273.0682	1	C 16 H 14 Cl O 2	100.00	273.0677	-0.5	-1.9	6.8	9.5	ok	even

5-(4-Chlorobenzyloxy)-1-indanone (**1e**)

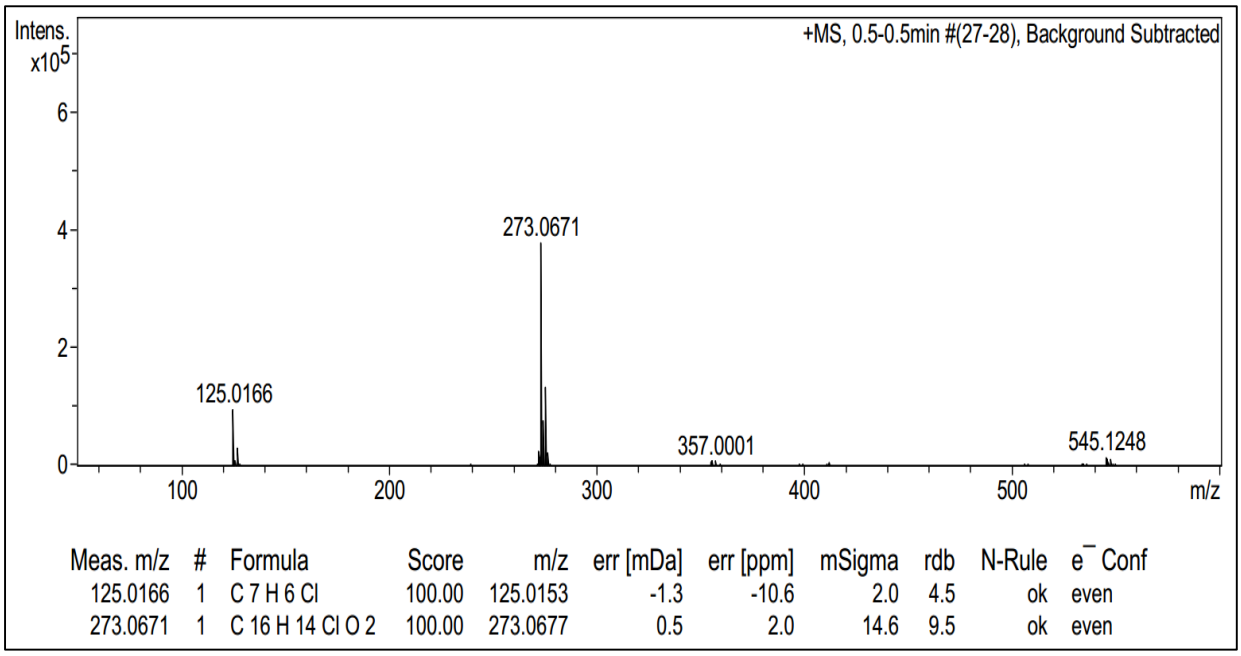

Meas. m/z	#	Formula	Score	m/z	err [mDa]	err [ppm]	mSigma	rdb	N-Rule	e⁻ Conf
125.0166	1	C 7 H 6 Cl	100.00	125.0153	-1.3	-10.6	2.0	4.5	ok	even
273.0671	1	C 16 H 14 Cl O 2	100.00	273.0677	0.5	2.0	14.6	9.5	ok	even

6-(4-Chlorobenzyloxy)-1-indanone (**1f**)

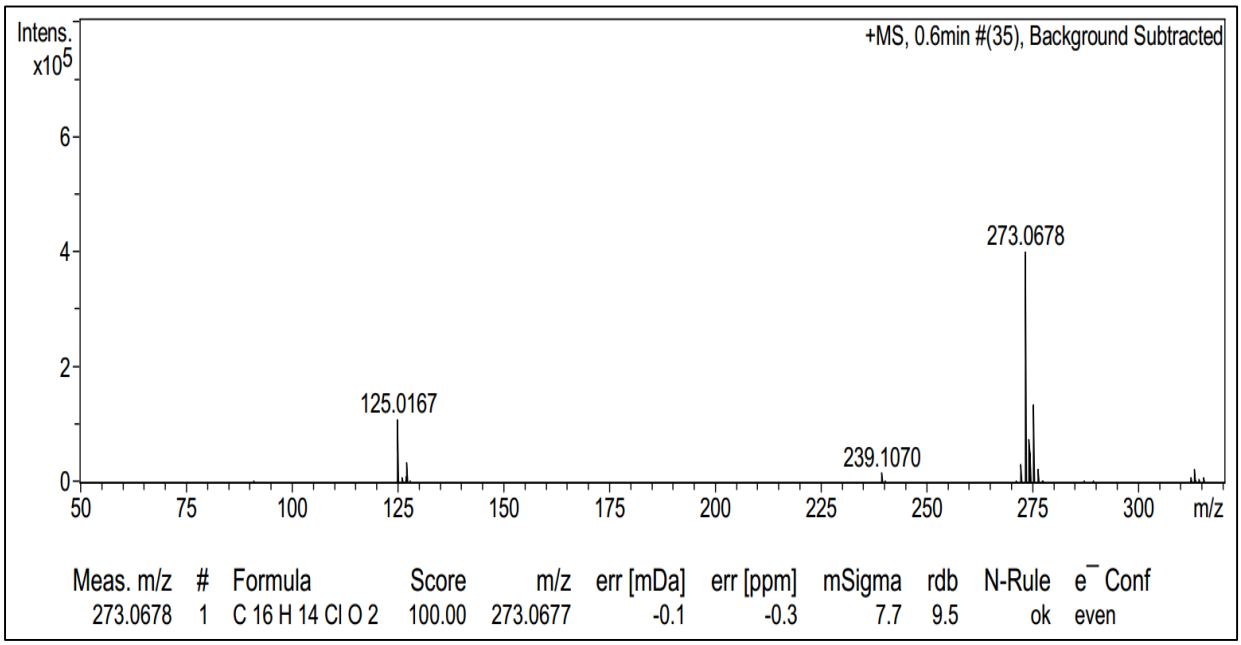

Meas. m/z	#	Formula	Score	m/z	err [mDa]	err [ppm]	mSigma	rdb	N-Rule	e⁻ Conf
273.0678	1	C 16 H 14 Cl O 2	100.00	273.0677	-0.1	-0.3	7.7	9.5	ok	even

6-(3-Chlorobenzyloxy)-1-indanone (**1g**)

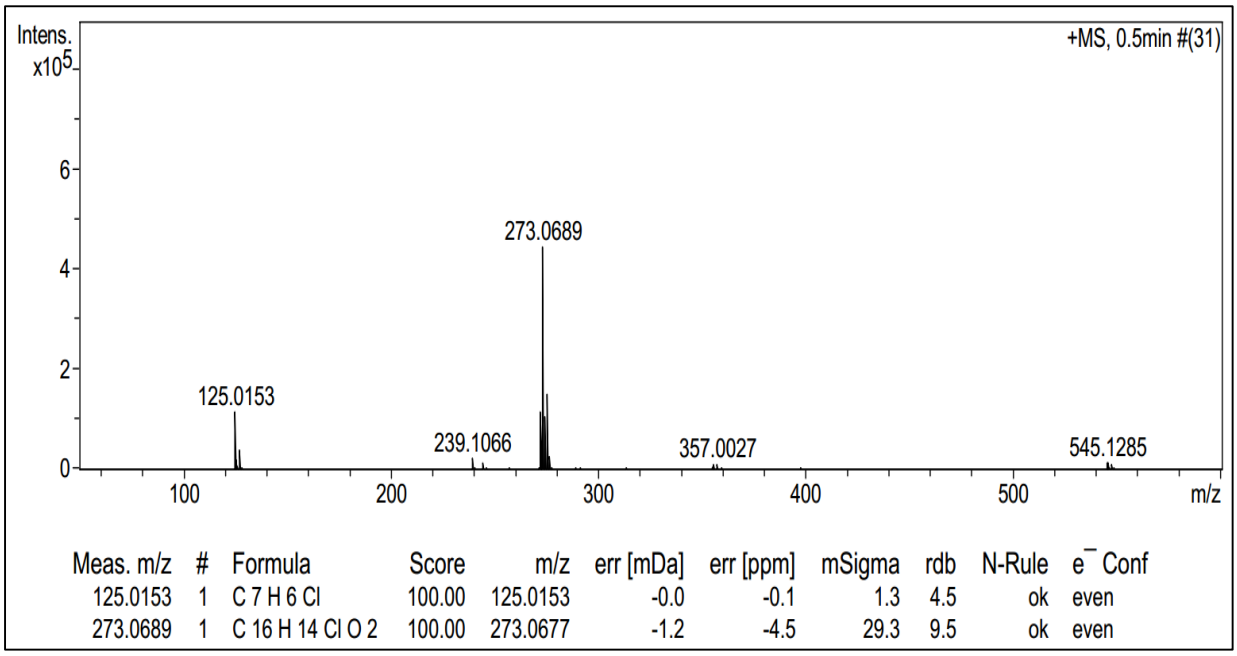

Meas. m/z	#	Formula	Score	m/z	err [mDa]	err [ppm]	mSigma	rdb	N-Rule	e⁻ Conf
125.0153	1	C 7 H 6 Cl	100.00	125.0153	-0.0	-0.1	1.3	4.5	ok	even
273.0689	1	C 16 H 14 Cl O 2	100.00	273.0677	-1.2	-4.5	29.3	9.5	ok	even

5-(2-Phenoxyethoxy)-1-indanone (**1h**)

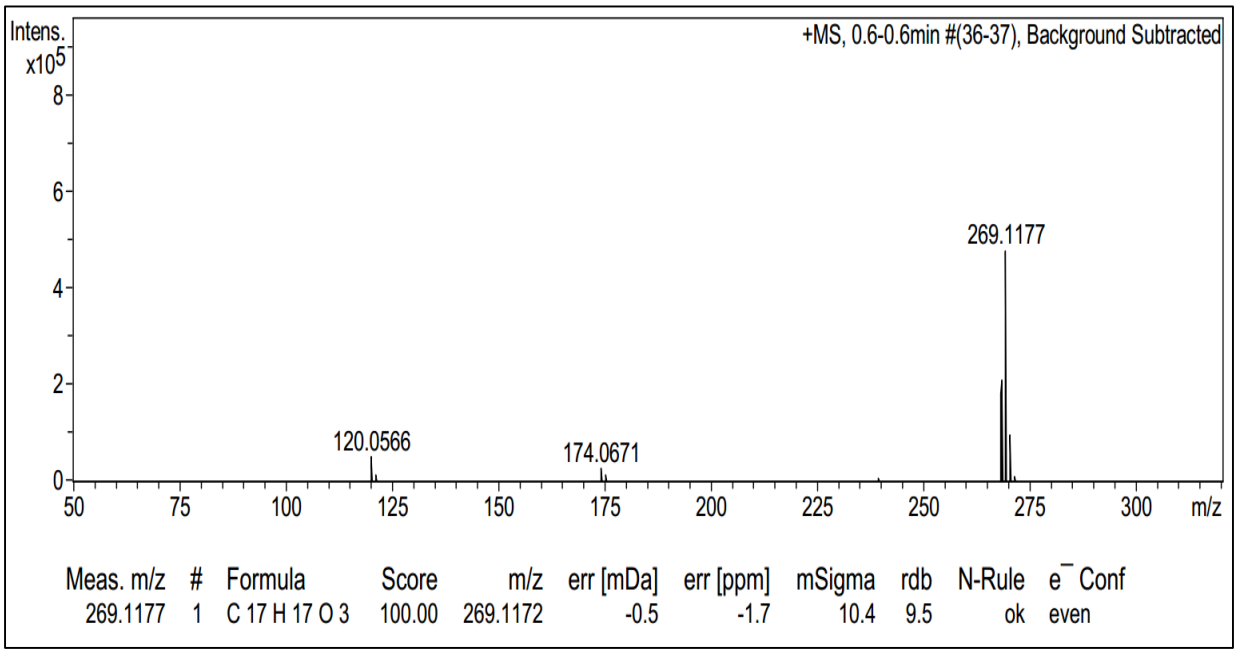

Meas. m/z	#	Formula	Score	m/z	err [mDa]	err [ppm]	mSigma	rdb	N-Rule	e⁻ Conf
269.1177	1	C 17 H 17 O 3	100.00	269.1172	-0.5	-1.7	10.4	9.5	ok	even

5-Benzyloxy-1-indanol (**1i**)

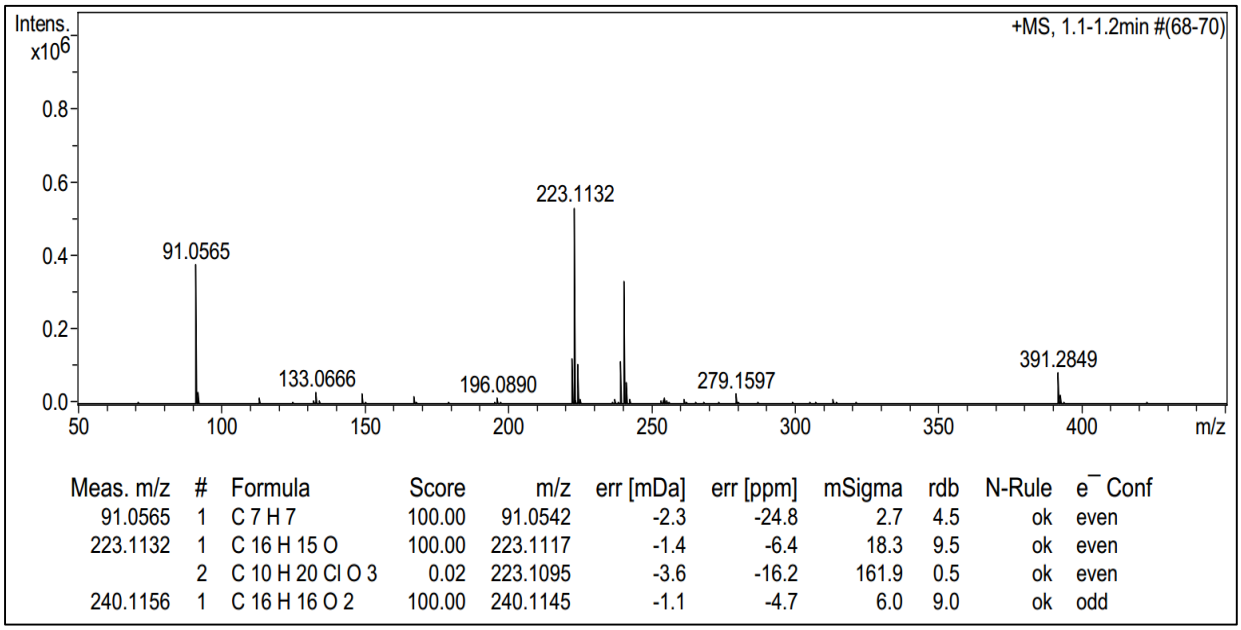

Meas. m/z	#	Formula	Score	m/z	err [mDa]	err [ppm]	mSigma	rdb	N-Rule	e¯ Conf
91.0565	1	C 7 H 7	100.00	91.0542	-2.3	-24.8	2.7	4.5	ok	even
223.1132	1	C 16 H 15 O	100.00	223.1117	-1.4	-6.4	18.3	9.5	ok	even
	2	C 10 H 20 Cl O 3	0.02	223.1095	-3.6	-16.2	161.9	0.5	ok	even
240.1156	1	C 16 H 16 O 2	100.00	240.1145	-1.1	-4.7	6.0	9.0	ok	odd

6-Benzyloxy-1-indanol (**1j**)

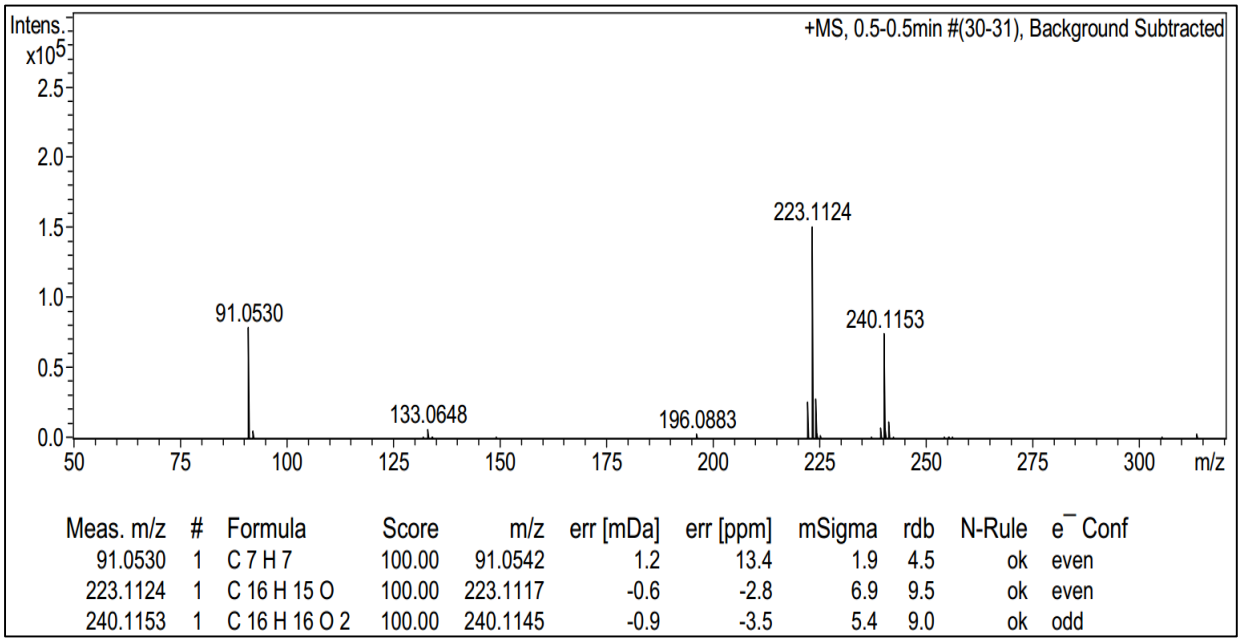

Meas. m/z	#	Formula	Score	m/z	err [mDa]	err [ppm]	mSigma	rdb	N-Rule	e¯ Conf
91.0530	1	C 7 H 7	100.00	91.0542	1.2	13.4	1.9	4.5	ok	even
223.1124	1	C 16 H 15 O	100.00	223.1117	-0.6	-2.8	6.9	9.5	ok	even
240.1153	1	C 16 H 16 O 2	100.00	240.1145	-0.9	-3.5	5.4	9.0	ok	odd

4-(4-Chlorobenzyloxy)-1-indanol (**1k**)

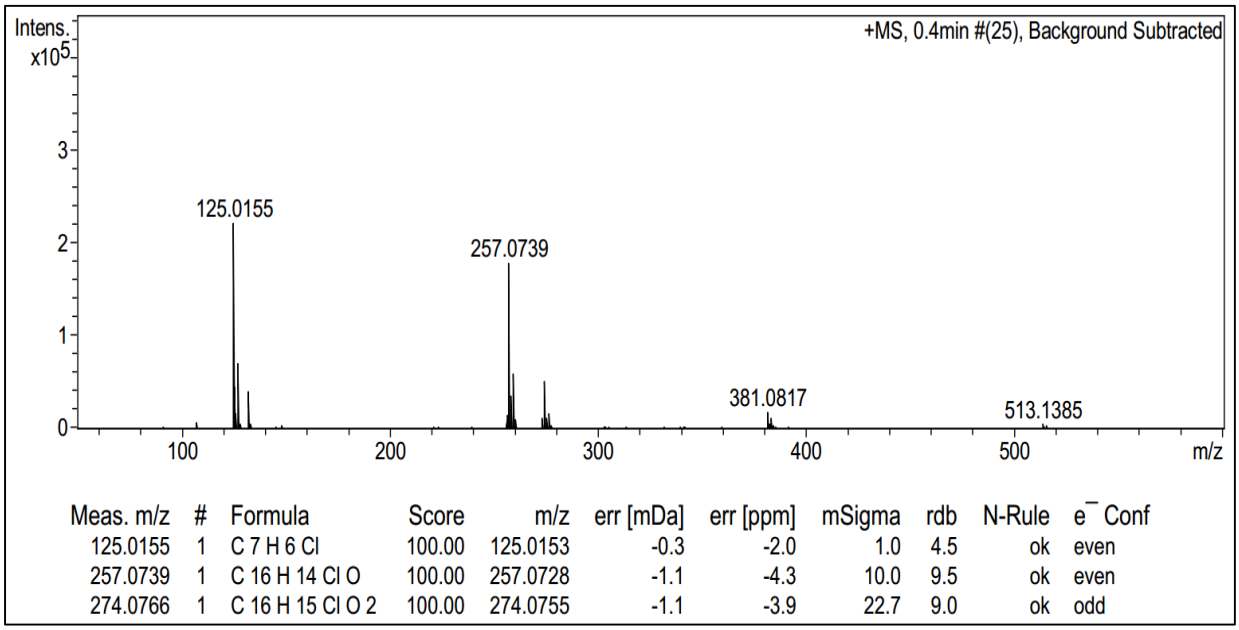

Meas. m/z	#	Formula	Score	m/z	err [mDa]	err [ppm]	mSigma	rdb	N-Rule	e¯ Conf
125.0155	1	C 7 H 6 Cl	100.00	125.0153	-0.3	-2.0	1.0	4.5	ok	even
257.0739	1	C 16 H 14 Cl O	100.00	257.0728	-1.1	-4.3	10.0	9.5	ok	even
274.0766	1	C 16 H 15 Cl O 2	100.00	274.0755	-1.1	-3.9	22.7	9.0	ok	odd

5-(4-Chlorobenzyloxy)-1-indanol (**1l**)

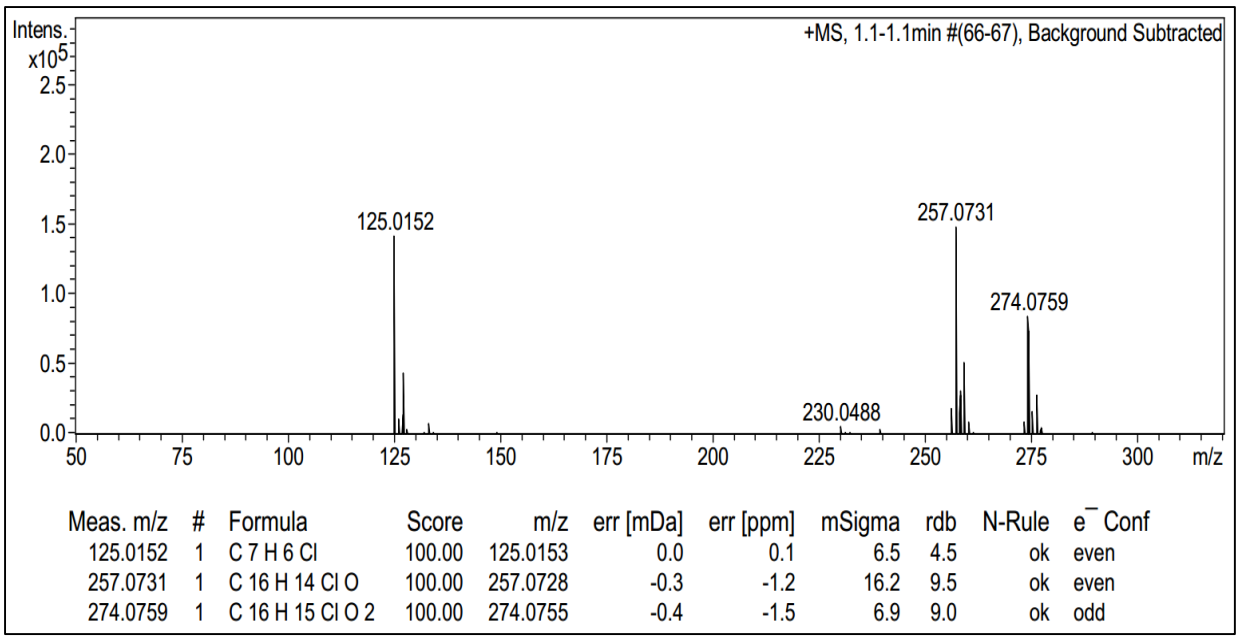

Meas. m/z	#	Formula	Score	m/z	err [mDa]	err [ppm]	mSigma	rdb	N-Rule	e¯ Conf
125.0152	1	C 7 H 6 Cl	100.00	125.0153	0.0	0.1	6.5	4.5	ok	even
257.0731	1	C 16 H 14 Cl O	100.00	257.0728	-0.3	-1.2	16.2	9.5	ok	even
274.0759	1	C 16 H 15 Cl O 2	100.00	274.0755	-0.4	-1.5	6.9	9.0	ok	odd

6-(4-Chlorobenzyloxy)-1-indanol (**1m**)

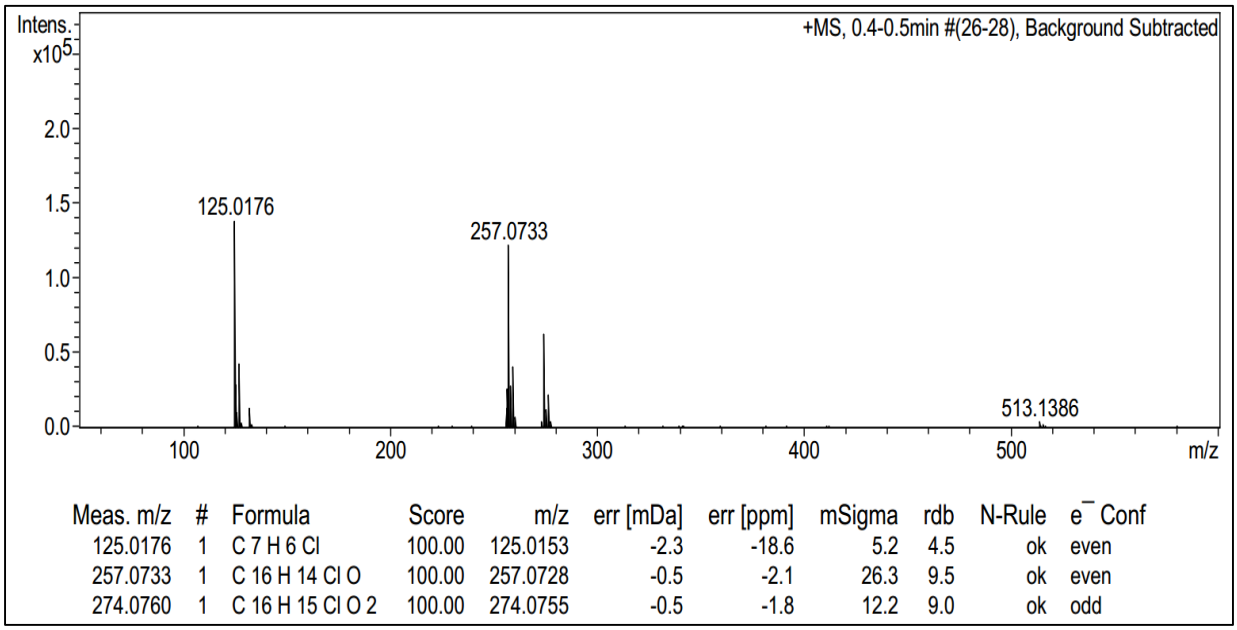

Meas. m/z	#	Formula	Score	m/z	err [mDa]	err [ppm]	mSigma	rdb	N-Rule	e⁻ Conf
125.0176	1	C 7 H 6 Cl	100.00	125.0153	-2.3	-18.6	5.2	4.5	ok	even
257.0733	1	C 16 H 14 Cl O	100.00	257.0728	-0.5	-2.1	26.3	9.5	ok	even
274.0760	1	C 16 H 15 Cl O 2	100.00	274.0755	-0.5	-1.8	12.2	9.0	ok	odd

6-(3-Chlorobenzyloxy)-1-indanol (**1n**)

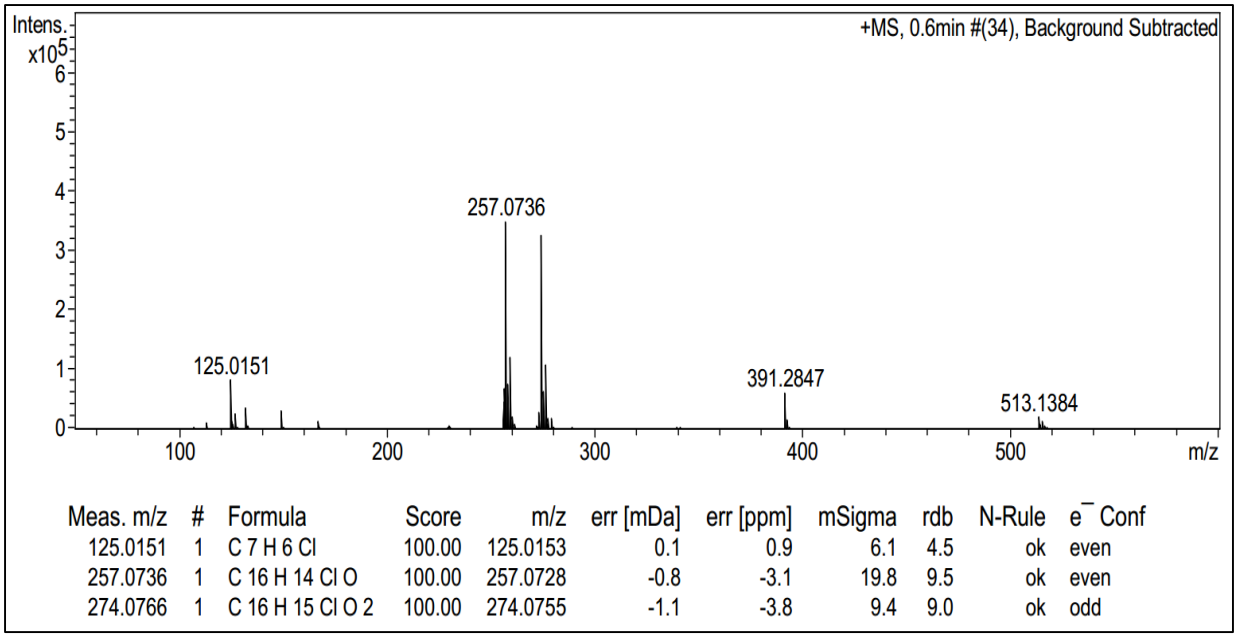

Meas. m/z	#	Formula	Score	m/z	err [mDa]	err [ppm]	mSigma	rdb	N-Rule	e⁻ Conf
125.0151	1	C 7 H 6 Cl	100.00	125.0153	0.1	0.9	6.1	4.5	ok	even
257.0736	1	C 16 H 14 Cl O	100.00	257.0728	-0.8	-3.1	19.8	9.5	ok	even
274.0766	1	C 16 H 15 Cl O 2	100.00	274.0755	-1.1	-3.8	9.4	9.0	ok	odd

4-Hydroxy-1-indanone (**2a**)

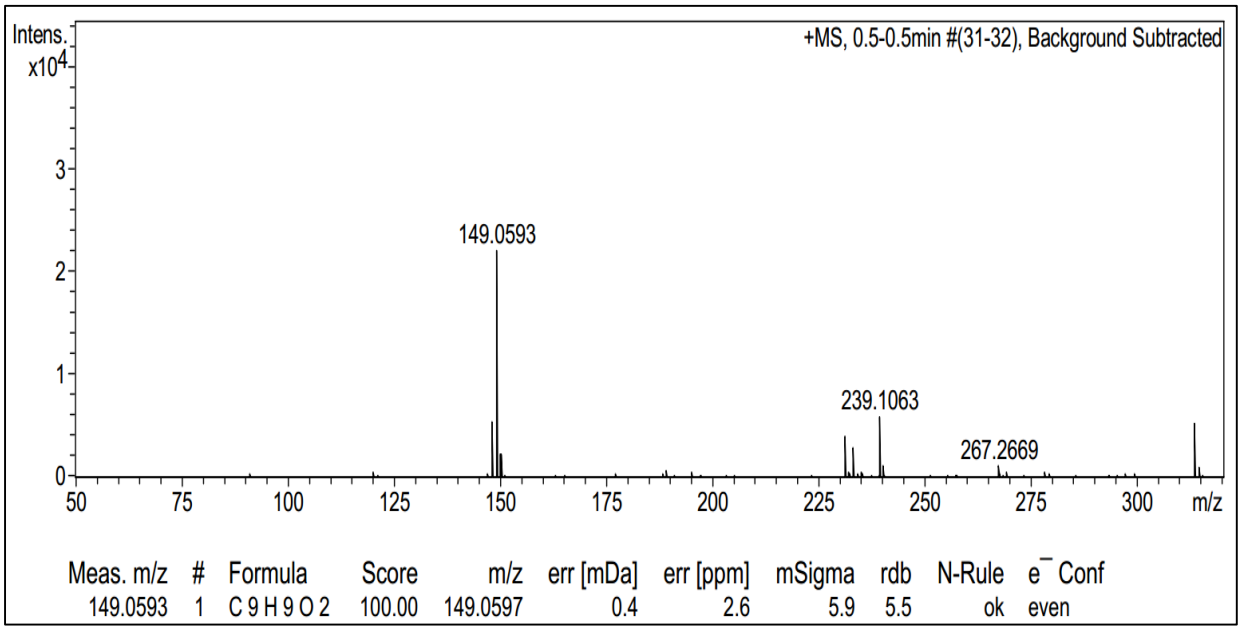

Meas. m/z	#	Formula	Score	m/z	err [mDa]	err [ppm]	mSigma	rdb	N-Rule	e⁻ Conf
149.0593	1	C 9 H 9 O 2	100.00	149.0597	0.4	2.6	5.9	5.5	ok	even

6-Hydroxy-1-indanone (**2c**)

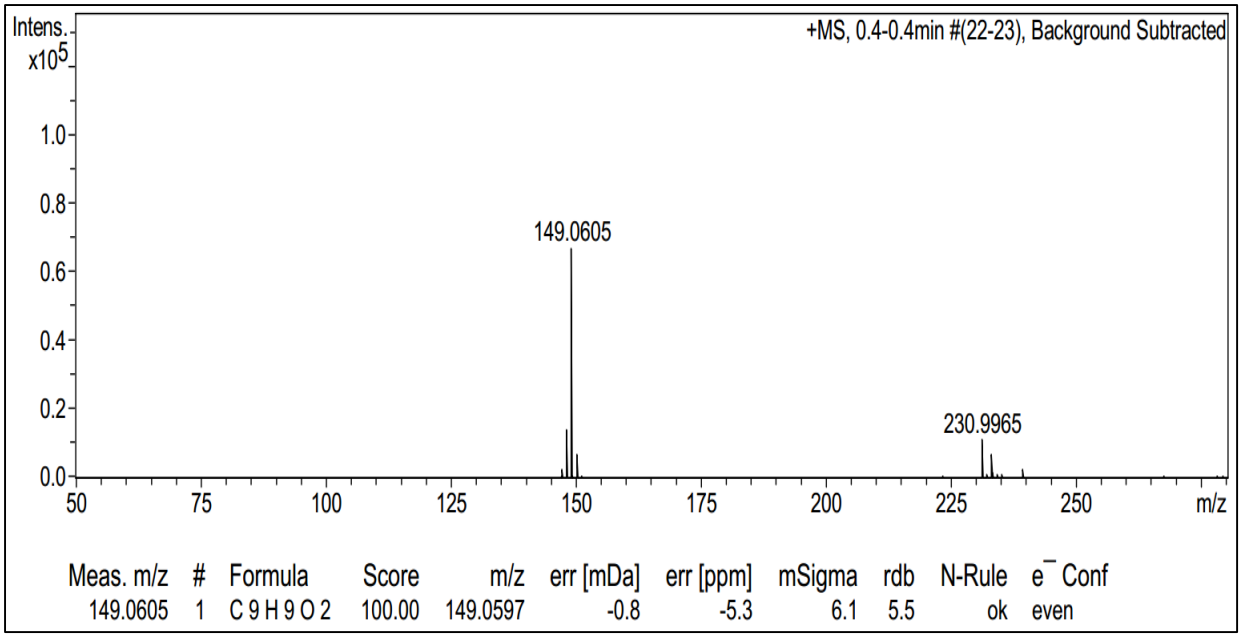

Meas. m/z	#	Formula	Score	m/z	err [mDa]	err [ppm]	mSigma	rdb	N-Rule	e⁻ Conf
149.0605	1	C 9 H 9 O 2	100.00	149.0597	-0.8	-5.3	6.1	5.5	ok	even

ANNEXURE C: HPLC

4-Benzyloxy-1-indanone (**1a**) – 1 mM

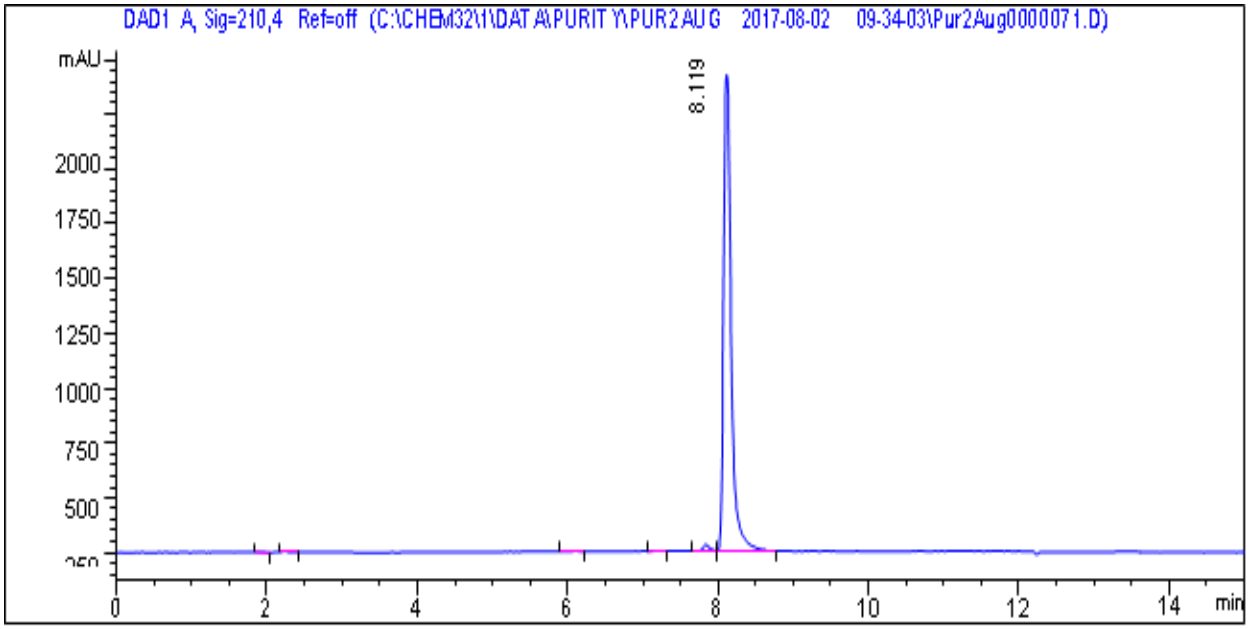

4-Benzyloxy-1-indanone (**1a**) – 100 µM

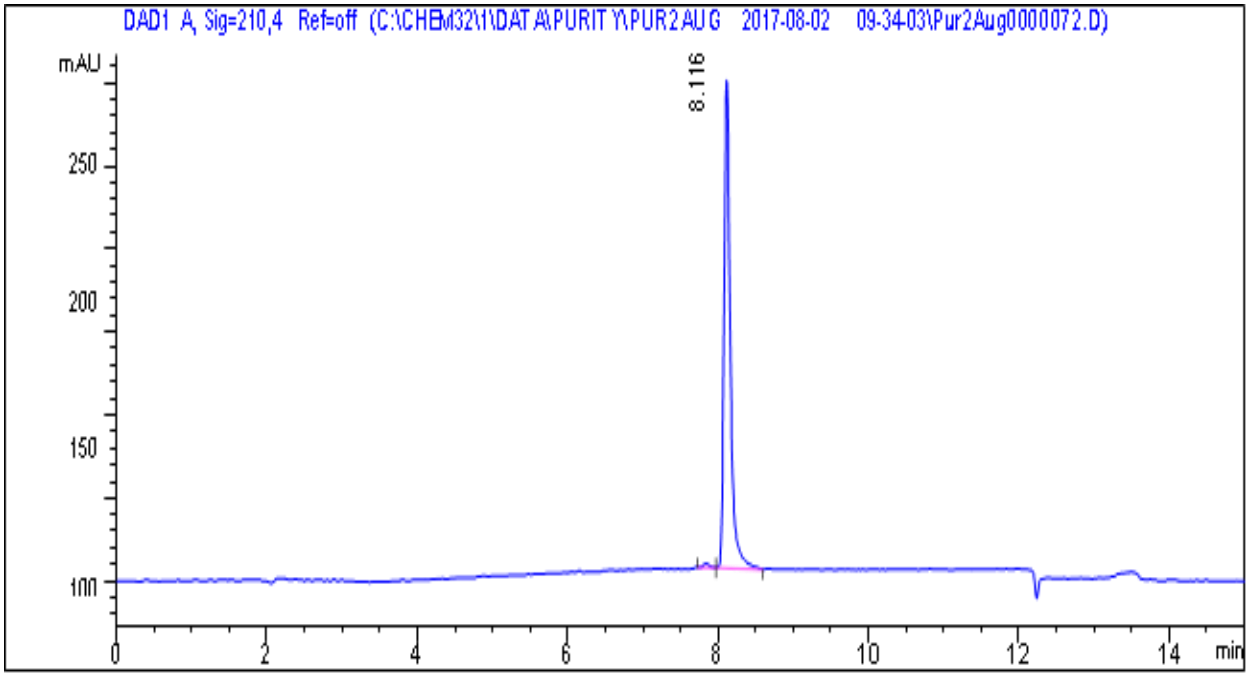

5-Benzyloxy-1-indanone (**1b**) – 1 mM

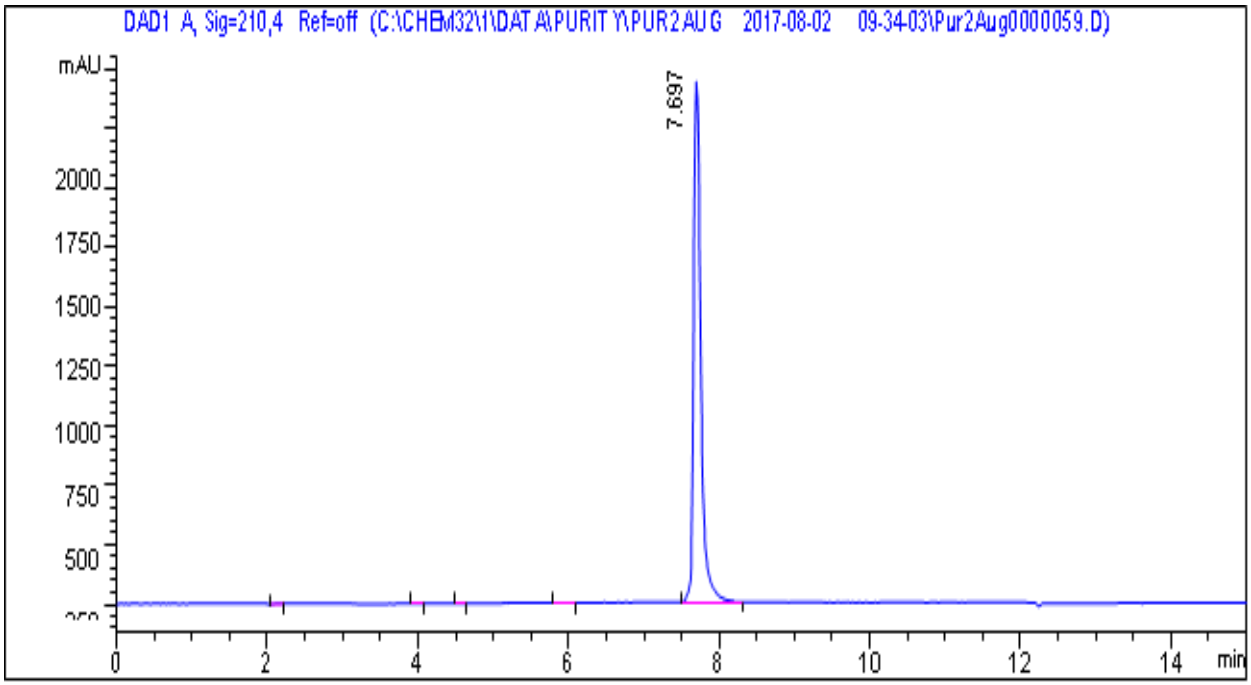

5-Benzyloxy-1-indanone (**1b**) – 100 µM

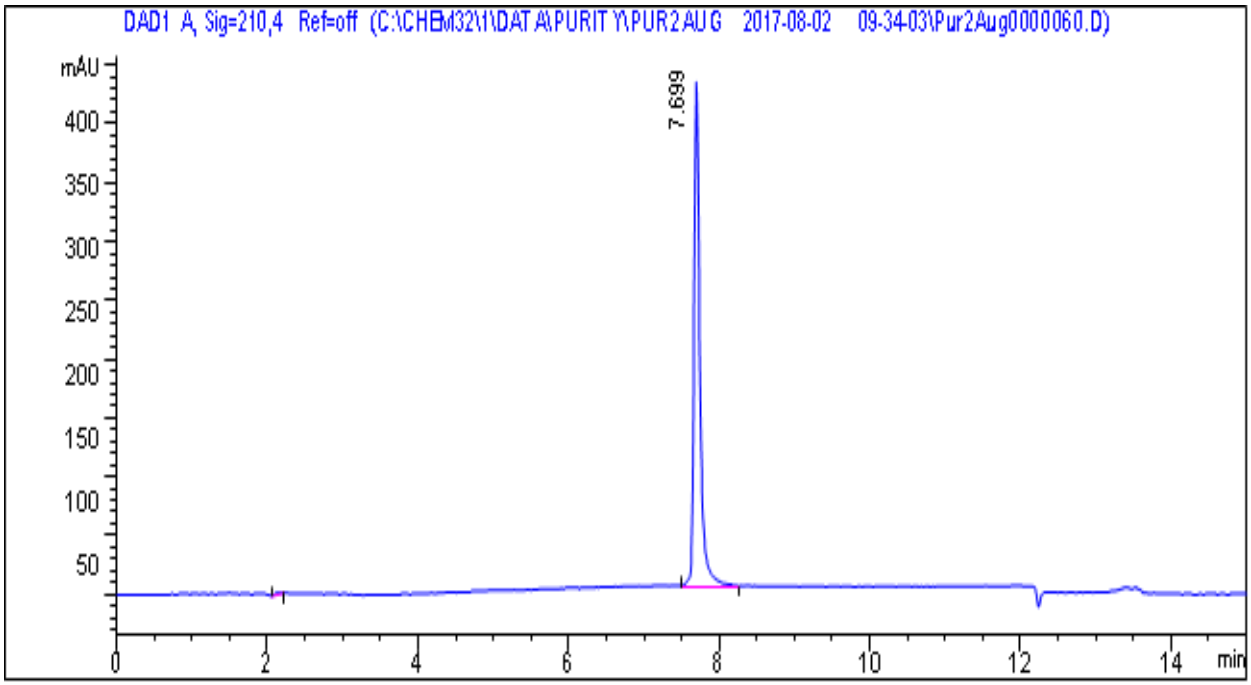

6-Benzyloxy-1-indanone (**1c**) – 1 mM

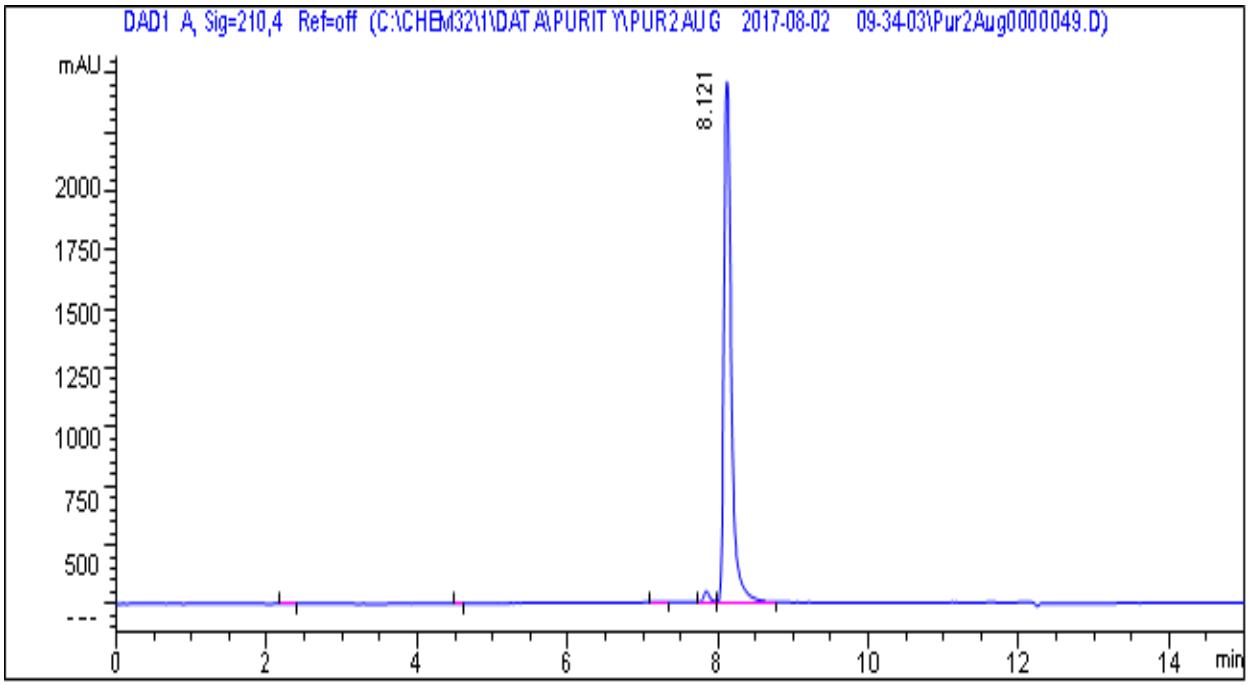

6-Benzyloxy-1-indanone (**1c**) – 100 µM

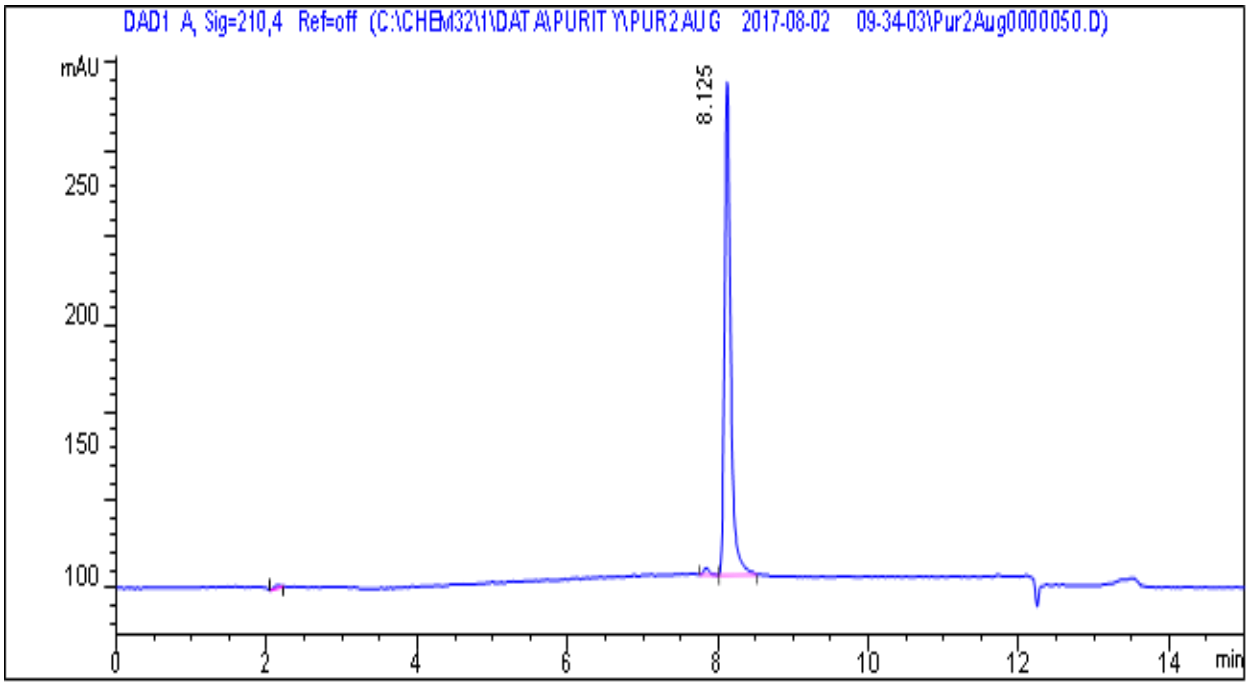

4-(4-Chlorobenzyloxy)-1-indanone (**1d**) – 1 mM

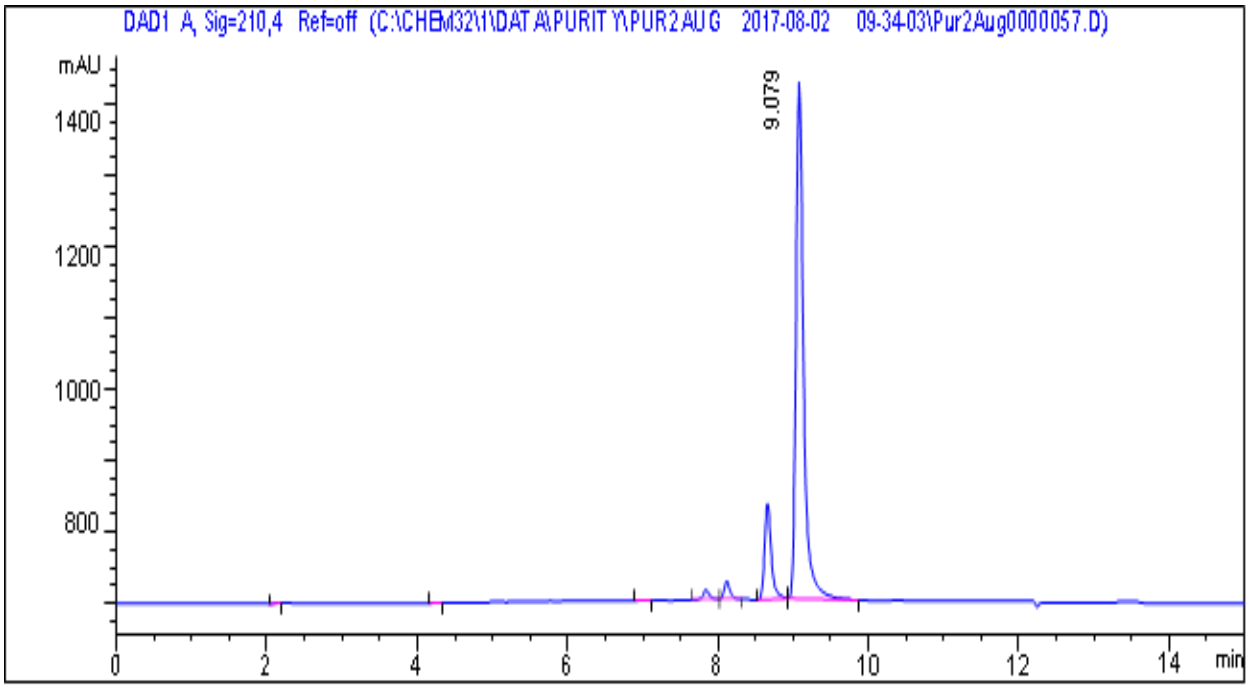

4-(4-Chlorobenzyloxy)-1-indanone (**1d**) – 100 µM

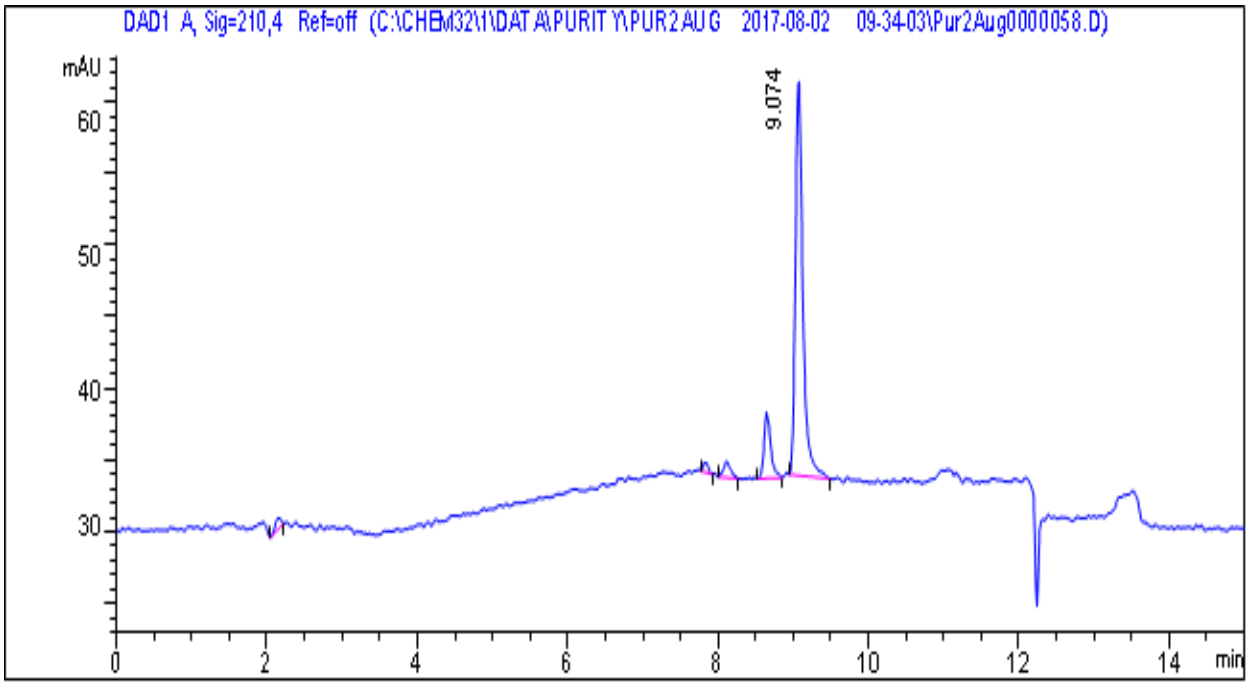

5-(4-Chlorobenzyloxy)-1-indanone (**1e**) – 1 mM

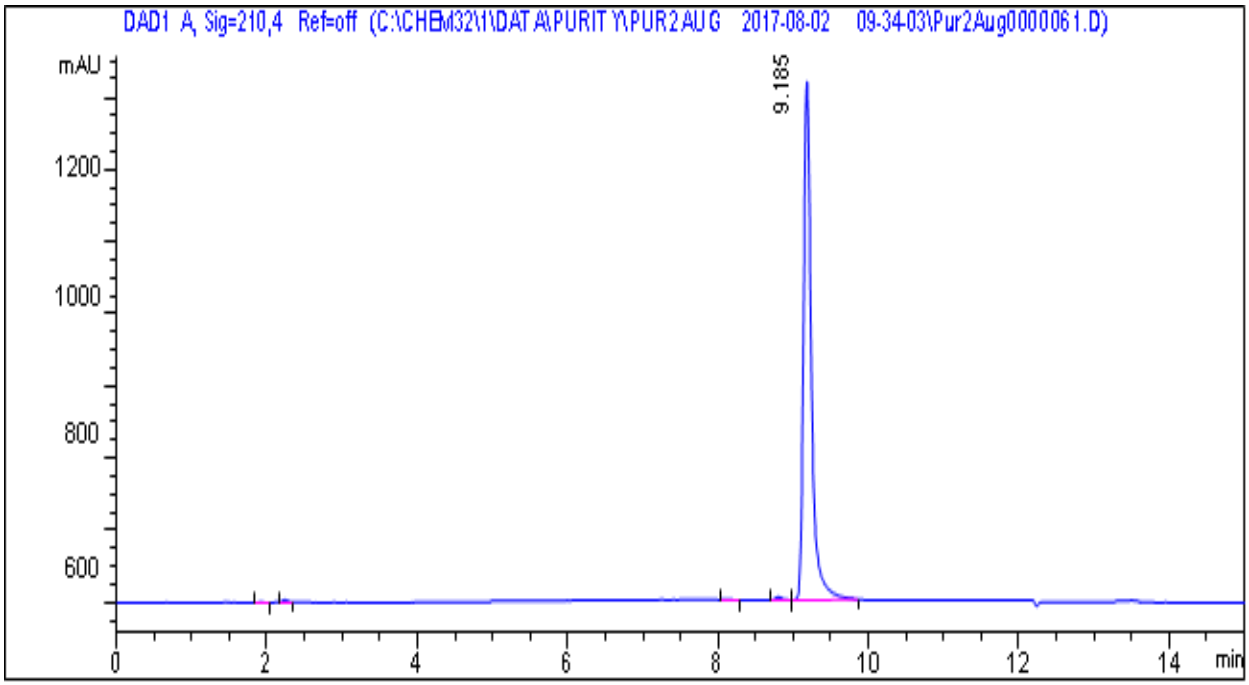

5-(4-Chlorobenzyloxy)-1-indanone (**1e**) – 100 µM

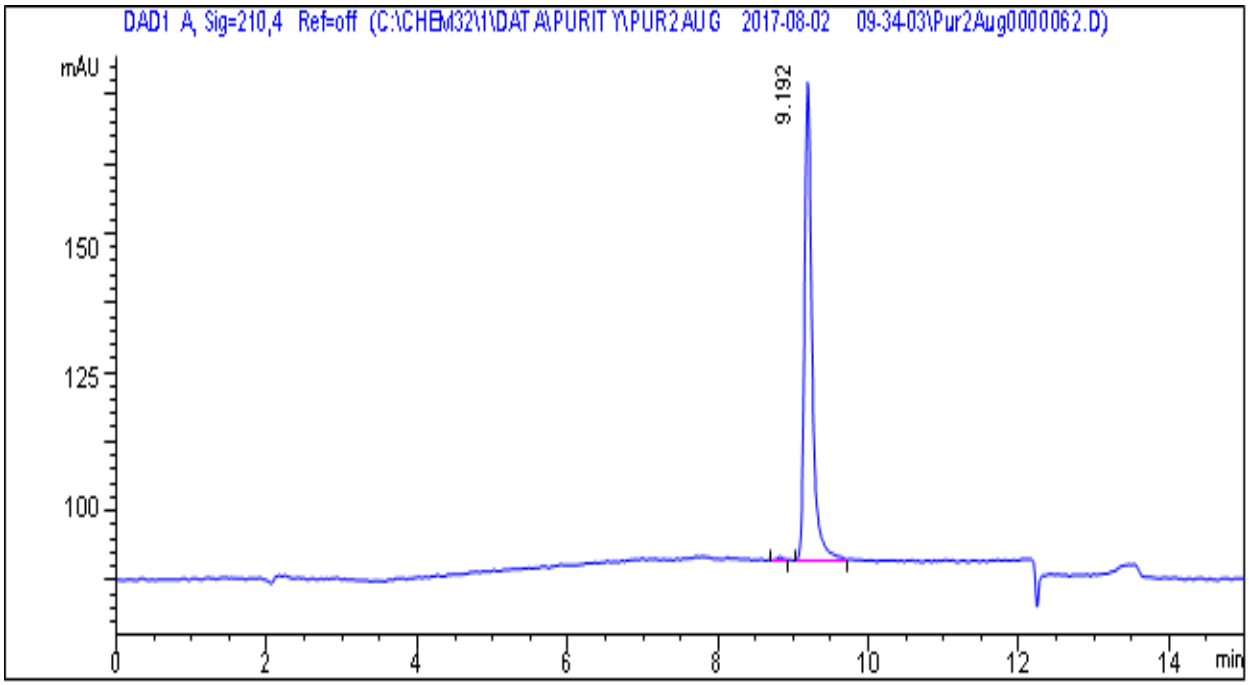

6-(4-Chlorobenzyloxy)-1-indanone (**1f**) – 1 mM

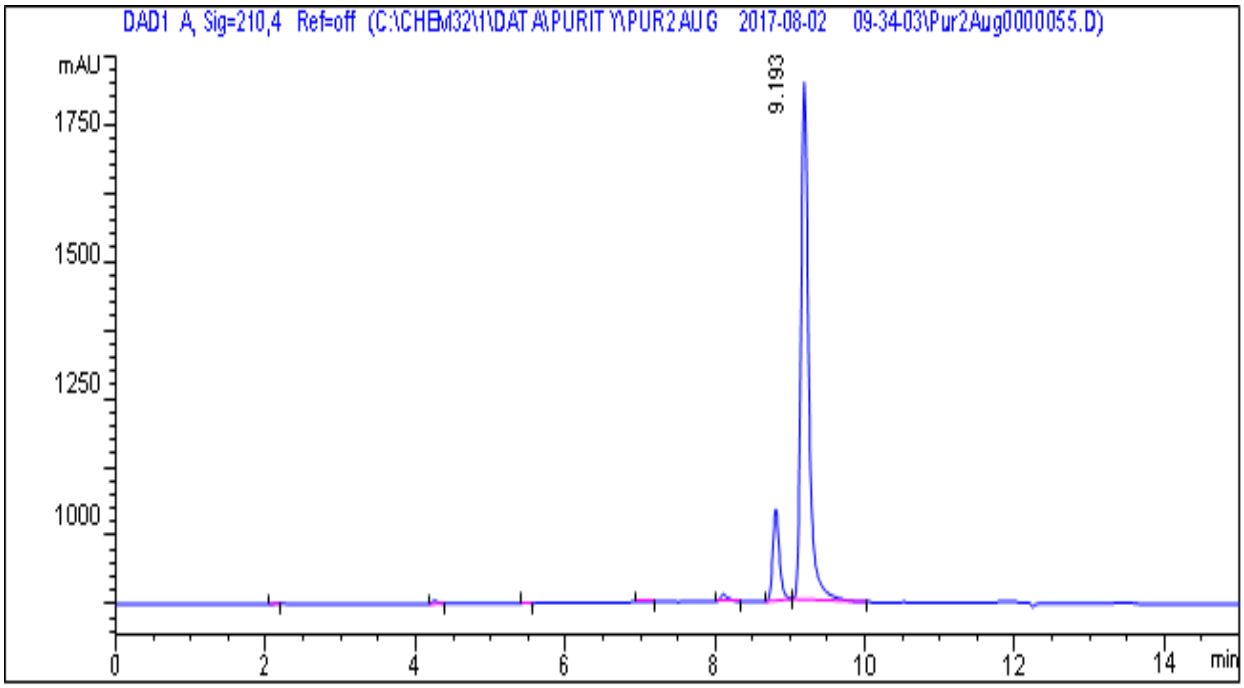

6-(4-Chlorobenzyloxy)-1-indanone (**1f**) – 100 µM

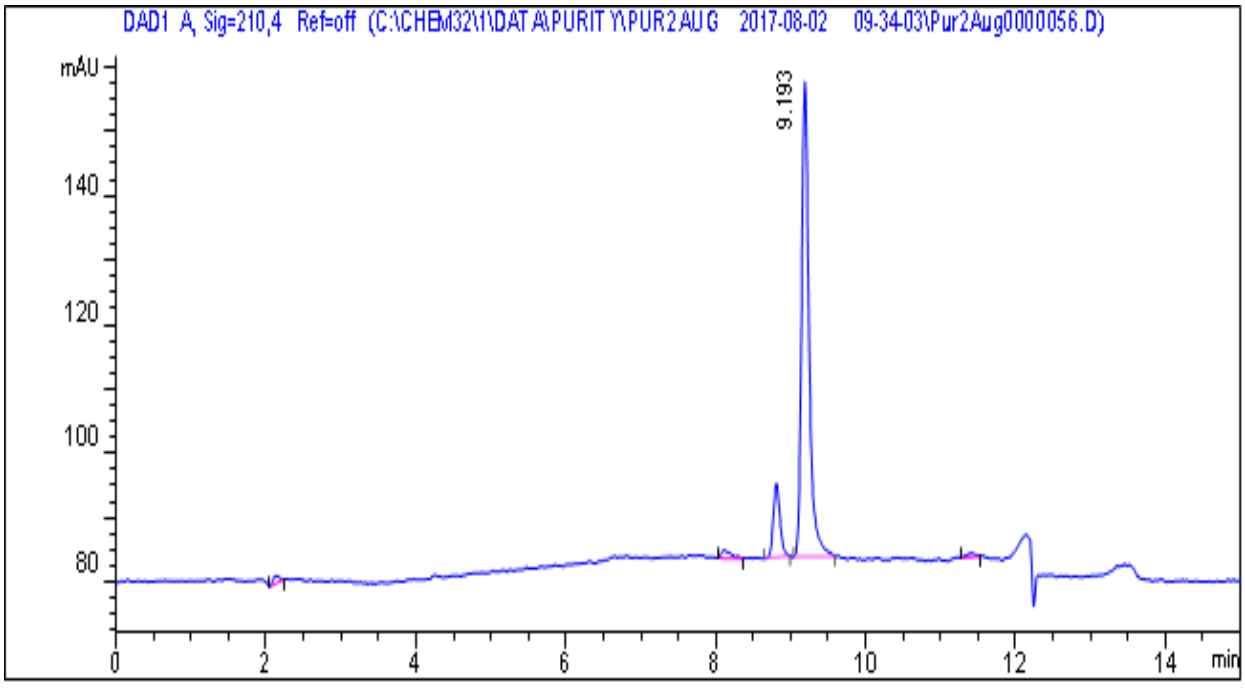

6-(3-Chlorobenzyloxy)-1-indanone (**1g**) – 1 mM

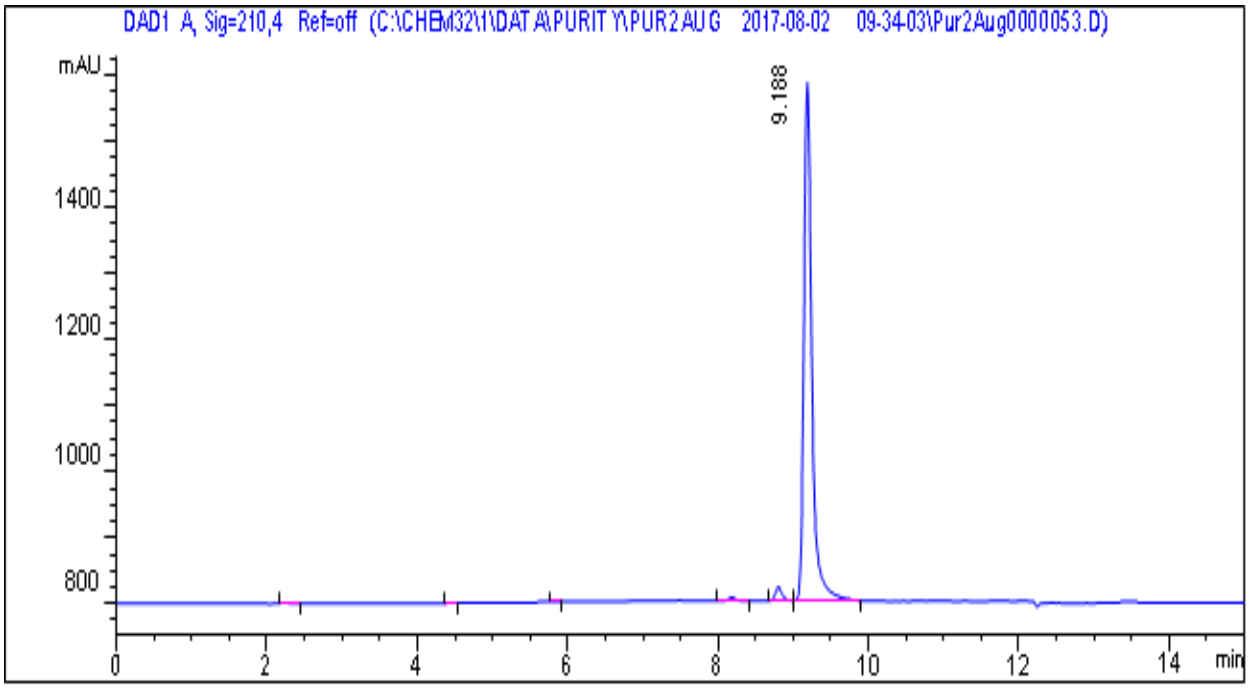

6-(3-Chlorobenzyloxy)-1-indanone (**1g**) – 100 µM

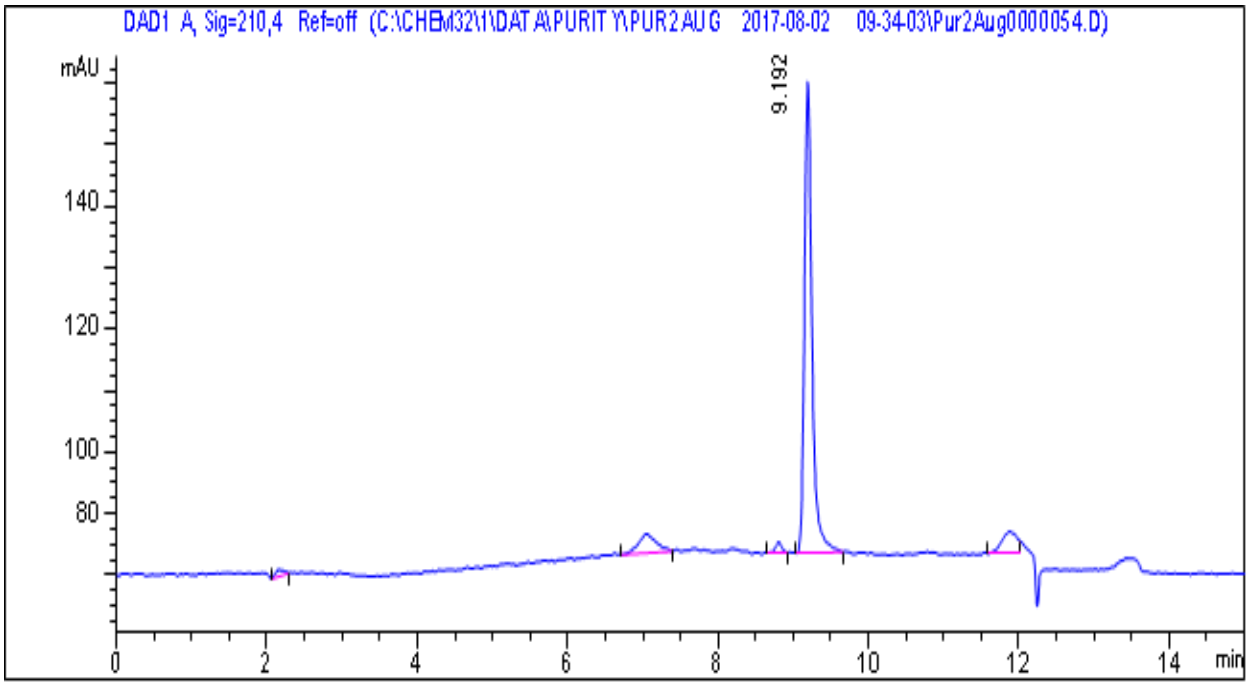

5-(2-Phenoxyethoxy)-1-indanone (**1h**) - 1 mM

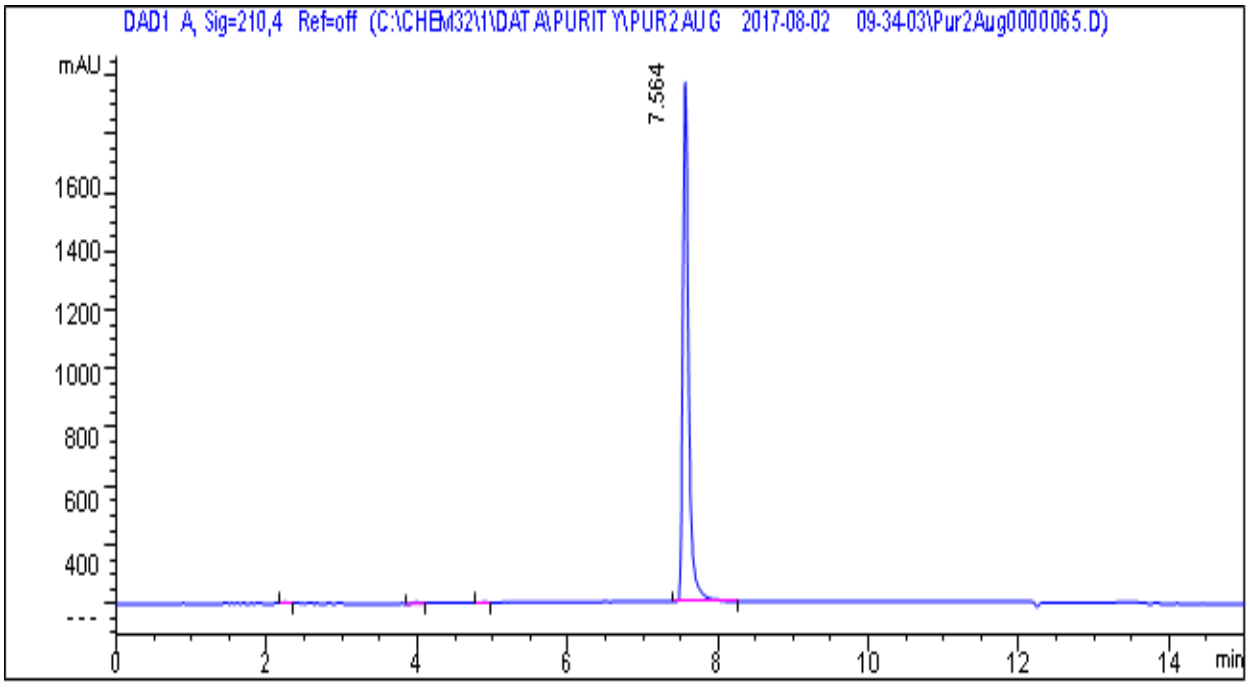

5-(2-Phenoxyethoxy)-1-indanone (**1h**) - 100 µM

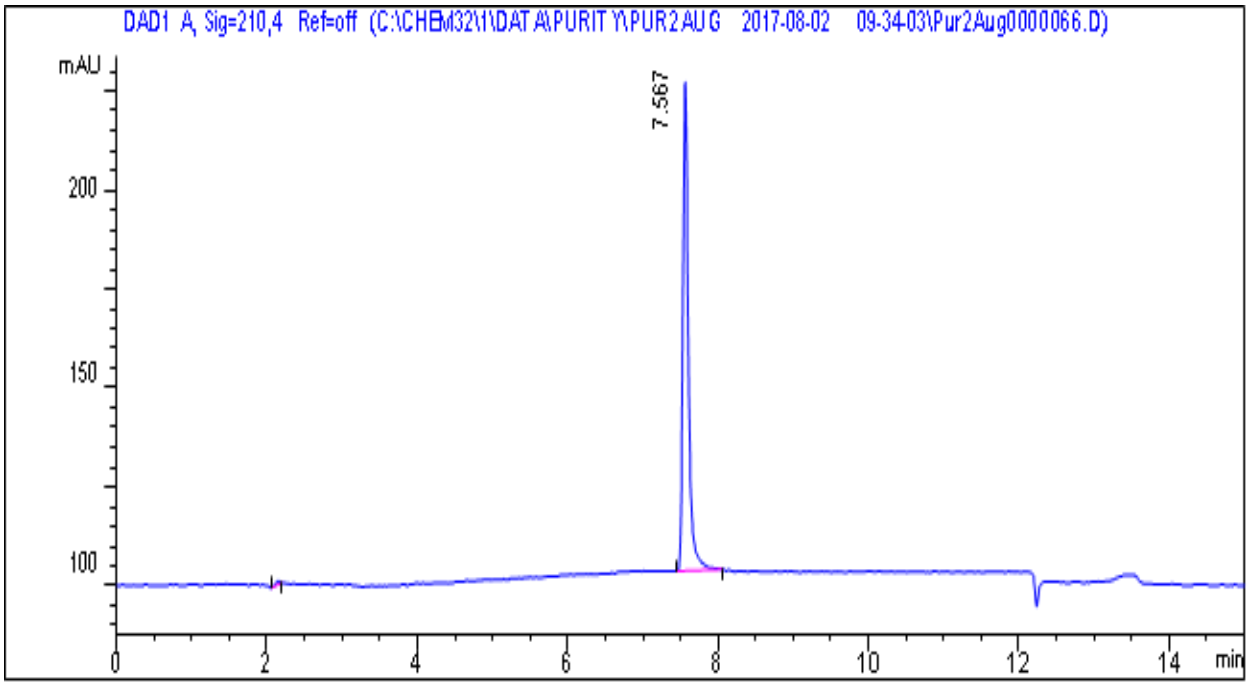

5-Benzyloxy-1-indanol (**1i**) - 1 mM

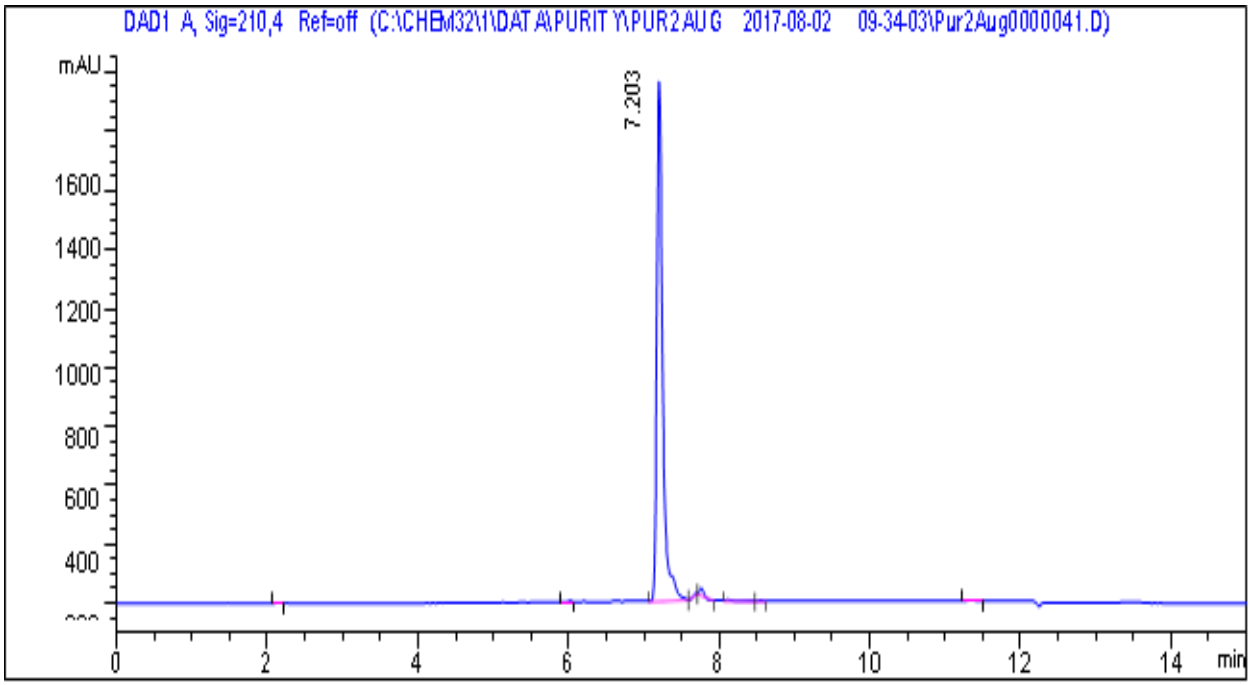

5-Benzyloxy-1-indanol (**1i**) - 100 µM

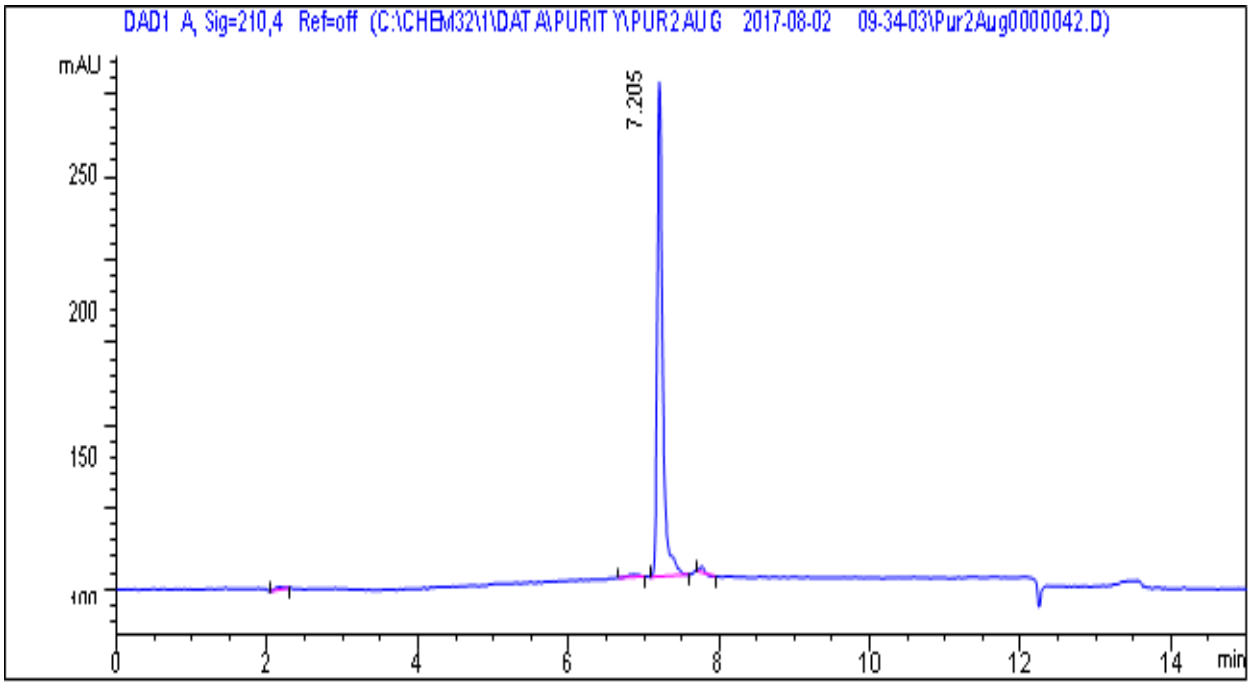

6-Benzyloxy-1-indanol (**1j**) - 1 mM

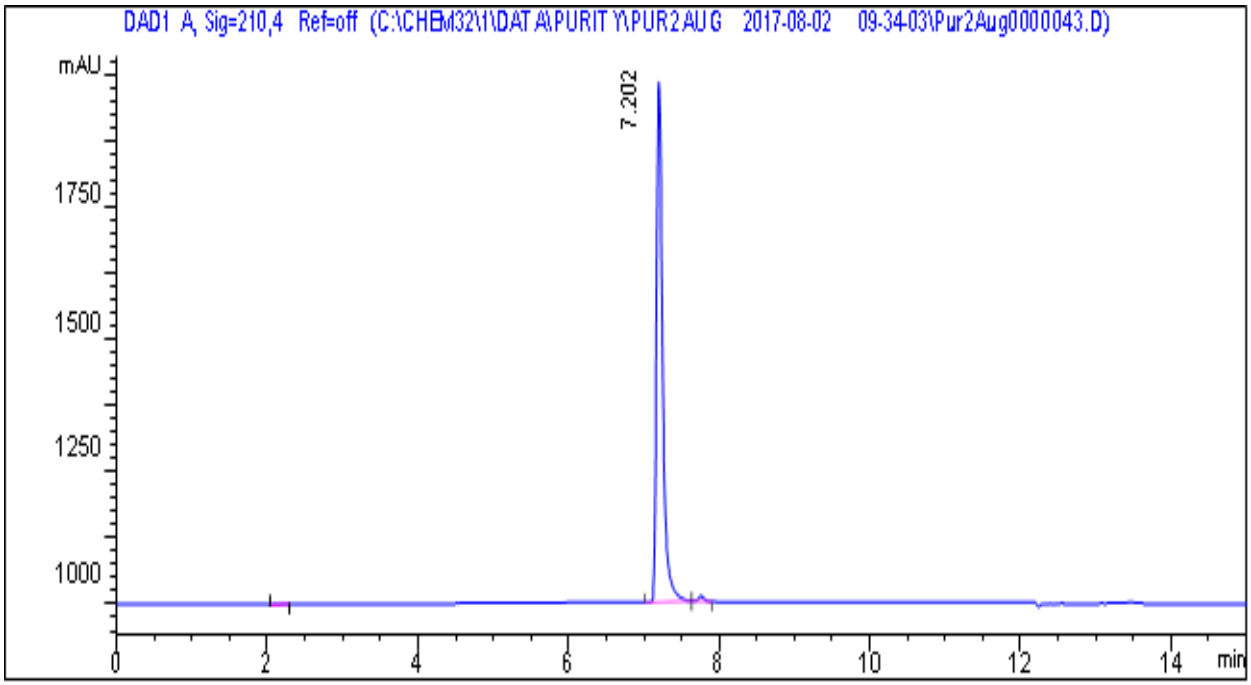

6-Benzyloxy-1-indanol (**1j**) - 100 µM

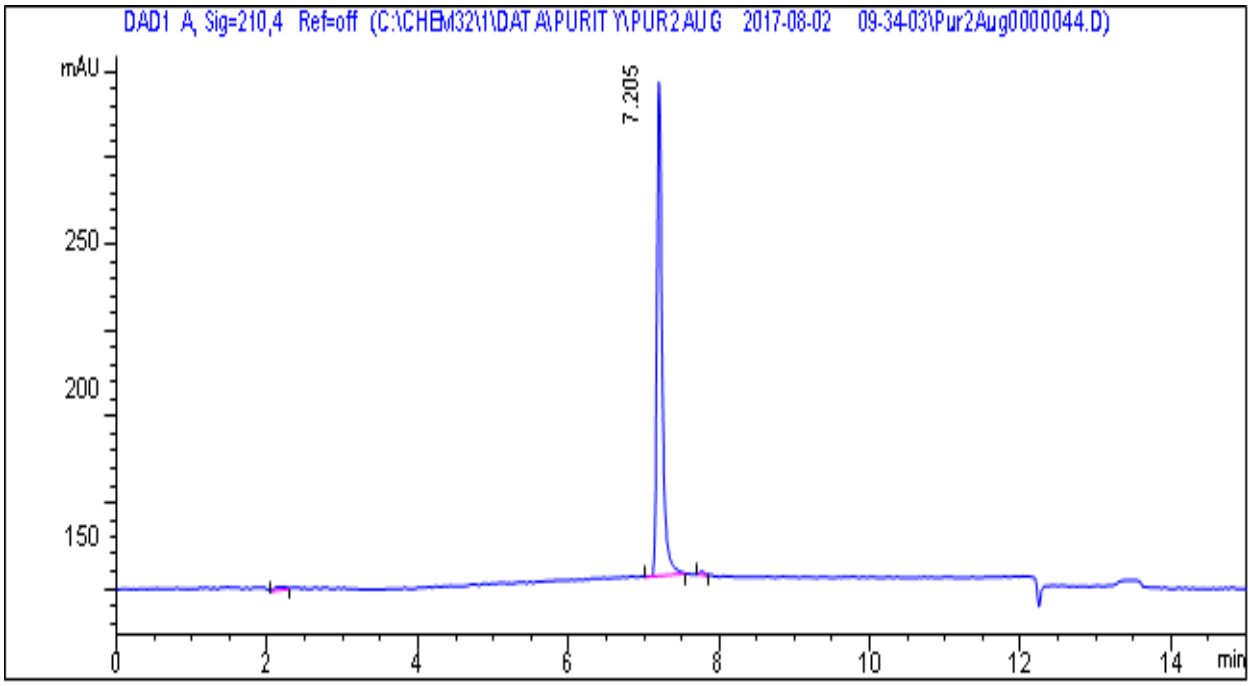

4-(4-Chlorobenzyloxy)-1-indanol (**1k**) - 1 mM

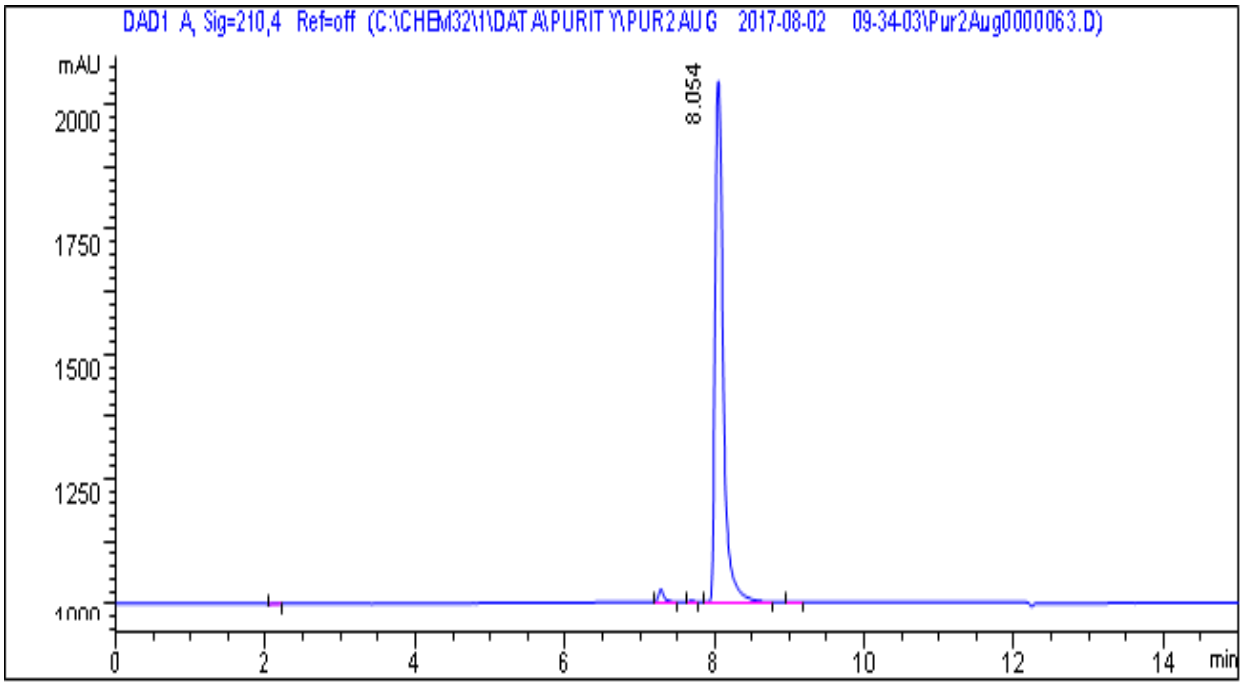

4-(4-Chlorobenzyloxy)-1-indanol (**1k**) - 100 µM

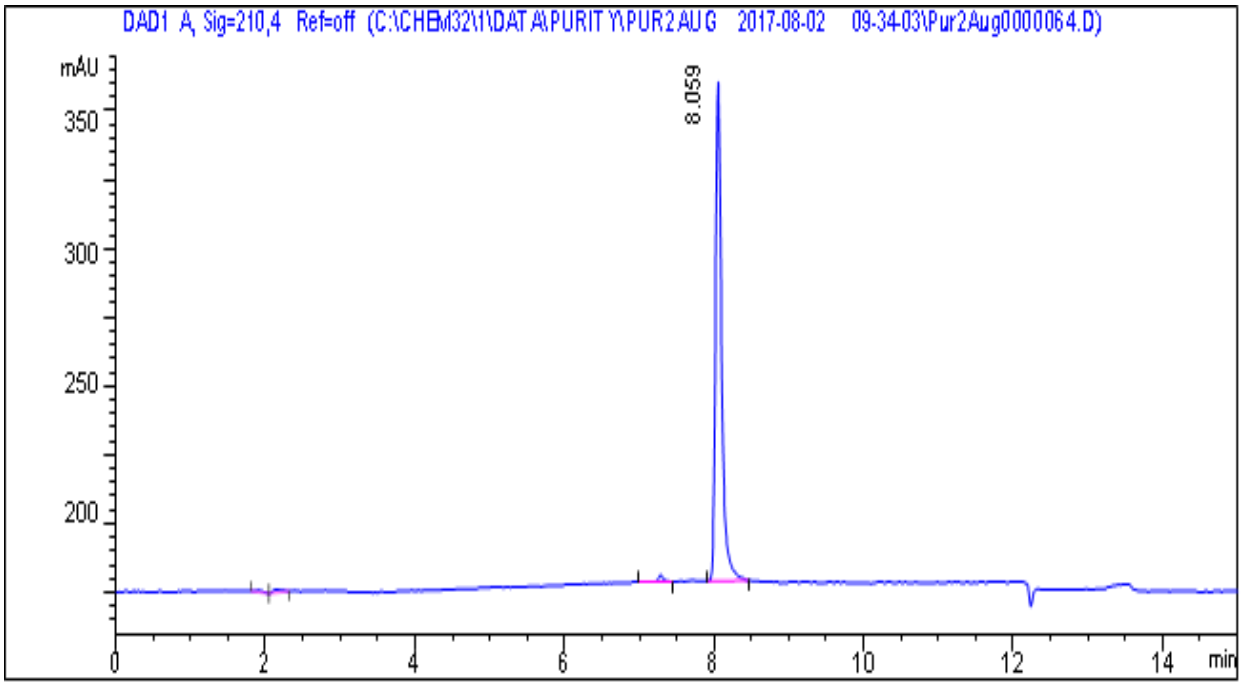

5-(4-Chlorobenzyloxy)-1-indanol (**1l**) - 100 mM

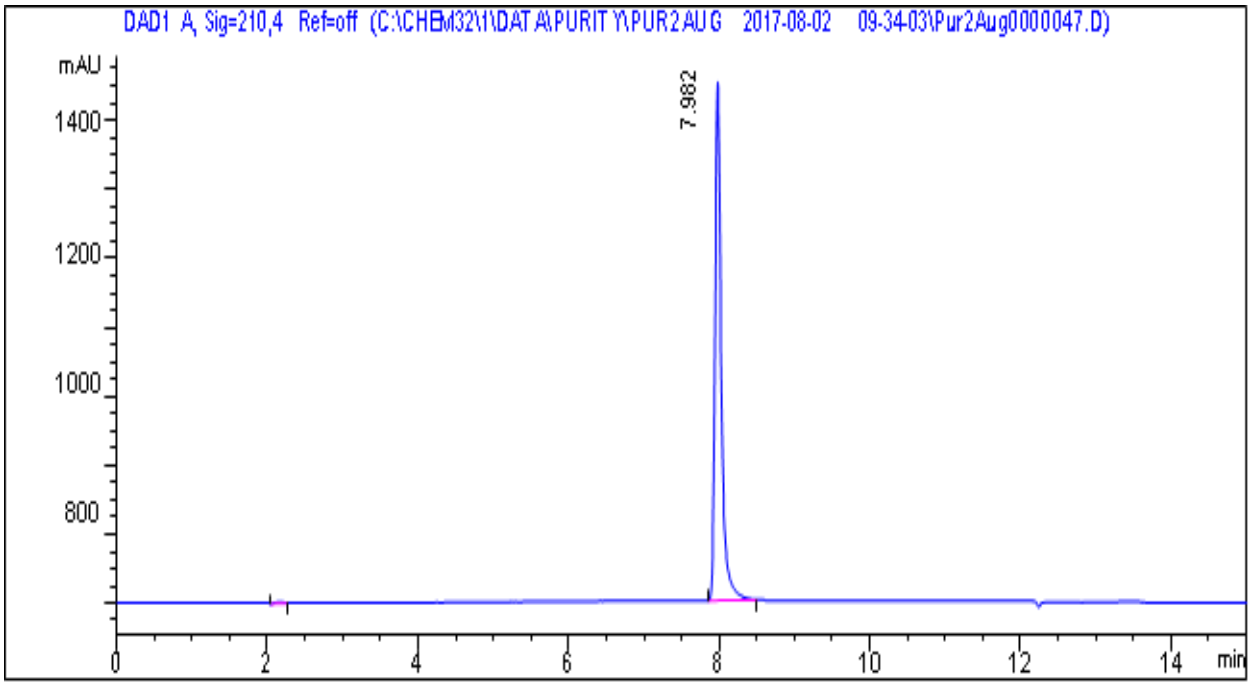

5-(4-Chlorobenzyloxy)-1-indanol (**1l**) - 1 µM

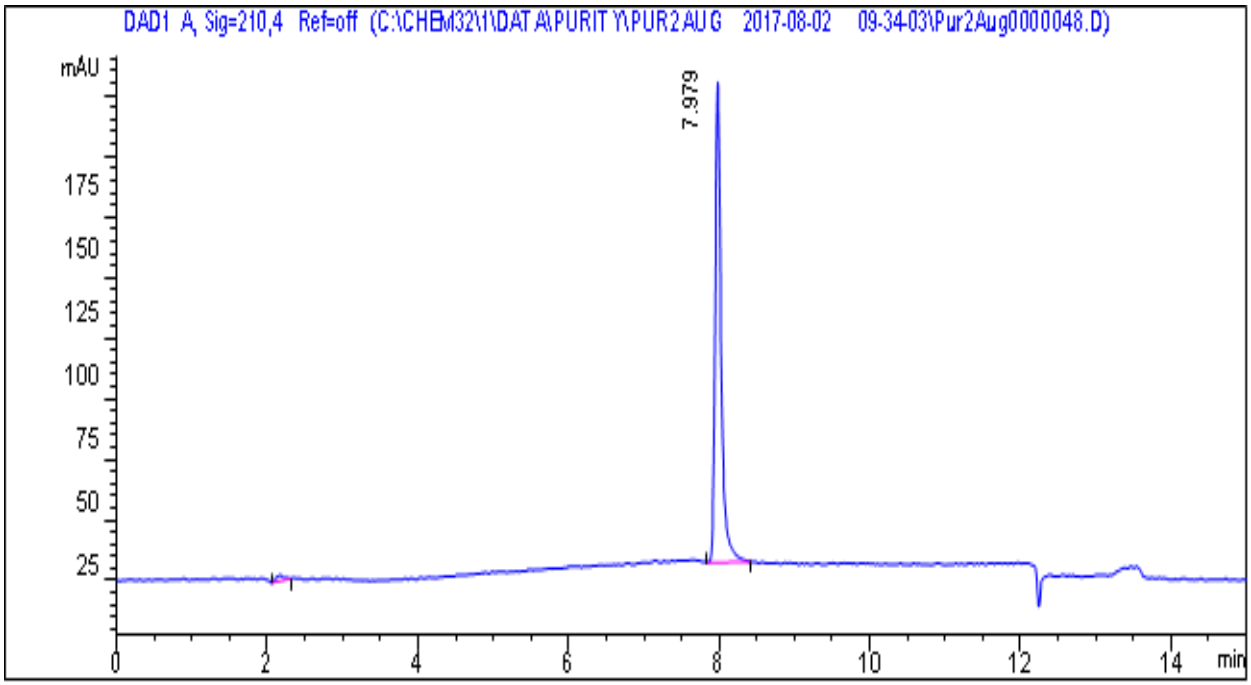

6-(4-Chlorobenzyloxy)-1-indanol (**1m**) - 1 mM

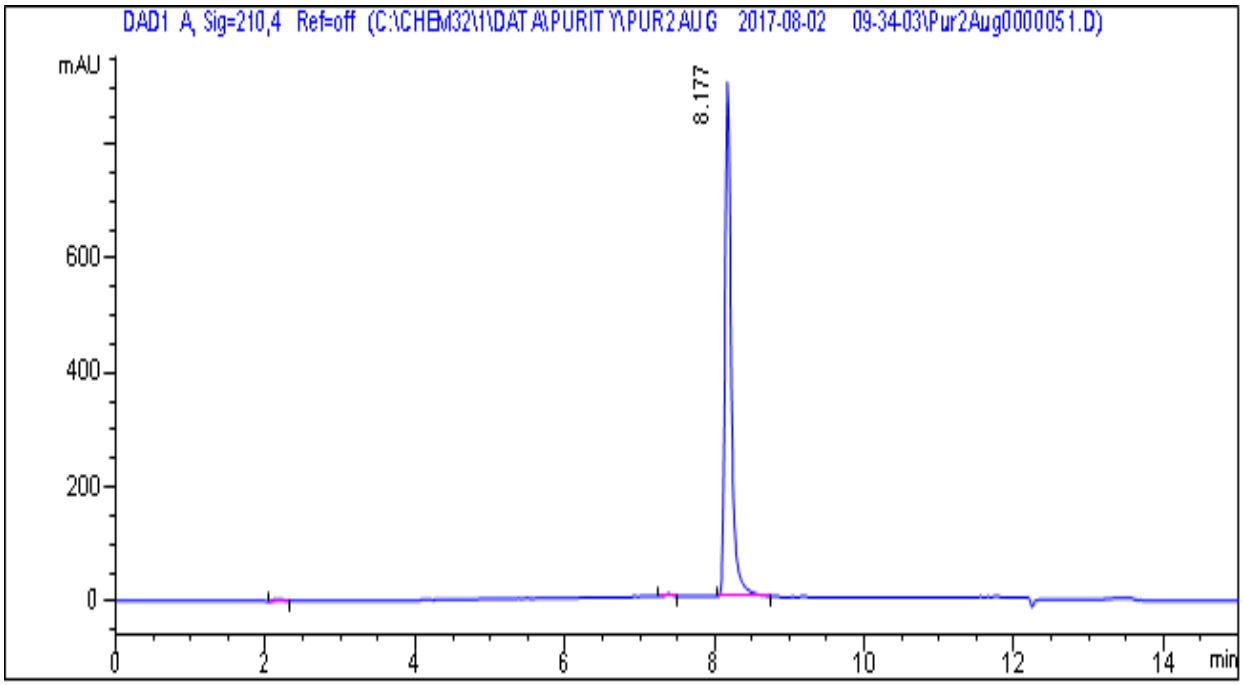

6-(4-Chlorobenzyloxy)-1-indanol (**1m**) - 100 µM

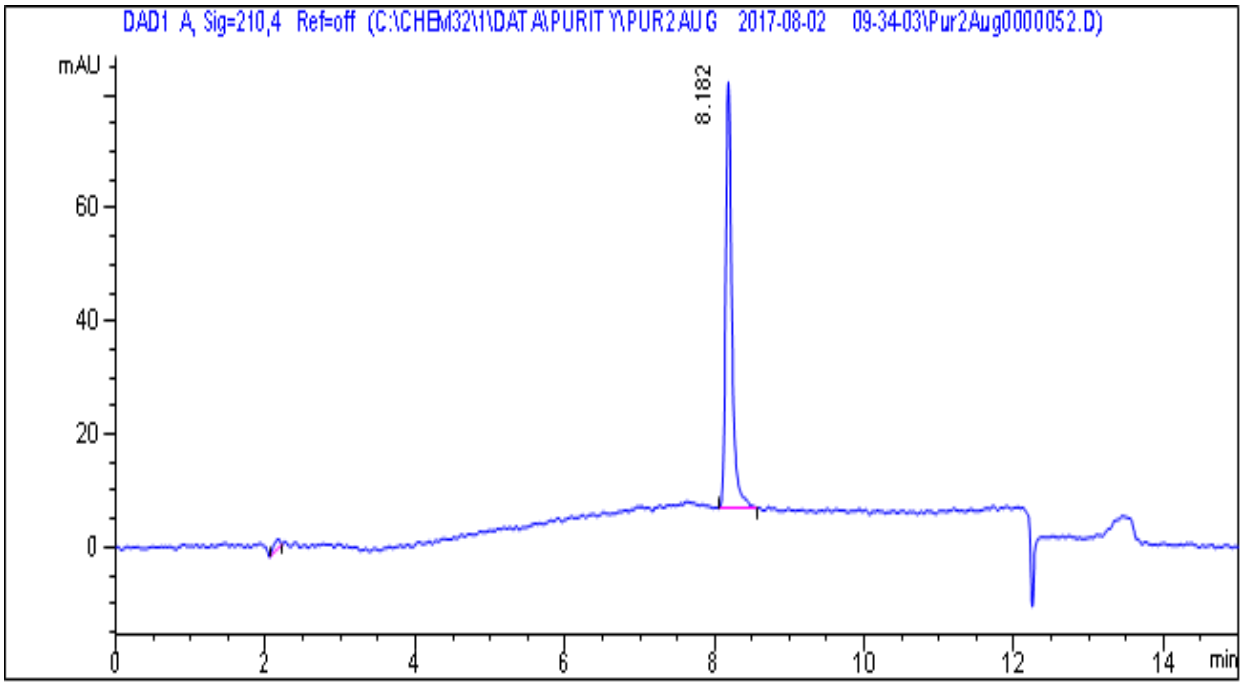

6-(3-Chlorobenzyloxy)-1-indanol (**1n**) - 1 mM

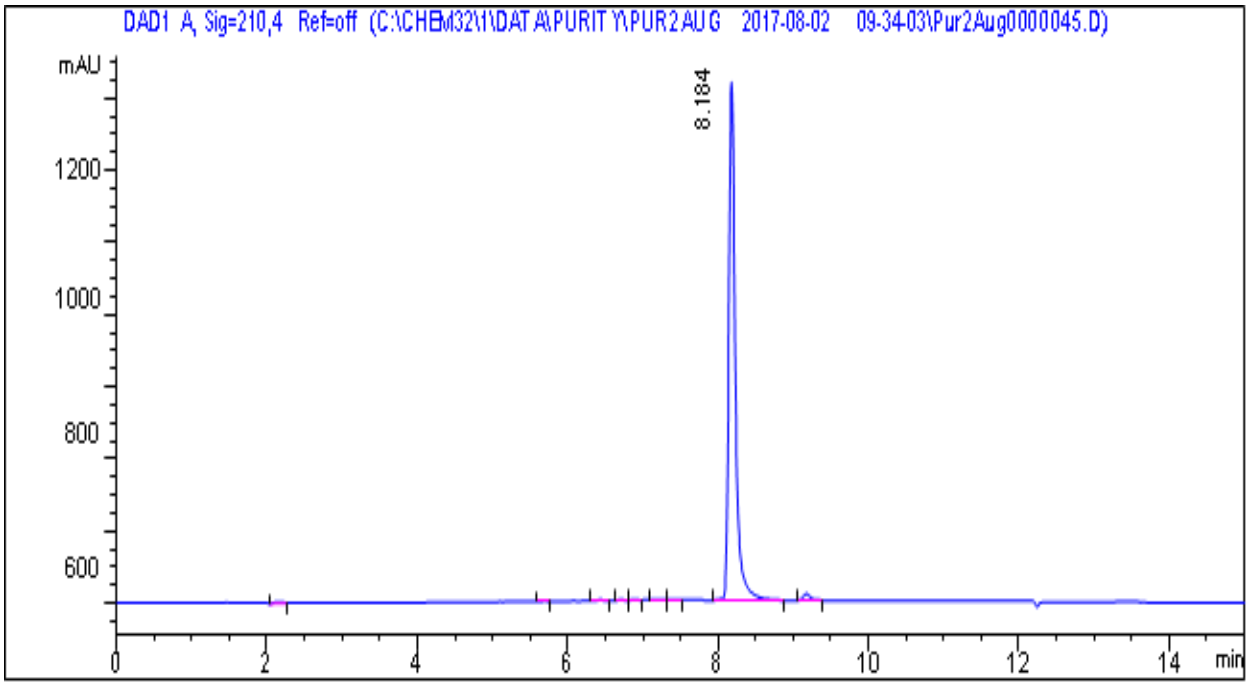

6-(3-Chlorobenzyloxy)-1-indanol (**1n**) - 100 µM

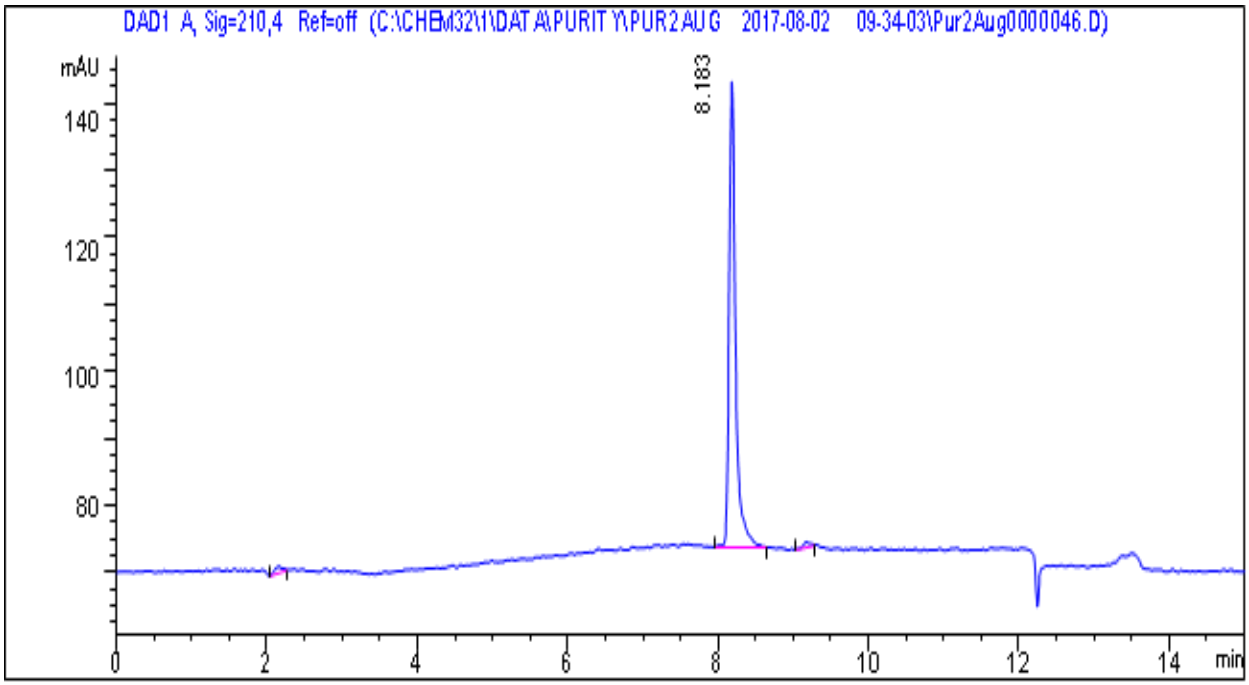

4-Hydroxy-1-indanone (**2a**) - 1 mM

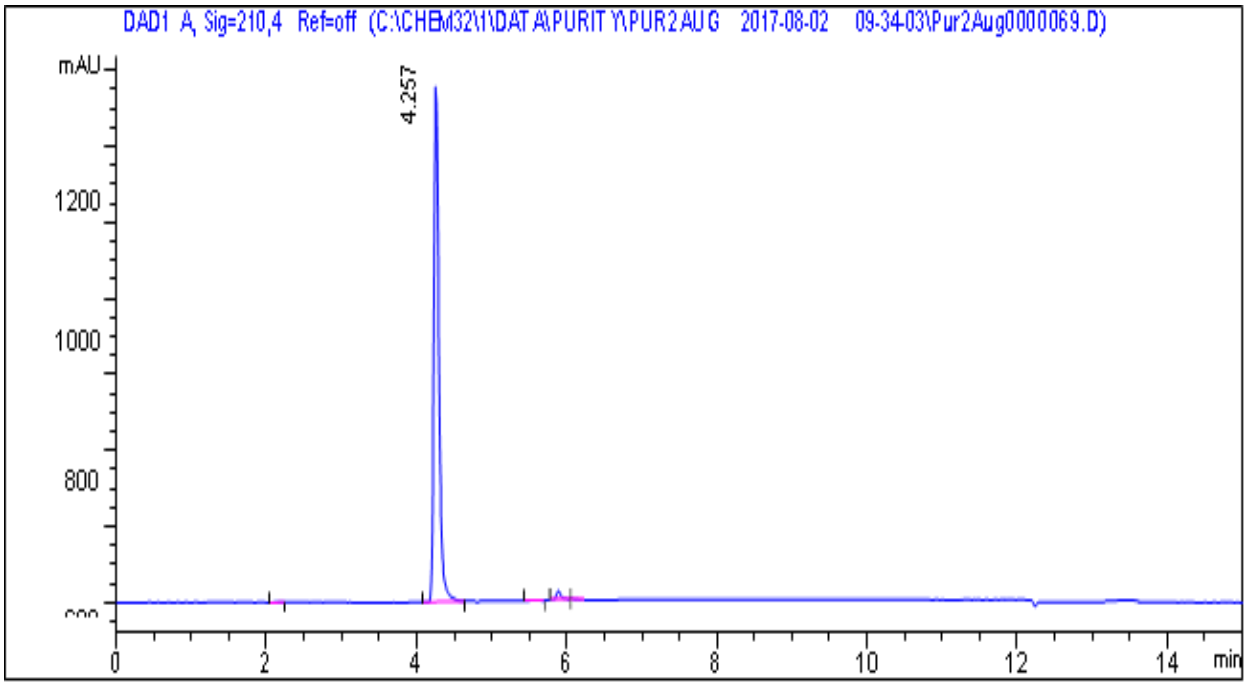

4-Hydroxy-1-indanone (**2a**) - 100 µM

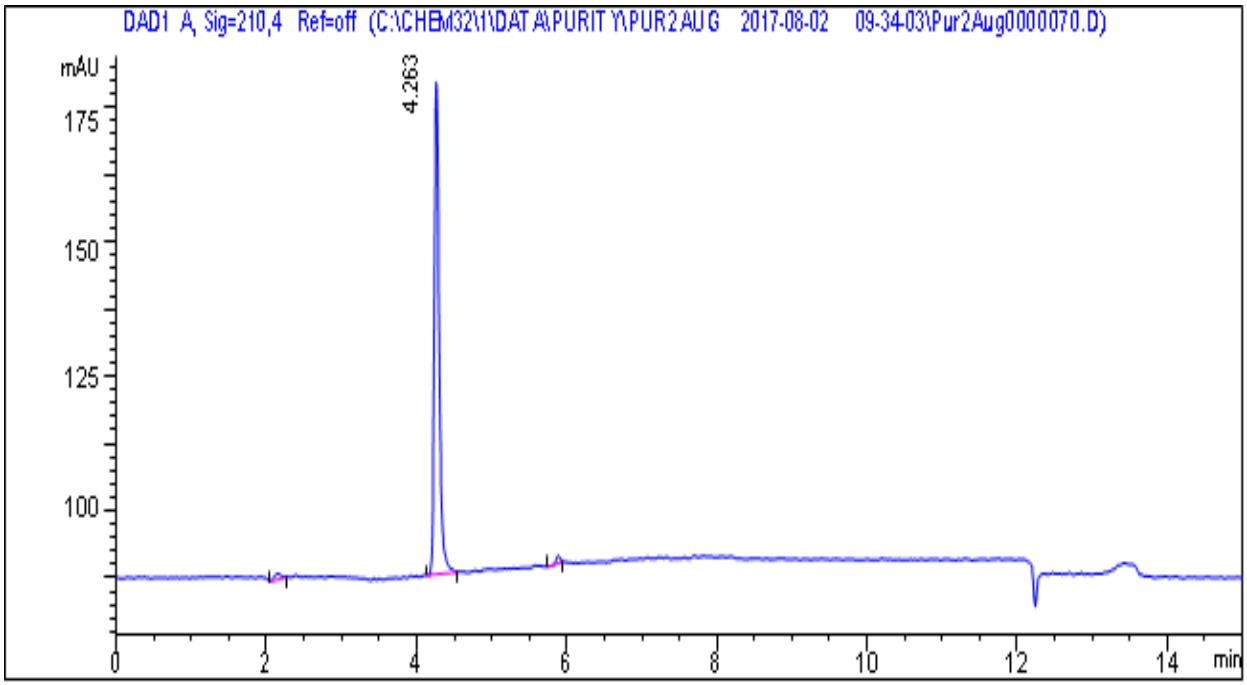

6-Hydroxy-1-indanone (**2c**) - 1 mM

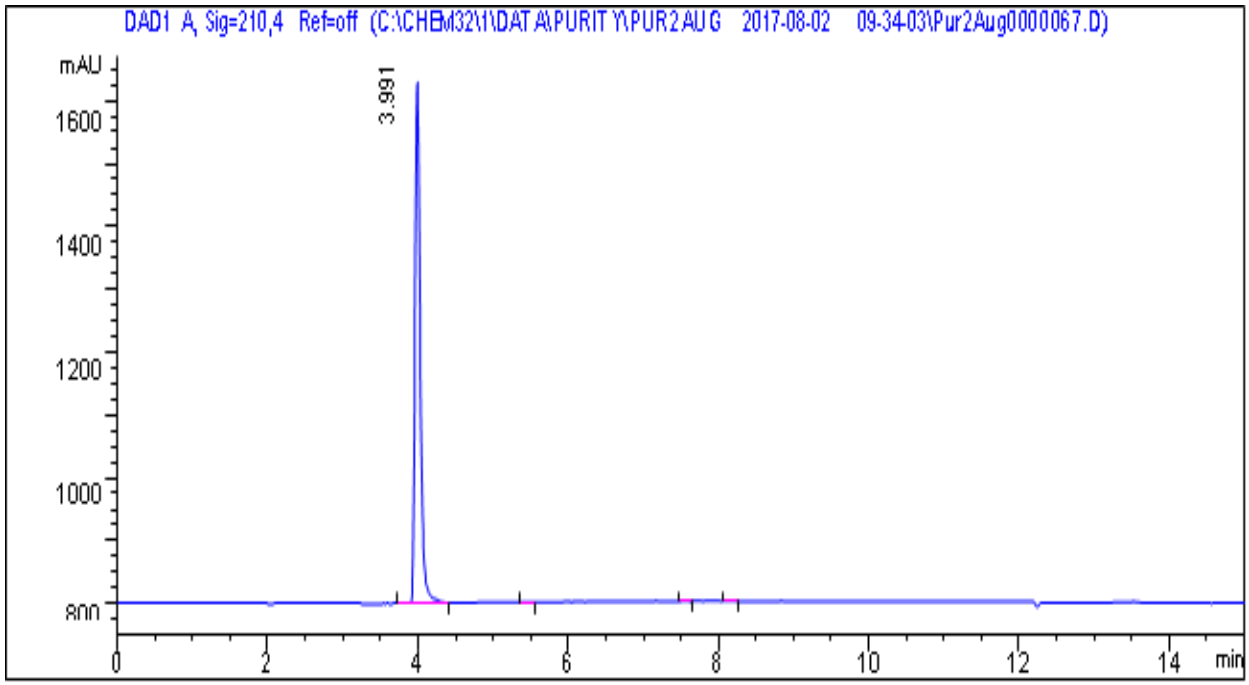

6-Hydroxy-1-indanone (**2c**) - 100 µM

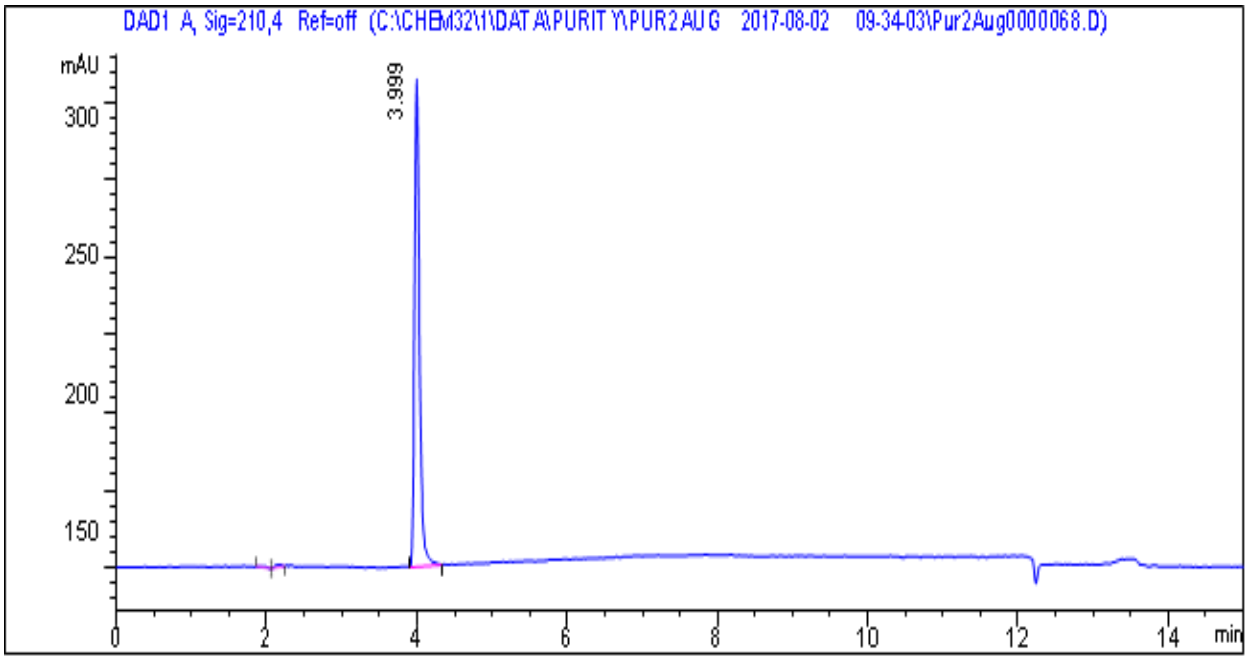

ANNEXURE D: PERMISSION

JOHN WILEY AND SONS LICENSE TERMS AND CONDITIONS

Oct 04, 2017

This Agreement between Ms. Elani Aucamp ("You") and John Wiley and Sons ("John Wiley and Sons") consists of your license details and the terms and conditions provided by John Wiley and Sons and Copyright Clearance Center.

License Number	4196401028093
License date	Sep 26, 2017
Licensed Content Publisher	John Wiley and Sons
Licensed Content Publication	British Journal of Pharmacology
Licensed Content Title	Monoamine oxidase: isoforms and inhibitors in Parkinson\'s disease and depressive illness
Licensed Content Author	Moussa B H Youdim,Y S Bakhle
Licensed Content Date	Feb 2, 2009
Licensed Content Pages	1
Type of use	Dissertation/Thesis
Requestor type	University/Academic
Format	Print and electronic
Portion	Figure/table
Number of figures/tables	3
Original Wiley figure/table number(s)	Figures 1, 3 and 7
Will you be translating?	No
Title of your thesis / dissertation	An investigation of indanone derivatives as inhibitors of monoamine oxidase
Expected completion date	Oct 2017
Expected size (number of pages)	130
Requestor Location	Ms. Elani Aucamp P.O. Box 413 Park South Vanderbijlpark, Gauteng 1910 South Africa Attn: Ms. Elani Aucamp
Publisher Tax ID	EU826007151
Billing Type	Invoice
Billing Address	Ms. Elani Aucamp P.O. Box 413 Park South Vanderbijlpark, South Africa 1910 Attn: Ms. Elani Aucamp
Total	0.00 USD
Terms and Conditions	

ELSEVIER LICENSE
TERMS AND CONDITIONS

Oct 04, 2017

This Agreement between Ms. Elani Aucamp ("You") and Elsevier ("Elsevier") consists of your license details and the terms and conditions provided by Elsevier and Copyright Clearance Center.

License Number	4196450698462
License date	Sep 26, 2017
Licensed Content Publisher	Elsevier
Licensed Content Publication	Journal of Molecular Biology
Licensed Content Title	Crystal Structure of Amine Oxidase from Bovine Serum
Licensed Content Author	Michele Lunelli,Maria Luisa Di Paolo,Marianna Biadene,Vito Calderone,Roberto Battistutta,Marina Scarpa,Adelio Rigo,Giuseppe Zanotti
Licensed Content Date	Mar 4, 2005
Licensed Content Volume	346
Licensed Content Issue	4
Licensed Content Pages	14
Start Page	991
End Page	1004
Type of Use	reuse in a thesis/dissertation
Intended publisher of new work	other
Portion	figures/tables/illustrations
Number of figures/tables /illustrations	1
Format	both print and electronic
Are you the author of this Elsevier article?	No
Will you be translating?	No
Original figure numbers	Figure 1
Title of your thesis/dissertation	An investigation of indanone derivatives as inhibitors of monoamine oxidase
Expected completion date	Oct 2017
Estimated size (number of pages)	130
Requestor Location	Ms. Elani Aucamp P.O. Box 413 Park South Vanderbijlpark, Gauteng 1910 South Africa Attn: Ms. Elani Aucamp
Publisher Tax ID	ZA 4110266048
Total	0.00 USD
Terms and Conditions	

Louise Jones <lj@iucr.org>

to me

Dear Elani

Thank you for your message.

Permission is hereby granted, on behalf of the IUCr, for you
to reproduce the material specified below, subject to the following conditions:

1. The original article in which the material appeared is cited.

2. IUCr's copyright permission is indicated next to the
figure in print. In electronic form, this acknowledgement
must be visible at the same time as the article, and must be hyperlinked to the articles in Crystallography Journals Online
Acta Cryst. (2010). F66, 1572-1578.

Best wishes
Louise

PNAS Permissions 10:50 PM (19 hours ago)

to me

Permission is granted for your use of the figures as described in your message. Please list a full citation for the PNAS article, and include "Copyright (2005) National Academy of Sciences, U.S.A." as a copyright note. Because this material published between 1993 and 2008, a copyright note is needed. There is no charge for this material, either. Let us know if you have any questions.

Best regards,
Kay McLaughlin for
Diane Sullenberger
Executive Editor
PNAS